The Pennsylvania State University

The Graduate School

Eberly College of Science

A SYSTEMATIC STUDY OF EXPRESSION AND FUNCTION OF *CAENORHABDITIS ELEGANS* GENES ENCODING P-TYPE ATPASES IN SUBFAMILY IV, THE GROUP OF PUTATIVE TRANSBILAYER AMPHIPATH TRANSPORTERS

A Thesis in

Intergative Biosciences

by

Nicholas N. Lyssenko

Submitted in Partial Fulfillment
of the Requirements
for the Degree of

Doctor of Philosophy

August 2007

The thesis of Nicholas N. Lyssenko was reviewed and approved * by the following:

Robert A. Schlegel
Professor of Biochemistry and Molecular Biology
Head of the Department of Biochemistry and Molecular Biology
Thesis Adviser
Chair of the Committee

Simon Gilroy
Professor of Biology

Andrea M. Mastro
Professor of Microbiology and Cell Biology

Wendy Hanna-Rose
Assistant Professor of Biochemistry and Molecular Biology

Graham H. Thomas
Associate Professor of Biology
and of Biochemistry and Molecular Biology

* Signatures are on file in the Graduate School.

ABSTRACT

In eukaryotic organisms, the cytofacial and exofacial monolayers of the plasma membrane and certain other cell membranes exhibit substantial differences with respect to lipid composition. The plasma membrane usually contains all of its phosphatidylserine (PS) and a larger portion of phosphatidylethanolamine in the inner leaflet. Viable cells normally conceal plasma membrane PS, while cells undergoing apoptosis or necrosis expose it on the cell surface. P-type ATPases in subfamily IV are the leading candidate transbilayer amphipath transporters (TATs), the proteins postulated to actively translocate PS to the cytofacial half of the compositionally polarized membranes. TATs of the single cell fungus *Saccharomyces sereviciae* are presently the best studied. Several mammalian members of the group are also under investigation. However, the currently available data fail to provide a comprehensive view of tissue-specific expression and developmental function of the subfamily members in a multicellular organism. Here are reported findings of the study aimed to systematically investigate subfamily IV P-type ATPases of the nematode *Caenorhabditis elegans*.

The *C. elegans* genome contains six open reading frames that encode P-type ATPases in subfamily IV. All six are transcribed. Expression of a nucleus targeted green fluorescent protein reporter under the control of *tat-2*, *tat-3*, *tat-4* or *tat-5* promoter sequence showed that the former three genes are active in tissue-specific patterns, while the latter gene is transcribed ubiquitously. Phenotypic analysis of nematodes with temporarily, via RNA interference, or permanently, by deletion mutagenesis, altered expression of *tat-1* through *5* shows that *tat-5* is an essential gene. *tat-5(RNAi)* animals exhibit morphological defects of the gonad, fertilization deficiencies and embryonic lethality. *tat-1* through *4* are nonessential. The *tat-3; tat-4* gene pair is nonessential as well. *tat-1* seems to be required for exposure of PS on the surface of apoptotic cells in the nematode gonad. *tat-2* and *tat-4* appear to mediate cholesterol metabolism in the digestive system. No notable phenotype was observed with *tat-3*. These findings from *C. elegans* suggest that *tat-1* through *4* are tissue specific genes that regulate membrane structure, and *tat-5* is the sole housekeeping TAT.

TABLE OF CONTENTS

List of figures…… vii
List of tables…… ix
List of abbreviations…… x
Acknowledgements..…….. xii

Chapter 1. A brief overview of the research project and the organization of this thesis 1

Chapter 2. An introduction to cell membranes, membrane phospholipid asymmetry and transbilayer lipid transport……..... 4

- Cell membrane as a two dimensional liquid…….. 4
- Asymmetric lipid distribution between the two monolayers of certain cell membranes……... 17
- Phospholipid transbilayer flip-flop…….. 20
- P-type ATPases in subfamily IV as putative transbilayer amphipath transporters.....……..... 29
- *Caenorhabditis elegans* as a model system for investigations of lipid bilayers……... 32
- References…… 34

Chapter 3. A brief review of the origins and major developments of the plasma membrane hypothesis…… 48

- Plasma membrane as the problem of permeability and osmosis…….. 48
- Plasma membrane as the problems of cell electrical resistance and cell surface area……... 57
- Early direct observations of cell membranes…… 70
- References…… 75

Chapter 4. Structure and transcription of *tat-1* through *5* genetic loci in *C. elegans*…….. 83

- Introduction…… 83
- Materials and methods…… 86
  - mRNA isolation and cDNA synthesis…… 86
  - Rapid amplification of cDNA ends (RACE)…….. 87
  - EST sequencing…… 89
- Results…… 89
  - *tat-1*…… 89
  - *tat-2* and *tat-3*…… 93
  - *tat-4* and *T24H7.6*…… 97
  - *tat-5* and *tat-6*…… 104
- Discussion …… 104

References…… 109

Chapter 5. Expression patterns of the GFP reporter under the control of *tat-2*, *3*, *4* or *5* promoter sequences…… 111

Introduction…… 111
Materials and methods…….... 115
YAC DNA isolation…… 115
Cosmid DNA isolation…….. 116
Expression cassette construction…….. 116
tat-1…… 116
tat-2…… 118
tat-3…… 120
tat-4…… 120
tat-5…… 124
Particle bombardment delivery of the expression cassettes into the nematode gonad…… 124
Image acquisition and processing…….. 128
Results…… 128
Biolistic transformation with *tat* expression cassettes that include a large portion of the 5' translated sequence failed to produce stable GFP-fluorescent transgenic lines…… 128
tat-2 is expressed in the alimentary, reproductive and excretory tissues…… 133
tat-3 is expressed in the alimentary, epithelial and reproductive systems…….. 139
tat-4 is expressed in the alimentary and reproductive systems…… 144
tat-5 is expressed broadly in many tissues…….. 148
Discussion…….. 150
Expression patterns of *tat-2* and *tat-4* are similar and distinct from the expression pattern of *tat-3*…… 150
Coordinated expression of *tat-2* and *tat-3* in the developing vulva and the uterine-vulval connection…….. 152
Expression and localization homology between TAT-2 and its mammalian counterparts…… 154
tat-5 is the most broadly expressed of the 4 investigated *tats*…….. 155
References…… 156

Chapter 6. Phenotypic analysis of *Caenorhabditis elegans* animals with altered expression of *tat-1*, *2*, *3*, *4* or *5*…… 159

Introduction…… 159
Materials and methods…… 163
C. elegans mutants and transgenes and animal maintenance…….. 163
tat RNAi vectors…… 165
dsRNA feeding of nematodes to induces RNAi…… 165

The assay for PS expose on the surface of apoptotic germ cells…. 166
Sterol deprivation assay……... 167
Results…… 168
tat-5 is an essential gene…… 168
tat-1, *tat-2*, *tat-3* and *tat-4* are nonessential and not required for apoptotic cell clearance…… 170
Apoptotic germline cell corpse staining with GFP-Annexin V is compromised in *tat-1(RNAi)* animals…… 170
tat-2 and *tat-4* mediation of sterol metabolism…… 174
tat-3; tat-4 double mutant is viable…… 180
Discussion…….. 183
tat-5 might be a housekeeping gene…….. 183
Involvement of the putative APLTs in sterol metabolism…… 183
Lipid asymmetry and TATs…..…… 189
Future research directions……... 191
References…… 192

LIST OF FIGURES

Chapter 2.

Figure 1. Chemical structure of a representative phospholipid, phosphatidylcholine..... 6
Figure 2. X-ray diffraction crystal structures of dilauroyl phosphatidylethanolamine and dimyristoyl phosphatidylcholine..... 8
Figure 3. Lipid phase behavior..... 10
Figure 4**.** Lipid translocation in the mammalian plasma membrane..... 28

Chapter 3.

Figure 1. Electrical properties of cell suspensions and tissues..... 60
Figure 2. The Langmuir trough and Langmuir monomolecular films..... 62
Figure 3. Most influential models of the cell membrane..... 64
Figure 4. A schematic of the surface of the oil droplet from the mackerel egg.... 67
Figure 5. An electron density profile, and its interpretation, of rabbit sciatic myelin..... 71
Figure 6. The unit membrane..... 72

Chapter 4.

Figure 1. Amplification of *tat-1*, *2* and *3* cDNA transcripts with a gene-specific and SL1-specific primers..... 90
Figure 2. Structure and transcription of the *tat-1* locus..... 91
Figure 3. Structure and expression of the *tat-2* locus..... 94
Figure 4. Structure and expression of the *tat-3* locus..... 96
Figure 5. Structure and expression of the *tat-4* locus..... 99
Figure 6. Structure and expression of the *tat-4* locus (part 2)..... 102
Figure 7. Structure and transcription of the *tat-4* locus..... 103
Figure 8. Transcription of *tat-5* and *tat-6*..... 105

Chapter 5.

Figure 1. Human and *C. elegans* P-type ATPases in subfamily IV..... 112
Figure 2. Construction of the *tat-1* expression cassette..... 117
Figure 3. Structure of the *tat-2* and *tat-3* expression cassettes and a list of transgenic lines carrying these cassettes as transgenes..... 119
Figure 4. Fusion sites of the *tat-4* 5' region with the sequence encoding NLS-GFP reporter in the *tat-4* expression cassettes..... 122
Figure 5. Structures of the *tat-4* expression cassettes and a list of transgenic lines carrying these cassettes as transgenes..... 123
Figure 6. Structure of the *tat-5b* and *tat-5a* expression cassettes and a list of transgenic lines carrying these cassettes as transgenes..... 125
Figure 7. GFP fluorescence in transgenic nematodes derived by bombardment

with pNL56.1…… 130
Figure 8. Expression of the *tat-2* reporter…….. 134
Figure 9 (starts on page 134). Expression of the *tat-2* reporter at the uterine-vulval connection in the early L4, middle L4 and late L4 animals……. 137
Figure 10. Expression of the *tat-2* reporter during spermatogenesis and in the spermatheca…….. 140
Figure 11 (starts on page 140)**.** Expression of the *tat-3* reporter…….. 143
Figure 12 (starts on page 144). Expression of the *tat-4* reporter…….. 147
Figure 13 (starts on page 148). Expression of the *tat-5b* reporter…….. 150
Figure 14. Expression of *tat-2* and *tat-3* in the developing vulva and the uterine-vulval connection…….. 153

Chapter 6.

Figure 1. Location of the deleted segments in the *tat-2*, *tat-3* and *tat-4* mutants relative the gene intron-exon structure…….. 164
Figure 2. *tat-5(RNAi)* phenotype…….. 169
Figure 3. The absence of persistent cell corpses in deletion mutants of *tat-2*, *tat-3* and *tat-4*……... 171
Figure 4. Compromised GFP-Annexin V staining of germline cell corpses in *tat-1(RNAi)* nematodes…….. 173
Figure 5 (starts on page 176). Hypersensitivity of *tat-2(tm1643)* and *tat-4* mutants to sterol deprivation…….. 179
Figure 6 (starts on page 181). Slight increase in sensitivity to sterol deprivation in *tat-3; tat-4* double mutants…….. 182
Figure 7. A speculative model TAT-2 and TAT-4 involvement in sterol metabolism in *C. elegans*……... 186

LIST OF TABLES

Chapter 2.

Table I. Spontaneous flip-flop half-lives and activation energies for synthetic label-carrying lipids in lipid-only bilayers……. 22
Table II. Lipid specificity and half-life for lipid flipping and translocating activities……. 24

Chapter 4.

Table I. WormBase IDs and given names of the 6 ORFs encoding P-type ATPases in subfamily IV……. 84

Chapter 5.

Table I. Expression of *tat-2*, *tat-3* and *tat-4* in *C. elegans* tissues…….. 152

LIST OF ABBREVIATIONS

ABC	ATP-binding cassette transporter
AC	anchor cell
APLT	aminophospholipid translocase
C5-DMB-	5-(5,7-dimethyl BODIPY)-1-pentanoic acid
C6-NBD-	6-[N-(7-nitrobenz-2-oxa-1,3-diazol-4-yl)-amino] hexanoylceramide
Chl	cholesterol
DIG	glycolipid-enriched complexes
DLPC	dilauroyl (12:0) phosphatidylcholine
DMPC	dimyristoyl phosphatidylcholine
DOPC	dioleoyl (18:0) phosphatidylcholine
DPPC	dipalmitoyl (16:0) phosphatidylcholine
DPPE	dipalmitoyl (16:0) phosphatidylethanolamine
DSPC	distearoyl phosphatidylcholine
EST	expressed sequence tag
DTC	distal tip cell
GFP	green fluorescent protein
GPI	glycosylphosphatidylinisotol
GSP	gene-specific primer
GUV	giant unilamellar vesicles
HDL	high-density lipoprotein
IPTG	isopropyl *β*-D-1-thiogalactopyranoside
MLV	multilamellar vesicles
M-MLV RT	Moloney Murine Leukemia Virus Reverse Transcriptase
NBD	7-nitrobenz-2-oxa-1,3-diazol-4-yl
NBD-DMPE	n-(7-nitrobenz-2-oxa-1,3-diazol-4-yl)-amino-1,2-dimyristoylphosphatidylethanolamine
NGM	nematode growth medium
NLS-GFP	nuclear localization signal - green fluorescent protein
ORF	open reading frame
PA	phosphatidic acid
PC	phosphatidylcholine
PE	phosphatidylethanolamine
PG	phosphatidylglycerol
PI	phosphatidylinositol
POPC	1-palmitoyl-2-oleyl phosphocholine
PS	phosphatidylserine
RACE	rapid amplification cDNA ends
RBC	red blood cell
RNAi	RNA interference
SGI	subgel I (another term for the lamellar crystalline, L_C, phase)
smNGM	sterol modified NGM
SpM	sphingomyelin
SV40 Tag	simian virus 40 large tumor antigen

TAT	transbilayer amphipath transporters
TEMPO-DPPC	dipalmitoyl phosphoethanolamine-n,n-dimethyl-n-(2',2',6',6'-tetramethyl-4'-piperidyl)
TGN	*trans*-Golgi network
ULV	unilamellar vesicles
uORF	upstream open reading frame
UTR	untranslated region
VPC	vulval precursors cells

ACKNOWLEDGEMENTS

I would like to thank Dr. Schlegel for creating a stimulating intellectual atmosphere in which I could grow and develop as an investigator and for subtle yet effective encouragement and support. Thanks also go to undergraduate students who helped me with my experiments, especially Yana Miteva, Katherine Minson, Julia Briggs and Chris McClellan, and to Dr. Peggy Halleck and other members of the Schlegel lab. I also would like to thank investigators who over the years supported my research projects with lucid discussions and useful advice: Simon Gilroy, Wendy Hanna-Rose, Graham Thomas, Jerry Workman, Esther Siegfried, the late Robert Simpson, Mark Tucker (at the Beltsville Agricultural Research Center, BARC) and Gregory McCarty (also at BARC).

Finally, I would like to express appreciation of my family's – Nicholas III, Richard and Catherine – support and understanding during my graduate studies and of all the fun we had in State College.

Chapter 1. A brief overview of the research project and the organization of this thesis

The research project whose findings are presented in this thesis aims to elucidate biochemical, physiological and developmental functions of subfamily IV P-type ATPases suspected of actively translocating phospholipids between the two monolayers of cell membranes and descriptively named transbilayer amphipath transporters (TATs) (this identifier is applied in this thesis to all members of the subfamily IV from all organisms). In order to properly evaluate the currently available evidence supporting the involvement of these proteins in lipid translocation, Chapters 2 and 3 consider in depth various biophysical aspects of cell lipid membrane lateral and transverse composition and structure, all postulated lipid flipping (facilitated diffusion) and translocating (active transport) activities and putative lipid transbilayer trasporting proteins, and some methodological issues related to measurements of lipid transbilayer movement. The empirical data and structural features of the transporters arguing for and against phospholipids as the primary translocated substrate of TATs are then outlined. The conclusion of this theoretical portion of the thesis is that, although TATs clearly contribute to the maintenance of proper membrane structure and function, further support is needed to ascertain that this contribution is indeed via lipid transbilayer translocation.

The experimental part of the project employs the nematode *Caenorhabditis elegans* as a model system to conduct a reverse genetics investigation of physiological and developmental roles of the *C. elegans* TATs. Chapter 2 contains a section that considers suitability of the nematode for lipid bilayer investigations. Reverse genetics – from the gene mutant to the phenotype - is a more uncertain approach to finding gene

functions, in comparison with the forward genetics – from the phenotypic screen to the gene. While gene deletion mutants for reverse genetics studies could be isolated by one of the dedicated *C. elegans* knockout groups in a relatively short period of time, these mutants may not exhibit easily notable abnormal phenotypes; the task of identifying deficiencies in the mutant could become arduous, as an investigator progresses from one faulty hypothesis to another. However, the more supplementary data, such as the expression pattern of the gene, are available, the stronger a hypothesis could be made regarding the gene function. Chapters 4 and 5 contain experimental data that describe transcription and tissue-specific expression of *C. elegans* TATs. A section at the beginning of Chapter 6 identifies major functional themes that emerge from findings regarding homologs of the nematode TATs in other organisms. Based on the theoretical considerations presented in Chapters 2 and 3, the newly collected *C. elegans* gene expression data and the overview of TAT research, two hypotheses are advanced: first, suppression of the TAT activity would lead to PS exposure on the surface of healthy cells and promotion of apoptotic cell clearance; and second, any subtle contribution from TATs to the maintenance of the membrane organization could be uncovered by eliminating another structural element, such as sterol.

A test of the first hypothesis found that suppression of the *C. elegans* TAT-1, against expectations, retards PS externalization in apoptotic germline cells. This observation further adds to the uncertainty with respect to the biochemical functions of TATs and throws in doubt the proposed direction of lipid translocation presumably conducted by these proteins. A test of the second hypothesis determined that, as predicted, *C. elegans* TAT-2 and TAT-4 become essential under the conditions of

severe sterol deprivation. Chapter 6 presents the data from the two tests and concludes with a discussion of TAT involvement in lipid translocation and lipid metabolism.

Chapter 2. An introduction to cell membranes, membrane phospholipid asymmetry and transbilayer lipid transport

Cell membrane as a two dimensional liquid

In a most general outline, cell membranes are thin (~ 70Å), mosaic (lipid-protein), oily sheets that partition the aqueous medium (Singer and Nicolson, 1972). The major constitutive components of cell membranes – the lipid and protein molecules – are characteristically amphipathic: composed of a hydrophobic and a hydrophilic moiety (Lee, 2003; Huang, 2001a). This dual nature compels membrane lipids and proteins to assemble and persist in excess water as bilayers (lamellae). Due to the hydrophobic effect (also called “the hydrophobic bond”), the hydrophobic moieties are forced into the interior of the lamella, where molecular interactions occur strictly through van der Waals and steric repulsive forces, so that the hydrophilic residues at the oil-water interface could interacts with each other and the surrounding water and other non-membrane molecules via dipolar and electrostatic forces (Meyer et al., 2006; Chandler, 2005; Langner and Kubica, 1999; Tanford, 1991; Cevc and Marsh, 1987; Israelachvili et al., 1980). The relatively inert lipids of the cell membrane provide the matrix – the lipid bilayer – in which proteins reside and perform various functions; in the absence of protein, membrane lipids could still exist as a bilayer, but it would be “lifeless” and devoid of most functions observed in the complete membrane; membrane proteins, conversely, lack the ability to form lamellae independently (Singer and Nicolson, 1972). Cell membranes envelop the whole cell (the plasma membrane), as well as most subcellular structures recognized as cell organelles (mitochondria, endoplasmic reticulum and others) (Nurse, 2000; Voet and Voet, 1995). While the importance of membranes in cell physiology and development is immense, many critical aspects of

membrane assembly and function still remain very poorly understood (Gummadi and Kumar, 2005; Vigh et al., 2005).

Based on chemical structure, most naturally occurring membrane lipids (a large fraction of the total lipids, or the cell lipidome) fall into one of three groups: glycerophospholipids (or simply phospholipids), sphingolipids and sterols (van Meer, 2005; Huang, 2001a). Phospholipids contain the characteristic and invariant L-glycerol 3-phosphate backbone: a glycerol ester-coupled with a phosphate group at the *sn-3* carbon (Figure 1). In the predominant – diacyl – phospholipids, both *sn-1* and *sn-2* carbons of the glycerol connect to nonpolar aliphatic chains via ester bonds. In rare species, the *sn-1* connection is via an ether bond (plasmalogens for example; Brites et al., 2004). Animal diacyl phospholipids usually carry a saturated even number – commonly 16 or 18 – carbon-long acyl chain at the *sn-1* position and an unsaturated even number between 16 and 22 carbon-long acyl chain at the *sn-2* position (Huang, 2001b). The unsaturated chain may contain between 1 and 6 *cis*-double bonds. The phosphate group in diacyl phospholipids forms an ester with a polar alcohol: commonly a choline, ethanolamine, inositol, glycerol or serine. Sphingolipids consist of a sphingoid long chain (usually C_{18}-sphingosine) linked with a long chain fatty acid via an amide bond at carbon 2 and with a polar head group, such as a phosphorylcholine in sphingomyelin or a galactose in galactosphingolipids, at the terminal hydroxyl carbon via an ester, *β*-glycosidic or some other type of bond (Futerman and Hannun, 2004). The sphingoid chain usually contains a *trans*-double bond at carbon 4 and a hydroxyl group at carbon 3; the esterified fatty acid may be 16 to 26 carbons in length and in the larger fraction, saturated or in the smaller faction, monounsaturated and *α*-hydroxylated.

The prevalent and structurally important sterol in mammalian cells is cholesterol: a quasi-planar molecule of a fused tetracyclic ring system linked with a branched isooctyl side chain (Mouritsen and Zuckermann, 2004). Phospholipid, sphingolipid and cholesterol biosyntheses from simple precursors are multi-step processes that involve many enzymatic reactions (Benveniste, 2004; Futerman and Hannun, 2004; Vance and Vance, 2004). Distantly related organisms, specific tissues in the same organism and

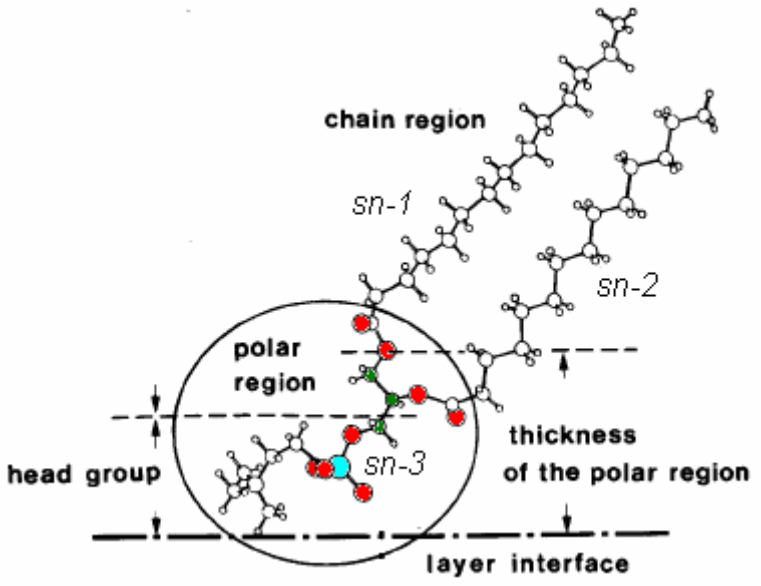

Figure 1. Chemical structure of a representative phospholipid, phosphatidylcholine. Oxygen atoms of the carboxyl groups and the phosphate residue are in red; carbon atoms of the glycerol are in green, the phosphorus atom is in blue (modified from Hauser et al., 1981).

even distinct membranes in the same cell frequently exhibit large differences with respect to membrane lipid composition (Ladha, 1998; van Helvoort and van Meer, 1995). While mammalian cells could contain hundreds of membrane lipid species, the lipid membrane content of rapidly growing *Escherichia coli* is 75% phosphatidylethanolamine (PE), 20% phosphatidylglycerol (PG) and 5% cardiolipin (Cronan, 2003; Dowhan, 1997). Thus, even a very limited assortment of lipids could ensure basic membrane properties; the great lipid diversity observed in higher

organisms probably serves to fine-tune individual membranes to specific environment and function.

Investigators of membrane biology frequently take a reductionist approach and cut through the great diversity and heterogeneity of lipids and membranes by focusing predominantly on certain model lipids, model lipid mixtures, artificial lipid bilayers and natural membranes (see for example Veatch and Keller, 2005). Unlike the natural counterparts, common synthetic model diacyl phospholipids, such as dilauroyl (12:0) and dioleoyl (18:0) phosphatidylcholine (DLPC and DOPC) and dipalmitoyl (16:0) phosphatidylethanolamine (DPPE), carry identical fully saturated fatty acid residues. Purified egg sphingomyelin is a common model sphingolipid. Depending on the method of preparation, model lipids and lipid mixtures arrange into a particular artificial model bilayer: dry or hydrated lamellar sheets, uni- or multilamellar vesicles (ULV, MLV), or solid supported lipid bilayers (Castellana and Cremer, 2006; Šegota and Težak, 2006; Nagle and Tristram-Nagle, 2000). Giant unilamellar vesicles (GUV) are a popular model lamella for the study of lipid rafts (Bagatolli, 2006). Each of these artificial bilayers holds certain investigative advantages and limitations. MLVs, for example, generate a strong signal in X-ray diffraction and other physicochemical analyses, but may also exhibit "unnatural" properties due to interactions between closely apposing lamellae. Historically, erythrocyte plasma membrane and myelin have been the most studied natural membranes (see Chapter 2). Often the assumption seems to be that findings in model artificial bilayers are directly applicable to biological membranes. However, besides the reductionist limitations of artificial systems, this also may not always be the case for another critical reason: synthetic bilayers are essentially lowest energy

equilibrium seeking systems, whereas the cell can expend energy and maintain membrane properties in a non-equilibrium state.

X-ray diffraction analyses show that single-species anhydrous crystals of model diacyl phospholipids and sphingolipids consist of bilayers stacked on top of each other (Marsh and Páli, 2006; Pascher et al., 1992; Hauser et al., 1981). Within the crystal bilayer, individual diacyl phospholipid molecules adopt a conformation in which the *sn-1* acyl chain, the glycerol and the phosphate residue stretch out in an almost straight line and the *sn-2* chain and the polar alcohol branch out from it at near right angles; all carbon-carbon bonds in the acyl chains are in the *trans*-conformation (Figure 2). As a consequence of this arrangement the *sn-1* chain is longer than the *sn-2* even when both consist of the same number of methylene groups and, especially in the case of small head group lipids such as PE, the alcohol residue lies almost parallel to the bilayer surface. Several lines of evidence from model bilayers and natural prokaryotic

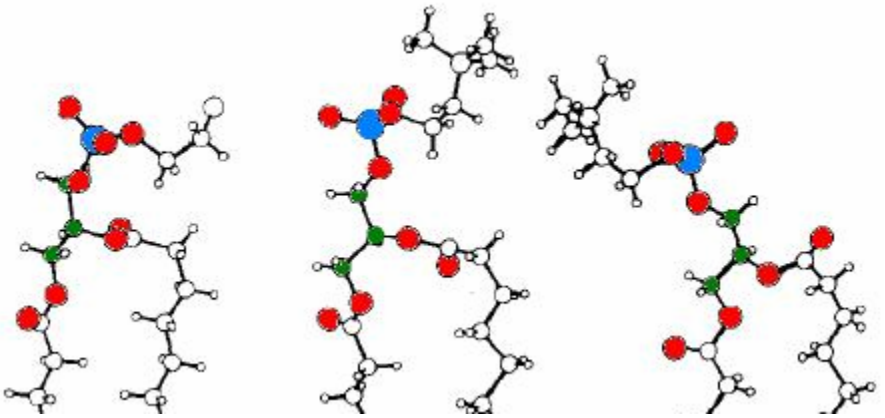

Figure 2. X-ray diffraction crystal structures of dilauroyl phosphatidylethanolamine (left) and dimyristoyl phosphatidylcholine (middle and right). Dimyristoyl PC is present in two conformations in crystals. Oxygen atoms of the carboxyl group and the phosphate residue are in red; carbon atoms of the glycerol are in green; and the phosphorus is in blue; acyl chains are shortened. (Modified from Hauser et al., 1981).

membranes indicate that under physiologically relevant conditions a major portion, but not all, of diacyl phospholipid rotamers exist in a conformation similar to that in the crystal structure (Hong et al., 1996; Seelig and Seelig, 1980). The phosphate and glycerol residues and the carboxyl and carbon-2 methylene groups of the acyl chains comprise even in fluid bilayers a somewhat rigidly ordered core of the molecule and assume the “h” shape; the phosphate can rotate and tilt around the long molecular axis, but the polar alcohol still remains “bent down” toward the bilayer surface because of the angle of the phosphodiester bond; the acyl chains beyond the first few ethelene groups are unrestrained and free to undergo bond isomerization.

Unlike, for example, many inorganic salts, which simply dissolve in water, hydrated phospholipids and sphingolipids instead swell and exhibit lyotropic and thermotropic mesomorphisms (Figure 3) (Milhaud, 2004; Wennerström and Sparr, 2003; Koynova and Caffrey, 1995; Chapman, 1993; Cevc and Marsch, 1987). A mesophase (or simply a phase) is a distinct lipid-water arrangement on both individual molecular and aggregate multimolecular levels. Phase transitions, or changes in the lipid-water arrangement, occur when molecules begin, or cease, displaying a new kind of motion (degree of freedom). Although phase behavior of a lipid as a function of temperature and water content depends to some extent on its chemical structure, most model diacyl phospholipids and sphingolipids generally exhibit a similar sequence of phase transitions (Figure 3A). After incubation at temperatures near 0ºC for long periods of time, single-species dispersions of model diacyl PC and PE relax to the stable and highly ordered lamellar crystalline (L_C) phase (also called subgel I, SGI) (Chang et al., 2006; Koynova et al., 1995). With reheating, a “crystallized” dispersion first undergoes a

transition, the *subtransition*, to the lamellar gel phase (L_β or $L_{\beta'}$, the prime indicates that the acyl chains tilt with respect to the bilayer surface). The critical difference between the crystal and the gel phases is the amount of water that resides between the apposing bilayers along the head-to-head contact plane: water enters the staked lipid bilayers during the crystal to gel transition and exits the lipid during the reverse progression (Figure 3B) (Chang et al., 2006; Cevic and Marsh, 1987). With respect to motion, the *subtransition* probably corresponds to the onset of slow oscillatory rotations by the acyl

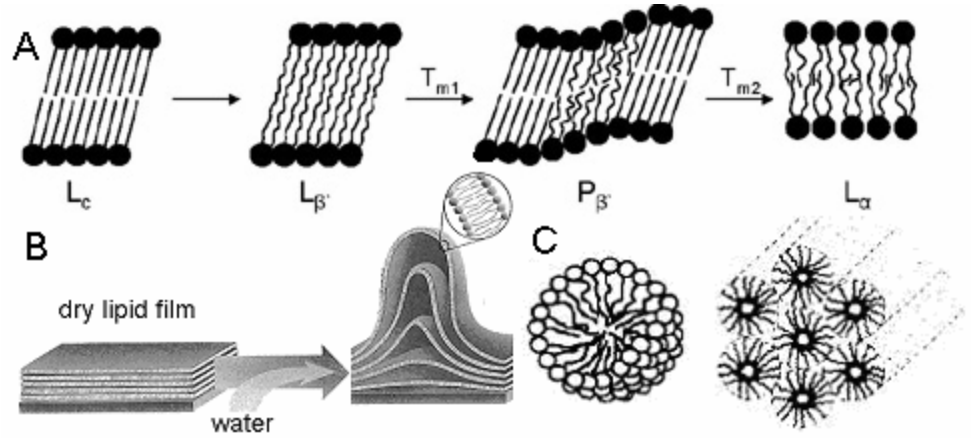

Figure 3. Lipid phase behavior. (A) Lamellar phases of diacyl phosphatidylcholine lipids. (B) Hydration and swelling of the dry lipid cake (modified from an Avanti Polar Lipids, Inc. drawing). (C) Nonbilayer phases: the spherical micelle phase (left) and the inverted hexagonal nonbilayer phase (right) (modified from Tate et al., 1991).

chains about the long molecular axis (Cevc and Marsh, 1987). Still higher temperatures induce dispersions of model diacyl PC lipids to undergo the *pretransition* to the ripple phase ($L_{\beta'} \rightarrow P_{\beta'}$), followed rapidly by the *main* transition to the liquid crystalline (fluid) phase ($P_{\beta'} \rightarrow L\alpha$). PE and phosphatidylserine (PS) lipids and sphingomyelin pass directly from gel to fluid (Browning and Seelig, 1980; Shipley et al., 1974). The *pre*- and *main* phase transitions arise mostly from the *trans* (*t*) to *gauche* (*g*) isomerization of the carbon-carbon bonds in the acyl chains of the diacyl phospholipids and the acyl and the sphingoid chains in sphingolipids (Huang, 2001a; Heimburg, 2000). In the gel state

nearly all C-C bonds of the fatty acid residues assume the lower energy *trans* conformation; with the transition to the fluid state a large portion of the bonds rotates to the *gauche* arrangement. However, a single *gauche* bond would introduce a sterically unfavorable 120° bend in the acyl chain; instead, two *gauche* and one *trans* bonds combine into a $g^{-}tg+$ or a $g+tg^{-}$ triplet, which forms a crankshaft-like kink. Each *gtg* triplet shortens the acyl chain along the long axis by 1.27Å. As a consequence of the *trans* to *gauche* isomerization and the concomitant diminution of the lateral cohesive interchain van der Waals interactions, fluid lipid bilayers are thinner, more spread out (larger area $Å^2$ and volume $Å^3$ per lipid molecule) and more diffusive (faster translational motion), compared with gel bilayers of the same lipid species (Huang, 2001a). Pure saturated diacyl phospholipids undergo the *main* transition at fairly high temperatures (T_m>37ºC); however, a single *cis*-double bond in either acyl chain dramatically lowers the T_m (Huang, 2001a). The *main* transition temperature of acyl chain saturated sphingolipids is around 37ºC. Thus, natural unsaturated phospholipids, but not necessarily all natural sphingolipids, are likely to exist at the physiologically relevant temperatures in the fluid molecular conformation.

While lamellar lipids – diacyl PC and sphingomyelin – form almost exclusively bilayer phases; lyso PC and unsaturated diacyl PE prefer under physiological conditions nonbilayer organization (Figure 3C) (Tate et al., 1991; Israelachvili et al., 1980; Gruner et al., 1985). The propensity of a particular phospholipid to form a nonbilayer phase is directly related to its critical packing shape. Single-chain large head group – conical – lipids tend to form spherical micelles; while double-chain small head group – inverted truncated conical – phospholipids can arrange into the inverted hexagon structure.

Lamellar phospholipids are consequently cylindrical in shape. Conical phospholipids, and especially PE, are major components of natural membranes (van den Brink-van der Laan et al., 2004; Sprong et al., 2001). An *in vivo* study found elevated levels of these molecules in highly curved membrane regions at the site of membrane fusion (Ostrowski et al., 2004). Investigations of model bilayers and purely theoretical considerations suggest a wide array of plausible functions for nonbilayer phospholipids: from regulation of bilayer lateral pressure to facilitation of membrane curvature and fusion (Chernomordik and Kozlov, 2005; van den Brink-van der Laan et al., 2004).

Phase behavior of model mixed lipid dispersions, commonly composed of two or three model lipids, reflects largely the differences among the T_m values of the lipid species present in the mixture, as well as certain imperfections of species miscibility (Almeida et al., 2005; Huang, 2001a; Lee, 1977). In a slowly-cooling fluid binary phospholipid dispersion, the lipid with the higher T_m begins gelling first, while the lower T_m component remains mostly in the liquid crystalline phase. This leads to coexistence of segregated gel and fluid phases (also described in this context as domains, Veatch and Keller, 2005) in some specific temperature range. When two phospholipid species intermix ideally, then experimentally observed phase behavior of the resultant binary mixture could be predicted from the T_m and transition enthalpy (ΔH) values for the pure dispersions of these species. However, with the exception of lipid systems composed of two structurally very similar – differing only by as little as two methylene groups – phospholipids, thermodynamic phase equations require a correction term for nonideality of mixing in order to describe phase behavior of binary mixtures satisfactorily. Nonideal mixing arises because the strength of interaction between two neighboring lipid

molecules of the same chemical structure and conformation rarely equals the strength of interaction between two dissimilar neighbors. For a binary mixture of A and B lipids, a thermodynamic energy term ρ (after Huang, 2001a and Lee, 1977), the nonideality of mixing parameter, compares the nearest neighbor interaction energy in AB pairs with the average of the interaction energies in AA and BB pairs:

$$\rho = Z[g_{AB} - \tfrac{1}{2}(g_{AA} + g_{BB})];$$

where Z is the number of nearest neighbors in the plane of the bilayer and g_{AB}, g_{AA} and g_{BB} are the molar interaction energies of AB, AA and BB nearest neighbor pairs, respectively. Hence the conformation of the phospholipid molecule changes during a phase transition, $\rho^{Gel} \neq \rho^{Fluid}$. The values of ρ^{Gel} and ρ^{Fluid} are estimated by introducing arbitrary numbers into the phase equation until a thermodynamically predicted phase behavior matches experimental data. In addition to the gel-fluid phase transition, miscibility constrains also affect the equilibrium intra-phase organization of lipids. Two phospholipids in the same phase with a positive ρ tend to separate into predominantly one-species domains (also called phases) and with a negative ρ, to form ordered patterns (also called compounds and even complexes). Although values of both ρ^{Gel} and ρ^{Fluid} parameters are positive for binary dispersions of model phospholipids, the latter term is usually insignificant (Almeida et al., 2005). Consequently, model phospholipid mixtures normally remain homogenous in the physiologically relevant liquid crystalline phase.

In dispersed binary mixtures of a model phospholipid or a sphingolipid and cholesterol the liquid state can exist in at least two phases: liquid disordered (L_d) and liquid ordered (L_O) (London, 2005; Simons and Vaz, 2004; Ipsen et al., 1987; see

McMullen et al., 2004 for a critical view). The former phase corresponds to the Lα, while the latter represents a new kind of organization that appears due to the peculiar association of cholesterol with phospho- and sphingolipids ($\rho < 0$). The nature of this association is still hotly debated (Simons and Vaz, 2004; McConnell and Radhakrishnan, 2003). One model, developed based on the studies of monomolecular Langmiur films (see Chapter 2), conceptualizes it as formation of reversible oligomeric chemical complexes that could consist for saturated PC lipids of 12 to the maximum of 60 lipid molecules, 4 to 12 of which would be cholesterol. An alternative proposal views the association as lattice assembly. Still another depicts phospholipid head groups as "umbrellas", which protect cholesterol hidden underneath from unfavorable interactions with water. Whatever the mechanism, association with cholesterol effects a significant change in the conformation of the lipid molecule: in the liquid ordered phase phospholipids and presumably, sphingolipids no longer exhibit acyl chain isomerization, but still laterally diffuse at only slightly reduced rates, in comparison with the L_d phase. The affinity of cholesterol for lipids decreases in the order sphingomyelin >> PS > PC > PE and is always higher for a more saturated lipid over a less saturated species (Barenholz, 2004; Silvius, 2003). In a binary dispersion of a model phospholipid and cholesterol the L_O phase can coexist with the L_d phase at cholesterol concentrations below 20-25 mole % and temperatures below ~ 40ºC; the whole dispersion adopts the L_O arrangement at cholesterol levels from 25 to 66 mole %, the limit of cholesterol solubility in the phospholipid bilayer (McMullen et al., 2004). Given the lipid composition of the erythrocyte membrane – low sphingolipid and high cholesterol content (sphingomyelin / PC / PE / PS / cholesterol, 16.0/22.2/19.6/8.9/33.3 mole %) – several

reviewers (Almeida et al., 2005; McMullen et al., 2004) suggested that this and similarly composed natural bilayers might exist completely in the liquid ordered phase. However, investigations of tertiary cholesterol-lipid dispersions, which may be more representative of the natural lipid bilayers, seem to detect presence of segregating L_O and L_d phase domains even at high (> 25 mole %) cholesterol levels (Feigenson, 2007; Veatch and Keller, 2005; de Almeida et al., 2003). Alternatively, some recent studies using novel methods altogether challenge the notions of the clear distinction between the L_O and L_d phases and the sharp transition from the coexistence of L_O and L_d domains to the entirely L_O dispersion in favor of gradual continuous change in the mixed fluid bilayer with the increasing cholesterol concentration (Heerklotz and Tsamaloukas, 2006). Clearly, more research must take place before a consensus regarding the cholesterol effect on model lipid bilayers emerges.

Given the heterogeneous lipid composition of the cell membrane, on the one hand, and the observations of lipid immiscibility and phase separation in model hydrated lipid mixtures, on the other, it is reasonable to propose that natural membranes could contain lateral lipid inhomogeneities, or domains, of a distinct composition from the bulk lipid; these domains would arise as a result of purely lowest energy equilibrium seeking behavior of the lipids without any input of energy from the cell (protein interference). This lipid domain hypothesis has a remarkably long and controversial history parceled into alternating periods of heightened interest and indifference. Its first formulation appeared in the 1920s and stated that the erythrocyte membrane could consist of separate phospholipid-only and sphingolipid-cholesterol regions (see Chapter 2). The Singer and Nicolson fluid mosaic model emphasized fluidity and denied existence of

lipid order in the cell membrane (Singer and Nicolson, 1972). It was, however, immediately challenged for ignoring lipid heterogeneity in general and gel phase domains, which – many investigators thought at the time – existed in some natural membranes, in particular (Oldfield and Singer, 1973). In the 1980s, Thompson proposed that sphingolipids could cluster into microdomains when present as a minor (less than 10 mole %) fraction in fluid dispersions of PC lipids (Brown, 1998). Extensive studies of this proposal eventually led to the conclusion that not all sphingolipids clustered and those that did formed rather small, as few as 20 molecules, domains. In the 1990s, Simons and Ikonen (1997; Rietveld and Simons, 1998) advanced the raft hypothesis. Rafts were nanoscale size long-lived closely packed sphingolipid-cholesterol clusters, which resided in the fluid matrix composed of unsaturated phospholipids. During Triton X-100 solubilization of cell membranes at 4ºC, rafts persisted as low-density detergent-insoluble glycolipid-enriched complexes (DIGs). Raft-associated (for example, GPI-anchored) proteins remained in DIGs after the Triton X-100 treatment. Some findings of transient confinement of a diffusing labeled protein to a particular region were viewed as due to transient association of this protein with rafts. In recent years, all aspects of the raft hypothesis came under severe scrutiny (Shaw, 2006; McMullen et al., 2004; Munro, 2003), and it underwent some substantial modifications (Hancock, 2006; Pike, 2006). The two main points of the criticism are: first, the Triton X-100 treatment might actually induce DIG formation, not preserve preexistent rafts (Tsamaloukas et al., 2006); and second, detailed light microcopy *in vivo* investigations of diffusing GFP labeled GPI and other proteins and fluorescent lipid analogs normally detect only even distribution of the probe throughout the plasma

membrane. Other studies also suggest that rafts could be only 5 to 20 nm in diameter and have half-lives in the 100 nanosecond range, a time period shorter than the half-live of protein-protein interactions in signal transduction and the reaction rate of many enzymes (Shaw, 2006). Thus, with the raft hypothesis in doubt, the fluid mosaic model remains the most accurate representation of the cell membrane organization. Although a molecule laterally diffusing in the plasma membrane could encounter certain constrains imposed by the cytoskeleton “fences” and anchored transmembrane protein “pickets” (Kusumi et al., 2005), overall the natural bilayer itself, without the protein organizing and modifying effect, is likely to be fluid and homogeneous.

Asymmetric lipid distribution between the two monolayers of certain cell membranes

The two monolayers of the animal plasma membrane typically differ with respect to the lipid composition (Devaux, 1991; Zachowski and Devaux, 1990). This was first unambiguously established for the erythrocyte membrane, in which the exofacial monolayer contains more sphingolipids and PC, while the cytofacial half accumulates more PE and all of the membrane PS (Bretscher, 1972; Rothman and Lenard, 1977). With a few notable exceptions, such as macrophages (Callahan et al., 2000) and embryonic myotubes (van den Eijnde et al., 2001), mammalian cells of other types also conceal PS in the inner monolayer of the plasma membrane (distribution of PE has been less investigated) (Devaux et al., 2006; Wang et al., 2004). Some reports indicate that membranes of the Golgi apparatus and of the vesicles that originate from either the Golgi or the plasma membrane also exhibit asymmetric phospholipid distribution (Alder-Baerens et al., 2006; Suzuki et al., 1997; Zachowski et al., 1989). The lipids of the endoplasmic reticulum seem to traverse the bilayer quickly in both directions by means

of a protein transporter with a very loose specificity, and this probably abrogates any asymmetry that could arise from synthesis of PC, PE, PS and phosphatidylinositol (PI) at the cytofacial monolayer of this organelle or any other sources (Vishwakarma et al., 2005; Marx et al., 2000). Lipids of the inner membrane of the mitochondrion similarly undergo rapid bidirectional flip-flop (Gallet et al., 1999). Thus, whether a membrane is asymmetric seems to correlate with its composition (Kol et al., 2002). Those membranes that contain sphingolipids and PS – the plasma membrane, Golgi apparatus, endosome and secretory vesicles – all might exhibit lipid asymmetry; on the other hand, membranes with insignificant amounts of sphingolipids and PS – the endoplasmic reticulum (PC / PE / PI : 60/25/10 mole % approximately; Sprong et al., 2001), mitochondrion and peroxisome – might, in contrast, actively promote lipid transbilayer intermixing via facilitated diffusion.

PS exposure is a critical well-documented step in the processes of apoptotic cell clearance and blood coagulation (Williamson and Schlegel, 2002; Schlegel and Williamson, 2001; Lentz, 2003). In apoptosis, PS serves as a marker that a dying cell, such as an apoptotic lymphocyte, exposes on the surface to identify itself to the phagocyte. PS is also continuously present, although at much lower levels in comparison with apoptotic cells, in the outer monolayer of fully differentiated macrophages, specialized phagocytes (Callahan et al., 2003;). Pretreatment of either apoptotic lymphocytes or macrophages with the PS-specific binding protein annexin V hinders engulfment of the former by the latter (Callahan et al., 2000; Krahling et al., 1999). PS-containing synthetic vesicles similarly hinder engulfment of lipid-symmetric (sealed ghosts in which lipid asymmetry is scrambled by the treatment with Ca^{+2};

Williamson et al., 1992) erythrocytes (Pradhan et al., 1994) and apoptotic lymphocytes (Fadok et al., 1992). Conversely, artificial erythrocyte surface-mimicking liposomes enriched with as little as 3 mole % PS, but not less, are efficiently removed from the murine circulation (Allen et al., 1988). PS-dependent clearance of artificial vesicles and engulfment of lipid-symmetric erythrocytes indicate that PS exposure on the surface of the apoptotic cell might be necessary and also sufficient for its recognition and uptake by the phagocyte at least in the erythrocyte and lymphocyte cell systems.

In blood coagulation, PS serves as a facilitator of enzymatic complex assembly on the surface of platelets and platelet-derived membrane blebs and microvesicles (Lentz, 2003; Monroe et al., 2002). Platelets normally conceal PS in the inner monolayer of the plasma membrane, but expose it when activated. The exposed PS renders the exofacial monolayer suitable for binding by several coagulations factors, including factor X_a and factor V_a, which combine into the prothrombinase complex, and prothrombin, which undergoes cleavage by the complex to thrombin. In parallel with the erythrocyte and lymphocyte cell systems, masking PS on the surface of platelets and platelet-derived bilayers hinders blood coagulation (Ravanat et al., 1992). Furthermore, individuals with Scott's syndrome, a rare congenital disorder, exhibit defects in PS exposure by activated platelets and consequently, suffer from provoked bleeding episodes (Zwaal et al., 2004).

Blood coagulation could be considered a kind of altruistic apoptosis on the part of platelets. A number of single-cell eukaryotic species exhibit mammalian-like apoptosis under adverse conditions. In overgrown *Saccharomyces sereviciae* cultures and colonies, chronologically older cells die exhibiting apoptotic markers, such as PS

exposure, commonly displayed by dying cells in higher organisms (Gourlay et al., 2006). *Dictyostelium discoideum* myxamoebae under certain unfavorable conditions can either undergo mammalian-like apoptosis with PS externalization or act as phagocytes and engulf dying neighbors (Tatischeff et al., 2001). These observations indicate that membrane asymmetry and PS concealment and exposure are very ancient evolutionary inventions perhaps already present in the protoeukaryote.

Phospholipid transbilayer flip-flop

Membrane lipid transbilayer (between monolayers) flip-flop can be viewed as a peculiar instance of transmembrane transport in which zwitterionic and charged lipid head groups traverse the hydrophobic milieu of the acyl chains. Substances normally pass through the cell membrane by means of simple diffusion, facilitated diffusion or active transport. Similarly, lipid flip-flop can occur by any one of the three mechanisms (Devaux, 1991). Currently available methods allow for quantitative measurements of the transbilayer lipid transport of only synthetic lipid molecules that carry a label, which could be an uncommon isotope, specific chemical group, spin adduct or fluorescent adduct (Devaux et al., 2002). Frequently, labeled lipids also have short (C_5 or C_6) one or both acyl chains, because molecules with shorter fatty residues exhibit better water solubility and are easier to incorporate into the bilayer of interest. Although inconsistent findings with different analogs of the same lipid occur, the assumption is that synthetic lipids nonetheless roughly reflect behavior of the corresponding natural counterparts (Devaux et al., 2002).

The rate of spontaneous lipid flip-flop (simple diffusion) in lipid-only bilayers depends on the structure of the traversing lipid molecule and lipid composition of the

bilayer. Lipids without or with a small head group diffuse transversely much faster than those with a large head group (Table I, B and D). Head group charge also influences the rate of flip-flop. Thus, phosphatidylglycerol (PG) undergoes flip-flop more often than PC, but not as often as PE; on the other hand, small head group but charged phosphatidic acid also flip-flops less frequently than PE (Table I, C). Consequently, lipids with a bulky label linked to the head group diffuse slower than lipids without an adduct (Table I, A and F). The length and probably, the degree of unsaturation of the acyl chains are two other structural factors that influence transverse diffusion: shorter-chain less-saturated lipids undergo flip-flop more frequently (Table I, C; Armstrong et al., 2003). Cholesterol, which has only a polar hydroxyl group, diffuses between the monolayers almost freely (half-life < 1 sec) (Hamilton, 2003). With respect to the lipid composition of the bilayer, the rate of transbilayer diffusion of a minor by content lipid correlates with the unsaturation level of the acyl chains in the bulk lipids (Armstrong et al., 2003) and is sensitive to cholesterol levels (Table I, E). Overall, the Arrhenius activation energy for lipid flip-flop in lipid-only bilayers is fairly high: around 100 kJ/mol (a quarter of the energy needed to break the covalent C-H bond); furthermore, even when this parameter is lower, ordered organization of the bilayer, as in the sphigomyelin-cholesterol lattice (Table I, E), may eliminate intralamellar fluctuations and discontinuities required for acquisition by individual molecules of the level of energy necessary for a flip; both of these factors ensure fairly slow, corresponding to half-lives in the range of hours to days, rates of transbilayer lipid diffusion.

Table I. Spontaneous flip-flop half-lives and activation energies for synthetic label-carrying lipids in lipid-only bilayers. (Rate of diffusion = 0.639/half-life for first order diffusion).

Label/lipid analog	Bilayer lipids, temperature	Translo-cation half-life	Activation energy	Source
(A) A nitroxide ring fused to the quaternary ammonium instead of a methyl in the PC head group (TEMPO-DPPC*) (C16:0)	Egg PC, 30ºC Egg PC, 35ºC	6.5 h 116 min	81 kJ/mol -	Kornberg and McConnell, 1971
(B) Thioglycerol Phosphatidylthioglycerol In both a sulfhydryl group in place of a hydroxyl group; oleoyl (C18:1) chains	PC, room PC, room	< 15 sec > 8 days	N/A N/A	Ganong and Bell, 1984
(C) *sn-2*: (CH_2)7-CH_2-pyrene in all				Homan and Pownall, 1988
sn-1: C8:0; head group: PC	POPC*, 37ºC	3.6 days	155 kJ/mol	
sn-1: C10:0; head group: PC	POPC, 37ºC	7.2 days	150 kJ/mol	
sn-1: C12:0; head group: PC	POPC, 37ºC	14 days	159 kJ/mol	
sn-1: C8:0; headg roup: PG*	POPC, 37ºC	2.9 days	142 kJ/mol	
sn-1: C12:0; head group: PG	POPC, 37ºC	2.9 days	146 kJ/mol	
sn-1: C8:0; headg roup: PA*	POPC, 37ºC	1.5 days	121 kJ/mol	
sn-1: C12:0; head group: PA	POPC, 37ºC	1.5 days	125 kJ/mol	
sn-1: C8:0; head group: PE	POPC, 37ºC	6 h	105 kJ/mol	
sn-1: C12:0; head group: PE	POPC, 37ºC	10 h	105 kJ/mol	
(D) *sn-1*: palmitoyl (C16:0) in both *sn-2*: 5-(5,7-dimethyl BODIPY)-1-pentanoic acid (C5-DMB) in both;				Bai and Pagano, 1997
Head group: H (diacylglycerol)	POPC, 37ºC	0.07 sec	N/A	
Head group: PC	POPC, 37ºC	7.5 h	N/A	
C5-DMB-ceramide	POPC, 37ºC	22 min	N/A	
C5-DMB-sphingomyelin	POPC, 37ºC	3.3 h	N/A	
(E) NBD-DMPE* (C14:0)	POPC POPC:Chl*-1:1 SpM:Chl*-6:4 All at 35ºC	29 min 82.5 min 34 min	85 kJ/mol 87 kJ/mol 53 kJ/mol	Abreu et al., 2004
(F) Perdeuterated DMPC* (C14:0)	DMPC, 20.5ºC	1.30 min	N/A	Liu and Conboy, 2005
Perdeuterated DPPC (C16:0)	DPPC, 36.6ºC	9.20 min	N/A	
Perdeuterated DSPC* (C18:0)	DSPC, 41.7ºC	312 min	N/A	
TEMPO-DPPC (same as in A)	DPPC, 36.1ºC	635 min	N/A	

*Abbreviations: PG – phosphatidylglycerol; PA – phosphatidic acid; POPC – 1-palmitoyl-2-oleyl-*sn*-glycero-3-phosphocholine; Chl-cholesterol; SpM – sphingomyelin; NBD-DMPE – n-(7-nitrobenz-2-oxa-1,3-diazol-4-yl)-amino-1,2-dimyristoylphosphatidylethanolamine; DMPC – dimyristoyl PC; DPPC – dipalmitoyl PC; DSPC – distearoyl PC.

In addition to intrinsic lipid factors, the rate of lipid transbilayer diffusion in the artificial bilayer is also sensitive to transbilayer peptides and synthetic flippases (also called synthetic translocases). Mere presence in the lipid lamella of random synthetic transbilayer peptides increases flip-flop of PG (down to the half-life of 10 min at higher peptide concentrations) and phosphatidic acid (Kol et al., 2001). Certain peptides also promote transbilayer diffusion of PE, while PC and PS appear altogether insensitive to the peptide effect (Kol et al., 2003). Synthetic flippases are water-soluble molecules that promote lipid flip-flop (Yaroslavov et al., 2006; Smith and Lambert, 2003). Substances in the carrier-like group of synthetic flippases form hydrogen bonds with the phosphate residue and in PS, also with the carboxyl group and traverse the hydrophobic milieu as charge-neutral lipid-flippase complexes (Smith and Lambert, 2003). The resultant decrease of the translocation half-life is fairly significant, down to 5 min for PC and PE and 30 min for PS. The PS-specific carrier can also induce PS exposure on the surface of healthy erythrocytes. These findings with the carrier-like flippases somewhat contradict the conclusions from transbilayer diffusion studies with labeled lipids alone and imply that the size of the head group and the charge on the ammonium (in PE and PS) or the tetraalkylammonium (in PC) cations impairs transverse lipid diffusion only marginally; instead, the greatest hindrance to lipid flip-flop arises from the lipid anion groups. Consequently and not surprisingly, given the critical function of this lipid in apoptosis, PS, with its two anions, appears to be the most resistant to transverse diffusion.

Investigations of transbilayer flip-flop of labeled lipid *analogs* in the erythrocyte, other mammalian and some nonmammalian membranes support the hypothesis that

eukaryotic cells may contain at least two lipid flippase (passive transport) and two lipid translocase (active transport) *activities*, named the scramblase (also called the bidirectional flipsite; names in parentheses are alternative names of the same activity present in the literature), ATP-independent flippase (the ER flippase), outward translocase (floppase) and inward translocase (flippase, aminophospholipid translocase, APLT) (Table II) (Devaux et al., 2006; Pomorski and Menon, 2006; Daleke, 2003; Bevers et al., 1999). The scramblase is the plasma membrane activity responsible for the rapid PS exposure on the surface of erythrocytes, platelets and lymphocytes (Table II) (Williamson et al., 1992, 1995, 2001; Schroit and Zwaal, 1991). It is likely to be present in all eukaryotic cells that conceal and then swiftly expose PS. It is ATP-independent, lipid head group-nonspecific, *bidirectional* and inducible by either high levels of intracellular Ca^{+2} or apoptosis. The sensitivity of this activity to sulphydryl oxidation, heating and protease cleavage suggests that it involves a protein component (de Jong and Kuypers, 2006; Comfurius et al., 1996). The ATP-independent flippase is an activity present in the endoplasmic reticulum (Pomorski and Menon, 2006). This activity also catalyzes rapid (although not as rapid as the scramblase, Table II), head group-nonspecific, bidirectional lipid movement (Vishwakarma et al., 2005; Marx et al., 2000). Unlike the scramblase, the ER flippase is constitutive and only poorly sensitive to protein modification treatments. The processes underlying the scramblase and the ER flippase activities are subjects of intense investigation and speculation (Devaux et al., 2006; Pomorski and Menon, 2006). A pore type protein transporter would most easily facilitate fast bidirectional lipid diffusion. However, extensive efforts to identify proteins behind the scramblase and ER flippase have yielded only false leads; as a result, the

Table II. Lipid specificity and half-life for lipid flipping and translocating activities.

Activity	Lipids/label	Cell type	Half-lives of flip/translo-cation	Source
Scramblase bidirectional, all phospholipids and sphingomyelin	C6-NBD-PC,-PS	erythrocyte platelets jurkat (human)	1.4 ms 8.2 μs 190 μs (37ºC)	Williamson et al., 2001
ER flippase bidirectional, all phospholipids and sphingomyelin	spin-PC spin-PE C6-NBD-PC C6-NBD-PE	rat liver microsomes	14.8 s 10.7 s 90.0 s 74.3 s (room)	Marx et al., 2000
Outward translocase from the inner to the outer monolayer, some specificity	C6-NBD-PC,-PE,-PS	erythrocytes	1.5 h (37ºC)	Connor et al., 1992
	[^{14}C] PC	erythrocytes	30 min (37ºC)	Kalin et al., 2004
	specifically C6-NBD-PS	ABCA1-GFP in MDCKII cells*	30 min (20ºC)	Alder-Baerens et al., 2005
Inward translocase from the inner to the outer monolayer; PS, PE, (PC)	C6-NBD-PS spin-PS	fibroblasts fibroblasts	7.2 min 3.6 min (20ºC)	Pomorski et al., 1996
	spin-PS spin-PE spin-PC spin-sphingomyelin	erythrocytes erythrocytes erythrocytes erythrocytes	5 min 1 h 8 h >> 10 h (37º)	Morrot et al., 1989

* In MDCKII cells expressing ABCA1-GFP chimeric protein.

research focus began to shift to more lipid-based mechanisms of the two activities.

The outward translocase (floppase) is a plasma membrane activity that translocates at low rates certain lipids from the inner to the outer monolayer of the plasma membrane (Table II) (Devaux et al., 2006; Daleke, 2003; Bevers et al., 1999). It is ATP-dependent, constitutive, only somewhat head group-specific and sensitive to various protein modification agents and broad-spectrum ATPase (vanadate) and ATP-

binding cassette (ABC) transporter (glibenclamide) inhibitors (Connor et al., 1992). The outward translocase activity is compromised in mutants of at least four ABC transporters. The ABC transporter superfamily consists of multispan transmembrane proteins that are likely to directly pump across cell bilayers a wide variety of cargoes, some of which – such as phospholipids, cholesterol, peptides and bile salts – are pretty big (Dean and Annilo, 2005). A crystal structure of a bacterial ABC transporter Sav1866 bound to ATP indicates that this protein forms a cavity suitable for passage of sizable substances (Dawson and Locher, 2006). Two putative ABC outward translocases, ABCB1 (MDR 1) and ABCC1 (MRP1), exhibit little lipid specificity and also contribute to non-specific extrusion from the cell of many different xenobiotic chemicals, including pharmacological drugs. Another putative outward translocase, ABCA1, is essential for intracellular cholesterol efflux to high-density lipoprotein (HDL) particles and clearance of apoptotic cells (Knight, 2004; Hamon et al., 2000). Two reports find that ABCA1 controls surface exposure of PS and PE (Alder-Baerens et al., 2005; Hamon et al., 2000); one report identifies its substrates as PC and sphingomyelin (Takahashi et al., 2006); and investigations in Williamson's and our labs show that translocation of the four proposed substrates is normal in ABCA1 gene mutants (RA Schlegel and P Williamson, personal communication). The final member of the outward translocase group, ABCB4, is required specifically for PC secretion into bile by hepatocytes and PC exposure on the cell surface of fiborblasts and erythrocytes (Kallin et al., 2004). Thus, there could be at least two kinds of outward translocases; "janitor" outward translocases, exemplified by ABCB1 and ABCC1, could simply pump nearly all molecules from the inner to the outer monolayer of the cell membrane in order to

prevent xenobiotics from diffusing into the cytosol; while lipid-specific outward translocases, such as ABCB4, could establish and maintain asymmetric lipid distribution across the plasma membrane by transporting outer monolayer-resident lipids to the outer monolayer.

The inward translocase (flippase) is the activity responsible for translocation of lipids from the exofacial to the cytofacial monolayer of lipid asymmetric cell membranes (from the Golgi apparatus to the plasma membrane). Until recently, the available evidence obtained with labeled lipids supported the view that this activity was ATP-dependent; constitutive; specific for PS and with a much lower affinity (K_m), PE; sensitive to protein modification reagents, vanadate and P-type ATPase specific inhibitors (AlF_4); and downregulated by cytosolic Ca^{+2} (Bevers et al., 1999). In the past few years, this view began to change somewhat due to findings in budding yeast. The yeast inward translocase, in addition to labeled PS and PE, unexpectedly also translocates labeled PC (Grant et al., 2001; Pomorski et al., 2003). The inward translocase of a protozoan parasite, *Leishmania infantum*, exhibits higher affinity for PE over PS and translocates PC as well (Araujo-Santos et al., 2003). These findings indicate that the inward translocase in different organisms might have different substrate specificities.

The asymmetric distribution of the plasma membrane lipids must be an equilibrium outcome of all constitutive translocase activities (Figure 4). Presently available evidence suggests a lipid translocation model in which the “janitor” outward translocases indiscriminately “sweep” all lipids from the cytofacial to the exofacial monolayer of the organelle at fairly slow rates. The head-group specific and more active

inward translocases pump certain lipids back to the inner monolayer. The cumulative effect of this bidirectional lipid traffic is the prevalence of spurious and toxic substances and PC and sphingomyelin, for which the mammalian inward translocases lack affinity, in the outer (“dirty” or unregulated) monolayer and accumulation of PS and PE in the inner (cleaned or regulated) half. Hence the center of the bilayer represents a diffusion barrier, potentially harmful xenobiotics located in its outer leaflet are hindred from readily diffusing into the cytosol. Over the background of these housekeeping activities,

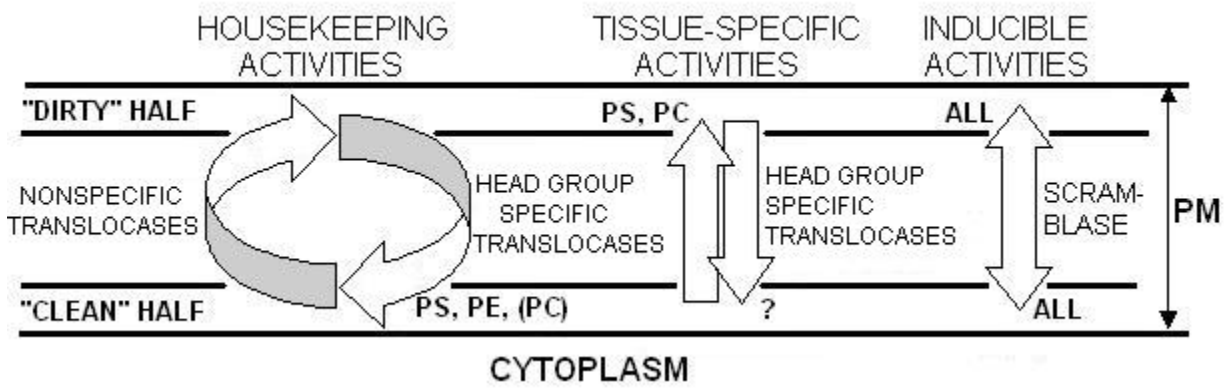

Figure 4. Lipid translocation in the mammalian plasma membrane.

the scramblase and certain head-group specific outward and inward translocases provide regulatory (maintain lateral pressure in each of the leaflets), inducible (PS exposure in apoptosis) and tissue-specific (PC secretion by hepatocytes) alterations of the lipid distribution. The housekeeping activities are likely to be widely conserved among eukaryotes, while the assortment of nonessential flippases and translocases would be different from species to species and cell type to cell type.

P-type ATPases in subfamily IV as putative transbilayer amphipath transporters

P-type ATPases in subfamily IV (also abbreviated as P_4-type ATPases) are the putative transbilayer amphipath transporters (TATs) responsible for the inward translocase activity. A member of this subfamily (ATP8A1) was co-purified with an inward translocase activity (referred to as ATPase II) from bovine adrenal chromaffin granules (Tang et al., 1996; Daleke and Lyles, 2000). ATP-dependent flip of labeled (always with the 7-nitrobenz-2-oxa-1,3-diazol-4-yl, NBD, tag) PS, PE and in some instances, PC is consistently deficient in the plasma membrane of cells with mutations in subfamily IV P-type ATPase-encoding genes in budding yeast (Elvington et al., 2005; Pomorski et al., 2003), mouse (Wang et al., 2004) and *L. donovani* (Perez-Victoria et al., 2006). Furthermore, heterologously expressed bovine ATP8A1 and its murine homolog (Atp8a1) respond to addition of specifically PS by increasing ATP hydrolysis and progressing through the catalytic cycle (initiating substrate-dependent dephosphorylation of the phosphorylated intermediate) (Paterson et al., 2006; Ding et al., 2000). These findings support at the very least a fairly restrained conclusion that the transporters in the novel subfamily of P-type ATPases participate in transbilayer translocation of NBD labeled PS and PE and depend on natural PS for full activity.

The most notable objection to the recognition of P-type ATPases in subfamily IV as TATs arises from structural considerations. The P-type ATPase superfamily contains five subfamilies (Kühlbrandt, 2004). The prokaryotic subfamily I and eukaryotic subfamilies II and III include exclusively metal cation and proton pumps. Transporters in subfamily V are orphan (without a substrate), although in yeast a member of this group regulates Ca^{+2} homeostasis (Cronin et al., 2002). As one reviewer noted (Kühlbrandt, 2004), “it is difficult to imagine how the binding site at the centre of a 10-helix bundle [in

the P-type ATPase] can adapt to translocate both ions and phospholipids". Furthermore, hypersensitivity of yeast subfamily IV P-type ATPase mutants to heavy metals (Co^{+2}, Zn^{+2}, Mn^{+2} and Ca^{+2}; Pomorski et al., 2003) reinforces the view that these proteins transport the same kind of cargo as the majority of the superfamily members. On the other hand, a structural comparison of a subfamily IV ATPase, Atp8a1, with a subfamily IIA transporter, the sarcoplasmic reticulum Ca^{+2}-ATPase (SERCA2) (by threading the former onto a crystal structure of the latter), indicates that, first, the putative TAT contains a mixture of hydrophobic and polar uncharged residues in the region that corresponds to the highly charged substrate binding site in the Ca^{+2} pump (Schlegel et al., 2003). And second, at the substrate entrance into the protein interior, SERCA2 contains a highly conserved aspartate and conserved glutamates; in the roughly equivalent area, Atp8a1 forms a long, 35-highly conserved residue crevasse that extends from a cytoplasmic domain down into the transmembrane region on the side exposed to the bilayer lipids. These two structural differences indicate that the transported substrates of the subfamily IV ATPases are likely to be bulky and hydrophobic, like phospholipids, instead of small and charged, like metal cations. Furthermore, in *Leishmania* a subfamily IV ATPase is required for cellular efflux of the lipid drug miltefosine (hexadecylphosphocholine) (Perez-Victoria et al., 2003). Thus, P-type ATPases of subfamily IV are the leading candidate lipid translocases.

Phenotypic defects caused by mutations in genes encoding putative TATs implicate these transporters in a number of cellular processes and mammalian diseases. The budding yeast genome encodes 5 polypeptides in the subfamily: Neo1p, is an essential endosomal ATPase, which interacts with Ysl2p, a potential guanine

nucleotide exchange factor for a small Arf-like GTPase Arl1p, and with Mon2p, a scaffold protein involved in multiple aspects of vesicular trafficking (Efe et al., 2005; Wicky et al., 2004). Drs2p and Dnf3p reside predominantly in the *trans*-Golgi network (TGN), where the two are required for translocation of PS, PE and PC to the cytoplasmic monolayer (Alder-Baerens et al., 2006; Natarajan et al., 2004). Dnf1p and Dnf2p perform aminophospholipid translocation functions in the plasma membrane (Pomorski et al., 2003). Drs2p forms a complex with Cdc50p; Dnf1p and Dnf2p with Lem3p and Dnf3p with Crf1p (Furuta et al., 2007; Saito et al., 2004). Cdcd50p, Lem3p and Crf1p are related proteins that may be noncatalytic subunits facilitating vesicular transport of the associated P-type ATPase. Cumulatively Drs2p and Dnf1-3p mediate various pathways of endocytosis and exocytosis (Chen et al., 2006; Graham, 2004). *Magnaporthe grisea*, the rice blast fungus, employs at least two putative TATs for infecting rice: one of these transporters controls a particular exocytosis pathway (Balhadere and Talbot, 2001; Gilbert et al., 2006). Mutagenesis of a *Leishmania* subfamily IV P-type ATPase confers the parasite with resistance against a pharmacological drug (Perez-Victoria et al., 2003). In mice, a putative TAT is a model of diabetes and obesity and affects insulin-induced glucose uptake (Dhar et al., 2006; 2004). Mutations in a human subfamily IV ATPase cause several kinds of cholestasis (impaired bile secretion) (Paulusma and Oude Elferink, 2005). The pattern that emerges from the mutant phenotype data is consistent with the role for the putative TATs in the maintenance of membrane structure and facilitation of vesicular transport, perhaps via regulation of phospholipid asymmetry, and in secretion and uptake of various substances.

Caenorhabditis elegans as a model system for investigations of lipid bilayers

The soil nematode *Caenorhabditis elegans* is an exceptionally powerful eukaryotic model system for developmental genetics. It offers numerous investigative benefits: a fully sequenced genome, ease of growth, short lifespan and extensive research support infrastructure, including several groups dedicated to isolation of null mutants upon request from any investigator. In many instances, *C. elegans* contains simplified versions of mammalian protein complexes, pathways and whole processes. Thus, apoptosis and apoptotic cell clearance in the nematode and mammals involve, to a large extent, the same kind of proteins, orchestrating the same sequence of events (Reddien and Horvitz, 2004; Hamon et al., 2006). This conservation of core proteins and the overall protein architecture and operation renders *C. elegans* a very useful study system in which findings for a large number of processes are directly applicable to mammalian organisms.

In recent years, several research groups began investigations of sterol metabolism in *C. elegans* with the view of developing this model organism into a productive sterol study system that would supplement cholesterol research in the much more cumbersome and expensive murine model (Paik et al., 2006; Entchev and Kurzchalia, 2005). Success of this undertaking to a large degree depends on whether the nematode sterol metabolism reflects the corresponding cholesterol turnover in mammals. Unlike mammals, *C. elegans* (as well as *Drosophila* and probably a majority of lower animals) is incapable of synthesizing sterol *de novo* and therefore, depends on exogenous sources for its supply (Chitwood, 1999). The sterol biosynthesis pathway is very ancient and the absence of it in certain animals is likely to be due to a loss (Cavalier-Smith and Chao, 2003). Except for this difference, the rest of *C. elegans* sterol

turnover seems to substantially reflect the corresponding process in mammals. In both the nematode and mammals, indiscriminate sterol uptake occurs in the intestine (Entchev and Kurzchalia, 2005). However, mammalian enterocytes actively re-secrete back into the intestinal lumen phytosterols, which disrupt endogenous cholesterol homeostasis at high serum levels (Yang et al., 2003). *C. elegans*, in contrast, metabolizes exogenous sterols, including cholesterol (Rottiers et al., 2006), to 7-dehydrocholesterol; nearly 70% of the non-dietary sterol in the nematode body is in this form (Merris et al., 2004). 7-Dehydrocholesterol differs from cholesterol by the presence of the Δ^7 bond, but otherwise the two are structurally identical. In a further similarity with mammals, 7-dehydrocholesterol serves as a precursor for steroid hormone biosynthesis: DAF-9, a cytochrome P450, synthesizes Δ^7-dafachronic acid, a ligand for DAF-12, a nuclear receptor that promotes reproductive development and suppresses dauer diapause, fat accumulation and life span (Motola et al., 2006; Beckstead and Thummel, 2006). Other still unidentified steroid hormones regulate molting (Slunder and Maina, 2001). Conversion of exogenous sterols to 7-dehydrocholesterol occurs in the intestine (Rottiers et al., 2006), which in *C. elegans* performs functions that in mammalian organisms are associated with the liver and adipose tissues. Biosynthesis of Δ^7-dafachronic acid takes place in the nematode steroidogenic organs, the hypodermis and the XXX cells (Gerisch and Antebi, 2004). Thus, both the nematode and mammals employ slightly different sterols for production of steroid hormones, which then perform secondary messenger functions in endocrine signaling pathways (Tatar et al., 2003).

In mammalian organisms, another critical function of cholesterol is to ensure proper membrane structure. Indeed, mammalian membranes contain large amounts of cholesterol. In contrast, *C. elegans* can survive on miniscule amounts of this substance (Entchev and Kurzchalia, 2005). Yet, the nematode contains proteins with sterol-sensing domains and caveolins; lipids extracted from nematode membranes contain (whether artificial or not) lipid rafts (Kuwabara and Labouesse, 2002; Scheel et al., 1999). The question then arises: is *C. elegans* membrane lipid structure similar to that of mammals? The answer to this question will certainly advance understanding of the mammalian bilayers as well. And second, the sterol heterotrophy of the nematode provides an opportunity to manipulate two lipid bilayer variables at the same time: sterol content and for example, (by means of genetics) the presence or absence of lipid bilayer modifying proteins, such as TATs.

References

Abreu MSC, Moreno MJ and WLC Vaz. (2004) Kinetics and thermodynamics of association of a phospholipid derivative with lipid bilayers in liquid-disordered and liquid-ordered phases. Biophysical Journal 87:353-365.

Alder-Baerens N, Lisman Q, Luong L, Pomorski T and JSM Holthuis. (2006) Loss of P4 ATPase Drs2p and Dnf3p disrupts aminophospholipid transport and asymmetry in yeast post-Golgi secretory vesicles. Molecular Biology of the Cell 17:1632-1642.

Alder-Baerens N, Muller P, Pohl A, Korte T, Hamon Y, Chimini G, Pomorski T and A Herrmann. (2005) Headgroup-specific exposure of phospholipids in ABCA1-expressing cells. Journal of Biological Chemistry 280:26321-26329.

Allen TM, Williamson P and RA Schlegel. (1988) Phosphatidylserine as a determinant of reticuloendothelial recognition of liposome models of the erythrocyte surface. Proceedings of the National Academy of Sciences of the United States of America 85:8067-8071.

Almeida PFF, Pokorny A and A Hinderliter. (2005) Thermodynamics of membrane domains. Biochimica et Biophysica Acta 1720:1-13.

de Almeida RFM, Fedorov A and M Prieto. (2003) Sphingomyelin/phosphatidylcholine/cholesterol phase diagram: boundaries and composition of lipid rafts. Biophysical Journal 85:2406-2416.

Araujo-Santos JM, Gamarro F, Castanys S, Herrmann A and T Pomorski. (2003) Rapid transport of phospholipids across the plasma membrane of *Leishmania infantum*. Biochemical and Biophysical Research Communications 306:250-255.

Armstrong VT, Brzustowicz MR, Wassall SR, Jenski LJ and W Stillwell. (2003) Rapid flip-flop in polyunsaturated (docosahexaenoate) phospholipid membranes. Archives of Biochemistry and Biophysics 414:74-82.

Bagatolli LA. (2006) To see or not to see: lateral organization of biological membranes and fluorescence microscopy. Biochimica et Biophysica Acta 1758:1541-1556.

Bai J and RE Pagano. (1997) Measurement of spontaneous transfer and transbilayer movement of BODIPY-labeled lipids in lipid vesicles. Biochemistry 36:8840-8848.

Balhedere PV and NJ Talbot. (2001) PDE1 encodes a P-type ATPase involved in appressorium-mediated plant infection by the rice blast fungus *Magnaporthe grisea*. Plant Cell 13:1987-2004.

Barenholz Y. (2004) Sphingomyelin and cholesterol: from membrane biophysics and rafts to potential medical applications. In PJ Quinn (Ed.), *Subcellular biochemistry, Volume 37: Membrane dynamics and domains* (pp. 167-215). New York, NY: Kluwer Academic / Plenum Publishers.

Beckstead RB and CS Thummel. (2006) Indicted: worms caught using steroids. Cell 124:1137-1140.

Benveniste P. (2004) Biosynthesis and accumulation of sterols. Annual Review of Plant Biology 55:429-457.

Bevers EM, Comfurius P, Dekkers DWC and FA Zwaal. (1999) Lipid translocation across the plasma membrane of mammalian cells. Biochimica et Biophysica Acta 1439:317-330.

Bretscher MS. (1972) Asymmetrical lipid bilayer structure for biological membranes. Nature New Biology 236:11-12.

van den Brink-van der Laan E, Killian JA and B de Kruijff. (2004) Nonbilayer lipids affect peripheral and integral membrane proteins via changes in the lateral pressure profile. Biochimica et Biophysica Acta 1666:275-288.

Brites P, Waterham HR and RJ Wanders. (2004) Functions and biosynthesis of plasmalogens in health and disease. Biochimica et Biophysica Acta 1636:219-231.

Brown RE. (1998) Sphingolipid organization in biomembranes: what physical studies of model membranes reveal. Journal of Cell Science 111:1-9.

Browning JL and J Seelig. (1980) Bilayers of phosphatidylserine: a deuterium and phosphorus nuclear magnetic resonance study. Biochemistry 19:1262-1270.

Callahan MK, Halleck MS, Kraling S, Henderson AJ, Williamson P and RA Schlegel. (2003) Phosphatidylserine expression and phagocytosis of apoptotic thymocytes during differentiation of monocytic cells. Journal of Leukocyte Biology 74:846-856.

Callahan MK, Williamson P and RA Schlegel. (2000) Surface expression of phosphatidylserine on macrophages is required for phagocytosis of apoptotic thymocytes. Cell Death and Differentiation 7:645-653.

Castellana ET and PS Cremer. (2006) Solid supported lipid bilayers: from biophysical studies to sensor design. Surface Science Reports 61:429-444.

Cavalier-Smith T and E E-Y Chao. (2003) Phylogeny of Choanozoa, Apusozoa, and other Protozoa and early eukaryote megaevolution. Journal of Molecular Evolution 56:540-563.

Cevc G and D Marsh. (1987) *Phospholipid bilayers: physical principles and models*. New York, NY: John Wiley & Sons.

Chandler D. (2005) Interfaces and the driving force of hydrophobic assembly. Nature 437:640-647.

Chang HH, Bhagat RK, Tran R and P Dea. (2006) Subgel studies of dimyristoylphosphatidylcholine bilayers. Journal of Physical Chemistry B: 110:22192-22196.

Chapman D. (1993) Lipid phase transitions. In M Shinitzky (Ed.), *Biomembranes: physical aspects* (pp. 29-62). Weinheim: Balaban Publishers.

Chen S, Wang JY, Muthusamy BP, Liu K, Zare S, Andersen RJ and TR Graham. (2006) Roles for the Drs2p-Cdc50p complex in protein transport and phosphatidylserine asymmetry of the yeast plasma membrane. Traffic 7:1503-1517.

Chernomordik LV and MM Kozlov. (2005) Membrane hemifusion: crossing a chasm in two leaps. Cell 123:375-382.

Chitwood DJ. (1999) Biochemistry and function of nematode steroids. Critical Reviews in Biochemistry and Molecular Biology 34:273-284.

Comfurius P, Williamson P, Smeets EF, Schlegel RA, Bevers EM and RF Zwaal. (1996) Reconstitution of phospholipid scramblase activity from human blood platelets. Biochemistry 35:7631-7634.

Connor J, Pak CH, Zwaal RFA and AJ Schroit. (1992) Bidirectional transbilayer movement of phospholipid analogs in human red blood cells. Journal of Biological Chemistry 267:19412-19417.

Cronan JE. (2003) Bacterial membrane lipids: where do we stand? Annual Review of Microbiology 57:203-224.

Cronin SR, Rao R and RY Hampton. (2002) Cod1p/Spf1p is a P-type ATPase involved in ER function and Ca^{2+} homeostasis. Journal of Cell Biology 157:1017-1028.

Daleke DL. (2003) Regulation of transbilayer plasma membrane phospholipid asymmetry. Journal of Lipid Research 44:233-242.

Daleke DL and JV Lyles. (2000) Identification and purification of aminophospholipid flippases. Biochimica et Biophysica Acta 1486:108-127.

Dawson RJP and KP Locher. (2006) Structure of a bacterial multidrug ABC transporter. Nature 443:180-185.

Dean M and T Annilo. (2005) Evolution of ATP-binding cassette (ABC) transporter superfamily in vertebrates. Annual Review of Genomics and Human Genetics 6:123-142.

Devaux PF, Lopez-Montero I and S Bryde. (2006) Proteins involved in lipid translocation in eukaryotic cells. Chemistry and Physics of Lipids 141:119-132.

Devaux PF, Fellmann P and P Herve. (2002) Investigation on lipid asymmetry using lipid probes. Comparison between spin-labeled lipids and fluorescent lipids. Chemistry and Physics of Lipids 116:115-134.

Devaux PF. (1991) Static and dynamic asymmetry in cell membranes. Biochemistry 30:1163-1173.

Dhar MS, Yuan JS, Elliott SB and C Sommardahl. (2006) A type IV P-type ATPase affects insulin-mediated glucose uptake in adipose tissue and skeletal muscle in mice. Journal of Nutritional Biochemistry 17:811-820.

Dhar MS, Sommardahl CS, Kirkland T, Nelson S, Donnell R, Johnson DK and LW Castellani. (2004) Mice heterozygous for *Atp10c*, a putative amphipath, represent a novel model of obesity and type 2 diabetes. Journal of Nutrition 134:799-805.

Ding J, Wu Z, Crider BP, Ma Y, Li X, Slaughter C, Gong L and X-S Xie. (2000) Identification and functional expression of four isoforms of ATPase II, the putative aminophospholipid translocase. Journal of Biological Chemistry 275:23378-23386.

Dowhan W. (1997) Molecular basis for membrane phospholipid diversity: why are there so many lipids? Annual Review of Biochemistry 66:199-232.

Efe JA, Plattner F, Hulo N, Kressler D, Emr SD and O Deloche. (2005) Yeast Mon2p is a highly conserved protein that functions in the cytoplasm-to-vacuole transport pathway and is required for Golgi homeostasis. Journal of Cellular Biology 118:4751-4764.

van den Eijnde SM, van den Hoff MJB, Reutelingsperger CPM, van Heerde WL, Henfling MER, Vermeij-Keers C, Schutte B, Borgers M and FCS Ramaekers. (2001) Transient expression of phosphatidylserine at cell-cell contant areas is required for myotube formation. Journal of Cell Science 114:3631-3642.

Elvington SM, Bu F and JW Nichols. (2005) Fluorescent, acyl chain-labeled phosphatidylcholine analogs reveal novel transport pathways across the plasma membrane of yeast. Journal of Biological Chemistry 280:40957-40964.

Entchev EV and TV Kurzchalia. (2005) Requirement of sterols in the life cycle of the nematode *Caenorhabditis elegans*. Seminars in Cell and Developmental Biology 16:175-182.

Fadok VA, Voelker DR, Campbell PA, Cohen JJ, Bratton DL and PM Henson. (1992) Exposure of phosphatidylserine on the surface of apoptotic lymphocytes triggers specific recognition and removal by macrophages. Journal of Immunology 148:2207-2216.

Feigenson GW. (2007) Phase boundaries and biological membranes. Annual Review of Biophysics and Biomolecular Structure 36: 63-77.

Futerman AH and YA Hannun. (2004) The complex life of simple sphingolipids. EMBO Reports 5:777-782.

Furuta N, Fujimura-Kamada K, Saito K, Yamamoto T and K Tanaka. (2007) Endocytic recycling in yeast is regulated by putative phospholipid translocases and the Ypt31p/32p-Rcy1p pathway. Molecular Biology of the Cell 18:295-312.

Gallet PF, Zachowski A, Julien R, Fellmann P, Devaux PF and A Maftah. (1999) Transbilayer movement and distribution of spin-labelled phospholipids in the inner mitochondrial membrane. Biochimica et Biophysica Acta 1418:61-70.

Ganong BR and RM Bell. (1984) Transmembrane movement of phosphatidylglycerol and diacylglycerol analogues. Biochemistry 23:4977-4983.

Gerisch B and A Antebi. (2004) Hormonal signals produced by DAF-9/cytochrome P450 regulate *C. elegans* dauer diapause in response to environmental cues. Development 131:1765-1776.

Gilbert MJ, Thornton CR, Wakley GE and NJ Talbot. (2006) A P-type ATPase required for rice blast disease and induction of host resistance. Nature 440:535-539.

Gourlay CW, Du W and KR Ayscough. (2006) Apoptosis in yeast – mechanisms and benefits to a unicellular organism. Molecular Microbiology 62:1515-1521.

Graham TR. (2004) Flippases and vesicular-mediated protein transport. Trends in Cell Biology 14:670-677.

Grant AM, Hanson PK, Malone L and JW Nichols. (2001) NBD-labeled phosphatidylcholine and phosphatidylethanolamine are internalized by tranbilayer transport across the yeast plasma membrane. Traffic 2:37-50.

Gruner SM, Cullis PR, Hope MJ and CPS Tilcock. (1985) Lipid polymorphism: the molecular basis of nonbilayer phases. Annual Review of Biophysics and Biophysical Chemistry 14: 211-238.

Gummadi SN and KS Kumar. (2005) The mystery of phospholipid flip-flop in biogenic membranes. Cellular and Molecular Biology Letters 10:101-121.

Hamilton JA. (2003) Fast flip-flop of cholesterol and fatty acids in membranes: implications for membrane transport proteins. Current Opinion in Lipidology 14:263-271.

Hamon Y, Trompier D, Ma Z, Venegas V, Pophillat M, Mignitte V, Zhou Z and G Chimini. (2006) Cooperation between engulfment receptors: the case of ABCA1 and MEGF-10. PLoS One 1:e120.

Hamon Y, Broccardo C, Chambenoit O, Luciani MF, Toti F, Chaslin S, Freyssinet JM, Devaux PF, McNeish J, Marguet D and G Chimini. (2000) ABC1 promotes engulfment of apoptotic cells and transbilayer redistribution of phosphatidylserine. Nature Cell Biology 2:399-406.

Hancock JF. (2006) Lipid rafts: contentious only from simplistic standpoint. Nature Reviews Molecular Cell Biology 7:456-462.

Hauser H, Pascher I, Pearson RH and S Sundell. (1981) Preferred conformation and molecular packing of phosphatidylethanolamine and phosphatidylcholine. Biochimica et Biophysica Acta 650:21-51.

Heerklotz H and A Tsamaloukas. (2006) Gradual change or phase transition: characterizing fluid-cholesterol membranes on the basis of thermal volume changes. Biophysical Journal 91:600-607.

Heimburg T. (2000) A model for the lipid pretransition: coupling of ripple formation with the chain-melting transition. Biophysical Journal 78:1154-1165.

van Helvoort A and G van Meer. (1995) Intracellular lipid heterogeneity caused by topology of synthesis and specificity in transport. Example: sphingolipids. FEBS Letters 369: 18-21.

Homan R and HJ Pownall. (1988) Transbilayer diffusion of phospholipids: dependence on headgroup structure and acyl chain length. Biochimica et Biophysica Acta 938:155-166.

Hong M, Schmidt-Rohr K and H Zimmermann. (1996) Conformational constraints on the headgroup and *sn-2* chain of bilayer DMPC from NMR dipolar couplings. Biochemistry 35:8335-8341.

Huang C-h. (2001a) Structural organization and properties of membrane lipids. In N Sperelakis (Ed.), *Cell physiology sourcebook*, 3rd edition (pp. 65-79). San Diego, CA: Academic Press.

Huang C-h. (2001b) Mixed-chain phospholipids: structure and chain-melting behavior. Lipids 36:1077-1097.

Ipsen JH, Karlström G, Mouritsen OG and H Wennerström. (1987) Phase equilibrium in the phosphatidylcholine-cholesterol system. Biochimica et Biophysica Acta 905:162-172.

Israelachvili JN, Marčelja S and RG Horn. (1980) Physical principles of membrane organization. Quarterly Review of Biophysics 13:121-200.

de Jong K and FA Kuypers. (2006) Sulphydryl modifications alter scramblase activity in murine sickle cell disease. British Journal of Haematology 133:427-432.

Kalin N, Fernandes J, Hrafnsdóttir S and G van Meer. (2004) Natural phosphatidylcholine is actively translocated across the plasma membrane to the surface of mammalian cells. Journal of Biological Chemistry 279:33228-33236.

Knight BL. (2004) ATP-binding cassette transporter A1: regulation of cholesterol efflux. Biochemical Society Transactions 32:124-127.

Kol MA, van Laak ANC, Rijkers DTS and JA Killian. (2003) Phospholipid flop induced by transmembrane peptides in model membrane is modulated by lipid composition. Biochemistry 42:231-237.

Kol MA, de Kruijff B and AIPM de Kroon. (2002) Phospholipid flip-flop in biogenic membranes: what is needed to connect opposite sides. Cell and Developmental Biology 13:163-170.

Kol MA, de Kroon AIPM, Rijkers DTS, Killian JA and B de Kruijff. (2001) Membrane-spanning peptides induce phospholipid flop: a model for phospholipid translocation across the inner membrane of *E. coli*. Biochemistry 40:10500-10506.

Kornberg RD and HM McConnell. (1971) Inside-outside transitions of phospholipids in vesicle membranes. Biochemistry 10:1111-1120.

Koynova R and M Caffrey. (1995) Phases and phase transitions of the sphingolipids. Biochimica et Biophysica Acta 1255:213-236.

Koynova R, Tenchov BG, Todinova S and PJ Quinn. (1995) Rapid reversible formation of a metastable subgel phase in saturated diacylphosphatidylcholines. Biophysical Journal 68: 2370-2375.

Krahling S, Callahan MK, Williamson P and RA Schlegel. (1999) Exposure of phosphatidylserine is a general feature in the phagocytosis of apoptotic lymphocytes by macrophages. Cell Death and Differentiation 6:183-189.

Kühlbrandt W. (2004) Biology, structure and mechanism of P-type ATPases. Nature Reviews Molecular and Cell Biology 5:282-295.

Kusumi A, Nakada C, Ritchie K, Murase K, Suzuki K, Murakoshi H, Kasai RS, Kondo J and T Fujiwara. (2005) Paradigm shift of the plasma membrane concept from the two-dimensional continuum fluid to the partitioned fluid: high-speed single-molecule tracking of membrane molecules. Annual Review of Biophysics and Biomolecular Structure 34:351-378.

Kuwabara PE and M Labouesse. (2002) The sterol-sensing domain: multiple families, a unique role? Trends in Genetics 18:193-201.

Ladha S. (1998) Lipid heterogeneity and membrane fluidity in a highly polarized cell, the mammalian spermatozoon. Journal of Membrane Biology 165:1-10.

Langner M and K Kubica. (1999) The electrostatics of lipid surfaces. Chemistry and Physics of Lipids 101:3-35.

Lee AG. (2003) Lipid-protein interactions in biological membranes: a structural perspective. Biochimica et Biophysica Acta 1612:1-40.

Lee AG. (1977) Lipid phase transitions and phase diagrams. II. Mixtures involving lipids. Biochimica et Biophysica Acta 472:285-344.

Lentz BR. (2003) Exposure of platelet membrane phosphotidylserine regulates blood coagulation. Progress in Lipid Research 42:423-438.

Liu J and JC Conboy. (2005) 1,2-diacyl-phosphatidylcholine flip-flop measured directly by sum-frequency vibrational spectroscopy. Biophysical Journal 89:2522-2532.

London E. (2005) How principles of domain formation in model membranes may explain ambiguities concerning lipid raft formation in cells. Biochimica et Biophysica Acta 1746:203-220.

Marsh D and T Páli. (2006) Lipid conformation in crystalline bilayers and in crystals of transmembrane proteins. Chemistry and Physics of Lipids 141:48-65.

Marx U, Lassmann G, Holzhutter HG, Wustner D, Muller P, Hohlig A, Kubelt J and A Herrmann. (2000) Rapid flip-flop of phospholipids in endoplasmic reticulum membranes studied by a stopped-flow approach. Biophysical Journal 78:2628-2640.

McConnell HN and A Radhakrishnan. (2003) Condensed complexes of cholesterol and phospholipids. Biochimica et Biophysica Acta 1610:159-173.

McMullen TPW, Lewis RNAH and RN McElhaney. (2004) Cholesterol-phospholipid interactions, the liquid-ordered phase and lipid rafts in model and biological membranes. Current Opinion in Colloid and Interface Science 8:459-468.

van Meer G. (2005) Cellular lipidomics. EMBO Journal 24:3159-3165.

Merris M, Kraeft J, Tint GS and J Lenard. (2004) Long-term effects of sterol depletion in *C. elegans*: sterol content of synchronized wild-type and mutant populations. Journal of Lipid Research 45:2044-2051.

Meyer EE, Rosenberg KJ and J Israelachvili. (2006) Recent progress in understanding hydrophobic interactions. Proceedings of the National Academy of Sciences of the United States of America 103:15739-15746.

Milhaud J. (2004) New insight into water-phospholipid model membrane interactions. Biochimica et Biophysica Acta 1663:19-51.

Morrot G, Herve P, Zachowski A, Fellmann P and PF Devaux. (1989) Aminophospholipid translocase of human erythrocytes: phospholipid substrate specificity and effect of cholesterol. Biochemistry 28:3456-3462.

Monroe DM, Hoffman M and HR Roberts. (2002) Platelets and thrombin generation. Arteriosclerosis, Thrombosis, and Vascular Biology 22:1381-1389.

Motola DL, Cummins CL, Rottiers V, Sharma KK, Li T, Li Y, Suino-Powell K, Xu HE, Auchus RJ, Antebi A and DJ Mangelsdorf. (2006) Identification of ligands for DAF-12 that govern dauer formation and reproduction in *C. elegans*. Cell 124:1209-1223.

Mouritsen OG and MJ Zuckermann. (2004) What's so special about cholesterol? Lipids 39:1101-1113.

Munro S. (2003) Lipid rafts: elusive or illusive? Cell 115:377-388.

Nagle JF and S Tristram-Nagle. (2000) Structure of lipid bilayers. Bichimica et Biophysica Acta 1469:159-195.

Natarajan P, Wang J, Hua Z and TR Graham. (2004) Drs2p-coupled aminophospholipid translocase activity in yeast Golgi membranes and relationship to in vivo function. Proceedings of the National Academy of Sciences of the United States of America 101:10614-10619.

Nurse P. (2000) The incredible life and times of biological cells. Science 289:1711-1716.

Oldfield E and SJ Singer. (1973) Are cell membranes fluid? Science 180:982-983.

Ostrowski SG, van Bell CT, Winograd N and AG Ewing. (2004) Mass spectrometric imaging of highly curved membranes during *Tetrahymena* mating. Science 305:71-73.

Paik YK, Jeong Sk, Lee EY, Jeong PY and YH Shim. (2006) *C. elegans*: an invaluable model organism for the proteomics studies of the cholesterol-mediated signaling pathways. Expert Review of Proteomics 3:439-453.

Pascher I, Lundmark M, Nyholm PG and S Sundell. (1992) Crystal structures of membrane lipids. Biochimica et Biophysica Acta 1113:339-373.

Paterson JK, Renkema K, Burden L, Halleck MS, Schlegel RA, Williamson P and DL Daleke. (2006) Lipid specific activation of the murine P_4-ATPase Atp8a1 (ATPase II). Biochemistry 45:5367-5376.

Paulusma CC and RPJ Oude Elferink. (2005) The type 4 subfamily of P-type ATPases, putative aminophospholipid translocases with a role in human disease. Biochimica et Biophysica Acta 1741:11-24.

Perez-Victoria FJ, Sanchez-Canete MP, Castanys S and F Gamarro. (2006) Phospholipid translocation and miltefosine potency require both *L. donovani* miltefosine transporter and the new protein LdRos3 in *Leishmania* parasites. Journal of Biological Chemistry 281:23766-23775.

Perez-Victoria FJ, Gamarro F, Ouellette M and S Castanys. (2003) Functional cloning of the miltefosine transporter. A novel P-type phospholipid translocase from *Leishmania* involved in drug resistance. Journal of Biological Chemistry 278:49965-49971.

Pike LJ. (2006) Rafts defined: a report on the Keystone symposium on lipid rafts and cell function. Journal of Lipid Research 47:1597-1598.

Pomorski T and AK Menon. (2006) Lipid flippases and their biological functions. Cellular and Molecular Life Sciences 63:2908-2921.

Pomorski T, Lombardi R, Riezman H, Devaux PF, van Meer G and JCM Holthuis. (2003) Drs2p-related P-type ATPases Dnf1p and Dnf2p are required for phospholipid translocation across the yeast plasma membrane and serve a role in endocytosis. Molecular Biology of the Cell 14:1240-1254.

Pomorski T, Muller P, Zimmermann B, Burger K and PF Devaux. (1996) Transbilayer movement of fluorescent and spin-labeled phospholipids in the plasma membrane of human fibroblasts: a quantitative approach. Journal of Cell Science 109:687-698.

Pradhan D, Williamson P and RA Schlegel. (1994) Phosphatidylserine vesicles inhibit phagocytosis of erythrocytes with a symmetric distribution of phospholipids. Molecular Membrane Biology 11:181-187.

Ravanat C, Archipoff G, Beretz A, Freund G and J-P Cazehave. (1992) Use of annexin-V to demonstrate the role of phosphatidylserine exposure in the maintenance of haemostatic balance by endothelial cells. Biochemical Journal 282:7-13.

Reddien PW and HR Horvitz. (2004) The engulfment process of programmed cell death in *Caenorhabditis elegans*. Annual Review of Cell and Developmental Biology 20:193-221.

Rietveld A and K Simons. (1998) The differential miscibility of lipids as the basis for the formation of functional membrane rafts. Biochimica et Biophysica Acta 1376:467-479.

Rothman JE and J Lenard. (1977) Membrane asymmetry. Science 195:743-753.

Rottiers V, Motola DL, Gerisch B, Cummins CL, Nishiwaki K, Mangelsdorf DJ and A Antebi. (2006) Hormonal control of *C. elegans* dauer formation and life span by a Rieske-like oxygenase. Developmental Cell 10:473-482.

Saito K, Fujimura-Kamara K, Furuta N, Kato U, Umeda M and K Tanaka. (2004) Cdc50p, a protein required for polarized growth, associates with the Drs2p P-type ATPase implicated in phospholipid translocation in *Saccharomyces cerevisiae*. Molecular Biology of the Cell 15:3418-3432.

Scheel J, Srivivasan J, Honnert U, Henske A and TV Kurzchalia. (1999) Involvement of caveolin-1 in meiotic cell-cycle progression in *Caenorhabditis elegans*. Nature Cell Biology 1:127-129.

Schlegel RA, Halleck MS and P Williamson. (2003) Phospholipid transporters in the brain. In BF Szuhaj and W van Nieuwenhuyzen (Eds.), *Nutrition and biochemistry of phospholipids* (pp. 1-13). Champaign, IL: AOCS Press.

Schlegel RA and P Williamson. (2001) Phosphatidylserine, a death knell. Cell Death and Differentiation 8:551-563.

Schroit AJ and RF Zwaal. (1991) Transbilayer movement of phospholipids in red cell and platelet membranes. Biochimica et Biophysica Acta 1071:313-329.

Seelig J and A Seelig. (1980) Lipid conformation in model membranes and biological membranes. Quarterly Reviews of Biophysics 13:19-61.

Šegota S and Đ Težak. (2006) Spontaneous formation of vesicles. Advances in Colloid and Interface Science 121:51-75.

Shaw AS. (2006) Lipid rafts: now you see them, now you don't. Nature Immunology 7:1139-1142.

Shipley GG, Avecilla LS and DM Small. (1974) Phase behavior and structure of aqueous dispersions of sphingomyelin. Journal of Lipid Research 15:124-131.

Silvius JR. (2003) Role of cholesterol in lipid raft formation: lessons from lipid model systems. Biochimica et Biophysica Acta 1610:174-183.

Simons K and WLC Vaz. (2004) Model systems, lipid rafts, and cell membranes. Annual Review of Biophysics and Biological Structure 33:269-295.

Simons K and E Ikonen. (1997) Functional rafts in cell membranes. Nature 387:569-572.

Singer SJ and GL Nicolson. (1972) The fluid mosaic model of the structure of cell membranes. Science 175:720-731.

Slunder AE and CV Maina (2001) Nuclear receptors in nematodes: themes and variations. Trends in Genetics 17:206-213.

Smith BD and TN Lambert. (2003) Molecular ferries: membrane carriers that promote phospholipid flip-flop and chloride transport. Chemical Communications 18:2261-2268.

Sprong H, van der Sluijs P and G van Meer. (2001) How proteins move lipids and lipids move proteins. Nature Reviews Molecular Cell Biology 2:504-513.

Suzuki H, Kamakura M, Morii M and N Takeguchi. (1997) The phospholipid flippase activity of gastric vesicles. Journal of Biological Chemistry 272:10429-10434.

Takahashi K, Kimura Y, Kioka N, Matsuo M and K Ueda. (2006) Purification and ATPase activity of human ABCA1. Journal of Biological Chemistry 281:10760-10768.

Tanford C. (1991) *The hydrophobic effect: formation of micelles and biological membranes*, 2nd edition. Malabar, FL: Krieger.

Tang X, Halleck MS, Schlegel RA and P Williamson. (1996) A subfamily of P-type ATPases with aminophospholipid transporting activity. Science 272:1495-1497.

Tatar M, Bartke A and A Antebi. (2005) The endocrine regulation of aging by insulin-like signals. Science 299:1346-1351.

Tate MW, Eikenberry EF, Turner DC, Shyamsunder E and SM Gruner. (1991) Nonbilayer phases of membrane lipids. Chemistry and Physics of Lipids 57:147-164.

Tatischeff I, Petit PX, Grodet A, Tissier J-P, Duband-Goulet I and J-C Ameisen. (2001) Inhibition of multicellualr development switches cell death of *Dictyostelium discoideum* towards mammalian-like unicellular apoptosis. European Journal of Cell Biology 80:428-441.

Tsamaloukas A, Szadkowska H and H Heerklotz. (2006) Nonideal mixing in multicomponent lipid/detergent systems. Journal of Physics – Condensed Matter 18:S1125-S1138.

Vance JE and DE Vance. (2004) Phospholipid biosynthesis in mammalian cells. Biochemistry and Cell Biology 82:113-128.

Veatch SL and SL Keller. (2005) Seeing spots: complex phase behavior in simple membranes. Biochimica et Biophysica Acta 1746:172-185.

Vigh L, Escribá PV, Sonnleitner A, Sonnleitner M, Piotto S, Maresca B, Horváth I and JL Harwood. (2005) The significance of lipid composition for membrane activity: new concepts and ways of assessing function. Progress in Lipid Research 44:303-344.

Vishwakarma RA, Vehring S, Mehta A, Sinha A, Pomorski T, Herrmann A and AK Menon. (2005) New fluorescent probes reveal that flippase-mediated flip-flop of phosphatidylinositol across the endoplasmic reticulum membrane does not depend on the stereochemistry of the lipid. Organic and Biomolecular Chemistry 3:1275-1283.

Voet D and JG Voet. (1995) *Biochemistry*. New York, NY: John Wiley & Sons.

Wang L, Beserra C and DL Garbers. (2004) A novel aminophospholipid transporter exclusively expressed in spermatozoa is required for membrane lipid asymmetry and normal fertilization. Developmental Biology 267:203-215.

Wennerström H and E Sparr. (2003) Thermodynamics of membrane lipid hydration. Pure and Applied Chemistry 75:905-912.

Wicky S, Schwarz H and B Singer-Kruger. (2004) Molecular interactions of yeast Neo1p, an essential member of the Drs2p family of aminophospholipid translocases, and its role in membrane trafficking within the endomembrane system. Molecular and Cellular Biology 24:7402-7418.

Williamson P and RA Schlegel. (2002) Transbilayer phospholipid movement and the clearance of apoptotic cells. Biochimica et Biophysica Acta 1585:53-63.

Williamson P, Christie A, Kohlin T, Schlegel RA, Comfurius P, Harmsma M, Zwaal RF and EM Bevers. (2001) Phospholipid scramblase activation pathways in lymphocytes. Biochemistry 10:8065-8072.

Williamson P, Bevers EM, Smeets EF, Comfurius P, Schlegel RA and RF Zwaal. (1995) Continuous analysis of the mechanism of activated transbilayer lipid movement in platelets. Biochemistry 34:10448-104455.

Williamson P, Kulick A, Zachowski A, Schlegel RA and PF Devaux. (1992) Ca^{2+} induces transbilayer redistribution of all major phospholipids in human erythrocytes. Biochemistry 31:6355-6360.

Yang C, Yu L, Li W, Xu F, Cohen JC and HH Hobbs. (2003) Disruption of cholesterol homeostasis by plant sterols. Journal of Clinical Investigation 114:813-822.

Yaroslavov AA, Melik-Nubarov NS and FM Menger. (2006) Polymer-induced flip-flop in biomembranes. Accounts of Chemical Research 39:702-710.

Zachowski A and PF Devaux. (1990) Transmembrane movements of lipids. Experientia 46:644-656.

Zachowski A, Henry JP and PF Devaux. (1989) Control of transmembrane lipid asymmetry in chromaffin granules by an ATP-dependent protein. Nature 340:75-76.

Zwaal RFA, Comfurius P and EM Bevers. (2004) Scott syndrome, a bleeding disorder caused by defective scrambling of membrane phospholipids. Biochimica et Biophysica Acta 1636:119-128.

Chapter 3. A brief review of the origins and major developments of the plasma membrane hypothesis

Most textbooks present scientific knowledge as a snapshot at a particular recent point in time. However, observing the unfolding of the research process over a substantial period is much more fascinating, insightful and instructive. Such an historical approach fosters a better understanding of the effects of equipment and techniques, model systems, other research fields and other factors on the scientific theory. It also uncovers interconnections between old and modern concepts and sometimes, points out that what is considered a new hypothesis could be in fact an old well-forgotten one. Initially the intention was to capture the origins of the plasma membrane hypothesis and its major developments in a short paragraph or two, but it quickly became apparent that this topic has received only fragmentary coverage in the published literature; or papers were simply old (Jacobs, 1962; Smith, 1962; Davson, 1962). This chapter was included in this thesis to begin to remedy this deficiency, as a foundation of a future in depth review of the membrane field.

Plasma membrane as the problem of permeability and osmosis

Osmotic responses and selective permeability of living cells discovered in the first half of the 19th century were consistent with the prediction that a boundary demarcated the living matter and ensured its discontinuity with the surrounding environment. The question of the mechanism of this boundary, however, was not satisfactorily answered for the next 100 years. Before the first observations of cell membranes with electron microscopes in the 1950s, the boundary could be neither seen nor “felt”, and its nature could be only inferred from models of the observed cellular responses in permeability, electrical conductance and other indirect

experiments. These models at first were constructed as simple analogies to physico-chemical phenomena, but later became quite sophisticated and took into consideration appropriate thermodynamic laws, chemical properties of substance and wide-ranging empirical observations of the living matter. Eventually membrane-based models and theories of osmosis and cell permeability had even become in the opinion of many investigators who prized theoretical simplicity too complex to be true (Jacobs, 1962). But, perhaps the greatest impediment to the development and acceptance of the plasma membrane hypothesis of the living boundary was the view held by a majority of researchers during a major part the 100-year period that the protoplasm was a colloidal substance and cell permeability and many other cellular responses were derivatives of its colloidal character. Thus, a proper understanding of the plasma membrane concept prevalent during the protoplasm era in the history of biology requires a consideration of the colloidal theory of the living matter.

Thomas Graham, a British investigator who studied diffusion and osmosis and invented dialysis, coined the word “colloid” in 1861 to describe substances characterized by low diffusibility and “the absence of the power to crystallize”: “As gelatine appears to be its type, it is proposed to designate substances of the class as *colloids*, and to speak of their peculiar form of aggregation as the *colloid condition of matter*. Opposed to the colloids is the crystalline condition” (quoted in Wilkie, 1960, Graham’s italics; Wilkie, 1961a; Fasten, 1919). Crystalloids, substances in the latter class, readily diffused and easily crystallized. Generally, a mixture of a colloid with water could exist in the liquid dispersed state of sol (Graham’s substitute word for “colloidal solution”) or the more viscous and solidified state of gel (Graham’s shorthand for

gelatin). Graham himself applied the term “gel” only to coagula of sols: hydrosol of gelatin, for example, could coagulate after addition of mercuric chloride. Later investigators used the term promiscuously to identify jellies and other solidified states of a colloid (Thomas, 1918). Graham also concluded that “the plastic elements of the animal body are found in” the class of colloids (Wilkie, 1960), and gelatin, agar and similar substances became “model systems” in the hands of those investigators who wanted to study chemical organization thought to be peculiar to the living matter (Fenn, 1916).

While Graham discovered colloids by way of diffusion and osmosis, Nägeli’s decision to investigate one particular colloid, starch, likely sprung out of his interest in the cell formation theory of his one time mentor, Schleiden (Smith, 1962). In Schleiden’s view new cells organized *de novo* in places with plenty of starch grains: “It is in this mass that organization always takes place, and the youngest structures are composed of another distinct, perfectly transparent substance…, when dried it imbibes water and swells…” (Schleiden, 1838, p. 237). Schleiden called the transparent substance “vegetable gelatine”: “It is this gelatine which is ultimately converted by new chemical changes into the actual cellular membrane [cell wall]… and into the material of vegetable fibre” (Schleiden, 1838, p. 237). Nägeli studied starch grains and updated his theory of *organisierte Substanzen* (organized substance) as represented by starch throughout his working life (Wilkie 1960; Wilkie 1961a, 1961b). In an 1879 paper on fermentation he reformulated the theory for the final time as an answer to the questions of intracellular organization and organic matter insolubility. By then it had become clear that cells executed many frequently irreconcilable chemical reactions simultaneously.

Such arrangement required special and temporal separation of the sites of fermentation within the cell, and this implied that the intracellular organization was fairly intricate. Regarding the question of organic matter insolubility Nägeli noted, “The molecular insolubility of organized compounds must be considered one of the most important properties for the existence of organism” (quoted in Wilkie, 1960). Indeed, why do cells not dissolve in water?

In Nägeli’s view the critical attribute of organized substance was its capacity to resist dissolution by water. “The fact that soluble sugar is converted into insoluble cellulose alone gives the assurance that the cell-wall of plants will persist under all external conditions and will not some time or other run off in solution” (quoted Wilkie, 1960). This resistance of organized compounds to the solvent was therefore a direct consequence of their assembly from simple units liable to water into larger aggregates. Nägeli proposed that starch grains consisted of small particles, “starch molecules”, which assembled into higher order compounds he called *Micellen* (micellae). Then, “because of their great weight, micellae in solution are much less mobile than molecules in solution, and consequently they readily adhere together” into *Micellverbände* (micellar associations) (quoted in Wilkie, 1960). Thus, Nägeli’s model of organized substance held that the reason cells didn’t dissolve was because their constitutive components held on to each other against the eroding action of water: the cell as a result was effectively one large *Micellverbänd*.

Like gelatin, cellulose (starch grains) gained the status of a “model system” of the living matter. Sachs, an eminent German botanist, proposed to apply Nägeli’s theory of *organisierte Substanzen* to all living substances as early as 1865, before it even

included the *Micellverbänd* level of organization. As late as 1929 an American investigator Seifriz chose “cellulose for comparison with protoplasm simply because the chemists have found out more about it from the point of view of structure than about any other substance which is closely related to protoplasm” (quoted in Wilkie, 1961b). There was little doubt at the beginning of the 20th century that the protoplasm comprised a colloid (Stiles, 1921a; Spaeth, 1916).

In a very extensive review of cell permeability research published over a period of time in the early 1920s, Stiles listed 10 notable theories of this phenomenon (Stiles, 1923a, 1923b). The theories differed mainly with respect to the colloidal process at the protoplasm surface invoked to explain permeability data. The vital equilibrium theory, for example, postulated that “a *slight* increase in the aggregation of the surface colloids would involve a rise in the viscosity of the cell surface and, if an equilibrium were established, the speed of diffusion of ions and molecules across the cell surface would thus be reduced” (Spaeth, 1916); the cell surface was essentially the same substance as the rest of the protoplasm and turned more or less liquid, and hence more or less permeable, depending solely on the presence and concentration of liquefying (thiocyanate) and deliquefying agents ($CaCl_2$) (Stiles, 1923b). Other theories focused on other colloidal properties, such as phase inversion and distribution of water between phases. A stand out in this group was the Charles Overton’s lipoid view, which, unlike all the rest, postulated that the surface of the protoplasm differed from the bulk of it qualitatively and contained a substantial amount of lipid.

Overton, a British investigator, employed an osmosis-based technique (Stiles, 1923c) to determine permeability of plant (*Spirogyra*) and animal (tadpole) cells to

hundreds of chemicals and showed that the capacity of a compound to enter the cell correlated with its oil-water partition coefficient and not its size (de Weer, 2000; Al-Awqati, 1999; Kleinzeller, 1999, 1995). Before Overton's work, investigations of purely inorganic phenomena had led to two views of solute passage through live and synthetic membranes (Stiles, 1921b). The sieve theory, put forward by Moritz Traube in 1867, presented membranes as molecular sieves with pores of certain size: only compounds smaller than the size of the pores could pass through. Traube discovered and studied colloidal precipitation membranes, now known as chemical gardens (Cartwright et al., 2002), and observed that permeability of these structures declined with time due to clogging of pores (Stiles, 1921b; Tinker, 1916). According to the alternative solution theory of membrane permeability, solutes could traverse a membrane only by dissolving in and diffusing through it to the opposite side. This theory originated with experiments of Liebig in 1849 and particularly, L'Hermite in 1855. The latter investigator illustrated the theory with the "three liquid layers" experiment: when a layer of castor oil separated water from alcohol, for example, in time the oil-soluble alcohol passed through the middle layer into water (Stiles, 1921b; Dandeno, 1909). Subsequent studies by Berthelot and Jungfleisch (in 1869 -1872) and Nernst (in 1891) showed that most solutes when dissolved in a mixture of two immiscible liquids preferred one liquid over the other (Stiles, 1921c). The partition coefficient of a solute expressed this preference as a ratio of the solute concentrations in the two solvents at equilibrium. Hence cell permeability of a compound was proportional to its oil-water partition coefficient, Overton proposed that "the general osmotic properties of the cell are due to the

impregnation of the boundary layers of the protoplasm by a substance … corresponding to a fatty oil" (quoted in Kleinzeller, 1995).

While *presence* of a lipid in the protoplasm boundary satisfactorily explained passage of hydrophobic solutes into cells, a *lipid-only* layer could not account for several well-established at the time cell permeability phenomena: entrance of water and small molecules, such as urea and glycerol; uptake of inorganic salts and organic metabolites, frequently against their concentration gradient; and transport of liquid in epithelial cells (Kleinzeller, 1995, 1999; Schultz, 1998; Brooks, 1938). Overton's solution was to further hypothesize that the protoplasm boundary layer was not a distinct structure, such as a physical membrane, but rather a discontinuous mixture of oily and water-soluble substances, which individually and perhaps, in combination facilitated several cell entrance pathways; diffusion through lipids was only one of such passages (Kleinzeller, 1999; Brooks, 1938). Overton then postulated existence of static pathways, those obeying the laws of diffusion, and active pathways, those that transported substances against the laws of diffusion: "Active participation of cells matters only for such solutes which are not at all, or only slowly, taken up by most cells by a strictly osmotic process" (quoted in Kleinzeller, 1999). A German investigator, Wilhelm Pfeffer, introduced a similar distinction between physical and physiological permeability before Overton. In Pfeffer's view however, the boundary was colloidal, proteinaceous, homogenous and continuous. Nevertheless, in 1904 a collaborator of Pfeffer's, Nathansohn, synthesized Overton's and Pfeffer's views into the first mosaic (Nathansohn's term), alternating lipid-protein, membrane theory of permeability (Stiles, 1923a).

The distinction between mosaic and continuous membrane theories has not always been grasped (not found in Kleinzeller, 1999; Shultz, 1998; or Smith, 1962; but emphasized by Davson, 1989; and Brooks, 1938). Furthermore, the meaning of the term “membrane” had remained mutable and very poorly defined until at least the 1940s. Nägeli called the protoplasm surface a membrane because, in his view, this word lacked a scientific definition and could apply to any surface organization (Smith, 1962). With the discovery of Traube’s colloidal precipitation membranes, it became apparent that colloids could form membranous structures with properties of selective permeability (Cartwright et al., 2002). In 1877 Pfeffer hypothesized that precipitation membranes and the colloidal protoplasm surface could organize by a similar mechanism and proposed a dynamic discontinuous model of the *Plasmahaut*, a German term equivalent to *Plasmamembran*. “The condition for the formation of the plasma membrane exists … wherever protoplasm masses offer a free surface. But on the other hand, the particles of the plasma membrane are distributed in the protoplasm when the plasma membrane is surrounded by protoplasm on all sides, and thus two opposing forces are at work – one working to form, the other to destroy, the plasma membrane” (Pfeffer, 1877, p.139). Pfeffer considered “*Plasmahaut*” to be a “stop-gap” term until a better understanding of the boundary was achieved. In 1888 a German physicist, Georg Quincke, suggested that the protoplasm could be enveloped with a very thin – too thin to observe with a light microscope, less than 100nm – continuous liquid membrane made up of fatty oils and liquid fats (Kleinzeller, 1999; Lipnick, 1991). Quincke studied, among other things, myelin figures (Zou and Nagel, 2006) and oil-water interactions; after observing amoeboid cells he noted that some peculiar aspects

of amoeboid movement and osmosis could be explained by the presence of a liquid oil film around these single-cell organisms (Lipnick, 1991). Stiles in his review (1922) defined the term “membrane” as referring to “a layer of protoplasmic material limiting the general body of the cytoplasm and differing from it in permeability properties”. By this very loose definition the fatty oil-impregnated boundary layer of Overton, the slightly aggregated colloidal surface of Spaeth and the liquid oil membrane of Quincke were all membranes.

The mosaic theory of Nathansohn envisioned the plasma membrane as a combination of a lipid and a protein components; the protein portion of the membrane facilitated selective permeability of lipid-insoluble substances and functioned as a sieve (Kleinzeller, 1999; Davson, 1989). Overton further suggested that the fatty material impregnating the surface of the protoplasm could be cholesterol esters, lecithin or some other similar lipid; this final elaboration of the mosaic theory explained the apparent wettability of cells (Kleinzeller, 1999). Investigations of Quincke, Overton and Nathansohn have significantly advanced the membrane hypothesis of the living boundary and formulated a nucleus of the modern understanding of the plasma membrane structure. Since then the view of the cell content has changed from a colloid to a sea water-like aqueous solution: “even those organisms that did develop the capacity to live out of water still carry the ocean with them” (Voet and Voet, 1995; see Alting, 2003 for modern views of protein gelation). The conclusion from cell permeability investigations that the protoplasm boundary contained lipids foreshadowed this change by suggesting an alternative answer to Nägeli’s insolubility question: the cell did not

dissolve because its constitutive components held onto each other, but because its content was enclosed into a semi-permeable sac of lipids.

Plasma membrane as the problems of cell electrical resistance and cell surface area

Exhaustive studies of cell permeability and osmosis had accumulated a great wealth of data about these phenomena, but had not arrived at a definitive view of the mechanism of the boundary that demarcated the living matter. Investigators had sought to explain the observed empirical behavior of the cell using the laws of thermodynamics and colloidal chemistry and had constructed many theories that fell into two broad groups depending on the proposed boundary mechanism: colloid membrane theories and continuous lipid or mosaic lipid-protein membrane theories. Experimentation with cell permeability and osmosis alone could not supply convincing evidence for one group of theories over the other. The research emphasis thus began to shift away from these two processes to other phenomena, new approaches and new study systems (Skou, 1998/2004; Davson, 1989, 1962; Robertson, 1981; Höber, 1930). The Gorter and Grendel experiment on red blood cells (RBCs), cell micromanipulation studies and other investigations provided independent sets of evidence for the presence of a permanent lipid membrane around cells. Membrane models derived from studies of the electrical conductivity of cell suspensions, mostly also RBCs, proved, however, to be the most influential in shaping up the plasma membrane hypothesis for the next 50 years.

Until the 1900s RBCs had been of little importance as a cell permeability model system. In 1779 a British biologist, William Hewson, described morphological responses of these cells to various salt concentrations in the medium (without invoking osmosis or permeability) and even noted that when frog RBCs rolled down a glass slide, “the solid

middle particle [nucleus] can be distinctly seen to fall from side to side in the hollow vesicle like a pea in a bladder" (quoted in Kleinzeller, 1995). But later cell theorists focused on the lack of the nucleus in mammalian RBCs and hesitated to consider corpuscles (the original term for RBCs) to be representative of true nucleus-containing cells (Kleinzeller, 1996). At the turn of the century Overton held essentially the same view as his predecessors and disregarded, for instance, the finding that RBCs exhibited selective permeability to electrolytes (Kleinzeller, 1999; Höber, 1930). The treatment of RBCs, however, changed when it became apparent that these cells were an ideal system for many cell membrane studies.

In 1902 Julius Bernstein summarized nearly 50 years of his own and other investigators' research on electrolyte permeability in muscle and nerve cells and proposed that a slightly permeable to ions membrane separated the cell content, which was essentially an electrolyte solution, from the surrounding environment (Seyfarth, 2006; Armstrong, 1999). In the 1910s a German physiologist Rudolf Höber investigated electrical resistance properties of RBC suspensions in order to detect the presence of the plasma membrane around cells and to test Bernstein's hypothesis (McAdams and Jossinet, 1995; Robertson, 1981; Davson, 1962; McClendon, 1924; Stiles and Jörgensen, 1914). Höber took advantage of the LC (tank) circuit, which consisted an inductor (L) and a capacitor (C) sequentially connected; after charging such a circuit, electrical current flowed between the two components back and forth at a particular frequency inversely proportional to the size of the inductor and the capacitor. The total circuit resistance exhorted a dampening effect on these oscillations by reducing the frequency and the amplitude of each oscillation until the current flow ceased. Höber

constructed LC circuits in which he incorporated a container for cell suspensions and electrolyte solutions by, for example, using an inductor made of wire wrapped around a hollow cylinder or inserting a glass tube with platinum electrodes in parallel with the capacitor. He then measured oscillation decay times in the circuits and calculated the impedance due to the test material as a function of frequency. His findings were that at low frequencies (10 kHz) RBC suspensions exhibited very high resistance, while at the highest frequencies tested (≈ 10 mHz), the resistance of these same suspensions was dramatically lower and similar to that produced by 0.1%-0.4% NaCl solutions. The impedance of haemolysed RBCs, in contrast, was not frequency dependent and equaled the low values observed with intact RBC suspensions at high frequencies. Höber concluded that his findings supported Bernstein's hypothesis and indicated the presence of both a highly resistant plasma membrane, which was responsible for the high resistance at low frequencies, and an intracellular electrolyte solution, which conducted electricity well at high frequencies.

In 1920s Hugo Fricke, a physicist, investigated electric properties of RBC suspensions with greatly improved instruments and found that experimental values of resistance and capacity as functions of frequency for this biological material were similar to those predicted by an electrical circuit in which a resistor (R_1) connected in parallel with another resistor (R_2) and a capacitor (Figure 1) (Ficke and Morse, 1925). R_1 and R_2 represented resistive properties of the cell suspension medium and the intracellular content, respectively, and C stood for the capacitance of the plasma membrane. At low frequencies the AC current flowed around the cells, while at high frequencies it flowed through cells. Fricke also extended Maxwell's equation for the

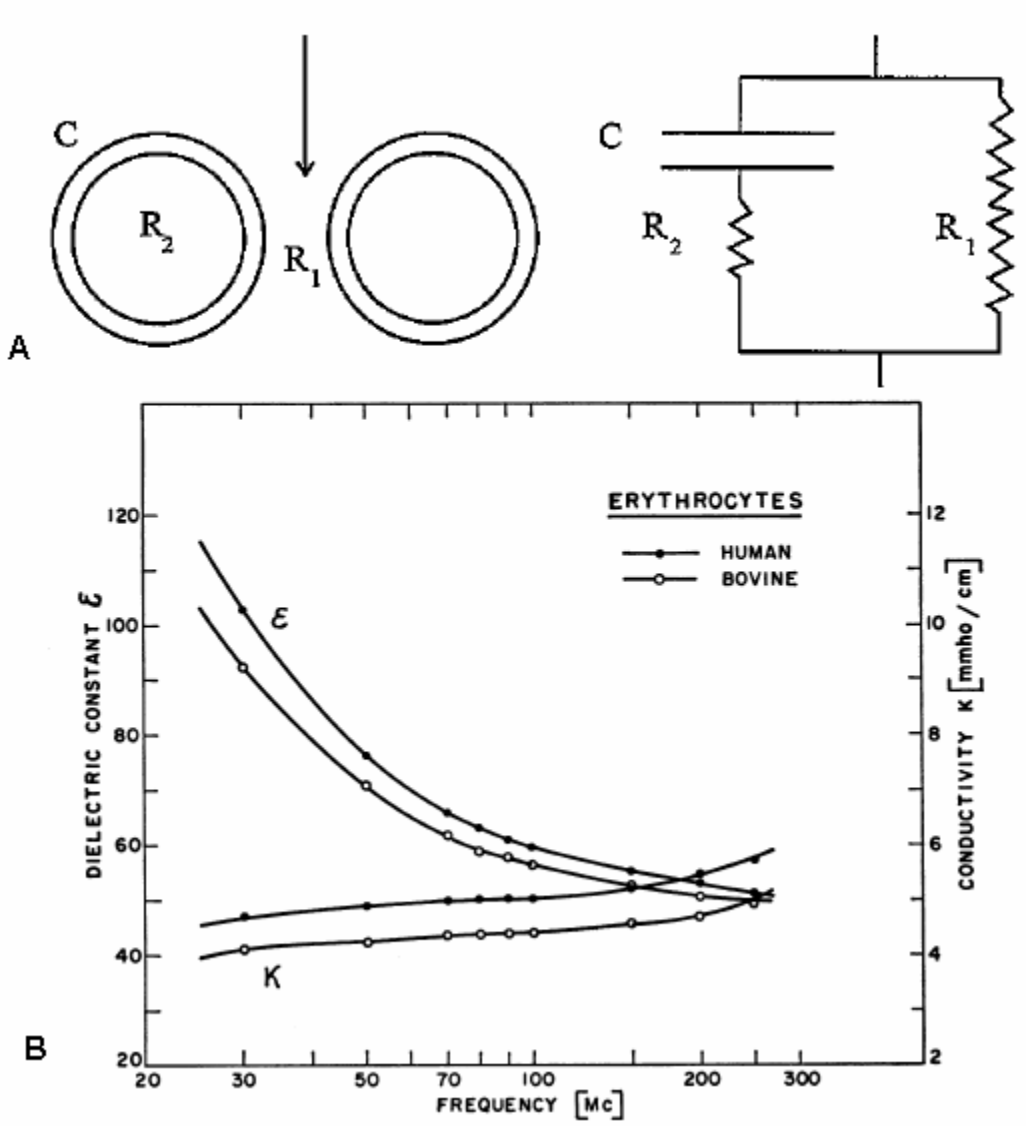

Figure 1. Electrical properties of cell suspensions and tissues. (A) The equivalent circuit model proposed by Fricke to represent electrical properties of RBC suspensions: R1 and R2 represented resistances of the cell medium and the intracellular content, respectively, and C stood for the capacitance due to the RBC plasma membrane (left – cell suspension; right – equivalent electrical circuit) (reproduced from McAdams and Jossinet, 1995). (B) Dielectric (ε) constant and conductivity (κ) of RBC suspensions as functions of applied frequency (reproduced from Pauly and Schwan, 1966).

conductivity of a dilute suspension of spherical particles to the case of oblate spheroids, such as RBCs, and calculated that capacitance of the dog RBC membrane was around 0.81 μF/cm^2. Fricke then assumed a value of 3 for the dielectric constant of the RBC plasma membrane and determined that this membrane must be 33Å thick (Fricke, 1925a; 1925b; Martinsen et al., 2002). Thus, electrical properties of RBC suspensions supported the view of the plasma membrane as a thin non-colloidal layer rich with dielectric substances, likely lipids.

In the 1920s Irving Langmuir showed that fatty acids formed monomolecular oriented films on the surface of water: the charged head groups of the fatty acid molecules were in contact with the liquid, while the hydrophobic chains protruded upward above the heads (Figure 2) (Langmuir, 1939). The fatty acid film provided a model for the arrangement of lipids in the plasma membrane. Fricke (1925c) used a Langmuir's value for the distance between two neighboring carbon atoms in a fatty acid carbon chain and calculated that only 20 to 30 sequentially bound carbons could fit in the 33Å RBC membrane perpendicular to the cell surface; the membrane, he concluded, was probably a monomolecular film of a lipid 20 to 30 carbon atoms in length. The dielectric constant value chosen by Fricke came, however, under scrutiny from Danielli (1935), who argued on purely theoretical grounds for a much higher constant and consequently, a much thicker membrane. Danielli together with his mentor Harvey (1935) also further modified Fricke's view of the plasma membrane by adding onto the lipid cell surface a layer of adsorbed protein. This modification was to explain the contradiction between the tension at the presumably lipid surface of certain cells,

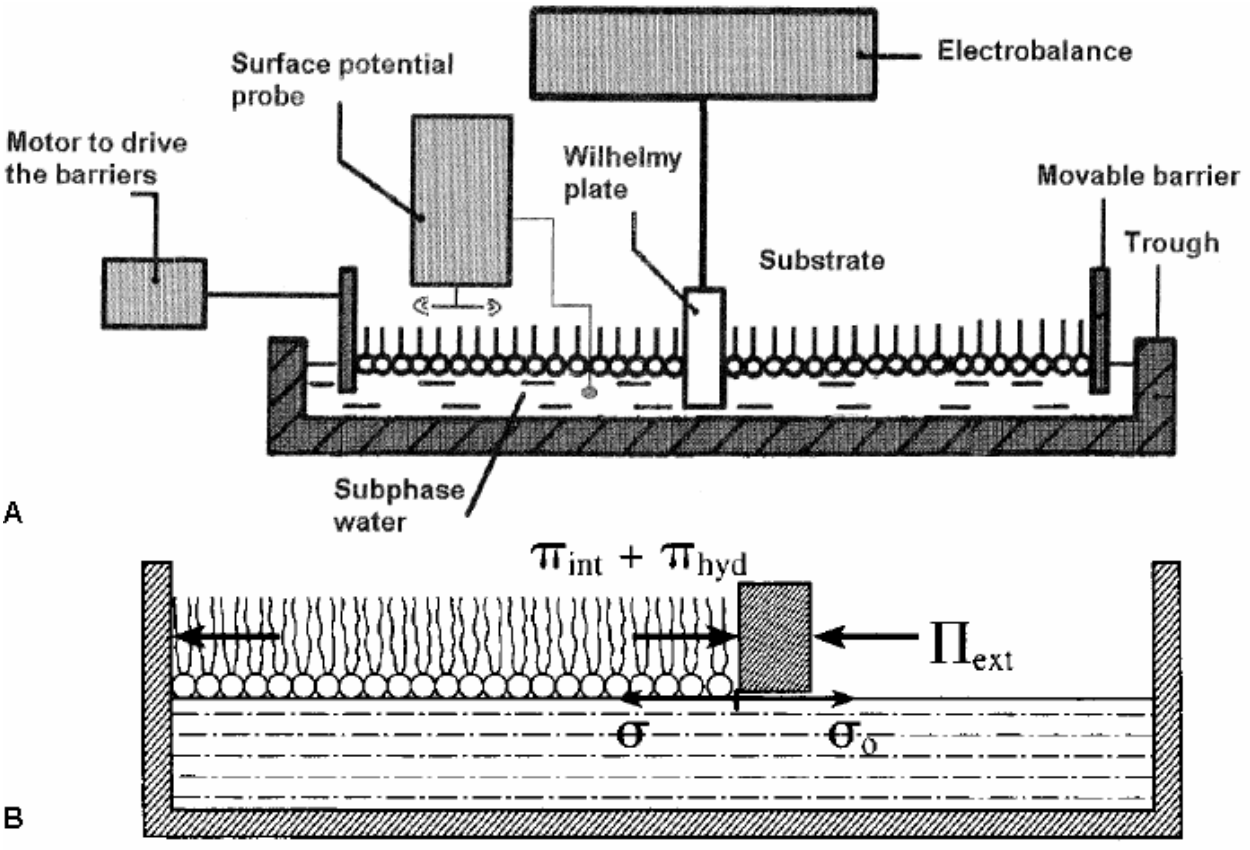

Figure 2. The Langmuir trough and Langmuir monomolecular films. (A) A Langmuir trough that contains the Wilhelmy plate for surface pressure measurements and a surface potential probe (modified from Dynarowicz-Latka et al., 2001). (B) Forces acting in the lipid monomolecular film. The total lateral surface pressure, which consists of lateral pressures due to lipid head group hydration (π_{hyd}) and the lateral interactions between lipid molecules (π_{int}), is balanced by an equal and opposite external pressure (Π_{ext}) applied to the barrier. σ and σ_0 are the interfacial tension of the film and pure water, respectively (modified from Marsh, 1996).

which was low, and the interfacial tension of cell-free lipids against water, which was, in the view of these investigators, comparatively quite high. Finally, together with Davson, Danielli (1935) proposed that the plasma membrane consisted of a disordered fatty middle surrounded on both side by an ordered layer of fatty molecules with hydrophobic chains pointed inward and polar heads outward and then, by a layer of adsorbed onto the lipid protein (Figure 3A).

When Danielli and Davson formulated their model of the plasma membrane, they were apparently unaware of the earlier and similar model by Gorter and Grendel (Davson, 1989). The latter two investigators determined that the area of water covered in the Langmuir trough by a monolayer of lipids extracted with acetone from RBCs was approximately twice as large as the cell surface area of the same amount of these cells (Gorter and Grendel, 1925). Hence the RBC plasma membrane separated two essentially aqueous phases, “the watery solution of hemoglobin” and the blood plasma, the plasma membrane lipids must arrange, Gorter and Grendel suggested, into a bilayer with the polar groups facing “to the inside and to the outside, in much the same way … as the molecules of a soap bubble are according to Perrin” (Gorter and Grendel, 1925). The two investigators then further elaborated their model by incorporating in it existing at the time observations of the lipid composition of the RBC and the behavior of lipids in Langmuir films (Davson, 1962). In 1913 Bürger and Beumer found sphingomyelin, cephalin, lecithin and cholesterol to be the major lipids in RBC extracts (Kirk, 1937). In the view of Perrin, in soap bubbles at least, two lipid monolayers that contacted along the hydrophobic surface experienced little cohesive forces and could easily slide past each other (Perrin, 1926). Inside a monolayer, however, extensive investigations

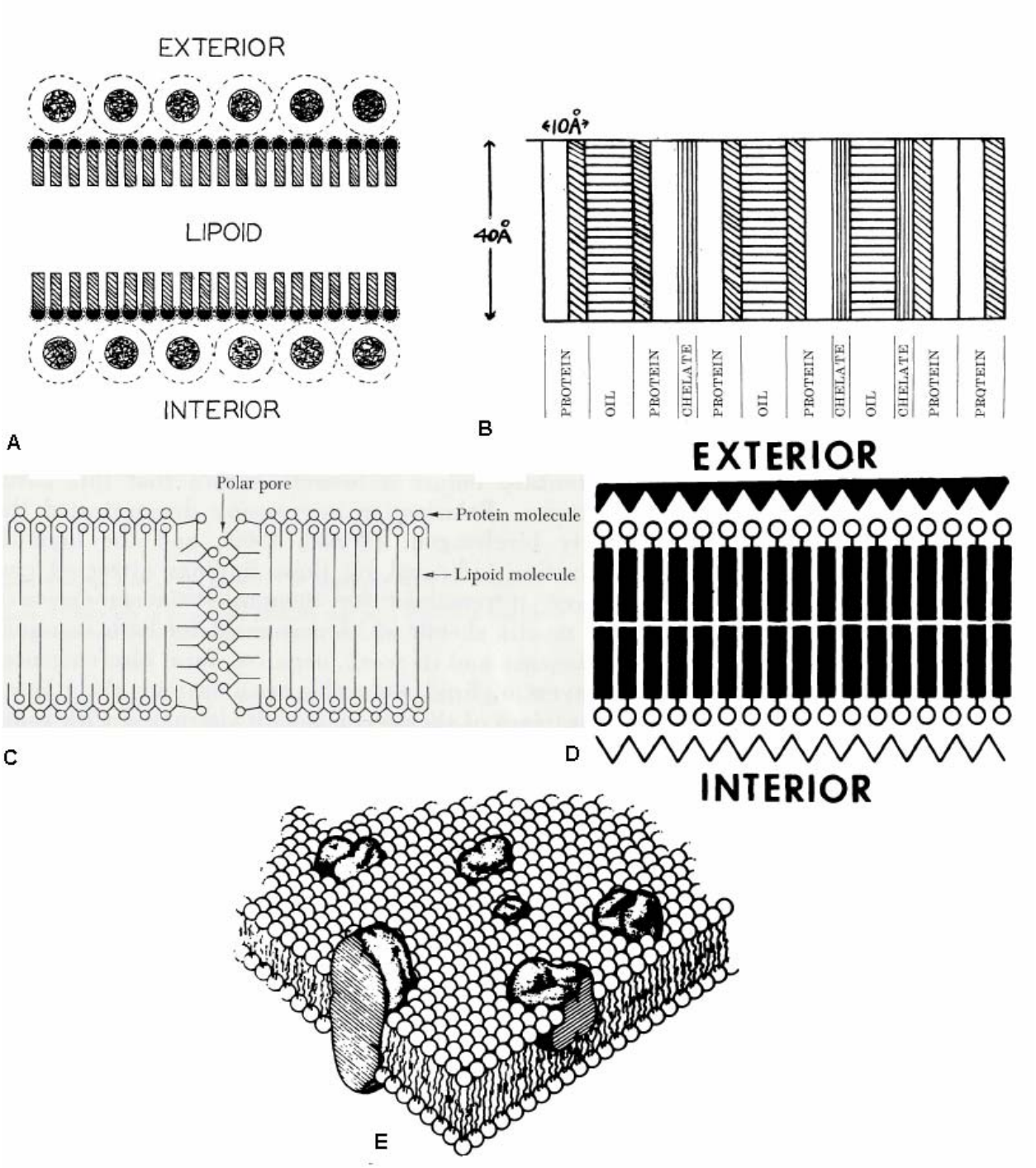

Figure 3. Most influential models of the cell membrane. (A) The Danielli-Davson model; the circles represent adsorbed protein (reproduced from Danielli and Davson, 1935). (B) The Brooks mosaic membrane model (reproduced from Brooks, 1938). (C) A modified version of the Danielli-Davson model; proteins both penetrate in between lipid molecules and form a polar pore for facilitated diffusion (reproduced from Branton and Deamer, 1972; the original in Danielli, 1954). (D) The unit membrane model; according to its author this model "resembled the earlier Danielli-Davson one but differed significantly in that only one bilayer was stipulated along

[**Figure 3 cont.**] with chemical asymmetry" (Robertson, 1982) (reproduced from Robertson, 1981; original in Robertson, 1959). (E) The fluid mosaic model of Singer and Nicolson (reproduced from Singer and Nicolson, 1972).

uncovered several lipid cooperative effects (Davson, 1962; Schulman and Stenhagen, 1938; Schulman and Rideal, 1937; Rideal et al., 1936; Schulman and Hughes, 1935). One of the most well-known and clearly demonstrated was the cholesterol's condensing effect: cholesterol addition caused lipid "expanded" (liquid) phospholipid films to "condense" into solid films of cholesterol-phospholid complexes; cholesterol also exhibited a preference for complex formation with sphingolyelin over glycerophospholipids (Cao et al., 2003; Schulman and Hughes, 1935). Gorter and Grendel speculated that monolayers of the RBC plasma membrane leaflets could consist of a mixture of lecithin expended areas and sphingomyelin-cholestrol condensed portions and thus, offered probably the earliest version of the lipid raft hypothesis (Welti and Glaser, 1994; Regen, 2002; Davson, 1962).

The Danielli-Davson and Gorter-Grendel plasma membrane models were certainly intuitive constructions inspired by the rapid advances in surface chemistry rather than hypotheses solidly rooted in experimental evidence. Nonetheless, both models have proven to be immensely influential and stimulating and have become focus points around which subsequent membrane investigations and discussions revolved. The Gorter-Grendel experiment had several critical design weaknesses (Zwaal et al., 1976; Branton and Deamer, 1972; Engelman, 1969; Bar et al., 1966). First, the use of acetone, a selective lipid solvent, led to a substantial loss of RBC lipids during the extraction. Second, the use of dried RBCs for calculations of the average RBC surface area led to an underestimation of this parameter by as much as 30%. Third and most

important, Gorter and Grendel assumed without any evidence that lipids packed inside the monolayers of the RBC plasma membrane very loosely. Thus, they measured the surface area of water covered by a monomolecular film of extracted RBC lipids as soon as this film exhibited the lowest measurable resistance to compression (Gorter and Grendel, 1925). Other investigators by that time had shown that lipid films could withstand substantial lateral surface pressures before collapsing: as the lateral pressure, usually exerted in the Langmuir trough onto the lipid film by means of a movable barrier (Figure 2), increased, the area per lipid molecule ($Å^2$/molecule) decreased (Langmuir, 1939). In 1938 Dervichian and Macheboeuf repeated the Gorter-Grendel experiment with another inefficient lipid extraction method and the same assumptions regarding the average surface area of the RBC, but instead measured the surface area of water covered by RBC lipids at near film-collapse lateral pressures and found that the ratio of the RBC lipid film area to the RBC surface area was 1 (Bar et al., 1966). Yet another reinvestigation of the Gorter-Grendel experiment found this ratio to change from 2.2, at the lowest film compression, to 1.1, at the near film collapse pressures (Bar et al., 1966). Without a good estimate of the lateral surface pressure in natural membranes, the Gorter-Grendel experiment could not be interpreted (Marsh, 1996; Engelman, 1969).

The kernel of the Danielli-Davson membrane model was already present in the Danielli-Harvey (1935) schematic of the surface of oil drops from mackerel eggs (compare Figures 3A and 4). Harvey's lab found that the surface tension of intact mackerel oil drops, as well as all investigated marine eggs and other cells, was much lower than the interfacial tension of mackerel body oil (Harvey and Shapiro, 1934).

Overton correctly explained such observations – good cell wettability and low cell surface tension – nearly 35 years earlier by the presence in the cell surface of lecithin and similar amphipathic lipids (Kleinzeller, 1999). Danielli and Harvey, however, erroneously assumed that all biologically relevant lipids exhibited comparatively high interfacial tension against water and hence, required a protein coat for good wettability (Danielli and Harvey, 1935; Haydon and Taylor, 1963). Nonetheless, even after the initial reasons for the inclusion of protein into the cell membrane structure disappeared, most membrane models still postulated existence of a polypeptide layer attached to the lipid leaflets in some fashion (Stoeckenius and Engelman, 1969; Haydon

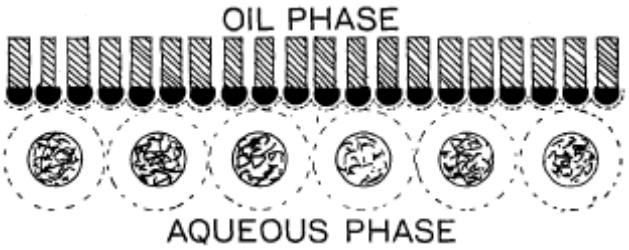

Figure 4. A schematic of the surface of the oil droplet from the mackerel egg (reproduced from Danielli and Harvey, 1935).

and Taylor, 1963). A larger deficiency of the Danielli-Davson membrane model was its inability to account for selective cell permeability of polar and charged substances (Skou, 1998/2004; Shultz, 1998). While Gorter and Grendel abstained from addressing cell permeability properties in the context of their membrane model altogether, Danielli and Davson advanced a permeability theory. In their view substances entered the cell through “relatively permanently existing” molecular size “pore structures” in the solid lipid membrane; the “pore-type structure” functioned as a molecular sieve, and “when

bathed in solutions of sodium salts, only sodium salts will be present in the lipoid layer, and water will pass readily through the film because water is relatively soluble in a phase consisting of a sodium salt" (Danielli and Davson, 1935). The theory was clearly insufficient.

In addition to the cell impedance studies and the Gorter and Grendel experiment, there were other fruitful approaches to the investigation of cell membranes. Chambers, Kite and others successfully employed various cell micromanipulation techniques (Chambers, 1938; Kite, 1913). Chambers with colleagues found, for example, that a droplet of oil applied to the plasma membrane of a mature marine egg could suddenly penetrate the membrane without disrupting it and then appear as a droplet on its cytopfacial side; when two droplets were applied at the same time and the egg medium agitated, the droplets moved relative to one another as if the membrane was fluid (Chambers and Kopac, 1937; Robertson, 1981). After an extensive review of the early membrane literature Branton and Deamer (1972) concluded that Plowe's (1931) experiments with the microneedle were probably the first direct and unambiguous demonstration of the existence of cell membranes. Schmitt et al. (1937) employed polarized light techniques to show presence of oriented perpendicular to the plane of the plasma membrane lipid molecules in RBC ghosts. There were many other insightful experiments and approaches that must be omitted here for the sake of brevity.

Stanley Schultz (1998), a modern reviewer of the membrane permeability research from the University of Texas Medical School, called the years between 1895 and 1940 a period of passivity: the community of membrane investigators, according to him, embraced during that time the unproductive paradigm of the plasma membrane as

an inert envelope and strived to explain permeability phenomena from the laws of passive diffusion. Schultz himself, however, upheld Thomas Kuhn's view of the scientific progress as a sequence of superseding paradigms and therefore, emphasized one view of the plasma membrane as paradigmatic at the expanse of richness and complexity of views and hypotheses present at any point in time. Certainly, Overton and Höbert clearly understood that simple diffusion could not account for all cell permeability processes (see above; Höbert, 1930; Harvey, 1911). Following Pfeffer they distinguished between physical and physiological/active permeability: lipid substances physically diffused through the lipid membrane inside the cell, while non-lipid chemicals, especially those moving against the concentration gradient, entered it by "physiological means". "Physiological/active permeability" subsequently became known as "ionic accumulation", then "special activity" and finally "active transport" (Teorell, 1956). The mechanism of active transport remained a mystery until Dean (1941) in a discussion of the fluxes of sodium and potassium in the muscle commented: "It is difficult to see how the muscle can get rid of the sodium by any equilibrium process…. Therefore there must be some sort of a pump…, which can pump out sodium or pump in the potassium." This insight launched the search that led to the identification of the sodium pump. The old theory of permeability by reversible chemical combination of the permeating substance with the membrane found its reinterpretation in the Osterhout's concept of the "carrier" (Osterhout, 1935; Harvey, 1911). Brooks revived Nathansohn's mosaic membrane (Figure 3B; Brooks, 1938), and Danielli later developed it into the concept of facilitated diffusion through protein pores (Figure 3C; Danielli, 1962). Thus, the field of membrane research advanced in the first part of the 20th century through

accrual of incremental changes and frequently, reinterpretation of existing concepts, rather than by major paradigmatic shifts.

Early direct observations of cell membranes

Significant advances in physics and in particular, critical discoveries in quantum mechanics enabled development of techniques and instruments capable of directly measuring certain parameters of lipids in a bilayer (nuclear magnetic and electron spin resonance, Raman spectroscopy) and visualizing cellular membranes (X-ray diffraction, electron microscopy, freeze-fracture) (Freedman, 2001; Israelachvili et al., 1980; Branton and Deamer, 1972; Sjöstrand, 1968). Invention of the methods for preparation of synthetic lipid bilayers – liposomes and bimolecular (black) lipid membranes – further facilitated progress in the field (Bangham, 1972; Tien and Diana, 1968). The inert, stable and repetitively ordered myelin sheath of the axon was well suited for X-ray diffraction analysis; first low resolution diffraction data indicated that myelin consisted of "cylindrical smectic fluid-crystalline lipid layers wrapped concentrically around the axon" (Schmitt et al., 1941). A 10Å resolution structure of the myelin sheath provided some dimensions for the internal organization of the myelin membrane (Figure 5): the transverse distance between the polar groups in the bilayer was found to be 35-38Å, depending on the source of myelin; the hydrocarbon chains packed closely near the water-lipid interface, but were pliant and disordered close to the bilayer center; the terminal methyl groups of the chains resided in the middle layer of about 15Å thick; and, the notable asymmetry of the electron density profile indicated preferential localization of cholesterol in the extrafacial leaflet of the membrane (Caspar and Kirchner, 1971; Blaurock, 1982; Nelander and Blaurock, 1978). Membranes other than myelin, however,

required mechanical compaction or dispersion by sonication in order to become suitable for X-ray diffraction analysis (Branton and Deamer, 1972; Sjöstrand, 1968). Such drastic treatments could have potentially altered membrane structure, but not always ensured a high quality X-ray diffraction pattern. More importantly, X-ray diffraction was an averaging technique; it could not, for example, determine whether the myelin sheath membrane was continuous with the plasma membrane of the Schwann cell (Branton and Deamer, 1972). Nonetheless, X-ray diffraction models of myelin were very useful for comparison with images obtained by electron microscopy to ascertain that both techniques faithfully represented membrane structure (Robertson, 1981; Finean, 1962).

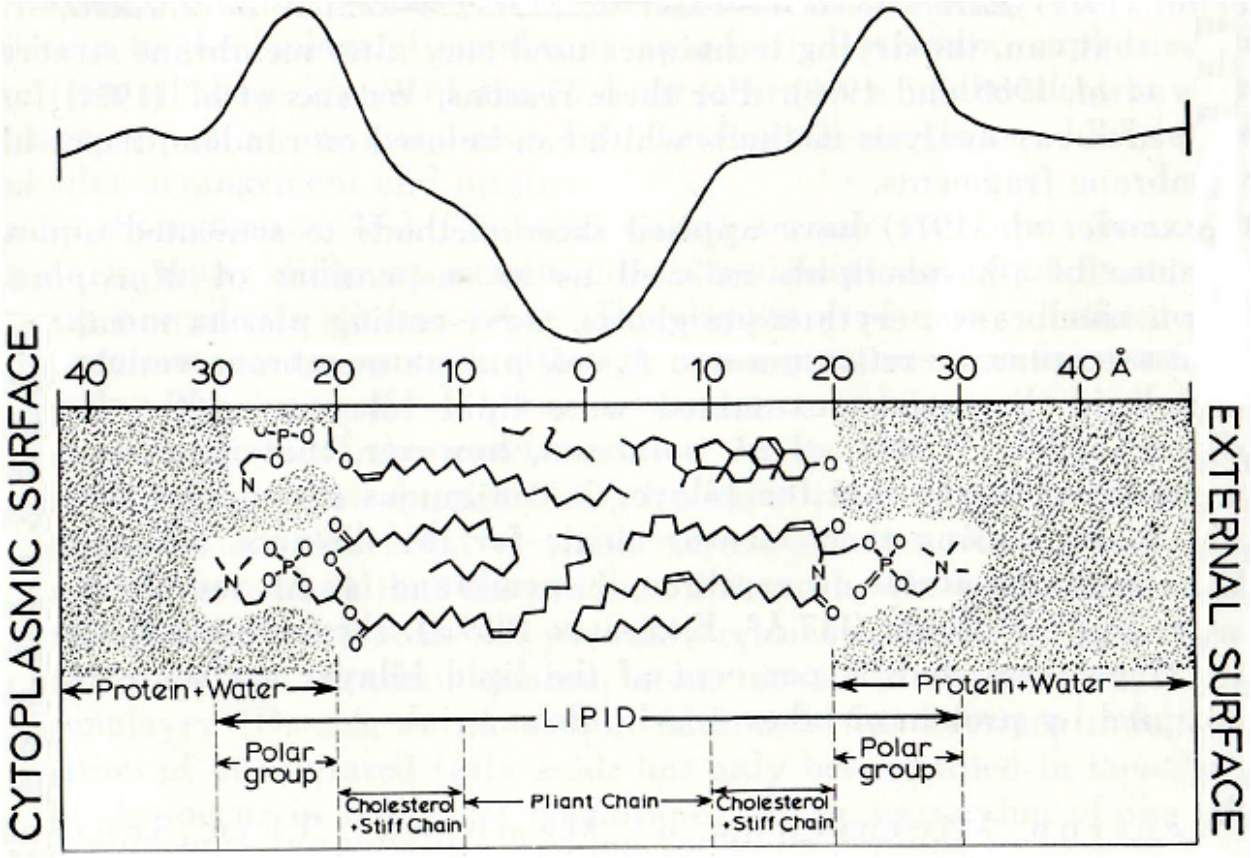

Figure 5. An electron density profile (top), and its interpretation (bottom), of rabbit sciatic myelin (modified from Branton and Deamer, 1972; original in Caspar and Kirschner, 1971).

In the early electron micrographs cell membranes appeared as dense thick lines (see for example Geren and Schmitt, 1954). Robertson (1957) was able, however, to improve image contrast through application of novel sample preparation methods (in particular, fixation with membrane-friendly permanganate; Luft, 1956) and to obtain micrographs in which cell membranes were clearly seen as “railroad tracks”: two dense dark 20Å-thick lines separated by a light 35Å-thick space (Figure 6). In Robertson’s interpretation, the dense lines represented protein and the light middle was the lipid bilayer; the whole triple-layer structure he called the unit membrane to emphasize that this was the most elementary and general organization of the cell membrane (Robertson, 1959) (Figures 3D, 6). The unit membrane was essentially the Danielli-Davson model with some modifications. In the following years investigators strived to

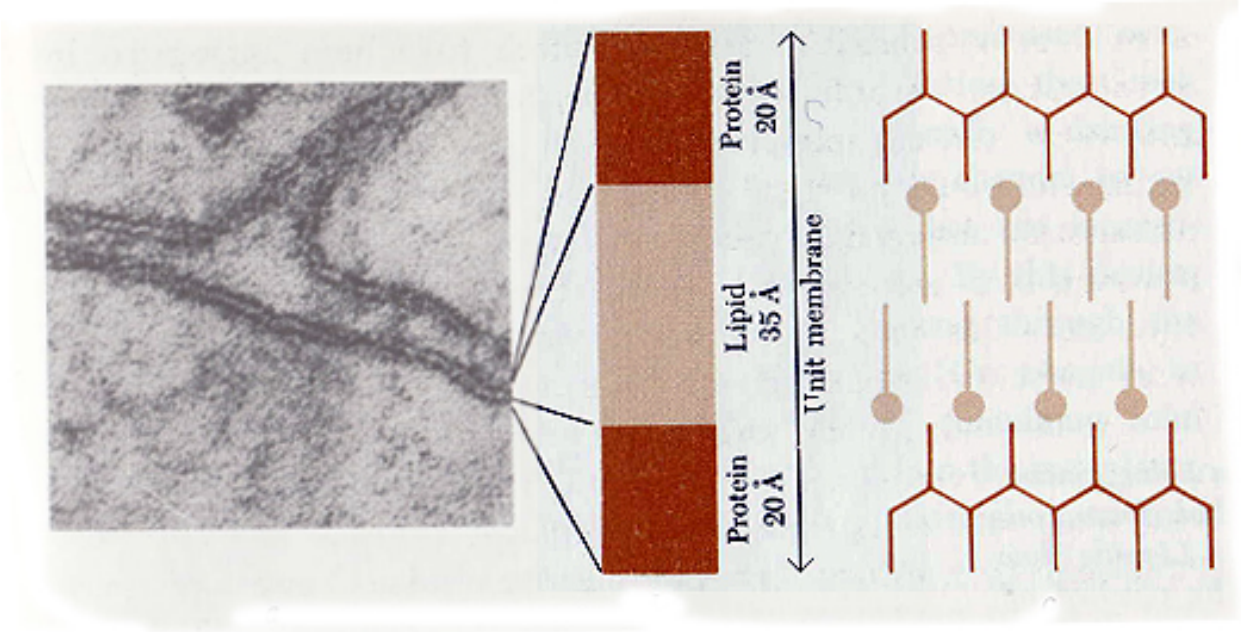

Figure 6. The unit membrane. An electron micrograph (left) of cell membranes at a junction of three cells and its graphic interpretation (right) (reproduced from Swanson, 1969).

determine whether the electron microscope “railroad track” image was indeed artifact-free and whether the lines and the light middle corresponded to protein and lipid, respectively, as Robertson proposed (Robertson, 1981; Rothfield and Finkelstein, 1968; Sjöstrand, 1968; Korn, 1966). These efforts yielded several suggestions most of which eventually turned out to be erroneous. Notable among these new proposals was the revival of Pfeffer’s concept of structural membrane subunits (particles) (see above) (Stoeckenius and Englman, 1969; Rothfield and Finkelstein, 1968; Korn, 1966). In some electron micrographs there were cross-bridges between the two dark lines; in others (outer segment frog retina images, for example), membranes appeared as arrays of spherical particles. These observations encouraged a biochemical search for an elementary structural unit, which, from theoretical considerations, could have been a lipoprotein micelle. “Dissolution” of myelin, erythrocyte and other membranes by detergents and lysolecithin into homogenous fragments at first seemed to support the subunit model; however, no evidence emerged to show that these fragments were indeed membrane subunits, and the model was eventually abandoned. Thus, the 1957 and 1959 papers by Robertson – exactly 50 years ago – were the first direct demonstrations of the existence of distinct structures – membranes – around all cells, inside the cell (endoplasmic reticulum) and around most cell organelles.

In 1972 Singer and Nicolson proposed the still current fluid mosaic model of the membrane structure (Figure 3E). This model rejected the existence of protein monolayers covering both sides of the bilayer on thermodynamic grounds; such a trilaminar structure would be thermodynamically unstable because the polar and ionic groups of the lipid would be blocked from contact with water by non-polar amino acid

residues of the protein. Instead, the lipid surface was postulated to be “naked”; protein molecules could associate with it only in some regions through either weak electrostatic interactions (peripheral) or in the case of integral proteins, much stronger hydrophobic contacts. The amphipathic integral proteins dipped into the hydrophobic bilayer interior or penetrated the whole width of the bilayer contacting aqueous solutions on both sides of it. Previous membrane models implied that the membrane monolayers were fluid but heterogeneous (Gorter-Grendel) or remained ambiguous regarding the state of lipids (Danielli-Davson). The Singer-Nicolson model, in contrast, strongly emphasized fluidity and homogeneity of the lipid leaflets and denied existence of any lipid order, although it allowed for the presence of small ordered patches due to protein-protein and protein-lipid interactions. The model rested to a large extent on evidence from freeze-etching micrographs and the Frye and Edidin experiment with cell fusion heterokaryons. Freeze-etching (or fracture) differed from standard thin section electron microscopy with respect to sample preparation and the observation plain; the sample did not need fixation and dehydration, instead it was rapidly frozen; fractured with a cooled microtome knife; etched (sublimation of a small amount of frozen water from the surface of the fracture plain); and shadowed with metal and replicated (Verkleij and Ververgaert, 1978). The replica was then observed with an electron microscope. Initially there was some uncertainty regarding the fracture plain through membranes; later it became apparent, however, that lipid bilayers fractured along the contact surface between the two leaflets. Individual protein molecules penetrating the bilayer appeared in freeze-fracture micrographs as particles on otherwise smooth lipid matrix. In the Frye-Edidin experiment the dynamics of intermixing of human and mouse antigenic components in

human-mouse fusion heterokaryons was followed by means of immunofluorescence (Frye and Edidin, 1970). Immunofluorescently labeled proteins appeared to achieve complete intermixing in a relatively short period of time after cell fusion: 40 min at 37ºC. Thus, the Singer-Nicolson membrane model introduced a dramatically different, previously unknown view of proteins in membranes, and in opposition to Gorter-Grendel, placed strong emphasis on lipid homogeneity over complexity of lipid interactions.

References

Al-Awqati Q. (1999) One hundred years of membrane permeability: does Overton still rule? Nature Cell Biology 1: E201-E202.

Alting AC. (2003) Cold gelation of globular proteins. Thesis. Wageningen University, the Netherlands.

Armstrong CM. (1999) A short history of ion channels and signal propagation. Current Topics in Membranes 48:283-301.

Bangham AD. (1972) Model membranes. Chemistry and Physics of Lipids 8:386-392.

Bar RS, Deamer DW and DG Cornwell. (1966) Surface area of human erythrocyte lipids: reinvestigation of experiments on plasma membrane. Science 153:1010-1012.

Blaurock AE. (1982) Evidence of bilayer structure and of membrane interactions from X-ray diffraction analysis. Biochimica et Biophysica Acta 650:167-207.

Branton D and DW Deamer. (1972) Membrane structure. In M Alfert, H Bauer, W Sandritter and P Sitte (Eds.), *Protoplasmatologia* Wien: Springer-Verlag.

Brooks SC. (1938) The chemical nature of the plasma membrane as revealed by permeability. American Naturalist 72:124-140.

Cao H, Tokutake N and SL Regen. (2003) Unraveling the mystery surrounding cholesterol's condensing effect. Journal of American Chemical Society 125:16182-16183.

Caspar DLD and D Kirschner. (1971) Myelin membrane structure at 10Å resolution. Nature 231:46-52.

Cartwright JHE, Garcia-Ruiz JM, Novella ML and F Otálora. (2002) Formation of chemical gardens. Journal of Colloid and Interface Science 256:351-359.

Chambers R. (1938) The physical state of protoplasm with special reference to its surface. American Naturalist 72:141-159.

Chambers R and MJ Kopac. (1937) The coalescence of living cells with oil drops. I. *Arbacia* eggs immersed in sea water. Journal of Cellular and Comparative Physiology 9:331-345.

Dandeno JB. (1909) Osmotic theories, with special references to van't Hoff's law. Bulletin of the Torrey Botanical Club 36:238-298.

Danielli JF. (1962) Structure of the cell surface. Circulation 26:1163-1166.

Danielli JF. (1954) The present position in the field of facilitated diffusion and selective active transport. Colston Papers 7:1-14.

Danielli JF. (1935) The thickness of the wall of the red blood corpuscle. Journal of General Physiology 19:19-22.

Danielli JF and H Davson (1935) A contribution to the theory of permeability of thin films. Journal of Cellular and Comparative Physiology 5:495-508.

Danielli JF and EN Harvey. (1935) The tension at the surface of mackerel egg oil, with remarks on the nature of the cell surface. Journal of Cellular and Comparative Physiology 5:483-494.

Davson H. (1989) Biological membranes as selective barriers to diffusion of molecules. In DC Tosteson (Ed.), *Membrane transport: people and ideas* (pp. 15-34). Bethesda, MD: American Physiological Society.

Davson H. (1962) Growth of the concept of the paucimolecular membrane. Circulation 26:1022-1037.

Dean RB. (1941) Theories of electrolyte equilibrium in muscle. Biological Symposia 3:331-348.

Dynarowicz-Latka P, Dhanabalan A and ON Oliveira Jr. (2001) Modern physiological research on Langmuir monolayers. Advances in Colloid and Interface Science 91:221-293.

Engelman DM. (1969) Surface area per lipid molecule in the intact membrane of the human red cell. Nature 223:1279-1280.

Fasten N. (1919) Colloids and living phenomena. Scientific Monthly 9:465-473.

Fenn WO. (1916) Similarity in the behavior of protoplasm and gelatine. Proceedings of the National Academy of Sciences of the United States of America 2:539-543.

Finean JB. (1962) The nature and stability of the plasma membrane. Circulation 26:1151-1162.

Freedman JC. (2001) Cell membranes and model membranes. In N Sperelakis (Ed.), *Cell physiology sourcebook*, 3rd edition (pp. 65-79). San Diego, CA: Academic Press.

Fricke H. (1925a) A mathematical treatment of the electrical conductivity and capacity of disperse systems. II. The capacity of a suspension of conducting spheroids surrounded by a non-conducting membrane for a current of low frequency. Physical Review 26:678-681.

Fricke H. (1925b) The electric capacity of suspensions of red corpuscles of a dog. Physical Review 26:682-687.

Fricke H. (1925c) The electric capacity of suspensions with special reference to blood. Journal of General Physiology 19:137-152.

Fricke H and S Morse. (1925) The electric resistance and capacity of blood for frequencies between 800 and 4½ million cycles. Journal of General Physiology 9:153-167.

Frye LD and M Edidin. (1970) The rapid intermixing of cell surface antigens after formation of mouse-human heterokaryons. Journal of Cell Science 7:319-335.

Geren BB and FO Schmitt. (1954) The structure of the Schwann cell and its relation to the axon in certain invertebrate nerve fibers. Proceedings of the National Academy of Sciences of the United States of America 40:863-869.

Gorter E and F Grendel. (1925) On bimolecular layers of lipids on the chromocytes of the blood. Journal of Experimental Medicine 41:439-443.

Harvey EN. (1911) Studies on the permeability of cells. Journal of Experimental Zoology 10:507-556.

Harvey EN and H Shapiro. (1934) The interfacial tension between oil and protoplasm within the living cell. Journal of Cellular and Comparative Physiology 5: 255-267.

Haydon DA and J Taylor. (1963) The stability and properties of bimolecular lipid leaflets in aqueous solution. Journal of Theoretical Biology 4:281-296.

Höbert R. (1930) The first Reynold A. Spaeth memorial lecture. The present conception of the structure of the plasma membrane. Biological Bulletin LVIII:117.

Israelachvili JN, Marčelja S and RG Horn. (1980) Physical principles of membrane organization. Quarterly Review of Biophysics 13:121-200.

Jacobs MH. (1962) Early history of the plasma membrane. Circulation XXVI:1013-1021.

Kirk E. (1937) The concentration of lecithin, cephalin, ether-insoluble phosphatide, and cerebrosides in plasma and red blood cells of normal adults. Journal of Biological Chemistry 123:637-640.

Kite GL. (1913) The relative permeability of the surface and interior portions of the cytoplasm of animal and plant cells. Biological Bulletin 25:1-7.

Kleinzeller A. (1999) Charles Ernest Overton's concept of a cell membrane. Current Topics in Membranes 48:1-49.

Kleinzeller A. (1996) William Hewson's studies of red blood corpuscles and the evolving concept of a cell membrane. American Journal of Physiology 271 (Cell Physiology 40):C1-C8.

Kleinzeller A. (1995) The postulate of the cell membrane. In A Kleinzeller (Volume Ed.), A Neuberger and LLM van Deenen (Series Eds.), Comprehensive Biochemistry 39. *Selected topics in the history of biochemistry. Exploring the cell membrane: conceptual developments* (pp. 27-90). Amsterdam: Elsevier.

Korn ED. (1966) Structure of biological membranes. Science 153:1491-1498.

Langmuir I. (1939) Pilgrim Trust Lecture. Molecular layers. Proceedings of the Royal Society of London. Series A, Mathematical and Physical Sciences 170:1-39.

Lipnick RL. (1991) Charles Ernest Overton: narcosis studies and a contribution to general pharmacology. In RL Lipnick (Ed.), Studies of narcosis, an English translation of Charles E. Overton's 1901 book *Studien uber die Narkose*. London: Chapman and Hall and Wood Library-Museum of Anesthesiology, 1991.

Luft JH. (1956) Permanganate – a new fixative for electron microscopy. Journal of Biophysical and Biochemical Cytology 2:799-802.

Marsh D. (1996) Lateral pressure in membranes. Biochimica et Biophysica Acta 1286:183-223.

Martinsen ØG, Grimnes S and HP Schwan. (2002) Interface phenomena and dielectric properties of biological tissue. In A Hubbard (Ed.), *Encyclopedia of surface and colloid science* (pp. 2643-2652). New York, NY: Marcel Dekker.

McAdams ET and J Jossinet. (1995) Tissue impedance: a historical overview. Physiological Measurement: 16:A1-A13.

McClendon JF. (1924) Electric conductivity of red blood corpuscles using high frequency alternating currents. Science 60:204.

Nelander JC and AE Blaurock. (1978) Disorder in nerve myelin: phasing the higher order reflections by means of the diffuse scatter. Journal of Molecular Biology 118:497-532.

Osterhout WJV. (1935) How do electrolytes enter the cell? Proceedings of the National Academy of Sciences of the United States of America 21:125-132.

Pauly H and HP Schwan. Dielectric properties and ion mobility in erythrocytes. Biophysical Journal 6:621-639.

Perrin JB. (1926) Nobel lecture. Discontinuous structure of matter. In *Nobel lectures, Physics 1922-1941*. Amsterdam: Elsevier Publishing Co., 1965.

Pfeffer W. (1877) *Osmotic investigations: studies on cell mechanics.* Trans. by GR Kepner; ed. by J Stadelman. New York, NY: Van Nostrand Reinhold, 1985.

Plowe JQ. (1931) Membranes in the plant cell. I. Morphological membranes at protoplasmic surfaces. Protoplasma 12:196-220.

Regen SL. (2002) Lipid-lipid recognition in fluid bilayers: solving the cholesterol mystery. Current Opinion in Chemical Biology 6:729-735.

Rideal EK, Adam NK, Gee G, Askew FA, Mitchell JS, Schulman JH, Gatty O, Gorter E, Danielli JF and A Hughes. (1936) Discussion on surface phenomena: films. Proceedings of the Royal Society of London. Series A, Mathematical and Physical Sciences 155:684-711.

Robertson JD. (1982) This week's citation classic. Current Contents 1:20.

Robertson JD. (1981) Membrane structure. Journal of Cell Biology 91:189s-204s.

Robertson JD. (1959) The ultrastructure of cell membranes and their derivatives. Biochemical Society Symposium 16:3-43.

Robertson JD. (1957) New observations on the ultrastructure of the membranes of frog peripheral nerve fibers. Journal of Biophysical and Biochemical Cytology 3:1043-1048.

Rothfield L and A Finkelstein. (1968) Membrane biochemistry. Annual Review of Biochemistry 37:463-496.

Schleiden MJ. (1838) Contribution to phytogenesis. Trans. by H Smith, appended to T Schwann, *Microscopical researches into the accordance in the structure and growth of animals and plants* (pp. 231-268). New York, NY: Kraus Reprint Co., 1969.

Schmitt FO, Dear RS and KJ Palmer. (1941) X-ray diffraction studies on the structure of the nerve myelin sheath. Journal of Cellular and Comparative Physiology 18:31-42.

Schmitt FO, Bear RS and E Ponder. (1936) Optical properties of the red cell membrane. Journal of Cellular and Comparative Physiology 9:89-92.

Schulman JH and AH Hughes. (1935) Monolayers of proteolytic enzymes and proteins. Mixed unimolecular films. Biochemical Journal 29:1243-1252.

Schulman JH and EK Rideal. (1937) Molecular interaction in monolayers: I. Complexes between large molecules. Proceeding of the Royal Society of London. Series B, Biological Sciences 122:29-45.

Schulman JH and E Stenhagen. (1938) Molecular interaction in monolayers. III. Complex formation in lipid monolayers. Proceedings of the Royal Society of London. Series B, Biological Sciences 126:356-369.

Schultz SG. (1998) A century of (epithelial) transport physiology: from vitalism to molecular cloning. American Journal of Physiology 274 (Cell Physiology 43):C13-C23.

Seyfarth E-A. (2006) Julius Bernstein (1839-1917): pioneer neurobiologist and biophysicist. Biological Cybernetics 94:2-8.

Singer SJ and GL Nicolson. (1972) The fluid mosaic model of the structure of cell membranes. Science 175:720-731.

Sjöstrand FS. (1968) Ultrastructure and function of cellular membranes. In AL Dalton and F Haguenau (Eds.), *Ultrastructure in biological systems. Vol IV. The membranes*. (pp. 151-210). New York, NY: Academic Press.

Skou JC. (1998/2004) The identification of the sodium pump. Republication of the 1998 Nobel Prize Lecture. Bioscience Reports 24:437-451.

Smith HW. (1962) The plasma membrane, with notes on the history of botany. Circulation 26:987-1012.

Spaeth RA. (1916) The vital equilibrium. Science XLII:502-509.

Stiles W. (1923a) Permeability. Chapters XIII and XIV (Theories of cell permeability). New Phytologist 22:204-224.

Stiles W. (1923b) Permeability. Chapters XIV (Theories of cell permeability, continued) and XV. New Phytologist 22:239-280.

Stiles W. (1923c) Permeability. Chapter XI (The determination of the permeability of plant cells to dissolved substances. New Phytologist 22:1-29.

Stiles W. (1922) Permeability. Chapter VIII (The plasma-membrane). New Phytologist 21:140-162.

Stiles W. (1921a) Pemeability. Chapters I and II. New Phytologist 20:45-55.

Stiles W. (1921b) Permeability. Chapter V. New Phytologist 20:186-194.

Stiles W. (1921c) Permeability. Chapter IV (Diffusion). New Phytologist. 20:137-149.

Stiles W and I Jörgensen. (1914) The measurement of electrical conductivity as a method of investigation in plant physiology. New Phytologist 13:226-242.

Stoeckenius W and DM Engelman. (1969) Current models for the structure of biological membranes. Journal of Cell Biology 42:613-646.

Swanson CP. (1969) *The cell.* 3rd edition. Englewood Cliffs, NJ: Prentice-Hall, Inc.

Teorell T. (1956) Eighth Spiers Memorial Lecture. Transport phenomena in membranes. Discussion of the Faraday Society 21:9-26.

Thomas AW. (1918) The nomenclature used in colloid chemistry. A plea for reform. Science 47:10-14.

Tien HT and AL Diana. (1968) Bimolecular lipid membranes: a review and a summary of some recent studies. Chemistry and Physics of Lipids 2:55-101.

Tinker F. (1916) The microscopic structure of semipermeable membranes and the part played by surface forces in osmosis. Proceedings of the Royal Society of London. Series A, Papers of a Mathematical and Physical Character 92:357-372.

Verkleij AJ and HJT Ververgaert. (1978) Freeze-fracture morphology of biological membranes. Biochimica et Biophysica Acta 515:303-327.

Voet D and JG Voet. (1995) *Biochemistry*. New York, NY: John Wiley & Sons.

de Weer P. (2000) A century of thinking about cell membranes. Annual Review of Physiology 62:919-926.

Welti R and M Glaser. (1994) Lipid domains in model and biological membranes. Chemistry and Physics of Lipids 73:121-137.

Wilkie JS. (1961a) Carl Nägeli and the fine structure of living matter. Nature 190:1145-1150.

Wilkie JS. (1961b) Nägeli's work on the fine structure of living matter – IIIb. Annals of Science 17:27-62.

Wilkie JS. (1960) Nägeli's work on the fine structure of living matter – I. Annals of Science 16:11-41.

Zou L-N and SR Nagel. (2006) Stability and growth of single myelin figures. Physical Review Letters 96:138301.

Zwaal RFA, Demel RA, Roelofsen B and LLM van Deenen. (1976) The lipid bilayer concept of cell membranes. Trends in Biochemical Sciences 1:112-114.

Chapter 4. Structure and transcription of *tat-1* through *5* genetic loci in *C. elegans*

Introduction

The *Caenorhabditis elegans* genome contains six predicted open reading frames (ORFs)[1] encoding peptides that would belong to subfamily IV of the P-type ATPase superfamily, the group of putative transbilayer amphipath transporters (TATs). Accordingly, these ORFs were named *tat-1* through *6* (Table I). The systematic cDNA sequencing project of Kohara identified at least one cDNA clone per each *tat* (Shin-i and Kohara, 1999). The *C. elegans* ORFeome cloning project also was able to isolate partial cDNA transcripts of the six ORFs (Lamesch et al., 2004). Thus, *tat-1* through *6* are all transcribed.

The structure of a genetic locus is usually uncovered through indirect sequencing and analysis of as many mRNA transcripts that arose from that locus as possible. The sequencing is indirect because mRNA is first reverse transcribed into more stable and easier to sequence cDNA. Unfortunately, cDNA synthesis from mRNA is generally inefficient and often generates many truncated cDNA clones. The method of cDNA production employed by Kohara's cDNA sequencing project uses the poly-dT primer that anneals to the mRNA poly(A) tail to prime cDNA polymerization from the very 3' to the 5' end of the mRNA transcript (Shin-i and Kohara, 1999). This particular method guarantees that all cDNA molecules contain an intact 3' end; but, because of poor processivity of reverse transcriptases, it also ensures that only some of these molecules

[1]The term "genetic locus" means here "the stretch of DNA that is characterized … by finding a complete open reading frame", as defined by Brenner (2000); an ORF may or may not give rise to a functional protein product; the term "gene" then signifies convergence of phenotypic and molecular data and identifies "a complete chromosomal segment responsible for making a functional product" (Snyder and Gerstein, 2003).

have a complete 5' end. The longer and more "difficult" the mRNA template, the fewer full-length cDNA transcripts it yields. The *tat* ORFs are rather long, 3.5 to 4.5 kb in length. Not surprisingly, Kohara's group cDNA libraries contain many full-length clones of only *tat-5*, a more abundantly expressed *tat*. The rest of the *tat* ORFs are represented by very few cDNA transcripts (only 4 for *tat-4*), none of which is complete. It is unlikely that a different similarly constructed cDNA library would contain more *tat* transcripts; alternative methods of cDNA synthesis, using random primers for example, produce even poorer results (NN Lyssenko, unpublished observations).

Table I. WormBase IDs and given names of the 6 ORFs encoding P-type ATPases in subfamily IV.

Given name	WormBase ID
tat-1	Y49E10.11
tat-2	H06H21.10
tat-3	W09D10.2
tat-4	T24H7.5
tat-5	F36H2.1
tat-6	F02C9.3

Rare full-length cDNA transcripts can be amplified using the polymerase chain reaction (PCR) and taking advantage of the data from Kohara's cDNA sequencing project and of the peculiar *C. elegans* pre-mRNA processing mechanism (Antebi et al., 2000). Pre-mRNA processing in the nematode involves *trans*-splicing of the 5' untranslated mRNA region (UTR) in the first exon to the RNA sequence carried by small nuclear ribonucleic particles (snRNP) of a particular type (Blumenthal, 1995; 2004). The end result of *trans*-splicing is the presence of a 22 nucleotide-long spliced leader (SL) sequence at the 5' end of the mRNA. A large (~ 70%) majority of C. elegans genes, but not all and not all transcripts of the same gene, undergo *trans*-splicing. The highly conserved SL1 sequence appears at the start of transcripts from standalone and first in

the operon genes; transcripts from cistrons located downstream (2nd and further down) of the first operon cistron (Blumenthal et al., 2002) can begin with the SL1, SL2 or any one of the related sequences collectively referred to as SL2-like. Thus, *C. elegans* full-length cDNA transcripts are open to amplification using a gene specific primer designed based on the 3' end data from Kohara's group to anneal within the ultimate exon and an SL1 or SL2 specific, gene non-specific, primer.

The PCR-based method of full-length cDNA transcript amplification with gene-specific and SL-specific primers is an expedient but not an exhaustive approach to full-length cDNA cloning and genetic locus characterization. First, it is only applicable to *trans*-spliced genes. Second, it omits leader-less transcripts of partially *trans*-spliced genes. Third, it might significantly distort the cDNA splice isoform composition and even cause loss of some alternative transcripts. Like in mammals, in *C. elegans* genes commonly contain many exons and introns, and the pre-mRNA processing involves extensive alternative splicing (Ast, 2004). Each ORF is likely to be a source of many alternative mRNA transcripts, some of which would be aberrant and a target of nonsense-mediated decay (NMD) (Weischenfeldt et al., 2005; Mango, 2001). The remaining translated mRNA splice isoforms could encode protein products with significantly divergent functions. Amplification of cDNA molecules via PCR could potentially enrich the cDNA transcript pool with some isoforms at the expense of others. A further distortion could occur during purification of the PCR products using agarose gel electrophoresis and cloning of cDNA molecules into a helper vector. A seemingly single band on the agarose gel could represent several similar size alternative transcripts. This necessitates sequencing of as many PCR-amplified cDNA clones from

the same gel band as feasible in order to sample the cDNA clone pool and identify all splice isoforms. However, sampling for alternative cDNA transcripts is similar to looking for the proverbial black swan: no matter how exhaustive the search, it could never exclude the possibility that one especially rare but important splice isoform eluded detection. For fairly long cDNA transcripts, sequencing to exhaustion could become prohibitively expensive. Despite the limitations, the PCR-based method of full-length cDNA transcript cloning has been successfully employed to sufficiently characterize many *C. elegans* genetic loci (Antebi et al., 2000). Here a combined approach of sequencing full-length PCR-amplified cDNA transcripts and near full-length clones from Kohara's group cDNA libraries is used to uncover structure and expression of *tat-1* through *5* genetic loci.

Materials and methods

mRNA isolation and cDNA synthesis

Mixed-stage Bristol strain N2 line *C*. *elegans* populations were grown on 14cm enriched peptone plates (20mM NaCl, 2% w/v peptone, 2.5% w/v agar) spotted with *Escherichia coli* strain OP50 (Lewis and Fleming, 1995). When a population approached starvation, it was washed off a plate with M9 buffer (45mM Na_2HPO_4, 25mM KH_2PO_4, 85mM NaCl and 1mM $MgSO_4 \cdot 7H_2O$) (Brenner, 1974) and collected into a 15ml conical tube. The tube was centrifuged at 500g for 30sec, and the supernatant removed. The nematode pellet was then re-suspended in TRIzol® reagent (Invitrogen, Carlsbad, California) as recommended by the manufacturer; treated with three cycles of rapid freeze in liquid nitrogen, followed by rapid thaw in a 37°C water bath; and stored at -80°C. Several nematode preparations were combined (~20ml final wet nematode

volume) in a 40ml Dounce homogenizer and treated to 20 strokes of the A (tight) pestle. Total RNA was then isolated from the nematode homogenate as recommended by the TRIzol® manufacturer. mRNA was purified from the total RNA with a Poly(A)Pure kit (Ambion, Austin, Texas).

cDNA was synthesized from the mixed-stage mRNA with either the $dT_{(18)}$ primer or the adaptor-dT primer (AAGCAGTGGTATCAACGCAGAGTAC$(T)_{20}$VX, where V is A, G or C and X is any deoxynucleotide) using Moloney Murine Leukemia Virus Reverse Transcriptase (M-MLV RT) (Promega, Madison, Wisconsin). The adaptor portion of the adaptor-dT primer was truncated as a result of inefficient primer synthesis. 1µg of the mRNA and 0.5µg, or 2.5µl, of 20µM stock of either primer were combined for 25µl-volume cDNA synthesis reactions.

Rapid amplification of cDNA ends (RACE)

Near full-length cDNA transcripts of *tat-1*, *tat-2*, *tat-3*, *T24H7.6* (*T24H7.5c*) and *tat-5* were amplified using gene-specific and SL-specific primers as described by Antebi et al. (2000). Gene-specific primers (GSPs) were selected to anneal in the ultimate exon of the ORF based on the data collected by Kohara's cDNA sequencing project and available through WormBase (Schwarz et al., 2006). The primers were:
GSP_*tat-1*_1 - CGCTACCGTAGTCTCTGTAAACAGTC;
GSP_*tat-2*_1 - ATTGAGAGCCTAAAACCGGTGCCTAC;
GSP_*tat-3*_1 - ACTGCTGAGAAGAATGGCCCGTAG;
GSP_ *T24H7.6*_1 - AGAATGGAAAGGCAGTGTGATGGTCG; and
GSP_*tat-5*_1 - ACGGGTGGATTGGTTACTCGCATTAG. SL-specific primers were:

SL1 - GGAATTCGGTTTAATTACCCAAGTTTGAG and

SL2 -AGAGGTTTTAACCCAGTTACTCAAG.

A 3’ fragment of *tat-3* was amplified with the adaptor-dT and GSP_*tat-3_2* (GAAGAAGTTCATCACTAGCCAG) primers.

A nested PCR approach was employed to amplify 5’ and 3’ cDNA ends of *tat-4* transcripts (Antebi et al., 2000). In the first round of 5’ RACE, 5’ portions of *tat-4* cDNA were amplified with the adaptor-SL1 (AACTGCAGCCGCGGCTCGAGGGTTTAATTACCCAAGTTTGAG) and GSP_*tat-4*_2 (TTCAGTAAGTGTTCCTGTTTTGTCTG) primers and in the second round, with the adaptor (AACTGCAGCCGCGGCTCGAG) and GSP_*tat-4*_3 (CTGAAAGAACATGTGTGACTGTTC) primers. *tat-4* 5’ RACE was also conducted with a slightly different set of primers: adaptor-SL1/GSP_*tat-4*_1 (GGAGATGCATCAGGCGCTGGTGAG) in the first round and adaptor/GSP_*tat-4*_2 in the second. In the first round of 3’ RACE, 3’ portions of *tat-4* cDNA transcripts were amplified with the GSP_*tat-4*_4 (CAGACAAAACAGGAACACTTACTG) and adaptor-dT primers. Second round amplification was conducted with either the GSP_*tat-4*_5 (ACGACGTTCCAATGATTCAG) or GSP_*tat-4*_6 (AGCCAACGACGTTCCAATG) and adaptor-dT primers.

Near all cDNA amplification reactions were conducted at least twice, once with the high-quality hot-start proof-reading PrimeSTAR™ (Takara Mirus Bio, Madison, WI) polymerase and once with Taq polymerase. For *tat-1*, *tat-2*, *tat-3* and *tat-4*, at least one 5’ fragment was sequenced from each of the two reactions. Amplified cDNA products

were separated on an agarose gel, purified using QIAEX II Gel Extraction kit (QIAGEN, Valencia, CA) and cloned into pGEM®-T Easy vector (Promega, Madison, WI).

A 5' cDNA fragment of *tat-6* was amplified with the SL1 and GSP_*tat-6*_1 (AATGTCCCTGTCTTGTCCGAC) primers.

EST sequencing

Partial cDNA clones (expressed sequence tags, ESTs) yk1228h06, yk34c11, yk1496c06, yk209d5, yk36b8, yk214f10 and yk126b10 were kindly provided by Dr. Kohara. The clones arrived as either ready for sequencing plasmids or phagemids packaged into phage particles. In the latter instances, EST-containing plasmids were excised from the phagemid in accordance with the instructions supplied with the clones.

Results

tat-1

The products of *tat-1* cDNA amplification with the GSP_*tat-1*_1 and SL1 primers reproducibly separated on the agarose gel into two distinct bands of about 3.8 and 4.3 kb (no product appeared with the SL2 primer) (Figure 1). Both bands were purified and cloned. 2 clones from each band were sequenced completely; 3 of these were *tat-1a.1* splice isoforms and one was a *tat-1b.1* isoform (Figure 2A). 2 more clones from each band were sequenced partially from both ends; 3 of these were again *tat-1a.1* isoforms and one was a *tat-1a.2* transcript. Partial EST clones yk1228h06, yk34c11 and yk1496c06 were sequenced; yk1228h06 was a *tat-1b.2* isoform, while the other two represented the *tat-1a.1* transcript. The three sequenced ESTs terminated with a poly(A) tail attached 11 or 12 (depending on whether an A at the poly(A) attachment site

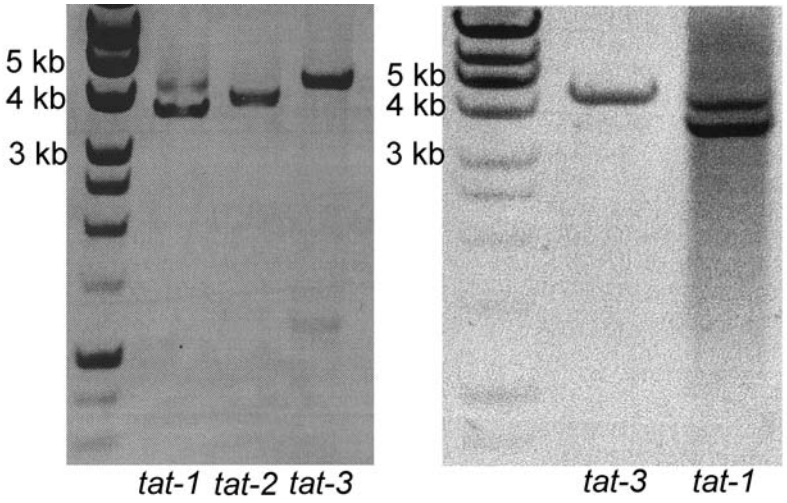

Figure 1. Amplification of *tat-1*, *2* and *3* cDNA transcripts with a gene-specific and SL1-specific primers using high-quality proofreading PrimeSTAR™ (Takara Mirus Bio, Madison, WI) DNA polymerase (left) or Taq polymerase (right).

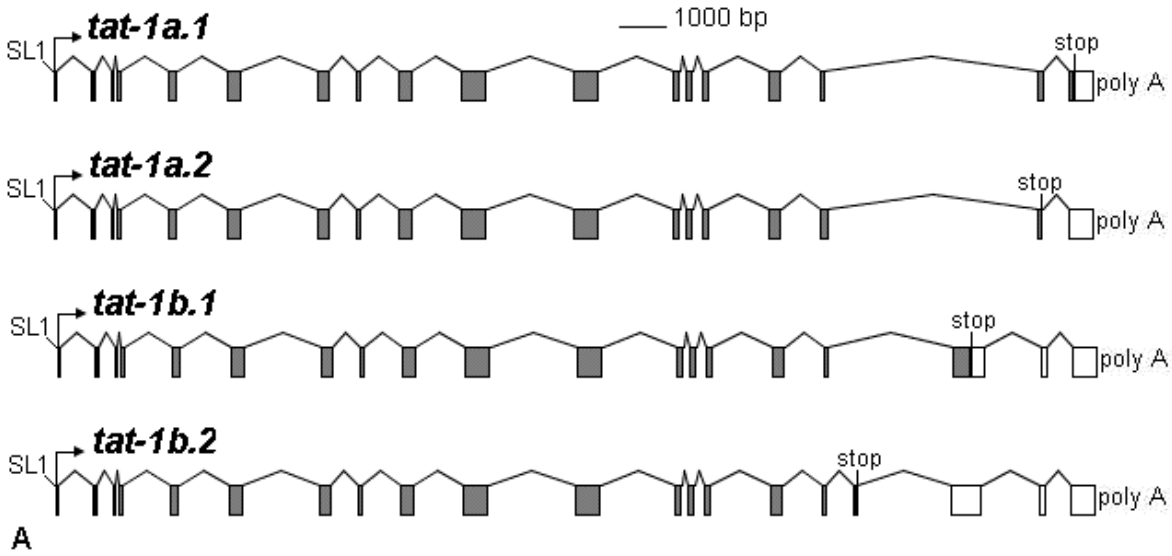

A

GCTCCTCGTCATTCTATGACCGAAAATCGATAATTTGTTTG
ATTTTTCATAATTCAACAAAAAATCGATAGCAAAGAAGTC
GAGGTCAAACACTTTTTGGAGCATAATG

B

```
TAT1A.1       FIPLATLLWDLVIKSLFTIAMPTPRELAVMYNKRTTSFNGFERLAS----------YSSN 1070
TAT1B.2       FIPLATLLWDLVIKSLFTIAMPTPRELAVMYNKRTTSFNGFERLAR----------KHVH 1070
TAT1A.2       FIPLATLLWDLVIKSLFTIAMPTPRELAVMYNKRTTSFNGFERLAR----------LACA 1070
TAT1B.1       FIPLATLLWDLVIKSLFTIAMPTPRELAVMYNKRTTSFNGFERLASSWAAYQGPTKDGAH 1080
              ******************************************

TAT1A.1       VLENMRLLTSSLRGSTTGSTRSRTAS--------EASLALAEQTRYGFAFS--------- 1113
TAT1B.2       LHTIIVAIERRLK------------------------AVCEWV---------------- 1089
TAT1A.2       SIYTHQIRQKKMMQIRSTG-----------------KLFIKRTRKHAAFD--------- 1103
TAT1B.1       VFANRFSLRKRIQPTSTTAASHPSATSPPPNGYVEKSQLNGKNGKHHRAKSPDYGSTELS 1140
                        :                                 :

TAT1A.1       -----------------QDESSAVAQTELIRN-------VDSTREKPTGR-- 1139
TAT1B.2       -------------------------------------------------
TAT1A.2       -----------------IISTWQYHWKYTIKN-------CIRSFTSTC---- 1127
TAT1B.1       TWSTRDEHEVEYKIPRGRKERSSYTNRAFIAEDNNVTSIVVNDEEDGSGTRL 1192
```

C

Figure 2. Structure and transcription of the *tat-1* locus. (A) The 4 detected splice isoforms of the *tat-1* ORF. (B) The 5' *tat-1* UTR contains a short upstream open reading frame (uORF) (boxed). (C) The divergent C terminus amino acid sequences in the protein products encoded by the four isoforms.

was part of the pre-mRNA or the poly(A) tail) bp downstream of a CATGAA putative poly(A) signal. 11 other 3' sequenced *tat-1* clones for which data were available from WormBase seemed to terminate at roughly the same location. Thus, a total of 4 alternative splice isoforms and a single putative poly(A) signal were identified among 4 fully and 7 partially sequenced (including the ESTs) *tat-1* cDNA clones (Figure 2A).

The lengths of the 4 transcripts are: *tat-1a.1* – 3958 bp (amplified with the GST and SL1 primers – 3688 bp); *tat-1a.2* – 4031 bp (3761 bp); *tat-1b.1* – 4626 bp (4356 bp); and *tat-1b.2* – 4699 bp (4429 bp). The first two isoforms seem to be responsible for the lower and the latter two, the upper bands on the agarose gels of the *tat-1* cDNA amplification products (Figure 1). It is noteworthy that mostly shorter alternative transcripts could be isolated even from the upper band. This may indicate that the longer isoforms are for some reason "resistant" to cloning. All 4 alternative transcripts are identical from the 5' end through a larger portion of the message toward the 3' end; the 5' UTR is 106 bp and contains an upstream open reading frame (uORF) (Figure 2B). There are cumulatively 20 exons in the *tat-1* ORF. Alternative splicing occurs with respect to exons 18 and 19, which are either present or absent, and exon 17, whose length depends on the choice between two competing splice donor sites; the ultimate and penultimate exons are conserved. Each one of the 4 splice isoforms has a different stop codon. In *tat-1a.2*, *tat-1b.1* and *tat-1b.2* the stop sequence is located not in the ultimate exon, but in the 19^{th}, 20^{th} or 18^{th} exon, respectively. The length of the 3' UTR correspondingly varies from 432 bp in *tat-1a.1* to 1323 bp in *tat-1b.2*. The alternative splicing and codon localization ensure that the protein products encoded by the 4

isoforms have dramatically divergent amino acid sequences at the C terminus (Figure 2C).

tat-2 and *tat-3*

The products of *tat-2* and *tat-3* cDNA amplification with the SL1 (there were no products with the SL2 primer) and GSP_*tat-2*_1 or GSP_*tat-3*_1 primers migrated on the agarose gel as single bands of about 4 and 4.6 kb, respectively (Figure 1). The bands were purified and cloned. For *tat-2*, three clones were sequenced completely and 10 partially from both ends. A total of 5 splice isoforms and 24 exons were detected (Figure 3A). The clones differed with respect to exon 23, which was skipped in about half (6/13) of the sequenced transcripts, and the first two exons. In one clone, exons 1 and 2 were absent (*tat-2a*); in 9 clones, only exon 1 was missing (*tat-2b.1* and *tat-2b.2*); and in 3 clones, both exons 1 and 2 were present (*tat-2c.1* and *tat-2c.2*). EST clone yk209d5 was sequenced. It contained a poly(A) tail 11 or 12 (depending on whether an A at the poly(A) attachment site was part of the pre-mRNA or the poly(A) tail) bp downstream from an AATAAA putative poly(A) signal. 4 other 3' sequenced *tat-2* clones for which data were available from WormBase all seemed to terminate at the roughly same location. Thus, 5 splice isoforms and a single putative poly(A) signal were identified among 14 partially or fully sequenced *tat-2* cDNA clones.

tat-2a transcript is 4213 bp long (3953 bp amplified with the GST_*tat-2*_1 and SL1 primers) and contains a short (44 bp) 5' UTR. *tat-2b.1* and *tat-2b.2* are 4269 (4009) and 4151 (3891) bp, respectively. The 5' UTR of these transcripts is 101 bp and has an uORF that encodes a 65 amino acid peptide and partially overlaps with the main ORF

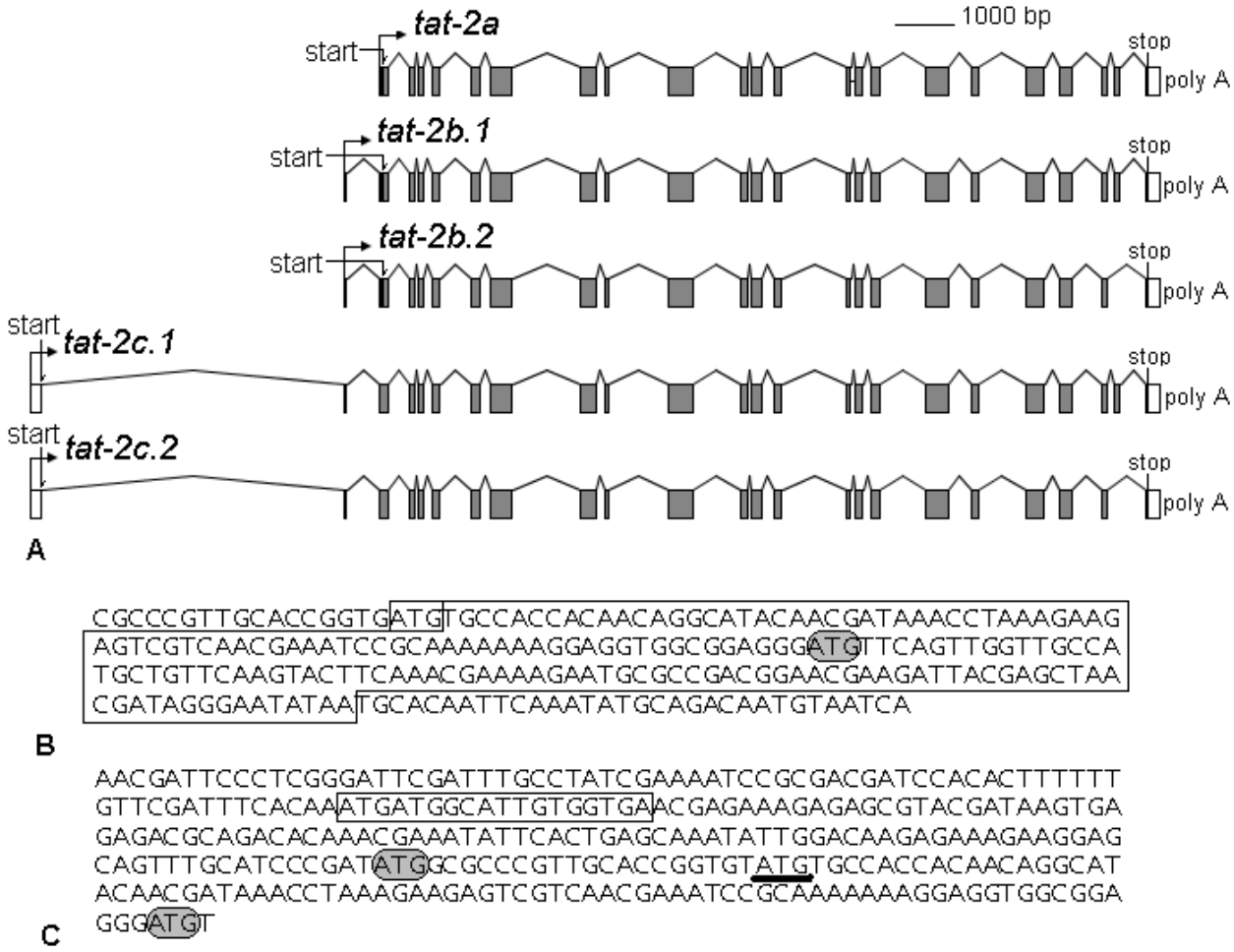

Figure 3. Structure and expression of the *tat-2* locus. (A) The 5 detected alternative splice transcripts of the *tat-2* ORF. (B) The 5' UTR of *tat-2b* isoforms contains a long uORF that partly overlaps with the main ORF (boxed); the start ATG of the main ORF is indicated by a shaded oval. (C) The 5' UTR of *tat-2c* isoforms has an uORF (boxed) and an ATG (first shaded oval) located in frame with the start codon ATG of the other splice variants (second shaded box); the start ATG (underlined) for the uORF in *tat-2b* transcripts is silent in *tat-2c* splice variants.

(Figure 3B). *tat-2c.1* and *tat-2c.2* are 4466 (4206) and 4348 (4088) bp, respectively; exon 1, present only in these two splice variants, contains an uORF and an ATG, which is in frame with the start codon ATG in the other isoforms (Figure 3C). Consequently, *tat-2c* transcripts encode a longer polypeptide, with additional 35 amino acids at its N terminus. The 5' UTR of *tat-2c* isoforms is 193 bp. In *tat-2* transcripts without exon 23, translation terminates at a stop codon located 19 bp into the ultimate exon. In transcripts with exon 23, translation also ceases in the ultimate exon but at a different stop codon positioned 33 bp away from the exon 5' end. The first 22 bp of the final exon are therefore translated in two different frames, depending on the presence of exon 23. The 3' UTR are 355 and 341 bp in transcripts without and with, respectively, exon 23.

For *tat-3*, 6 clones were fully sequenced (Figure 4A). One of these clones lacked a middle 1.5 kb region. The missing sequence did not contain canonical splice donor and acceptor sites at the very ends. Hence short transcripts, such as this, would have been eliminated during cDNA product purification on the agarose gel, the aberrant clone likely arose from a regular length transcript through deletion mutagenesis in the host *E. coli* cell. The other five clones consisted of 13 exons each and differed only slightly: the length of the ultimate exon depended on the choice between two alternative splice acceptor sites. In 4 clones (*tat-3a*) this exon was 6 nucleotides shorter than in the fifth clone (*tat-3b*). *tat-3* 3' cDNA products amplified with the adaptor-dT and GSP_*tat-3*_2 primers segregated on the agarose gel into at least 5 bands (Figure 4C). The bands were purified in three sets: the upper band, the two closely spaced middle bands together and the two closely spaced lower bands together, and cloned. One clone was

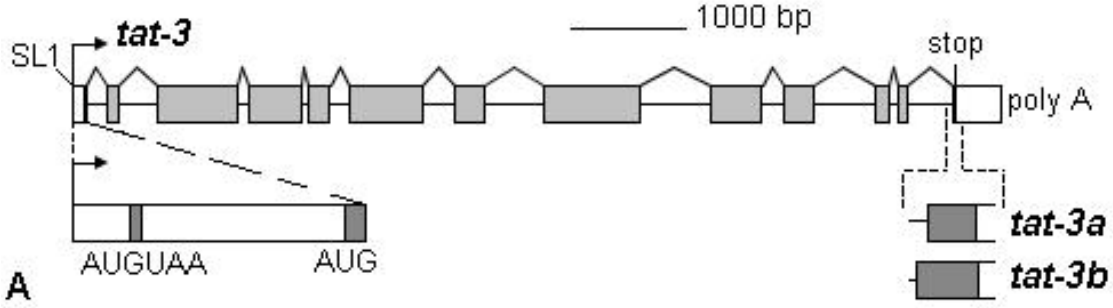

TTTCAGAGAACGTCACCGCATATAAATGTAACAAAAGT
GCAAAGGGCACTTGAAACGAATCCTATCGAATCCACAA
AAATCAAATTTGCAATTTATTCTCGATTTCCAGAGAAT
TGTGAATG

B

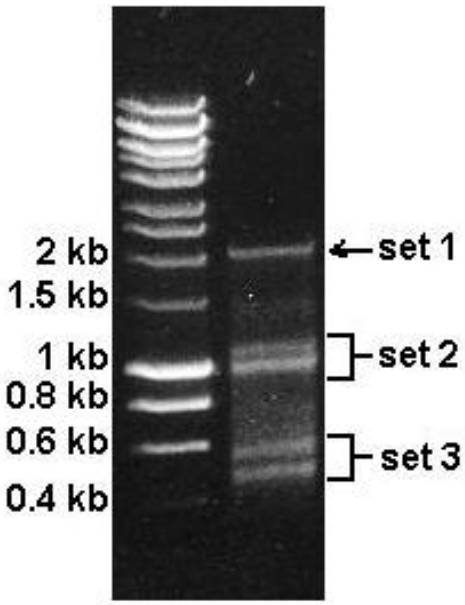

Figure 4. Structure and expression of the *tat-3* locus. (A) Only two slightly different *tat-3* transcripts were detected. (B) The 5' *tat-3* UTR contains an uORF (boxed). (C) products of cDNA amplification with the adaptor-dT and GSP_*tat-3*_2 primers segregated into five bands; the bands were purified from the gel in three sets as noted.

sequenced from each set. The upper and middle set clones were not *tat-3* transcripts. The lower set clone was a 439 bp 3' *tat-3* fragment that contained a poly(A) tail 11 bp downstream of an AATAAA putative poly(A) signal. This clone (480 bp amplified length with the adaptor-dT primer) likely represented the lower of the two short bands. It could be that the other short band was another version of the *tat-3* 3' end. On the other hand, 10 3' sequenced clones from WormBase all seemed to terminate at the roughly same location. Thus, 2 slightly different isoforms and a single putative poly(A) signal were identified among 5 (not including the aberrant transcript) 5' and one 3' fully sequenced *tat-3* cDNA clones.

The *tat-3* transcripts are 4776 (4508 bp amplified in 5' RACE) and 4782 (4514) bp long. The *tat-3* 5' UTR is 119 bp and contains an upstream ATG (uATG) followed immediately by a stop codon (Figure 4B). The 3' UTR is 421 bp.

tat-4 and *T24H7.6*

cDNA transcript data available from WormBase suggested that the *tat-4* locus contained two peculiar ORFs transcribed and translated separately and together as a single ORF (*T24H7.5b* isoform) (Figure 5A). cDNA amplification with the GSP_ *T24H7.6*_1 and either SL1 or SL2 primers yielded products that traveled on the agarose gel as single bands of about 800 bp (Figure 5B). The bands were purified and cloned. 10 clones amplified with the SL1 primer and two clones with the SL2 primer were completely sequenced. All 12 were identical and corresponded to the transcript marked in WormBase as the *T24H7.5c2* isoform of *tat-4* (*T24H7.5*) (Figure 5A). These findings,

however, suggested that *T24H7.5c2* was a separate second ORF in a cluster of two, and its proper identification was *T24H7.6*.

For *tat-4* 5' and 3' RACE, primers were chosen to anneal to regions encoding amino acid sequences conserved in all or at least, the subfamily IV P-type ATPases. This ensured that if there were transcripts without these particular highly conserved sequences, the protein products of such transcripts would likely lack functionality. Very low yields after a single round of PCR amplification necessitated application of nested PCR. For 3' RACE, *tat-4* cDNA was first amplified with the GSP_*tat-4*_4 (anneals to the sequence encoding the DKTGT motif, which is absolutely conserved in all P-type ATPases; Palmgren and Axelsen, 1998) and adapter-dT primers (Figure 5A, C). Then, the products of the first round were amplified with either the GSP_*tat-4*_5 or GSP_*tat-4*_6 (both anneal to the region encoding the ND--MI motif; the ND pair is conserved in nearly all P-type ATPases, and MI, in all P-type ATPases in subfamily IV; Palmgren and Axelsen, 1998) and adapter-dT primers. The products of the second round amplified with GSP_*tat*-4_5 separated on the agarose gel into 4 bands and with GSP_*tat-4*_6, 5 bands (Figure 5D). The 4 bands present in both reactions were purified and cloned. The two middle bands were isolated together. 11 clones from the upper band were sequenced. 3 of these were transcripts of some other, not *tat-4*, ORFs. One terminated in the *tat-4* predicted exon 16 without a clearly distinguishable poly(A) signal in a close proximity upstream of the poly(A) tail (Figures 5A and 7B). The other 9 all contained exon 16; 5 of these clones terminated with a poly(A) tail in the ultimate exon of *T24H7.6* 14 or 17 (depending on whether an AAA triplet at the poly(A) site was part of the poly(A) tail or the pre-mRNA transcript) nucleotides downstream of a GATAAA putative poly(A)

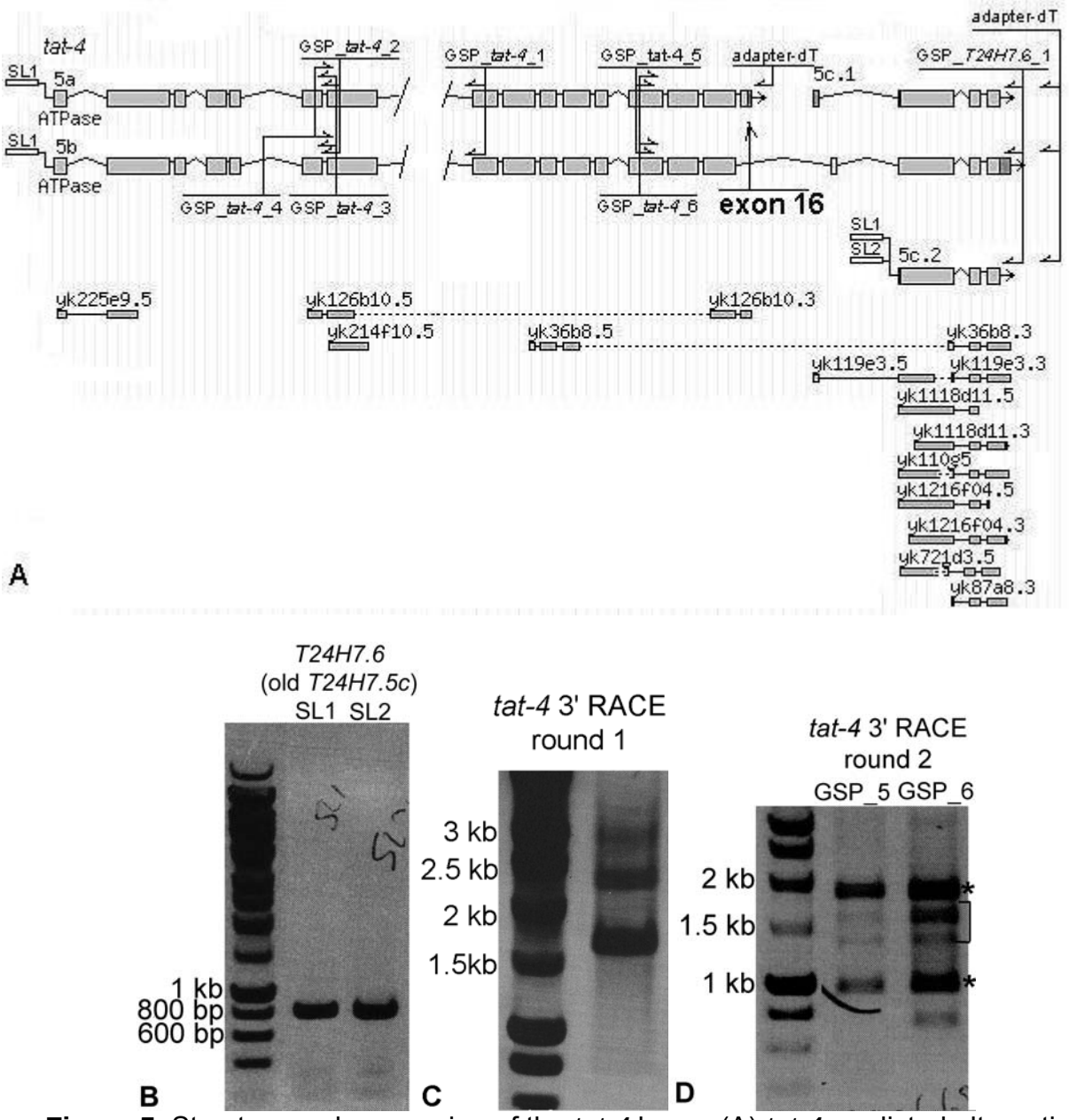

Figure 5. Structure and expression of the *tat-4* locus. (A) *tat-4* predicted alternative transcripts, available from Kohara's group *tat-4* cDNA clones and localization of the annealing sites for the primers used to amplify *tat-4* cDNA. *tat-4* and *T24H7.6* (*T24H7.5c.2* in the figure) ORFs were predicted to be transcribed and translated in some isoforms together (*T24H7.5b* isoform). (B) cDNA amplification products generated using either the SL1 or SL2 and GSP_*T24H7.6*_1 primers. (C) Products of the first round of *tat-4* 3' end amplification with the GSP_*tat-4*_4 and adaptor-dT primers; the visible bands were likely to be not *tat-4* cDNA products. (D) Products of the second round of *tat-4* 3' end amplification with either the GSP_*tat-4*_5 or GSP_*tat-4*_6 and adaptor-dT primers; the upper and lower bands (marked with a star) individually and the middle two bands (marked with a bracket) together were purified and cloned.

signal. 6 *T24H7.6* (formerly *T24H7.5c*) clones for which data were available from WormBase seemed to terminate at approximately this same location. For the remaining 2 clones, 3' sequences could not be obtained. 3 clones of the middle set were sequenced and all were of some other, not *tat-4*, ORF transcripts. 4 clones of the lower band were sequenced. 3 of these terminated in exon 16, 10 or 11 bp (depending on whether an A at the poly(A) site is from the pre-mRNA or the poly(A) tail) downstream of a CATAAA putative poly(A) sequence (Figure 7B); only a partial sequence of the fourth clone could be obtained. Yk36b8, yk214f10 and yk126b10 partial 3' clones were sequenced. All contained exon 16. Yk36b8 terminated with a poly(A) tail in the ultimate exon of *T24H7.6* at the same site as the 5 upper band clones. Yk124f10 and yk126b10 terminated in exon 16, the latter had a poly(A) tail at the same site as the 3 lower band clones, and the former a few base pairs downstream from that location, 14 or 15 bp away from the CATAAA putative poly(A) signal. These findings indicated that all *tat-4* transcripts might include exon 16, which contains a stop codon and several weak poly(A) signals; when these signals fail to induce polyadenylation, then it occurs at the strong putative poly(A) signal in the *T24H7.6* ultimate exon. Thus, *tat-4* and *T24H7.6* are separate but partially overlapping ORFs encoding two independent protein products.

The 3' *tat-4* end was also amplified with the GSP_*T24H7.6*_1 and GSP_*tat-4*_6 primers (Figure 6C). The products of this reaction segregated into several bands. The distinct band around 1.7 kb was the right size to have been arisen from *tat-4* transcripts that terminated in the ultimate *T24H7.6* exon. The faint band just below the 1.7 kb band could represent another still undetected minor splice isoform of *tat-4*. The band at 800

bp was cloned and two of the isolated clones sequenced. The sequenced clones were *T24H7.6* transcripts amplified with the GSP_*T24H7.6*_1 primer and apparently some contamination in the cDNA preparation that could function as the SL2 primer.

For 5' *tat-4* RACE, two slightly different combinations of primers were used. In one set, cDNA was first amplified with the adaptor-SL1/GSP_*tat-4*_2 primer pair and then the adaptor/GSP_*tat-4*_3 pair (Figure 5A, 6A). GSP_*tat-4*_2 and GSP_*tat-4*_3 were partially overlapping primers that annealed to the sequence encoding the absolutely conserved P-type ATPase DKTGT motif (Palmgren and Axelsen, 1998). In the other set, the first amplification was with the adaptor-SL1/GSP_*tat-4*_1 and then the adaptor/ GSP_*tat-4*_2 primer pairs (Figure 6B). In both cases, second round cDNA amplification products migrated on the agarose gel as single bands. The bands were purified and cloned. 3 clones from each band were sequenced. All 6 were identical. The *tat-4* middle part, between the regions where GSP_*tat-4*_2 and GSP_*tat-4*_6 primers anneal, was sequenced in EST clones yk126b10 and yk36b8, which were in that middle portion identical. Thus, 4 *tat-4* isoforms different only with respect to the termination site were detected among six 5', nine 3' and 3 EST fully sequenced clones.

tat-4a.1, *tat-4a.2* and *tat-4a.3* isoforms consist of 16 exons and are around 3700 bp each (Figure 7A). The two slight differences among these transcripts are the location of the poly(A) site in exon 16 (Figure 7B) and consequently, the length of the 3' UTR, which varies from 57 (in *tat-4a.1*) to 109 bp (in *tat-4a.3*). The *tat-4b* alternative transcript terminates in the ultimate exon of *T24H7.6* and therefore, contains three additional exons, which comprise the *T24H7.6* ORF. *tat-4b* is 4618 bp in length and its 3' UTR is

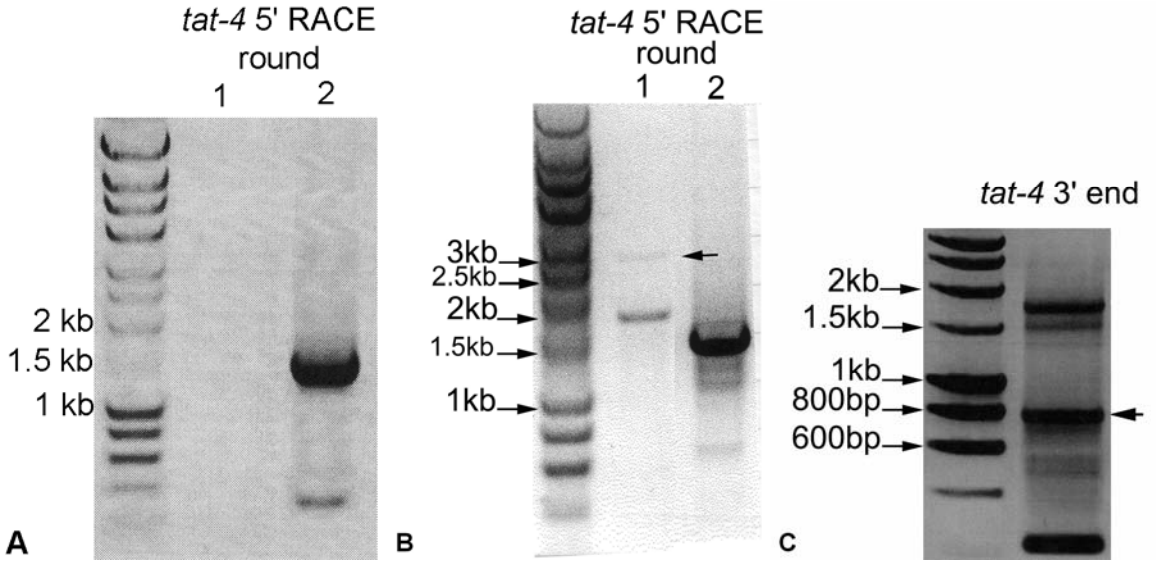

Figure 6. Structure and expression of the *tat-4* locus (part 2). (A and B) Amplification of 5' *tat-4* cDNA fragments with two different combinations of primers. (B) The leftward directed arrow indicates the location of expected size product in the first round of amplification. (C) Amplification of *tat-4b* 3' end with two gene-specific primers. The band indicated with the leftward directed arrow was cloned.

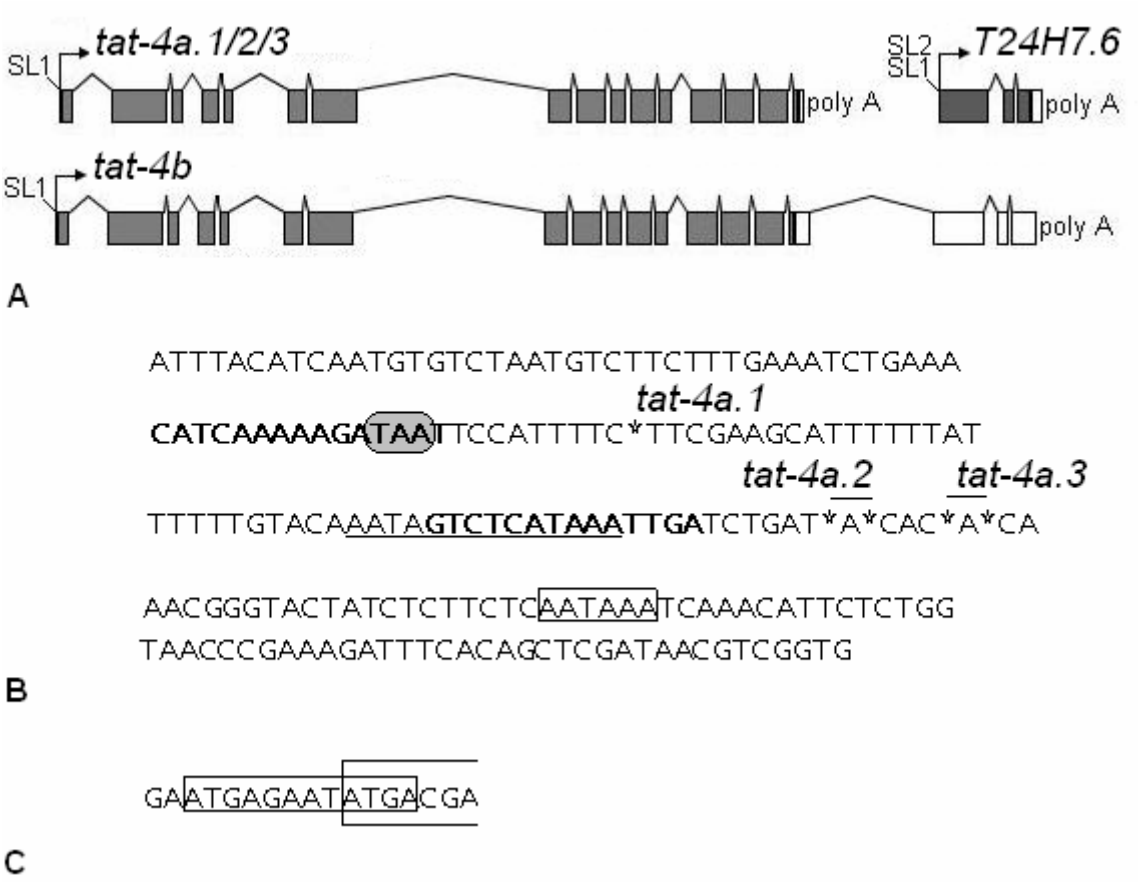

Figure 7. Structure and transcription of the *tat-4* locus. (A) The 4 detected alternative transcripts of the *tat-4* ORF. (B) Exon 16 of the *tat-4* ORF. Locations of poly(A) sites in the three isoforms that terminate in this exon are indicated with a single star, or two stars when there is an ambiguous – either poly(A) or pre-mRNA – A nucleotide at the poly(A) site. The stop codon is in a shaded oval. Nucleotides in bold and underlined are regions located an appropriate distance away from the putative poly(A) site to serve as poly(A) signals. Curiously, exon 16 contains a canonical poly(A) signal sequence (boxed) that do not seem to function. (C) The 5' UTR of *tat-4* contains an uORF (boxed) that partially overlap with the main ORF.

969 bp. The 5' UTR in the 4 transcripts is only 10 bp; nonetheless, it contains an uORF that partially overlaps with the main ORF (Figure 7C).

tat-5 and *tat-6*

Products of cDNA amplification with the GSP_*tat-5*_1 and either SL1 or SL2 primers migrated on the agarose gel as single bands (Figure 8A). Both bands were purified and cloned. Only two clones from each band were partly sequenced. One of these clones was a *tat-5a* isoform carrying an SL2 sequence. This was noteworthy because it suggested that *tat-5a* and *tat-5b* were *trans*-splicing isoforms. No further characterization of this locus was conducted. cDNA transcript data available from WormBase provided a relatively clear and sufficient description of *tat-5* transcription.

tat-6 is a very close homolog of *tat-5*. *tat-6* cDNA could be amplified with a carefully selected *tat-6*-specific primer, indicating that this ORF is transcribed (Figure 8B).

Discussion

The data presented here confirm the findings from Kohara's systematic cDNA sequencing and the ORFeome cloning projects that the 6 *C. elegans tat* ORFs encoding P-type ATPases in subfamily IV are all transcribed. *tat-6* is a close (73% identity on the nucleotide level) homolog of *tat-5a*. The paucity of EST clones representing this ORF in Kohara's cDNA library (only 1 clone) and the faintness of the agarose gel band composed of *tat-6* 5' cDNA amplification products (Figure 8B) suggest that *tat-6* transcripts are rare. Beyond confirming that it is indeed a template for mRNA synthesis, no further characterization of the *tat-6* ORF was undertaken. *tat-5*, in contrast, seems to

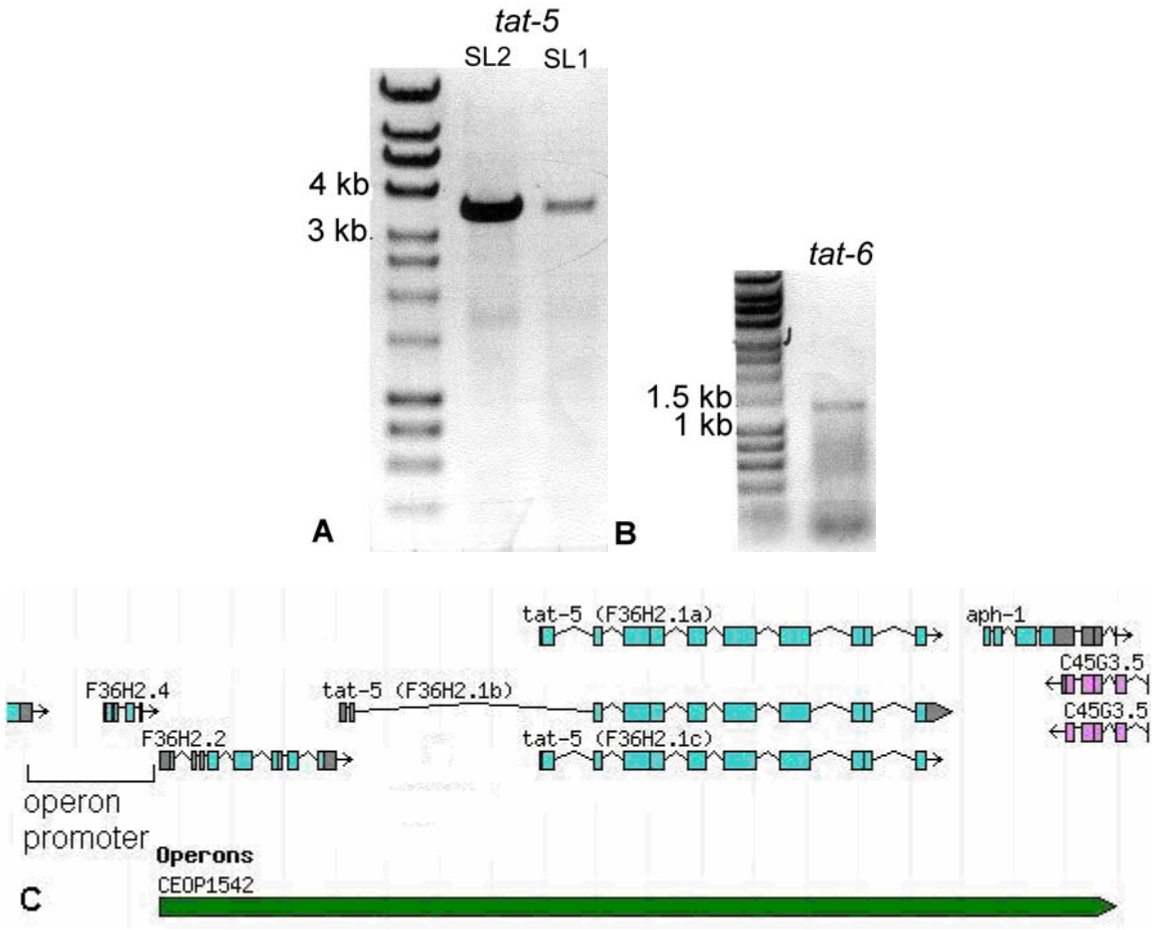

Figure 8. Transcription of *tat-5* and *tat-6*. (A) *tat-5* 5' RACE products. (B) *tat-6* 5' RACE products. (C) Structure and transcription of the *tat-5* locus as predicted from the data collected by Kohara's cDNA sequencing project.

be the most transcribed of all the *tats*. Kohara's cDNA sequencing project identified and partially sequenced enough full-length and partial *tat-5* clones to derive a sufficiently clear view of the structure and transcription of the *tat-5* ORF (Figure 8C). This ORF contains 12 exons, which through alternative splicing combine into 3 alternative transcripts. The *tat-5b* isoform is the second cistron in a three-cistron operon. The other two cistrons are *F36H2.2*, an ORF encoding a peptide with similarity to transmembrane nucleoside transporters, and *aph-1*, a gene encoding a transmembrane subunit of γ-secretase, an atypical aspartyl protease that cleaves amyloid β-precursor and other single-span transmembrane proteins (Wolfe, 2006; Goutte et al., 2002; Francis et al., 2002). Genes located in the same operon in *C. elegans* share the same promoter sequences (which are located upstream of the leading cistron), exhibit similar expression patterns and might participate in the same processes (Eichmuller et al., 2004; Lercher et al., 2003). Thus, the presence of *F36H2.2*, *tat-5b* and *sph-1*, three transmembrane proteins, in the same operon might be of some presently unclear functional significance.

The almost identical *tat-5a* and *tat-5c* isoforms lack the two first short exons of the ORF and instead begin with the third exon, which is not present in *tat-5b* (Figure 8C). *tat-5* cDNA amplification revealed that *tat-5a* could be amplified with the SL1 and SL2 primers. Transcripts from cistrons located in subordinate positions (2^{nd} and so forth) in an operon could contain either an SL1 or SL2 sequence. *tat-5a/c* and *tat-5b* transcripts are therefore likely to be products of alternative *trans*-splicing to two competing acceptor sites located over 3 kb away from each other in the pre-mRNA (alternatively, a second promoter located within the long second intron of *tat-5b* could

control *tat-5a/c* expression). *sph-1* lacks a promoter sequence within a 5 kb region immediately upstream of the gene (Francis et al., 2002). Thus, the common promoter upstream of *F36H2.2* could be the sole driver of expression for the three-cistron message.

tat-1 through *4* ORFs separate in two groups based on structure and transcription. *tat-1* and *tat-2* consist of 20 and 24, respectively, generally smaller, while *tat-3* and *tat-4*, of 13 and 16, respectively, generally larger exons. Pre-mRNA transcripts of the former group undergo alternative splicing with respect to exons located at the 5' and 3' ends of the message, and as a consequence, the resultant mRNA molecules encode protein products with divergent N and C terminuses. mRNA transcripts of the latter group exhibit either a minor difference (*tat-3*) or differ only in the untranslated region (*tat-4*). In *C. elegans* transcripts terminate with a poly(A) tail added 10 to 18 bp downstream of a poly(A) signal, which in a majority of cases is the AAUAAA motif (Hajarnavis et al., 2004). *tat-2* and *tat-3* ORFs contain a single AATAAA poly(A) signal each. A CATGAA motif appears to be the poly(A) signal in *tat-1*. CATGAA sequences are known to function as poly(A) signals in a number of genes (Hajarnavis et al., 2004). The *tat-4* ORF seem to contain at least two weak poly(A) signals in a close (<100 bp) proximity of the stop codon. The CATAAA motif is likely to be the poly(A) signal in the nearly identical *tat-4a.2* and *tat-4a.3* transcripts. CATAAA sequences occur as a polyadenylation signal in other genes (Hajarnavis et al., 2004). The identity of the poly(A) signal in *tat-4a.1* is unclear, although the region where it must be located contains many adenosine nucleotides (Figure 7B). In those cases when the signals immediately downstream of the *tat-4* stop codon fail to induce poly(A) tailing (*tat-4b*), it

occurs at the putative poly(A) signal in the ultimate exon of the *T24H7.6* ORF, the downstream neighbor of *tat-4*. *T24H7.6* transcripts carry both SL1 and SL2 sequences. It seems that *tat-2* and *T24H7.6* form a two-cistron operon whose pre-mRNA molecules frequently fail to undergo processing into individual, single-ORF, mRNA messages. The resultant bi-cistronic transcripts include two main complete ORFs.

Nearly all (except *tat-2a*) *tat-1* through *4* mRNA transcripts contain an uORF. In mammals, uORFs frequently suppress translation efficiency of the main ORF by recruiting and stalling the ribosome (Morris and Geballe, 2000). The stop codons of uORFs could also be recognized as premature, which would trigger degradation of the transcript via NMD. The later mechanism of mRNA stability control is known to occur in *C. elegans* (Lee and Schedl, 2004). However, not all uORF are functional. Active uORF are usually conserved in homologous genes across many species (Iacono et al., 2005). A brief analysis of a small selection of murine and human subfamily IV P-type ATPases revealed that murine *Atp10c*, *Atp10b* and *Atp10d* and human *ATP10c* and *ATP10d* all contain at least one uORF (data not shown). Thus, at least some of the uORFs in the *C. elegans tat-1* through *4* could be evolutionary conserved and functional.

The data presented here provide a sufficient but not exhaustive description of structure and transcription of the *tat-1* through *5* ORFs. Several issues remained unaddressed. The middle part of *tat-4* was sequenced in only 2 clones. Furthermore, *tat-4* alternative transcripts represented in Kohara's cDNA library by the clone yk119e3 were not identified (Figure 5A). Only one clone of *tat-3* 3' end was sequenced. These and other deficiencies should be resolved in the future research.

References

Antebi A, Yeh W-H, Tait D, Hedgecock EM and DL Riddle. (2000) *daf-12* encodes a nuclear receptor that regulates the dauer diapause and development age in *C. elegans*. Genes and Development 14:1512-1527.

Ast G. (2004) How did alternative splicing evolve? Nature Reviews Genetics 5:773-782.

Blumenthal T. (2004) Operons in eukaryotes. Briefings in Functional Genomics and Proteomics 3:199-211.

Blumenthal T, Evans D, Link CD, Guffanti A, Lawson D, Thierry-Mieg J, Thierry-Mieg D, Chiu WL, Duke K, Kiraly M and SK Kim. (2002) A global analysis of *Caenorhabditis elegans* operons. Nature 417:851-854.

Blumenthal T. (1995) *Trans*-splicing and polycistronic transcription in *Caenorhabditis elegans*. Trends in Genetics 11:132-136.

Brenner S. (2000) Genomics. The end of the beginning. Science 287:2173-2174.

Brenner S. (1974) The genetics of *Caenorhabditis elegans*. Genetics 77:71-94.

Eichmuller S, Vezzoli V, Bazzini C, Ritter M, Furst J, Jakab M, Ravasio A, Chwatal S, Dossena S, Botta G, Meyer G, Maier B, Valenti G, Lang F and M Paulmichl. (2004) A new gene-finding tool: using *Caenorhabditis elegans* operons for identifying functional partner proteins in human cells. Journal of Biological Chemistry 279:7136-7146.

Francis R, McGrath G, Zhang J, Ruddy DA, Sym M, Apfeld J, Nicoll M, Maxwell M, Hai B, Ellis MC, Parks AL, Xu W, Li J, Gumey M, Myers RL, Himes CS, Hiebsch R, Ruble C, Nye JS and D Curtis. (2002) *aph-1* and *pen-2* are required for Notch pathway signaling, γ-secretase cleavage of βAPP, and presenilin protein accumulation. Developmental Cell 3:85-97.

Goutte C, Tsunozaki M, Hale Va and JR Priess. (2002) APH-1 is a multipass membrane protein essential for the Notch signaling pathway in *Caenorhabditis elegans* embryos. Proceedings of the National Academy of Sciences USA 99:775-779.

Hajarnavis A, Korf I and R Durbin. (2004) A probabilistic model of 3' end formation in *Caenorhabditis elegans*. Nucleic Acids Research 32:3392-3399.

Iacono M, Mignone F and G Pesole. (2005) uAUG and uORFs in human and rodent 5' untranslated mRNAs. Gene 349:97-105.

Lee M-H and T Schedl. (2004) Translation repression by GLD-1 protects its mRNA targets from nonsense-mediated mRNA decay in *C. elegans*. Genes and Development 18:1047-1059.

Lewis JA and JT Fleming. (1995) Basic culture methods. In HF Epstein and DC Shakes (Eds), *Methods in cell biology: Caenorhabditis elegans: modern biological analysis of an organism (Methods in Cell Biology, Vol 48)* (pp. 3-29). New York, NY: Academic Press.

Lamesch P, Milstein S, Hao T, Rosenberg J, Li N, Sequerra R, Bosak S, Doucette-Stamm L, Vandenhaute J, Hill DF and M Vidal. (2004) *C. elegans* ORFeome version 3.1: increasing the coverage of ORFeome resources with improved gene predictions. Genome Research 14:2064-2069.

Lercher MJ, Blumenthal T and LD Hurst. (2003) Coexpression of neighboring genes in *Caenorhibditis elegans* is mostly due to operons and duplicate genes. Genome Research 13:238-243.

Mango SE. (2001) Stop making nonSense: the *C. elegans smg* genes. Trends in Genetics 17:646-653.

Morris DR and AP Geballe. (2000) Upstream open reading frames as regulators o mRNA translation. Molecular and Cellular Biology 20:8635-8642.

Palmgren MG and KB Axelsen. (1998) Evolution of P-type ATPases. Biochimica et Biophysica Acta 1365:37-45.

Shin-i T and Y Kohara. (1999) NEXTDB: the expression pattern map database for *C. elegans*. Genome Informatics 10:213-214.

Snyder M and M Gerstein. (2003) Genomics. Defining genes in the genomic era. Science 300:258-260.

Schwarz EM et al. (2006) WormBase: better software, richer content. Nucleic Acids Research 34(Database issue): D475-478.

Weischenfeldt J, Lykke-Andersen J and B Porse. (2005) Messenger RNA surveillance: neutralizing natural nonsense. Current Biology 15:R559-562.

Wolfe MS. (2006) The γ-secretase complex: membrane-embedded proteolytic ensemble. Biochemistry 45:7931-7939.

Chapter 5. Expression patterns of the GFP reporter under the control of *tat-2*, *3*, *4* or *5* promoter sequences

Introduction

Investigations in mammalian systems suggest that open reading frames (ORFs) encoding P-type ATPases in subfamily IV, the group of putative transbilayer amphipath transporters (TATs), are expressed in tissue-specific patterns (Halleck et al., 1999; Harris and Arias, 2003). The human and murine genomes contain at least 14 TAT-coding ORFs each, which segregate into 5 divisions (classes and major subclasses) with 2 to 4 closely related potentially redundant members per division (Figure 1). The 6 *C. elegans* TAT ORFs, named *tat-1* through *6*, fall into subclasses 1a and 1b, one in each, and classes 2 and 5, two in each (Figure 1). Class 6 members are not found in the nematode, although classes 5 and 6 could be considered as one division represented in *C. elegans* by *tat-3* and *tat-4*. Expression patterns of the nematode *tats* would help recognition of aberrant phenotypes in mutants of these genes.

Single-cell resolution expression patterns are usually obtained in *C. elegans* indirectly using expression cassettes that reside in the nematode as a transgene and represent the endogenous gene of interest (Okkema and Krause, 2005). An expression cassette could be constructed by inserting a sequence encoding a reporter peptide, commonly the *Aequorea victoria* green fluorescent protein (GFP), in frame with the targeted ORF into a fragment of a *C. elegans* chromosome that includes the ORF and its promoter and terminator regions. Or, it could be made by fusing a gene promoter fragment in frame with the GFP sequence, followed by a heterologous terminator. The expression vector (the expression cassette in a backbone vector) is co-delivered with a

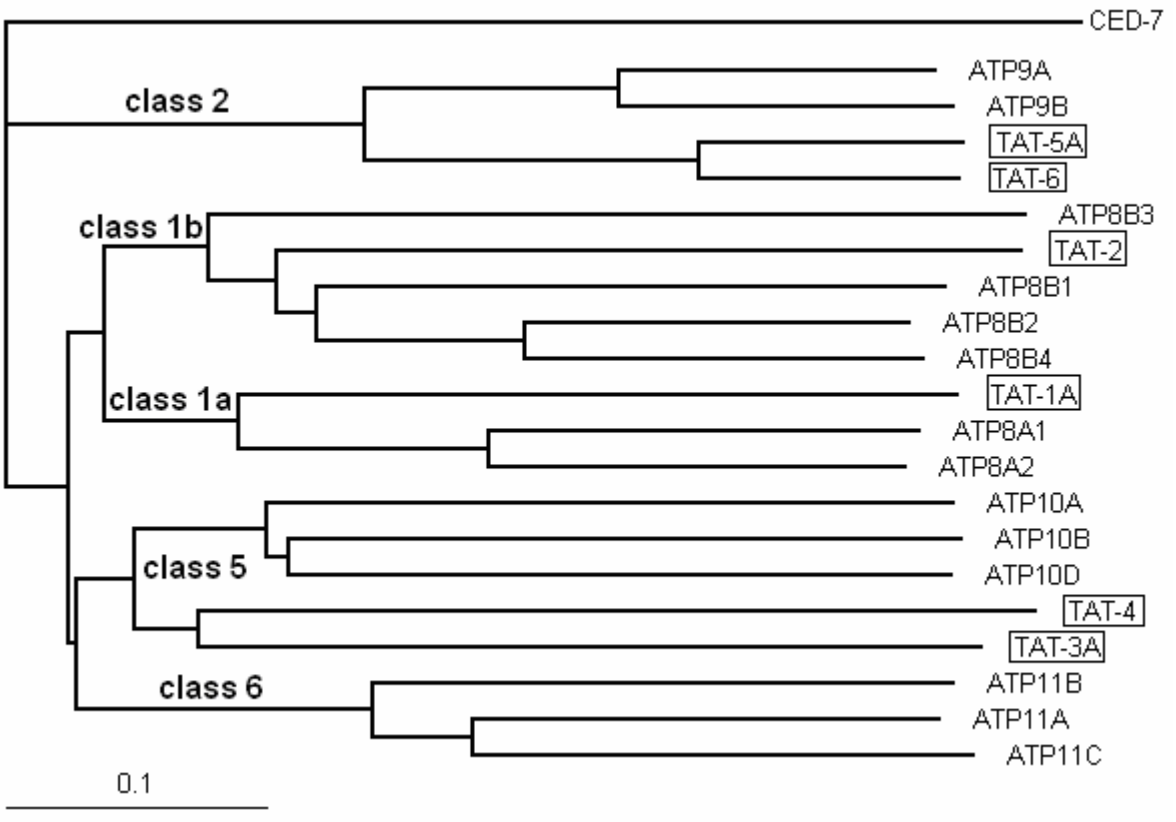

Figure 1. Human and *C. elegans* P-type ATPases in subfamily IV. The division in classes is after Halleck et al. (1999). Alignment by ClustalW, *C. elegans* ABC transporter CED-7 is used as the outgroup.

construct carrying a selectable marker gene and in some cases, fragmented genomic DNA (to limit formation of tandem repeats of the expression cassette) into the nematode gonad syncytium through either microinjection or particle bombardment. The former method generates repetitive or complex extrachromosomal arrays composed of many (perhaps tens to hundreds) copies of the expression and selection vectors and when added, exogenous DNA (Evans, 2006). These arrays are lost during cell division at varying rates depending on the array properties, and this leads to formation of “mosaic” animals and appearance in each generation of nematodes altogether without the array. Particle bombardment produces both extrachromosomal and short integrated arrays (Praitis et al., 2001). In the latter case, a few copies of the expression and selection vectors (DNA is not added with this method) co-integrate directly into a *C. elegans* chromosome. The resultant short transgenes are stable and behave almost like endogenous genes. The downside of the particle bombardment method is that the few integrated expression cassettes could occasionally be all rearranged, abbreviated or “unfortunately” inserted during the process of integration and therefore, be partly or completely nonfunctional (Somers and Makarevitch, 2004; NN Lyssenko, unpublished data). “Unfortunate” insertion occurs when a circular expression vector breaks within the expression cassette and as a result, the cassette is incomplete or, when the break occurs in the GFP-coding sequence, silenced altogether. “Unfortunate” insertions become an especially acute limitation when the size of the expression cassette greatly exceeds the length of the backbone sequence and hence, the probability of the break occurring in the cassette is very high (when the cassette and the backbone are the same length, the probability of a cassette break is 50%; when the cassette is twice as

long as the backbone, the probability is 66%). The ability of a transgene to faithfully represent transcription of the endogenous gene depends on the structure of the expression cassette (must include as many *cis*-regulatory sequences as possible) and in the case of integrated short arrays, also on the structure and chromatin context of the transgenic locus. Generally, integrated transgenes derived through particle bombardment are considered to reflect endogenous expression more faithfully than extrachromosomal array-based expression cassette (Praitis et al., 2001).

The *C. elegans tat* ORFs are long and likely to be poorly transcribed. Furthermore, some evidence from the budding yeast *Saccharomyces cerevisiae* indicates that P-type ATPases in subfamily IV could be inactivated by addition of a label (Wicky et al., 2004). Thus, a good initial approach to finding expression patterns of the *tat* ORFs would be to use transcriptional fusions of *tat* promoter regions with a sequence encoding nuclear localization signal-containing GFP (NLS-GFP). Concentrating GFP in the nucleus enhances fluorescence signal and greatly aids in identifying expressing cells and tissues. Where possible, the whole intervening region between the ORF of interest and the preceding gene should be taken as the promoter sequence. In *C. elegans*, the first few introns also frequently harbor *cis*-regulatory elements (Okkema and Krause, 2005). However, in *tats* with short 3' utranslated regions (UTR) not much of the translated sequence and therefore, not many exons and introns could be included in the expression cassette, because the N terminus of the encoded products contains transmembrane regions and could also include endoplasmic reticulum (ER)-targeting motifs, which would prevent the NLS-GFP reporter from localizing to the nucleus. Here, derived via particle bombardment integrated and

extrachromosomal transgenes composed of *tat* promoter regions transcriptionally fused with the sequence encoding NLS-GFP are used to determine expression patterns of the *tat* ORFs.

Materials and methods

YAC DNA isolation

S. cerevisiae carrying yeast artificial chromosomes (YACs) Y49E10 or Y17G9 were obtained from the *Caenorhabditis* genome sequencing group at the Sanger Institute. 10ml aliquots of synthetic minimal glucose -ura medium (0.67% Difco™ yeast nitrogen base without amino acids [Difco Laboratories acquired by BD, Franklin Lakes, NJ], 2% dextrose, 0.08% Bio101© Systems CSM -ura w/ 40mg/L ADE [Qbiogene, Irvine, CA]) were inoculated with a large colony of yeast and grown overnight at 30ºC in a rotating wheel. The cell number of the cultures was determined using a hemocytometer; the cultures were then washed twice with cold 50mM EDTA, pH 8: centrifuged at 500g for 5-10min and then re-suspended in 10ml of 50mM EDTA, pH 8 by vortexing. Aliquots containing $5x10^7$ washed cells or whole suspensions (≥ 2.5 10^8 cells) were centrifuged again, and the pellet was resuspended in 600ml of the sorbitol/potassium phosphate/EDTA buffer (1M sorbitol, 50mM potassium phosphate, pH 7.5, 0.02M EDTA, pH 8). These suspensions then received 2µl of 2-mercapthoethanol and 50U of zymolyase (Zymo Research via VWR) and were incubated at 30ºC in a rotating wheel (gentle rotations) for 1-2 hours with periodic visual monitoring. Spheroplasts were pelleted by centrifugation in a bucket centrifuge at 3000g for 5-6min; the pellet was re-suspended in 180ml of ATL buffer (DNeasy® kit, Qiagen), and 20µl of proteinase K (DNeasy® kit, Qiagen) was added to the suspension, which was then incubated for 2

hours at 55ºC in a heatblock. Total DNA was isolated from the digestions using a DNeasy® kit (Qiagen, Valencia, CA).

Cosmid DNA isolation

Escherichia coli cells carrying cosmids T24H7, W09D10 or F36H2 were obtained from the *Caenorhabditis* genome sequencing group at the Sanger Institute. T24H7 cosmid was unstable in cells grown >30ºC or stored for prolonged (>3 days) periods of time at 4ºC. DNA was extracted from cell cultures with the cosmids using a QIAGEN plasmid midi kit (QIAGEN, Valencia, CA).

Expression cassette construction

tat-1

A DNA segment in Y49E10 YAC that contains the *tat-1* promoter (the intervening portion between the *tat-1* and *pie-1* ORFs) and the first 4 *tat-1* exons and introns was amplified in three fragments using proof-reading polymerase PrimeSTAR™ (Takara Mirus Bio, Madison, WI) with the nested PCR approach (Figure 2). The fragments were cloned into pGEM®-T Easy helper vector (Promega, Madison, WI) to derive pNL57.1, pNL58.2 and pNL59.3 constructs. These three and all subsequent *tat-1* constructs were stable only when host *E. coli* cultures grew at <30ºC. The PCR inserts in pNL57.1 and pNL58.2, which were a proximal promoter and a 5' transcribed fragments of the ORF, respectively, were sequenced where possible; the inverted repeats (identified using the einverted program of the EMBOSS software suite; Olson, 2002) prevented sequencing of the remainder. After several cloning steps, vectors pNL66.1, which contains the

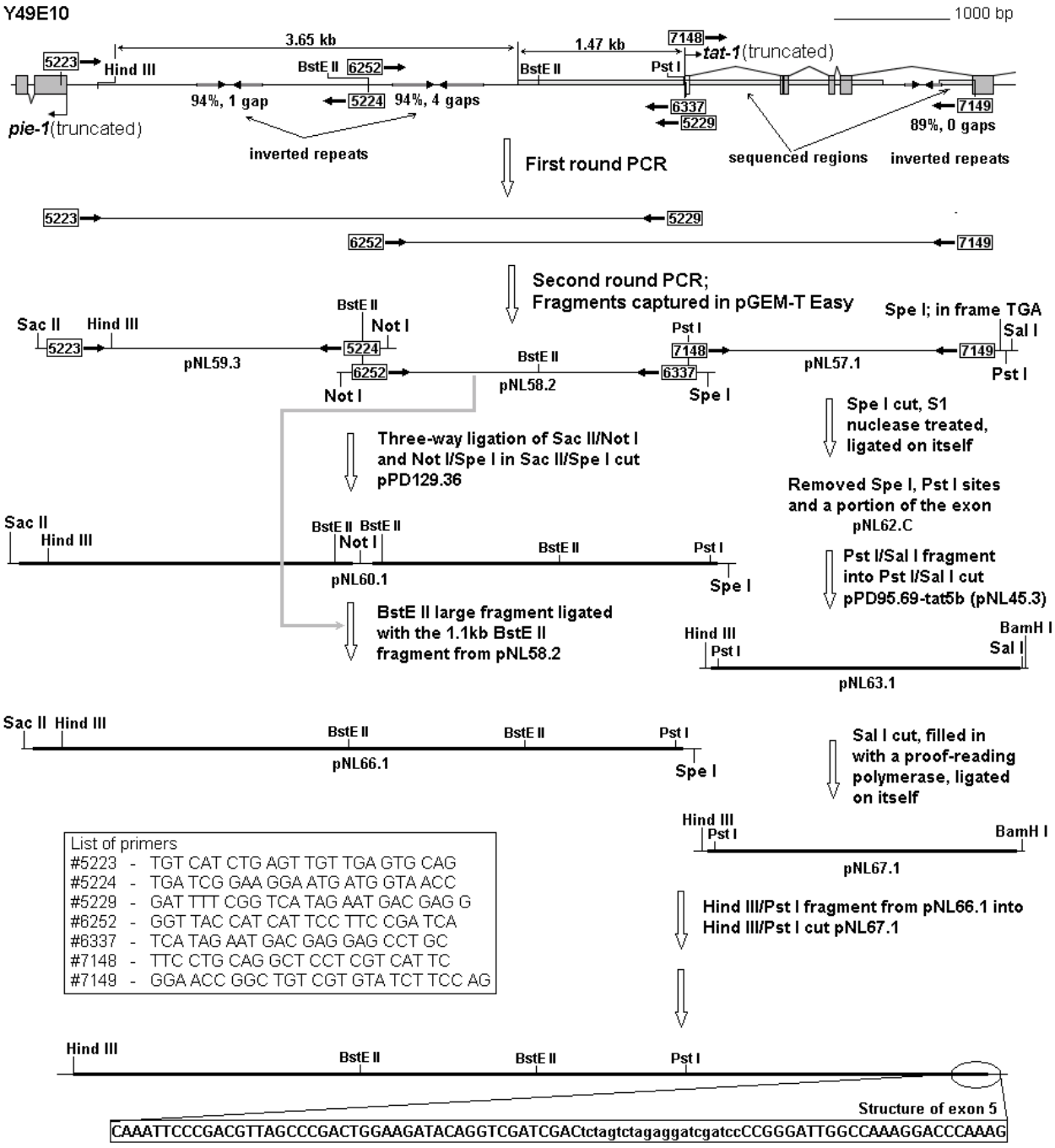

Figure 2. Construction of the *tat-1* expression cassette.

whole *tat-1* promoter, and pNL67.1, which includes the front 5' end portion of the ORF fused in frame with an NLS-GFP sequence (in pPD95.69 from the Fire lab vector kit), were derived (Figure 2). In the final step, repeated several times, the Hind III/Pst I fragment from pNL66.1 was ligated into Hind III/Pst I cut pNL67.1 to derive only deletion mutant versions of the intended expression cassette. To circumvent this problem, the cassette was generated using the overlap PCR approach: in the first round the promoter segment in pNL66.1 was amplified with primers 5223 and 6337 and the *tat-1* 5' end-reporter segment in pNL67.1, with primers 7148 and 8021 (TCAGAGGTTTTCACCGTC); in the second round the two overlapping first round products were amplified with primers 5223 and 8021 to recover the full length *tat-1* expression cassette. The size of the second round product was verified on an agarose gel and the DNA was used for particle bombardment.

tat-2

An 8.6 kb segment that includes 6 introns of the *tat-2* ORF and a 1.1 kb proximal promoter region was amplified from Y17G9 in three overlapping fragments using proof-reading polymerase PrimeSTAR™ (Takara Mirus Bio, Madison, WI) with primer pairs 7155 (GGATCCATATGGTTCCGACGTTG) and 7154 (TGTACTTTTCCCCTCTTGTGAAC), 7153 (CATTTTATGCAGAGTTCGAGTCAC) and 7152 (GAAGAGTGGCGGTAAAATTCGG), and 7151 (TCTTCTAACTCTCGGGCCATTTG) and 7150 (TAACATCCAAAAGCAGTAACATCC). The 3.2 kb fragment amplified with 7155 and 7154 primers and spanning introns 2 through 5 and exons 2 through 5 was sequenced. The three fragments were then assembled together into pPD95.69 (Fire lab vector kit) to derive pNL78.1 (Figure 3A). A

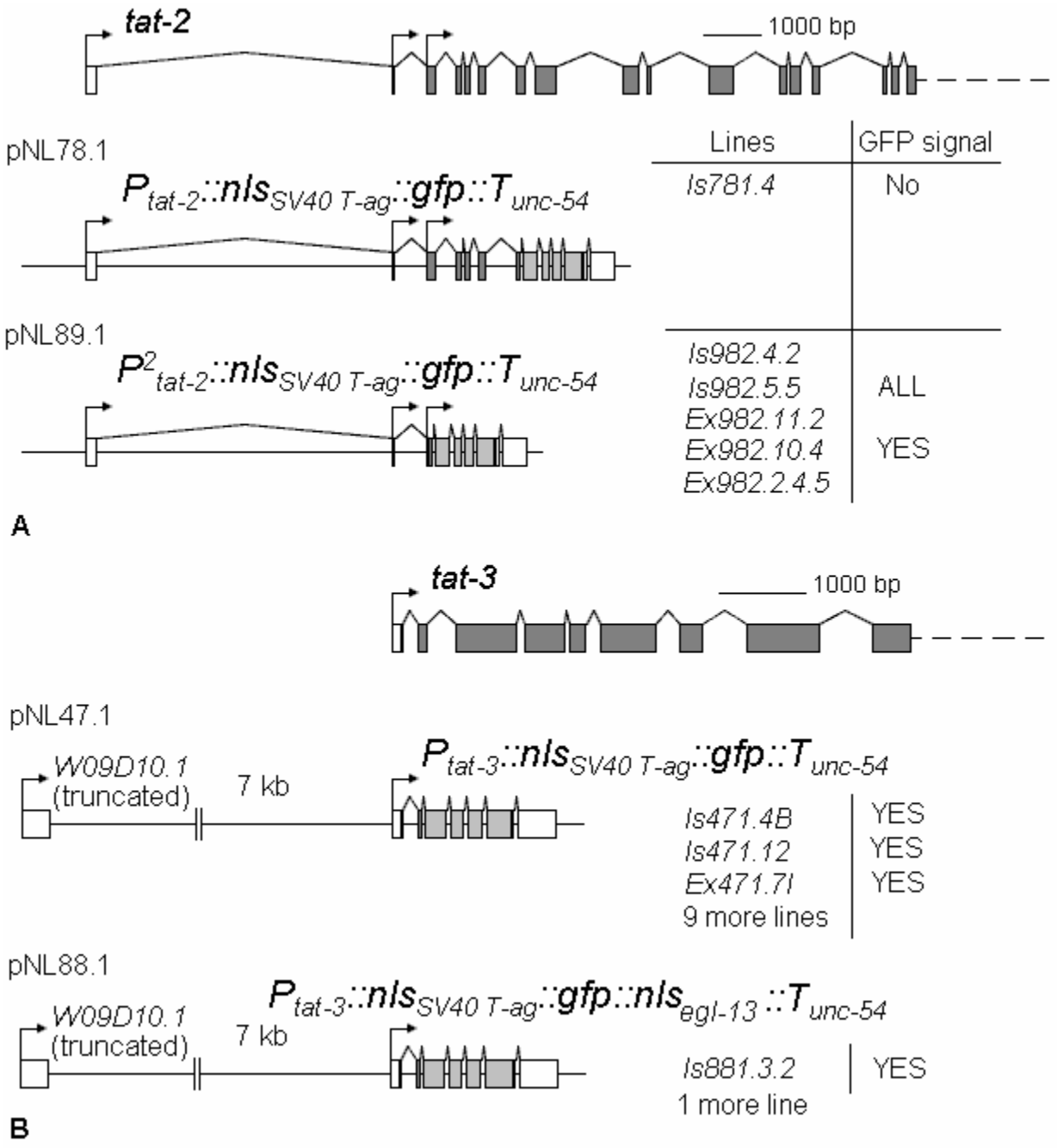

Figure 3. Structure of the *tat-2* (A) and *tat-3* (B) expression cassettes and a list of transgenic lines carrying these cassettes as transgenes.

second shorter *tat-2* expression cassette was made by amplifying a *tat-2* segment that contains introns 1 and 2 and exons 1 and 2 with primers 7154 and 9060 (GCGGATCCTGAACAGCATGGCAACCAACTG) and then inserting it into pNL78.1 in place of the 7154/7155 fragment to derive pNL89.1. The 7154/9060 segment was sequenced. pNL78.1 and pNL89.1 were used for particle bombardment.

tat-3

The *tat-3* promoter sequence (the 7 kb segment between *tat-3* and the preceding ORF, plus the first exon-intron pair) was obtained from the W09D10 cosmid in two overlapping fragments: as a distal 5.6 kb Spe I/Sph I restriction digest fragment and as a proximal 1.8 kb PCR fragment amplified with primers 4282 (CCAAATCCCAACTTTCTGCCA) and 4281 (GACGTCGGATCCTTCCACGTCCACCGACTTCTG). The PCR amplified segment was sequenced. The two fragments were reassembled into pPD95.69 (Fire lab kit) to derive pNL47.1, and then the full promoter was cut out from pNL47.1 as the Pst I/Nco I fragment and inserted into Pst I/Nco I cut pNL74.4 (a derivative of pPD95.69 in which a second NLS from EGL-13 was added to the C terminus of GFP) to derive pNL88.1. pNL47.1 and pNL88.1 were used for particle bombardment (Figure 3B).

tat-4

The *tat-4* promoter sequence (a 2.1 kb fragment between *tat-2* and the preceding gene, plus the first *tat-4* exon and intron) was amplified from the T24H7 cosmid using primers 5583 (CTGCAGCGATATGTCATCAACTCCGGTC) and 5584 (GGATCCGTCAGTGAAGTCTCGGTAGTTG). The amplified fragment was sequenced and inserted into Pst I/BamH III cut pPD95.69 (Fire lab vector kit) as a Pst I/BamH III

segment to derive pNL53.5. The new construct was then cut with BamH III, the overhangs filled in and the linear piece ligated on itself to derive the pNL56.1 vector, in which the 5' translated portion of *tat-4* was fused out of frame with the translated reporter sequence (Figures 4 and 5). The 2.1 kb *tat-4* promoter sequence was further cut as a Pst I/Xma I segment out of pNL56.1 and inserted into Pst I/Xma I cut pNL74.4 (a derivative of pPD95.69 in which a second NLS was added) to derive pNL76.1. During this step of vector construction a C nucleotide next to the Xma I site disappeared and this brought the *tat-4* 5' translated portion in pNL76.1 in frame with the reporter sequence (Figure 4). Another *tat-4* expression cassette was constructed through a three-way ligation of the 3.3 kb Xba I/Bgl II T24H7 fragment, which contains two complete ORFs upstream of *tat-4*, with the Bgl II/EcoR I fragment from pNL76.1 and EcoR I/Xba I cut pPD95.69 to derive pNL85.2 (Figure 5). The fifth *tat-4* expression cassette was made by fusing the longer 7.8 kb Sal I/Bgl II T24H7 fragment, which includes a third long upstream ORF in addition to the first two short ORFs immediately preceding *tat-4*, with Bgl II/EcoR I cut pNL76.1 and EcoR I/Sal I cut pPD95.69 to derive pNL86.1. The final and shortest *tat-4* expression cassette was assembled by amplifying a 1.6 kb *tat-4* promoter fragment that excludes the first intron with primers M13-rev (standard primer) and 9059 (GCGGATCCTGGTCGAGGTGTCGTCATATTC) from pNL53.5 and then replacing the longer Nhe I/BamH III fragment in pNL53.5 with the shorter Nhe I/BamH III fragment from the PCR product to derive pNL91.1. pNL53.5, pNL56.1, pNL76.1, pNL85.2, pNL86.1 and pNL91.1 were used for particle bombardment (Figure 5).

Figure 4. Fusion sites of the *tat-4* 5' region with the sequence encoding NLS-GFP reporter in the *tat-4* expression cassettes.

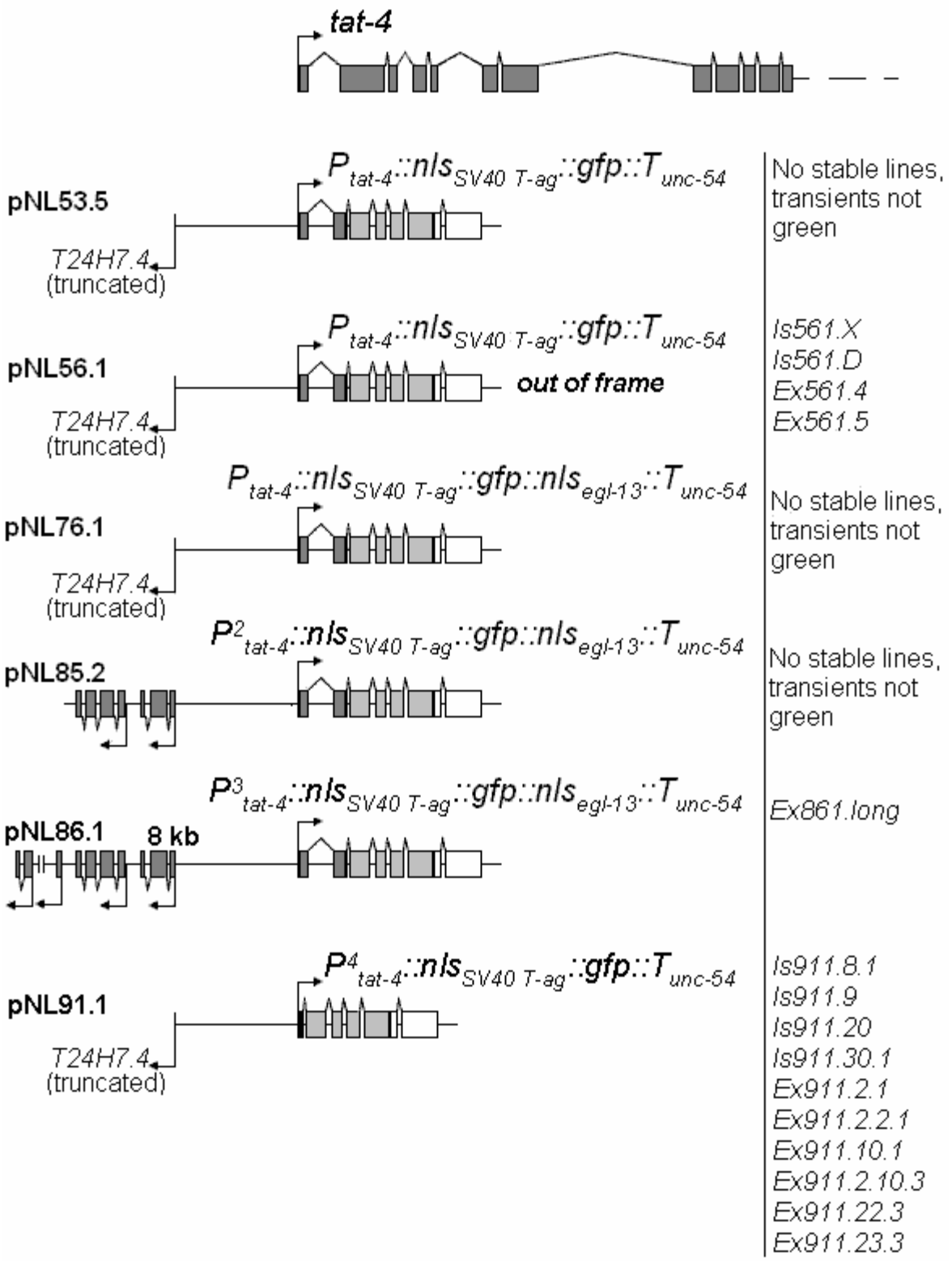

Figure 5. Structures of the *tat-4* expression cassettes and a list of transgenic lines carrying these cassettes as transgenes.

tat-5

The 6.4 kb Swa I/Sal I *tat-5b* promoter fragment that includes two complete upstream ORFs (the first ORF of the operon in which *tat-5* is the second cistron and an independent ORF upstream of the operon) was cloned from the F36H2 cosmid into EcoR I/Sal I cut pBluescript. The promoter was then cut out as Pst I/Sal I segment and ligated into Pst I/Sal I cut pPD95.69 (Fire lab vector kit) to derive pNL45.3, in which the translated portion of *tat-5b* is out of frame with the translated reporter sequence. To bring the two into the same frame the Xba I site was destroyed in pNL45.3 to derive pNL48.1 (Figure 6).

A 4.7 kb *tat-5a* promoter fragment was obtained from F36H2 in two portions as the Sal I/Nco I restriction segment and as a PCR fragment amplified with primers 4188 (TCGACGTCTTCGTCCACATTTAG) and 4189 (GGATCCTACTCGAACCGTTCGTGAG). The PCR product was sequenced. The two portions were assembled into pPD95.69 to derive pNL46.1 (Figure 6). pNL48.1 and pNL46.1 were used in particle bombardment.

Particle bombardment delivery of expression cassettes into the nematode gonad

DNA delivery into the nematode gonad was conducted as described by Praitis et al. (2001) with some modifications. *tat* expression cassette vector DNA and DNA of the vector carrying *unc-119(+)* (pDP#MM016B; Maduro and Pilgrim, 1995) (a gift of Dr. W Hanna-Rose) were isolated from *E. coli* cultures using the QIAprep Spin Miniprep kit (Qiagen, Valencia, CA). 4.5µg of an expression vector were combined with 1.5µg of the

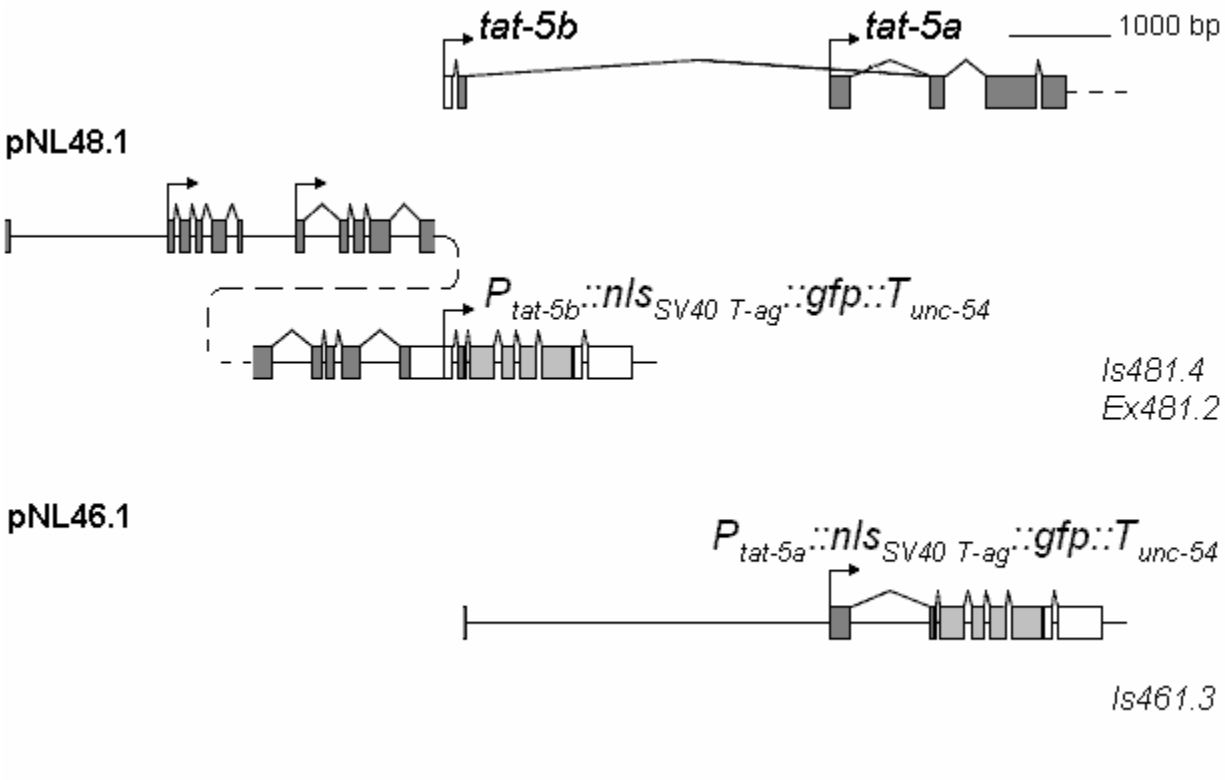

Figure 6. Structure of the *tat-5b* and *tat-5a* expression cassettes and a list of transgenic lines carrying these cassettes as transgenes.

unc-119(+) vector for the total of 6µg of DNA (in the 3:1 ratio after Kinchen et al., 2005) used to coat 3mg of gold particles.

Vector DNA was coated onto gold particles as described by Tucker et al. (2002). Around 3mg of gold particles (in almost all cases 1µm in diameter; in the remaining cases 1.6µm gold particles were used) (Bio-Rad Laboratories, Hercules, CA) were placed into a high quality siliconized 1.5ml microcentrifuge tube (Bio Plas, San Rafael, CA). The particles were then washed three times with alcohol and once with distilled water: washed with 200µl of either alcohol or water by vigorous vortexing for 1min (very brief vortexing with water), briefly (<10sec with alcohol and slightly longer with water) centrifuged at no more than 100 g in a standard tabletop centrifuge, liquid removed without loss of the gold particles. After washing, the gold particles were re-suspended in the amount of water that was determined by the formula: 55 – the number of µls of the DNA solution containing 6µg of vector DNA = µl amount of water for gold particle re-suspension (the total DNA solution plus water volume did not exceed 55µl). Following re-suspension, the gold particles, while being vortexed, were quickly combined in the following order with the DNA solution, 50µl of 2.5M $CaCl_2$ and 20µl of 0.1M spermidine and then vigorously vortexed for 3 more minutes. The coated particles were pelleted to remove the supernatant, washed once with alcohol (as above) and re-suspended by vigorous vortexing in 100µl of alcohol. The suspension was sonicated for 5-10sec in a water-bath sonicator and then immediately spotted in 10µl aliquots onto macrocarriers (due to evaporation of alcohol there was enough suspension to spot 8-9 macrocarriers).

unc-119 mutant nematodes (a gift of Dr. W Hanna-Rose) were grown on 14cm enriched peptone plates (see Chapter 3) spotted with *E. coli* bacteria of either C600 (a

kind gift of Dr. C Malone) or OP50 strain. Before bombardment nematode plates were passaged (animals washed off with M9 buffer to one side of the plate held under incline and then transferred by pipetting to new plates) 1 to 2 or 3 every day for 2 or 3 days. Even with frequent passages, plates always contained significant areas in which nematodes cleared all food and collected into heaps. The heaped animals were in most cases spread out with a bent and moistened Pasteur pipette immediately before bombardment.

Particle bombardment was conducted using a PDS-1000/He system (Bio-Rad Laboratories, Hercules, CA) (kindly provided by Dr. S Gilroy) as recommended by the manufacturer. In almost all cases 1350psi rupture disks were used. All other parameters were standard presets used for plant bombardment (Tucker et al., 2002). Each nematode plate was bombarded in most cases only once.

After bombardment, most nematodes were washed off a bombarded plate with M9 buffer and transferred to 2 or 3 fresh plates. The original and the new plates were incubated under standard conditions (see Chapter 5) for 1 to 3 weeks before screening for transgenic animals. For early screening (only 1 week incubation), plates were flooded with M9 buffer and then all animals that swam were collected onto fresh NGM (see Chapter 5) plates. Some of these animals were only transiently transgenenic and produced exclusively uncoordinated (*unc-119*) progeny. Only one stably transgenenic line, considered independent, was selected per screened plate. Integrated lines were identified by whether homozygous for the transgene animals (not producing *unc-119* progeny) could be derived. Stably transgenic lines, either integrated or

extrachromosomal, were maintained under regular conditions for many generations without loss of the transgene.

Image acquisition and processing

For imaging, transgenic animals were anesthetized with 10mM sodium azide (Sulston and Hodgkin, 1988). Nomarski and fluorescence images were arranged for presentation and publication with the ImageJ program (a freeware from the National Health Institutes).

Results

Biolistic transformation with *tat* expression cassettes that include a large portion of the 5' translated sequence failed to produce stable GFP-active transgenic lines

Vectors carrying 6 different *tat-4* expression cassettes were used for biolistic transformation of *C. elegans* (Figures 4 and 5). In pNL53.5 a sequence for a nucleus-targeted GFP is fused in frame to the second *tat-4* exon. The resultant expression cassette encodes a chimeric reporter peptide that contains 65 amino acids of the TAT-4 N terminus. pNL76.1 is the same as pNL53.5, except for the presence of a second NLS signal from *egl-13* at the 3' end of the GFP segment in the former vector. pNL85.2 and pNL86.1 are derivatives of pNL76.1 in which the *tat-4* upstream promoter fragment is progressively longer: 1.5 kb in pNL76.1, 3 kb in pNL85.2 and 8 kb (including 3 complete upstream ORFs) in pNL86.1. Particle bombardments (at least 8 plates per construct) with the pNL53.3, pNL76.1, pNL85.2 and pNL86.1 vectors yielded transiently transgenic (non-uncoordinated) animals that lacked any notable GFP fluorescence and a single extrachromosomal stable line *Ex861.long* (Figure 5). The absence of GFP signal in the transiently transformed nematodes suggests that the chimeric reporter encoded by the four vectors was either synthesized and inactivated or not expressed at all. In either

case, however, the *unc-119(+)* sequence from the selection vector should not have been affected and albeit not fluorescent, stably transgenic animals should have been recovered. The inability to readily generate stably transformed non-uncoordinated and non-fluorescent lines with pNL53.5, pNL76.1, pNL85.2 and pNL86.1 (discounting the *Ex861.long* line, see below) was therefore rather puzzling.

In comparison with pNL53.5, pNL56.1 contains 4 extra nucleotide pairs at the site of fusion between the 5' portion of the *tat-4* ORF and the reporter (Figures 4 and 5). As a result, the *tat-4* translated segment present in the construct is out-of-frame with the downstream translated reporter sequence and in-frame with a sequence that terminates with a stop triplet 30 nonsense codons later; without the *tat-4* ATG, the translated segment encoding NLS-GFP starts with the ATG of the SV40 Tag NLS fragment located at the 5' of the sequence that codes for GFP (see Fire lab vector kit documentation). Particle bombardment with pNL56.1 produced 2 integrated and 2 extrachromosomal lines (Figure 5). Strong GFP fluorescence could be seen in animals of the extrachromosomal lines in the spermathecas, coelomocytes and a single head neuron (Figure 7); weaker signal emanated from the intestine (data not shown). Since pNL53.5 and pNL56.1 carry identical *tat-4* promoter segments, reporter expression in the latter vector suggests that the chimeric reporter in the former construct would be also likely expressed. The absence of GFP fluorescence in transiently transgenic lines bombarded with pNL53.5 must therefore be due to misfolding and inactivity of the chimera between the N terminus of TAT-4 and the NLS-GFP.

Ex861.long, the sole stable line recovered after biolistic transformation with the four *tat-4* expression vectors encoding the chimeric reporter, is likely able to persist

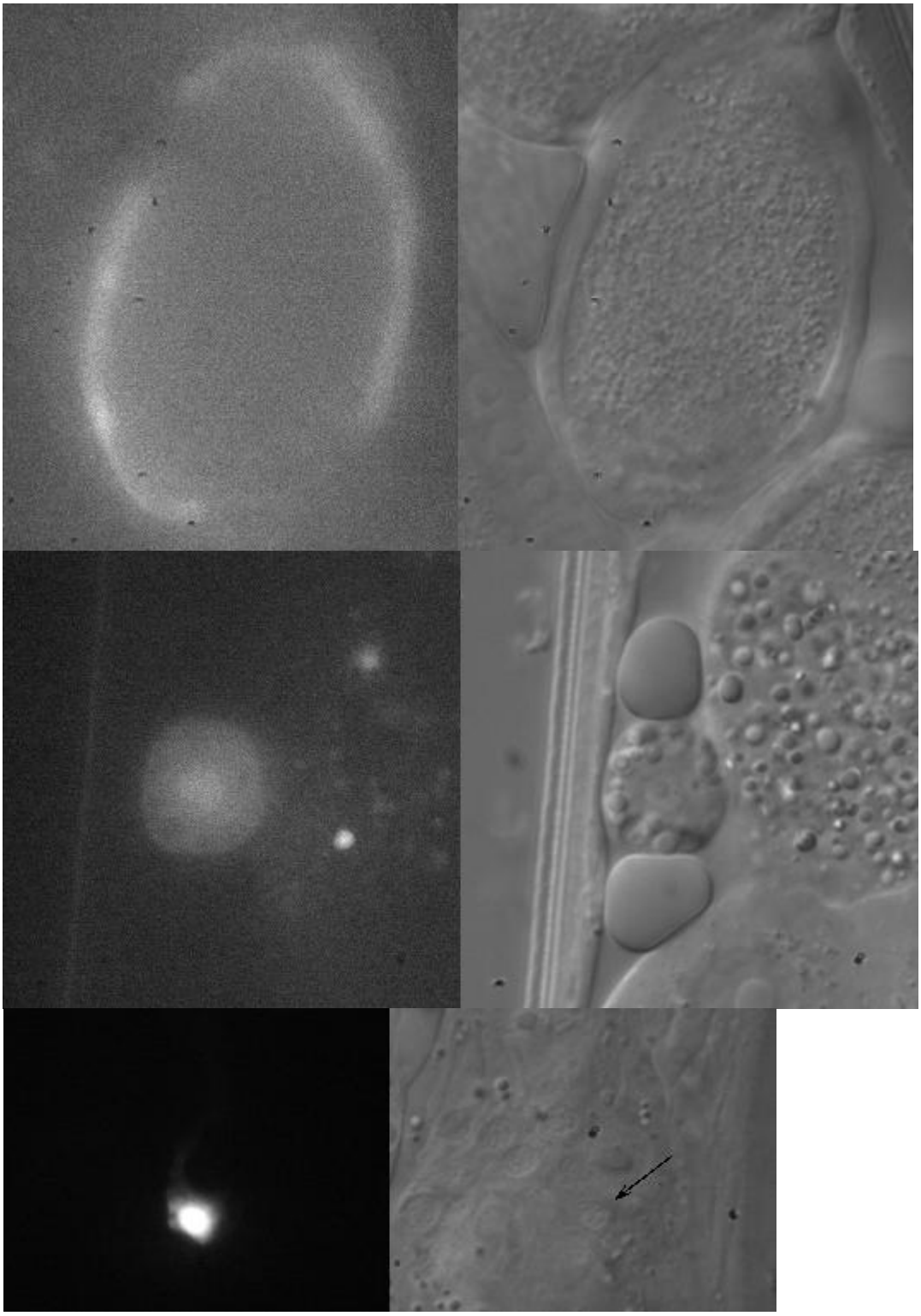

Figure 7. GFP fluorescence in transgenic nematodes derived by bombardment with pNL56.1. GFP signal could be seen in the spermatheca (upper row), coelomocytes (middle row) and a head neuron (lower row).

because all of its *tat-4* expression cassettes are unfortunately inserted and rearranged; the chimera as a result is not expressed. Indeed, in *Ex861.long* animals faint GFP fluorescence could be observed in some cells of the head region (data not shown). This expression pattern differs drastically from GFP expression in lines generated with pNL56.1 and pNL91.1 (see below) and suggests that a GFP-coding sequence came in the *Ex861.long* array under control of some unintended promoter. If indeed the chimeric reporter peptide composed of the TAT-4 N terminus and the NLS-GFP was misfolded, inactivating the GFP domain and causing loss of the encoding transgene, then exclusion of the 5' end translated sequence from the *tat-4* expression cassette would readily fix this deficiency. In pNL91.1 a reporter sequence is ligated into the first *tat-4* exon only 18 bp downstream of the start codon (Figures 4 and 5). As predicted, particle bombardment with this vector generated numerous stably transgenic lines exhibiting strong GFP fluorescence.

Like TAT-4, TAT-2 also seems to have a domain at its N terminus that forms with the NLS-GFP reporter a misfolded inactive chimera that causes loss of transgenes. *tat-2* expression cassette in pNL78.1 vector encodes a chimeric reporter that harbors either 165 (in *tat-2a* and *tat-2b* isoforms) or 200 (in *tat-2c*) amino acids from the N terminus of TAT-2 (Figure 3A). Biolistic transformation of *C. elegans* with pNL78.1 yielded transiently transgenic animals that lacked notable GFP fluorescence and a single integrated line, *Is781.4*. Nematodes carrying the *Is781.4* transgene did not exhibit a notable GFP signal (data not shown). In contrast, particle bombardment with pNL89.1, which hosts an ORF for a chimeric reporter with only either 9 (in *tat-2a* and *tat-2b* isoforms) or 44 (in *tat-2c*) amino acids from the N terminus of TAT-2, readily generated

5 GFP-fluorescing stable lines (Figure 3A). Furthermore, stably transgenic “green” lines could not be obtained with a *tat-1* and a *tat-5a* (pNL46.1) expression cassettes that encode chimeric reporters containing 81 TAT-1 and 90 TAT-5a N terminal amino acids, respectively (Figures 2 and 6). The single integrated line, *Is461.3*, made with pNL46.1 lacks GFP signal. Again, particle bombardments with pNL47.1 and pNL48.1, which express chimeric reporter peptides that include only 9 amino acids of the TAT-3 N terminus and 22 amino acids of the TAT-5b N terminus, respectively, readily produced GFP-fluorescent stable lines (Figures 3B and 6). Thus, it seems that the N terminus of not only TAT-4, but also likely of all the other TATs contains a domain which adversely interacts with the NLS-GFP domain in chimeric reporter fusions and causes loss of the transgenes encoding those chimeric reporters.

The poisonous region in the N terminus of TATs is probably a lipid membrane associated domain. A highly accurate transmembrane helix prediction software, SOSUI (Hirokawa et al., 1998), was used to identify the location of the first transmembrane helix in the TAT sequences. The *tat* expression cassettes were then designed to ensure that the reporter sequence fused with the targeted ORF upstream of the segment encoding the first helix. Nonetheless, as the finding that short N terminal portions of TAT-2 direct the NLS-GFP reporter to the plasma membrane (see below) suggests, in addition to transmembrane helices N termini of TATs also likely contain other membrane-associate domains. Chimeras of the NLS-GFP and a membrane domain would tend to misfold and trigger the unfolded protein response (UPR), which then could induce apoptosis of the cells in which the aberrant peptide accumulated (Bernales et al., 2006).

tat-2 is expressed in the alimentary, reproductive and excretory tissues

2 integrated and 3 extrachromosomal transgenic lines carrying *tat-2* expression cassettes from pNL89.1 were made via biolistic transformation (Figure 3A). The 5 lines differ with respect to the intensity of GFP signal but otherwise generally exhibit nearly identical reporter expression patterns. In all cells with GFP expression, fluorescence seems to emanate mostly from plasma membrane regions (Figures 8-10). This suggests that the 9 (in *tat-2a* and *tat-2b* isoforms; see Figure 3 in Chapter 3) and 44 (in *tat-2c*) amino acid TAT-2 sequences present in the chimeric peptides encoded by the *tat-2* expression cassette override the weak SV40 Tag NLS and target the reporter to the plasma membrane compartment.

tat-2 reporter expression can be first detected in the 2-fold stage embryos in 2 sets of pharyngeal cells, the developing pharyngeal-intestinal valve and a set of cells at the posterior intestine (Figure 8A). Reporter expression appears in the intestine by the first larval (L1) stage (Figure 8B). In the alimentary system of L4 and adult animals, the strongest GFP fluorescence arises from the pharyngeal-intestinal valve (Figure 8C) and the rectal gland cells; weaker signal is observed in the intestine (data not shown). Within the pharynx, *tat-2* reporter is expressed in the 4 gland cells located in the posterior bulb (Figure 8D) and in some cells whose identity could not be ascertained in the procorpus. GFP fluorescence is also observed in the excretory canal and the excretory pore cells in the excretory system of the adult (Figure 8D and data not shown).

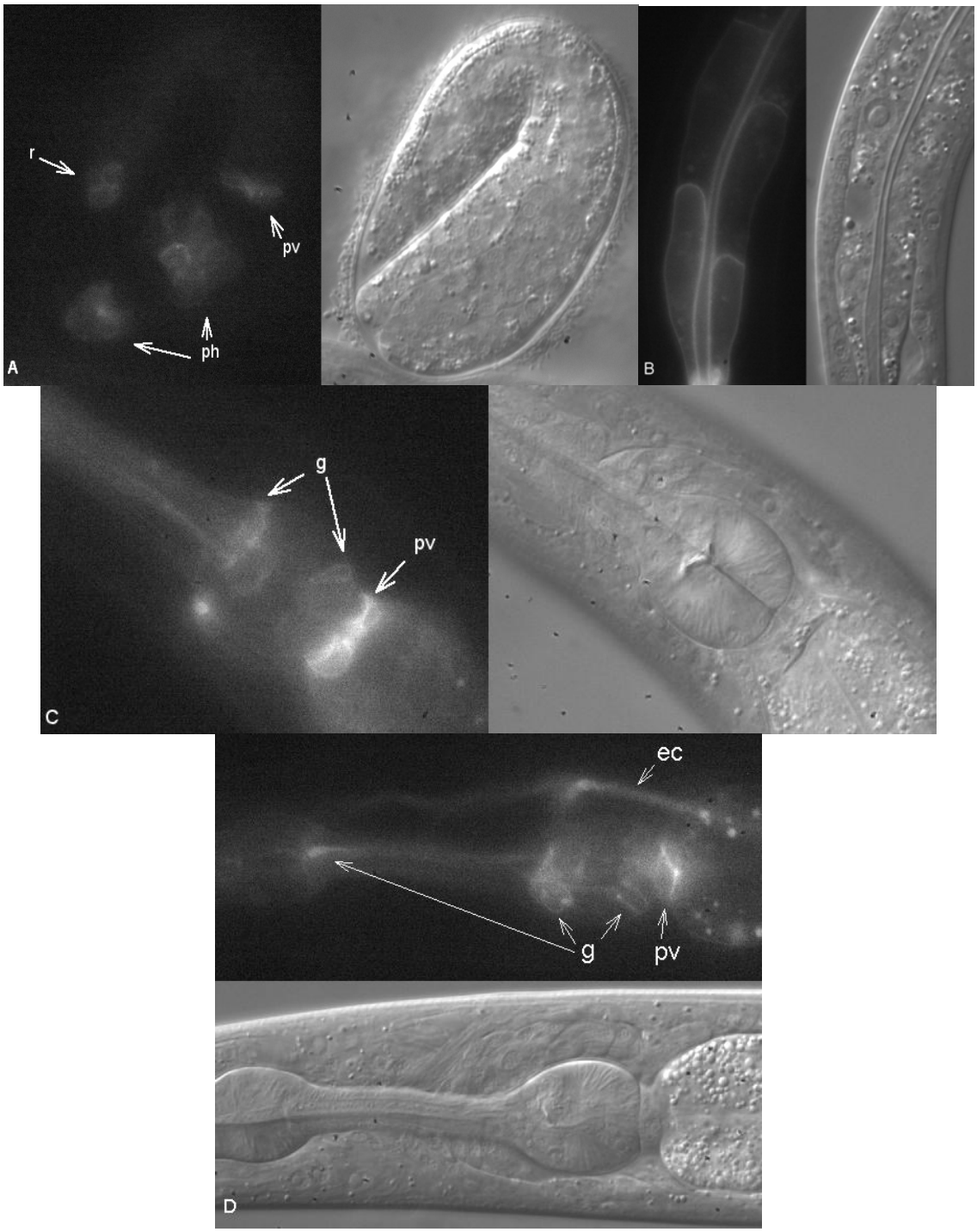

Figure 8. Expression of the *tat-2* reporter in the 2-fold stage embryos (A), in the intestine of L2 animals (B) and in the pharynx, pharyngeal-intestinal valve and excretory canal of the adult (C and D). Abbreviations: ec – excretory canal, g – gland cells of the pharynx, ph – pharynx, pv – pharyngeal-intestinal valve, r – rectum.

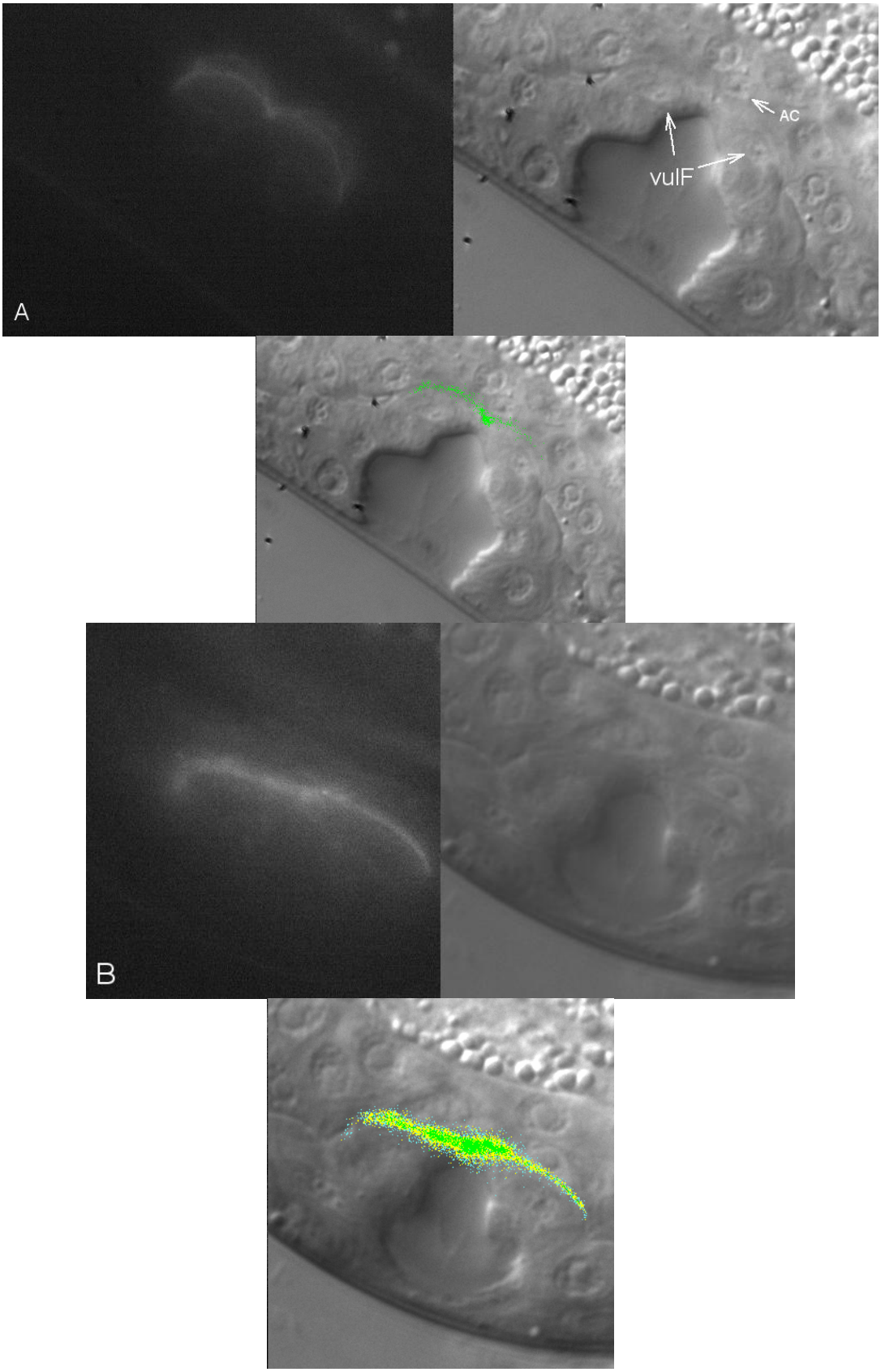

Figure 9 (continues on the next page).

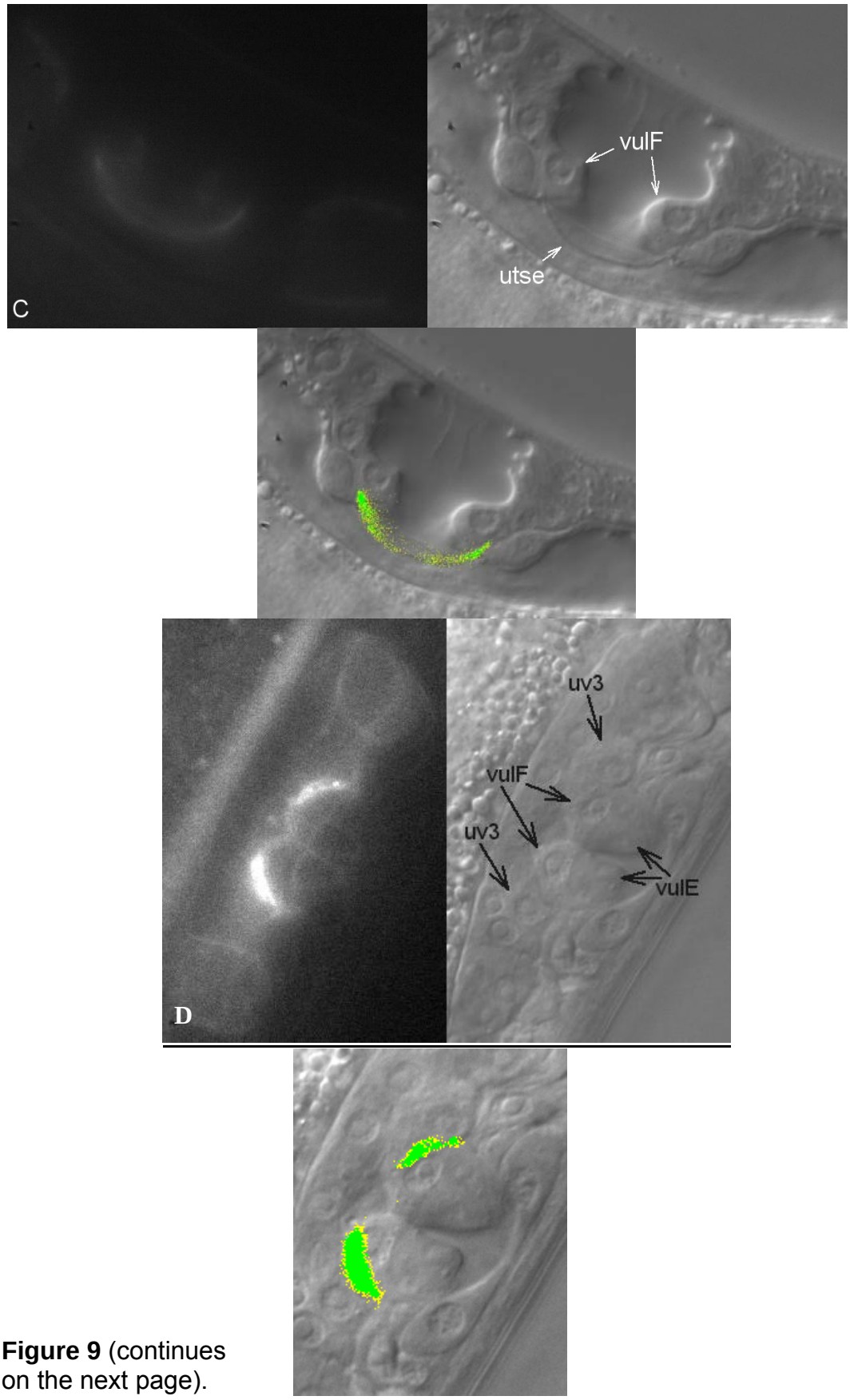

Figure 9 (continues on the next page).

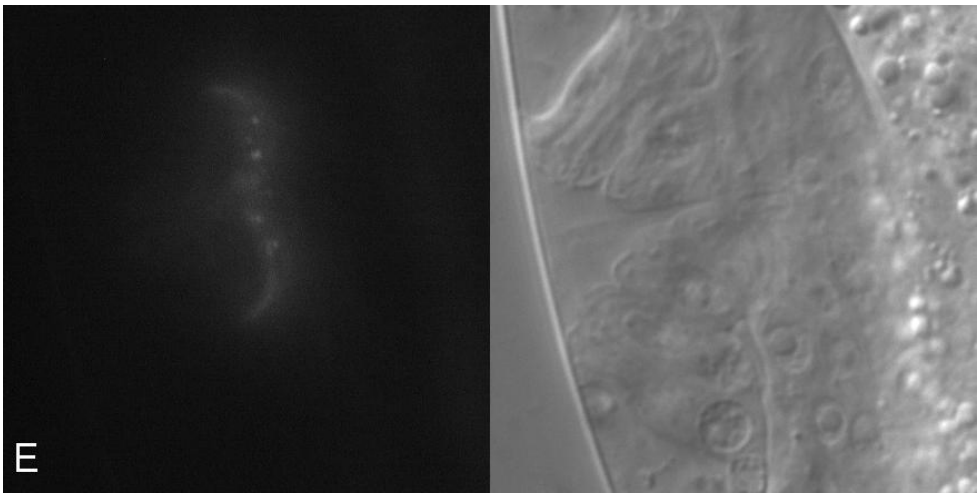

Figure 9 (starts on page 134). Expression of the *tat-2* reporter at the uterine-vulval connection in the early L4 (A and B), middle L4 (C) and late L4 (D and E) animals. The three panels in A-D are, from left to right and down, a UV light image, a bright light Nomarski image and an overlay of the pseudocolored background-erased UV image onto the bright light image. In the pseudocolored images, the strength of the GFP signal declines from green to yellow to light blue. The animal depicted in D carried an extrachromosomal array, all the rest were animals of an integrated line. Abbreviations are the names of relevant cells as discussed in the text.

In the reproductive system, GFP signal first clearly appears in early L4 animals along the contact surface between the developing vulva and uterus (Figure 9A). The signal persists in the same area throughout the L4 stage and then vanishes after the uterine-vulval connection is complete in the adult (Figure 9B-E and data not shown). Formation of the uterine-vulval connection involves the anchor cell (AC) and a subset of VU intermediate precursor cells on the uterine side and the vulF cells on the side of vulva (Choi et al., 2006; Hanna-Rose and Han, 1998; Newman and Sternberg, 1996). Toward the later part of the L3 stage, the AC resides over the opening in the basement membranes separating the uterus from the vulva and contacts the vulF cells and some members of the VU intermediate precursor lineage. The AC induces 6 adjacent cells of the later type to assume the π fate and divide once. Then, 4 π daughters located the closest on each side of the AC along the anterior-posterior axis become mononuclear uterine-vulval 1 cells (uv1); the remaining π progeny fuse together into the “H”-shaped syncytial uterine-seam (utse) cell. The “parallel bars” of the utse stretch out and connect to the seam cells in the epidermis, while the “cross bar” forms into a thin planar laminar process that runs dorsal over the AC and uv1 cells. The AC fuses with the utse by the middle L4 to liberate a three-layer stacked vulF-uv1-utse structure. GFP fluorescence of the *tat-2* reporter seems to emanate in early L4 animals from the vulF plasma membrane regions that are adjacent to the AC and the π lineage cells (Figure 9A); the epicenter of the GFP signal is located ventrally underneath the AC (Figure 9A-B). By the middle L4 stage, the epicenter shifts outward away from the dorsoventral axis that passes through the center of the vulva (Figure 9C) and by the late L4, seems to reside in the plasma membrane regions between the vulF and uv3 cells (Figure 9D). In

extrachromosomal lines, in addition to the expression along the uterine-vulval contact plane, the plasma membrane of the vulE cells also radiates weak fluorescence (Figure 9D); this signal could be an artifact of reporter over-expression (Chang et al., 1999). The fully formed vulva in the adult is devoid of *tat-2* reporter expression even in extrachromosomal lines, but the uterus exhibits moderate fluorescence (data not shown). Expression of the *tat-2* reporter also seems to occur during the L4 stage in the germline syncytium differentiating into spermatids in the proximal gonad (Figure 10A). Following spermatogenesis, spermatids enter the spermatheca passively by being swept in with the first ovulating oocytes and then rapidly undergo morphogenesis into spermatozoa. At the L4 stage, “empty” spermathecas give out a very weak GFP signal (Figure 10A). In contrast, in adult previously ovulated hermaphrodites, GFP fluorescence in the plasma membrane of both somatic cells of spermatheca and spermatozoa is extremely bright (Figure 10B). Thus, *tat-2* expression in the *C. elegans* reproductive system appears to exhibit an intricate developmentally coordinated pattern.

tat-3 is expressed in the alimentary, epithelial and reproductive systems

Over a dozen independent transgenic lines carrying *tat-3* expression cassettes were derived (Figure 3B). *tat-3* reporter fluorescence is first detectable in the two-fold embryos in the pharynx (data not shown); this signal is very strong from the very beginning and remains strong through the rest of the nematode lifecycle (Figure 11C and D). Very strong fluorescence then appears in the seam cells of L1 animals (Figure 11A). By the L4 stage, weak GFP signals are detectable in the nuclei of the hypodermis (Figure 11B). Adult hermaphrodites also exhibit strong *tat-3* expression in some cells of the head region, such as the XXXs (Figure 11C), and the tail region (data not shown). In

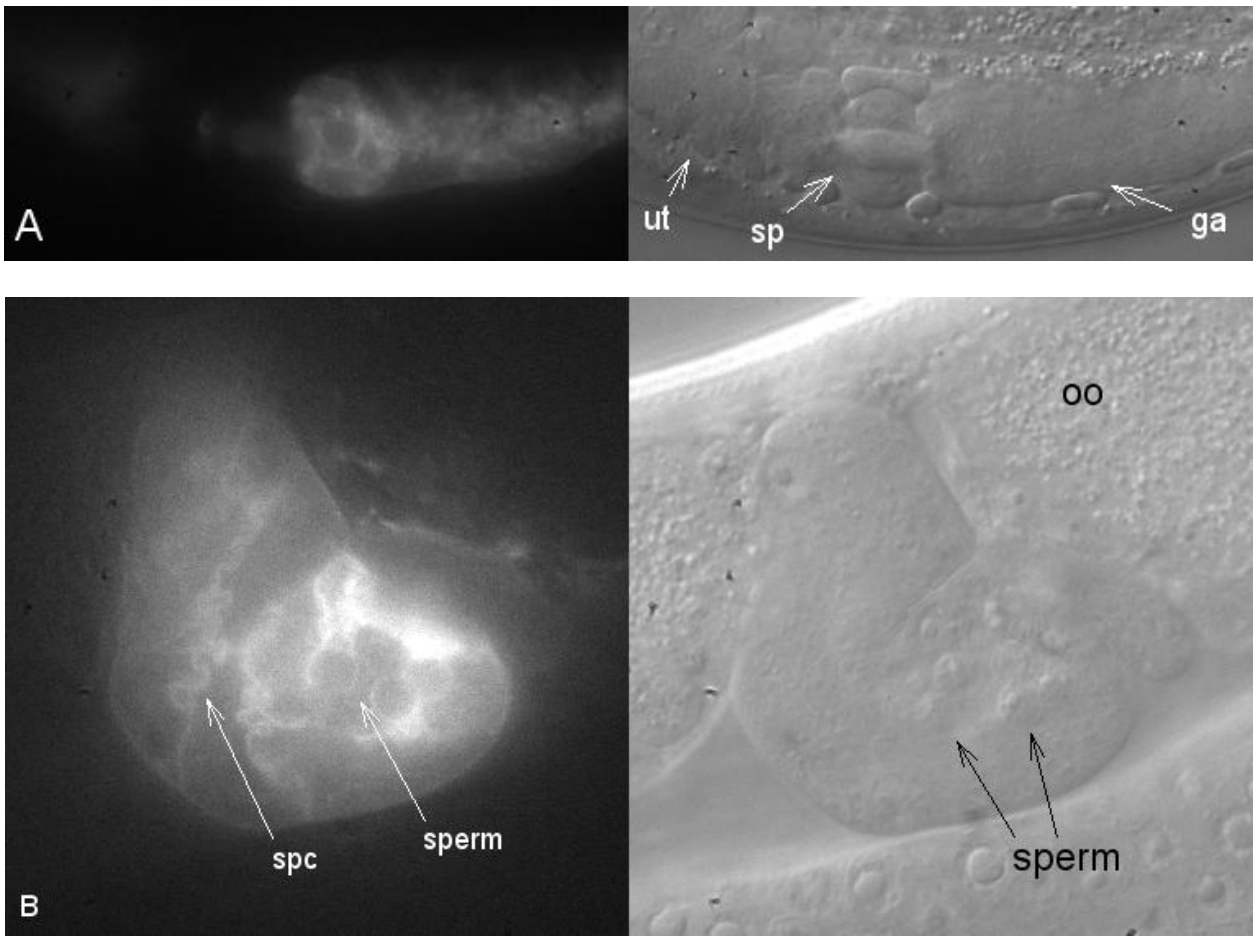

Figure 10. Expression of the *tat-2* reporter during spermatogenesis (A) and in the spermatheca (B). Abbreviations: ga – gonad arm; oo – oocyte; sp – spermatheca; spc – somatic cell of the spermatheca; ut – uterus.

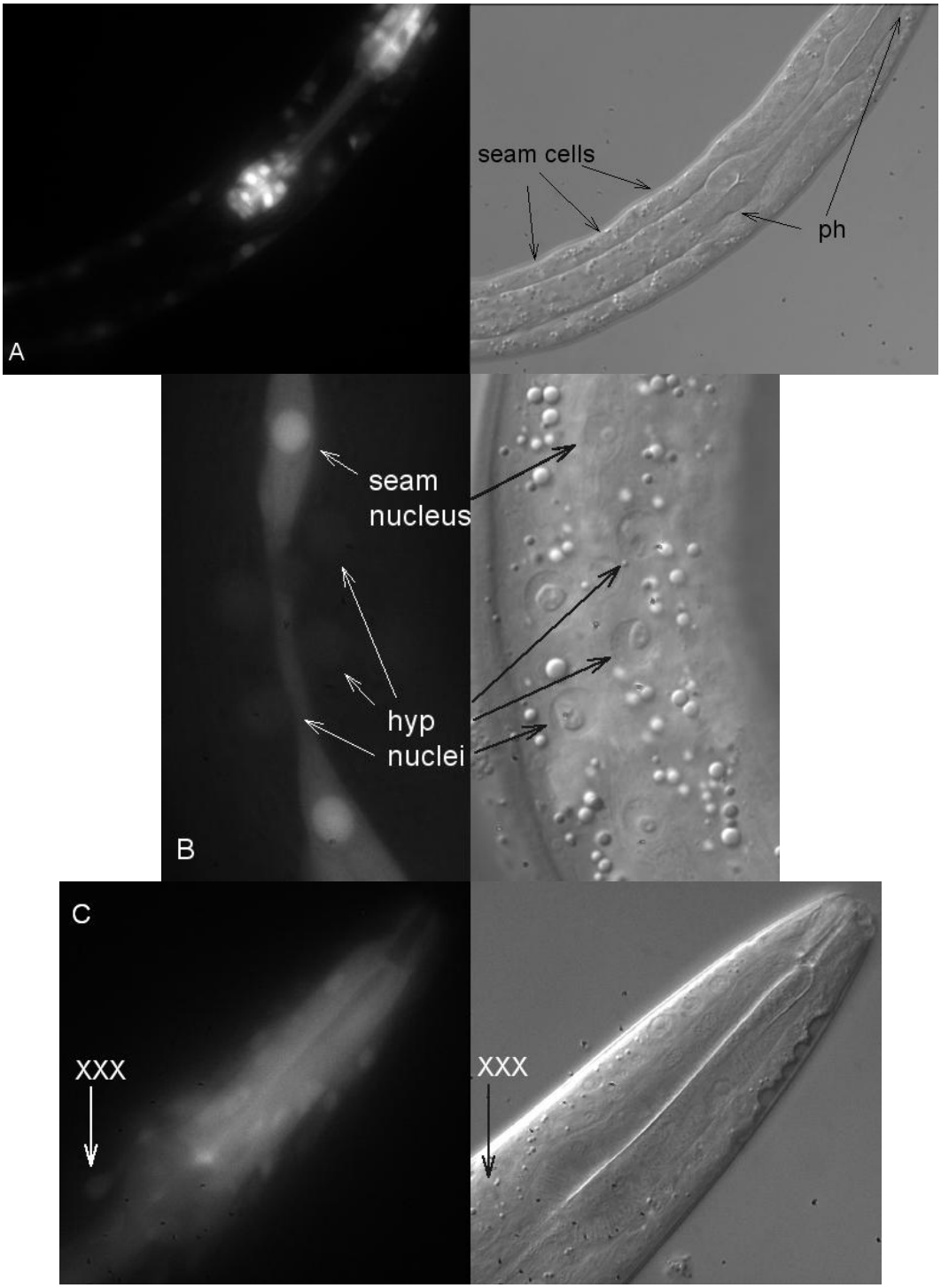

Figure 11 (continues on the next page).

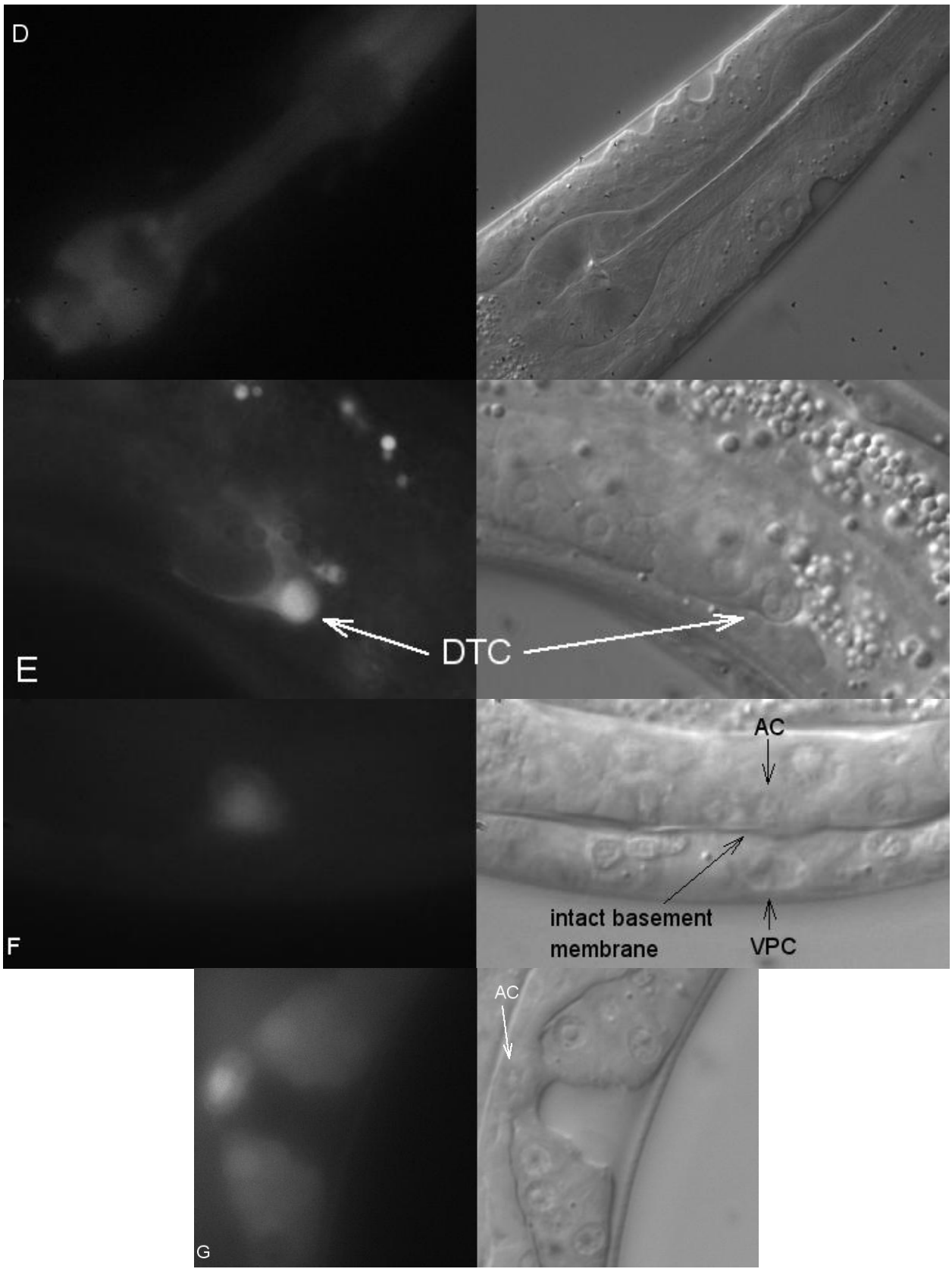

Figure 11 (continues on the next page).

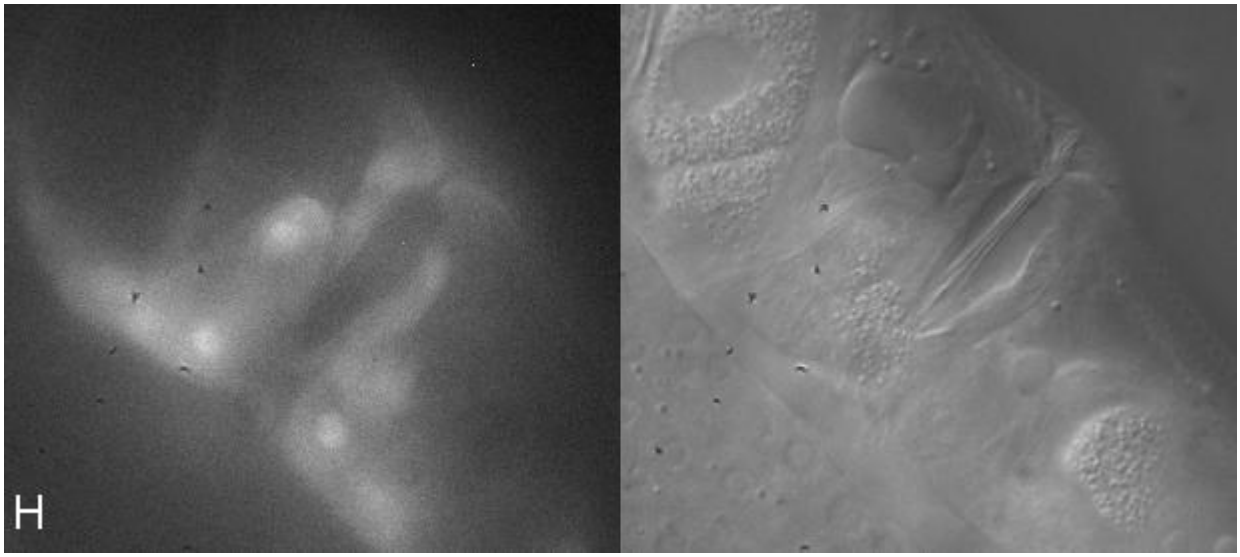

Figure 11 (starts on page 140)**.** Expression of the *tat-3* reporter in the pharynx, the seam cells and some other head region cells in an L1 animal (A), the seam cells and hypodermis of an L4 animal (B), the pharynx and head region cells of an adult (C and D), the DTC (E), the AC and VPCs (F and G) and the adult vulva (H). Abbreviations: ph – pharynx; hyp – hypodermis. The remaining abbreviations are names of different cells discussed in the text.

the reproductive system, the distal tip cells (DTCs) begin expressing the reporter from the onset of gonad migration (Figure 11E). The AC also exhibits strong fluorescence as soon as it chooses its fate (Figure 11F). Early in the development of the uterine-vulval connection, the vulval precursors cells (VPCs), shielded from the AC by two intact basement membranes separating the uterus from the epidermis, are devoid of the reporter signal (Figure 11F). However, it seems that, as soon as the AC degrades the membranes and sends a process to the nearest VPCs, these AC-contacted cells begin exhibiting *tat-3* expression. By the early L4 stage, GFP fluorescence is the strongest in the vulF cells and the weakest, if at all, in the vulva cells furthest removed from the uterus (Figure 11G). This graded pattern of expression persists through the L4 until all vulval cells begin expressing the *tat-3* reporter in the adult (Figure 11H). In extrachromosomal lines with very strong reporter fluorescence, GFP signal, perhaps ectopic, is also seen in the uterus and the spermatheca (data not shown).

tat-4 is expressed in the alimentary and reproductive systems

4 integrated and 6 extrachromosomal lines carrying *tat-4* expression cassettes from pNL91.1 were made (Figure 5). *tat-4* reporter fluorescence is first clearly seen in 3-fold stage embryos in the cells of the pharyngeal-intestinal valve and some cells in the posterior intestine (Figure 12A). Strong expression in these tissues continues through the remainder of the animal lifecycle (Figuire 12B). The GFP signal in the posterior intestine seems to emanate from the three oblong rectal gland cells (Figure 12C). GFP fluorescence in the intestine becomes pronounced in L1-L2 animals (Figure12D). *tat-4* reporter is also expressed in the spermatheca and the uterus. Similar to *tat-2*, *tat-4*

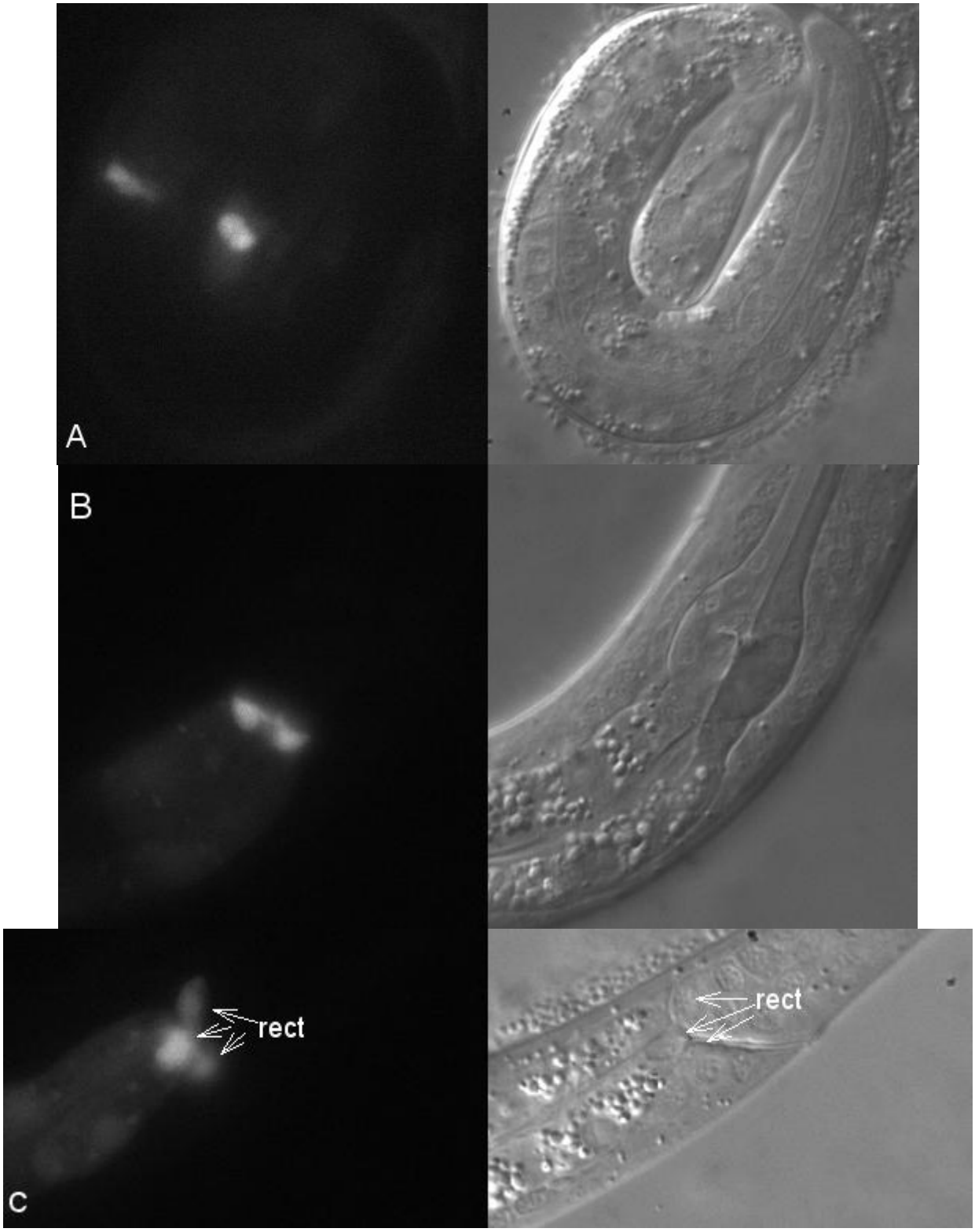

Figure 12 (continues on the next page).

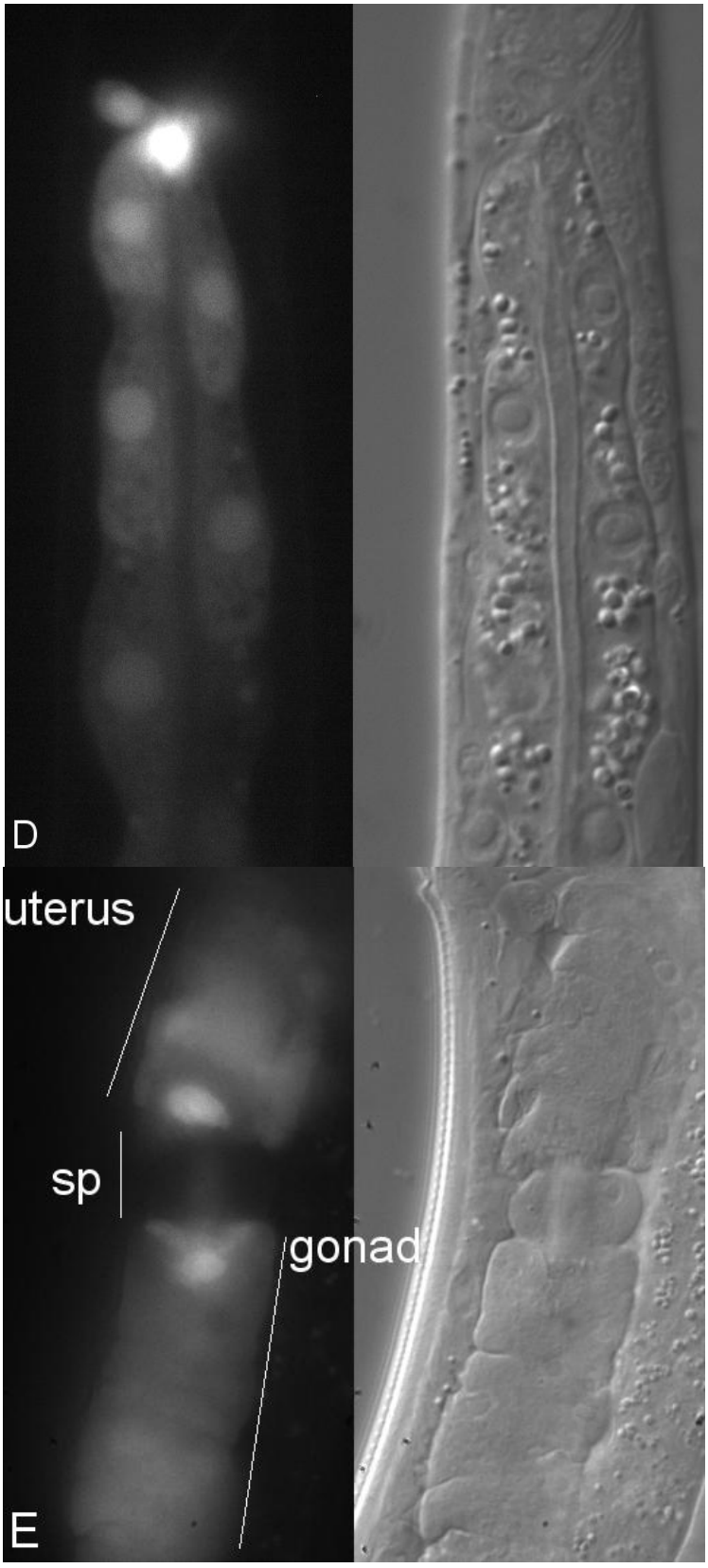

Figure 12 (continues on the next page).

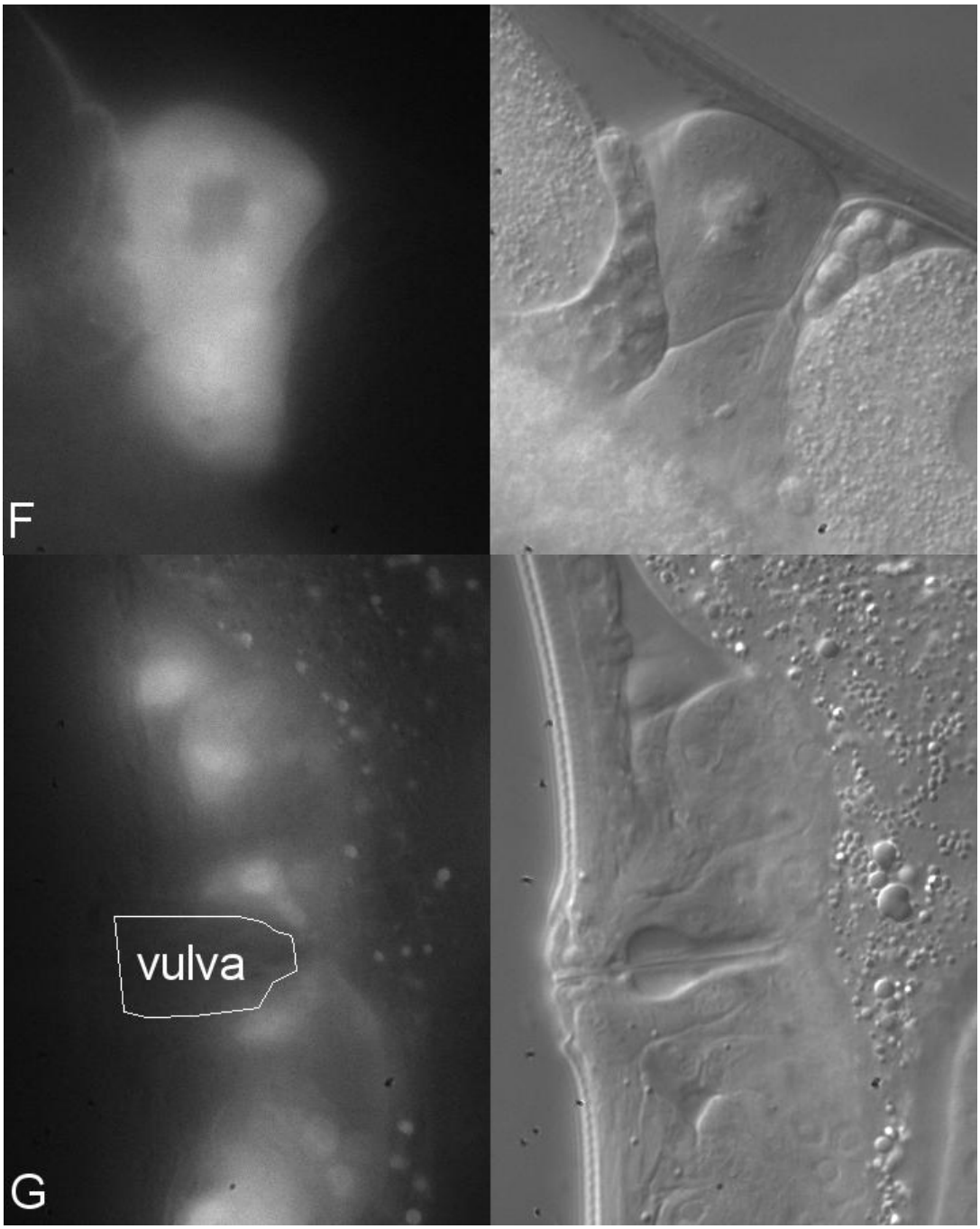

Figure 12 (starts on page 144). Expression of the *tat-4* reporter in the embryo (A), the pharyngeal-intestinal valve (B), the rectal gland cells (C), the intestine (D) and the reproductive system (E-G). Abbreviations: rect – rectal gland cells; sp – spermatheca.

reporter fluorescence is seen in L4 animals in the proximal gonad, where spermatogenesis takes place, and in the uterus (Figure 12E). In the adult, however, the brightest signal emanates from the spermatheca (Figure 12F). Expression in the vulva is not observed (Figure 12G).

tat-5 is expressed broadly in many tissues

2 transgenic lines, one integrated (*Is481.4*) and one extrachromosomal (*Ex481.2*), carrying *tat-5b* expression cassettes from pNL48.1 were made (Figure 6). In both lines GFP signal emanates broadly from many somatic tissues at all developmental stages, except very early embryos. Because the reporter is only weakly nuclear and some cells are obscured by fluorescence from neighboring tissues, it is difficult to ascertain whether indeed all cells express *tat-5b*. The *Is481.4* line embryos begin exhibiting GFP fluorescence clearly at the comma stage (Figure 13A). Larval and adult animals of this line seem to express the reporter in all inspected somatic tissues and cells (intestine, pharynx, seam cells, vulva, spermathecas, AC, DTCs, neural cells and others) (Figure 13B and C); there is seemingly no expression in the germline, and a few tissue types remain to be investigated (muscle). Animals of the *Ex481.2* line exhibit stronger but mosaic fluorescence in the same cell types as the *Is481.4* nematodes, except GFP signal is also seen in some nuclei of the *Ex481.2* germline (Figure 13D). The latter finding is surprising since extrachromosomal arrays are, as a norm, suppressed in germ cells (Praitis et al., 2001); it may, however, indicate that germline nuclei also, although weakly, express *tat-5b*. Thus, *tat-5* is the most broadly expressed of the 4 investigated *tats*.

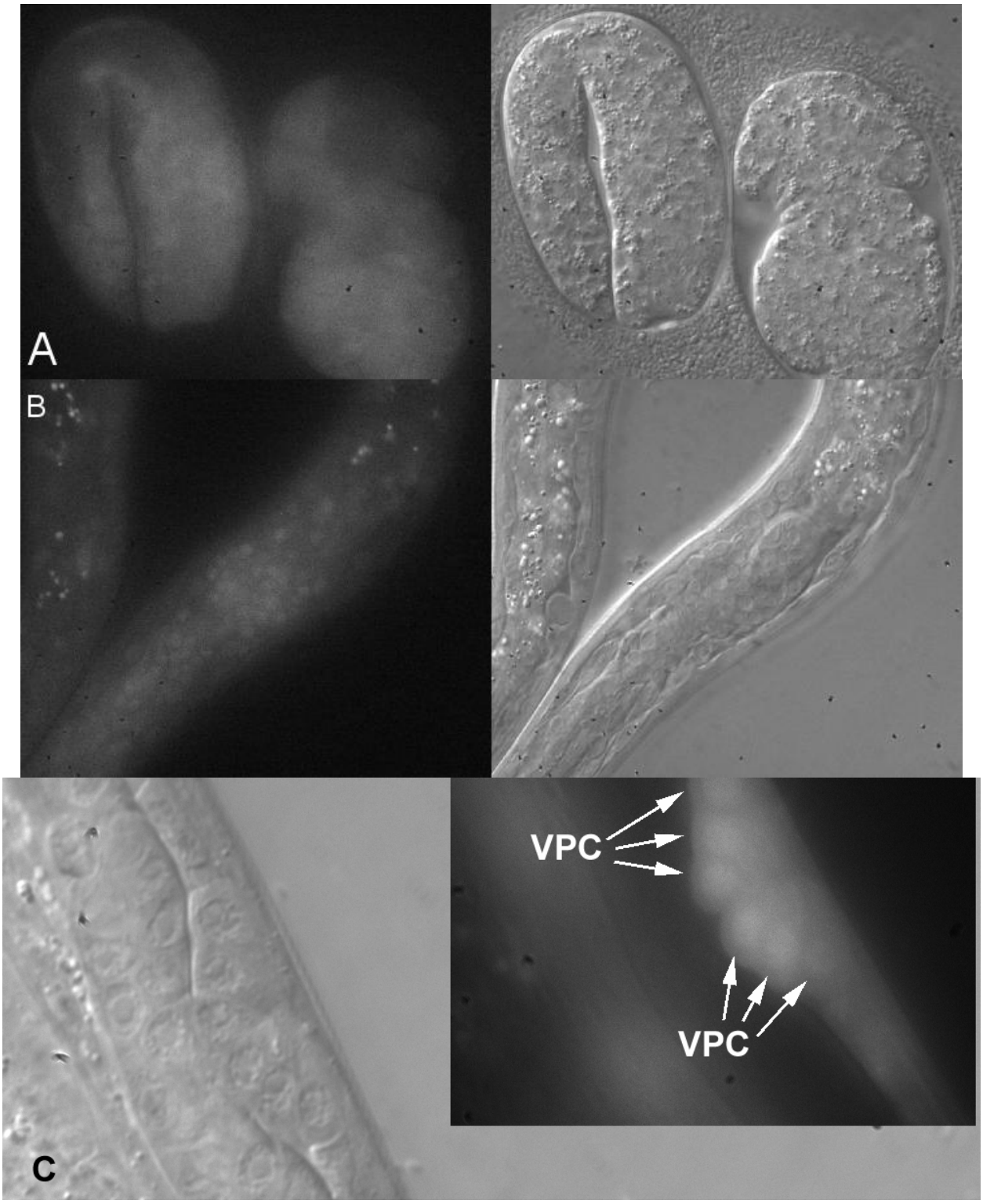

Figure 13 (continues on the next page).

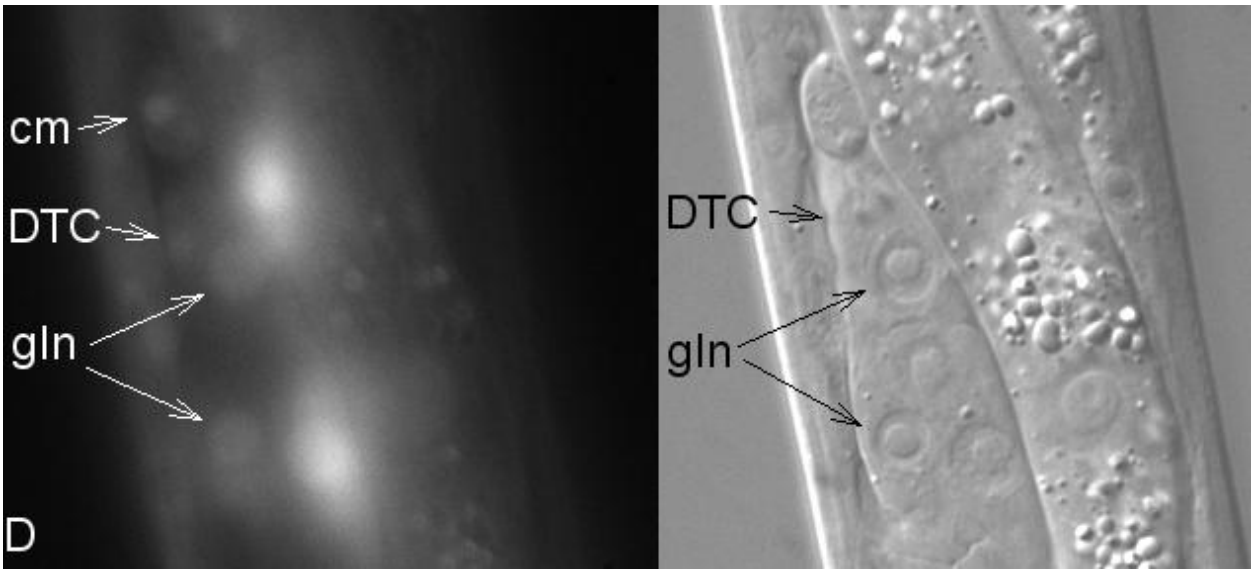

Figure 13 (starts on page 148). Expression of the *tat-5b* reporter in the *Is481.4* line embryos (A), the head region (B) and the developing vulva (C) and in the *Ex481.2* line gonad (D). Abbreviations: AC – anchor cell, cm – coelomocyte; DTC – distal tip cell; gln – germline nucleus; VPC – vulval precursor cell. The gonad arm in D is before the turn.

Discussion

Expression patterns of *tat-2* and *tat-4* are similar and distinct from the expression pattern of *tat-3*

Reporters of *tat-2*, *tat-3* and *tat-4* expression are active in certain specific tissues (Table I). This finding is consistent with observations of mammalian genes that encode P-type ATPases in subfamily IV and are expressed in tissue-specific patterns as well (Halleck et al., 1999; Harris and Arias, 2003). Although *tat-3* and *tat-4* are related with respect to the amino acid sequence of the gene product (Figure 1), the two are not turned on in the same tissues. Instead, it seems that *tat-4* is expressed in the same cell types as *tat-2*. *tat-2* and *tat-4* reporters exhibit strong expression in the pharyngeal-intestinal valve, intestine, rectal gland cells, spermatheca, spermatids, sperm and uterus. *tat-2* is additionally active in the gland cells of the pharynx, the excretory system and a few critical cells of the developing vulva. *tat-3* expression pattern is completely different. *tat-3* reporter product is found in the pharynx (but not the gland cells), DTCs, AC, seam cells, hypodermis, adult vulva and some cells of the head and tail regions. Very weak *tat-3* reporter signals in extrachromosomal lines arise from the spermatheca and uterus, two organs in which *tat-2* and *tat-4* are also on. Expression of *tat-4* in the same tissues as *tat-2* and the lack of activity of both *tat-2* and *tat-4* in cells in which *tat-3* is transcribed suggest that the function of *tat-3* and *tat-4* peptide products might be the same, but the temporal and tissue-specific distribution of this function is so complex that it requires two independent promoters to institute. *tat-2* might then perform a role which is different from the one executed by the other two genes.

Table I. Expression of *tat-2*, *tat-3* and *tat-4* in *C. elegans* tissues

Cells and tissues	*tat-2*	*tat-3*	*tat-4*
Alimentary system			
Gland cells of the pharynx	+++	-	-
Pharynx other than the gland cells	-	+++	-
Pharyngeal-intestinal valve	+++	-	+++
Intestine	++	-	++
Rectal gland cells	+++	-	+++
Reproductive system			
DTCs	-	+++	-
AC	-	+++	-
Developing vulva	+++	+++	-
Adult vulva	-	+++	-
Uterus	++	+	+++
Proximal gonad at spermatogenesis	+++	-	+++
Adult spermatheca	+++	+	+++
Excretory system			
Excretory canal cell	+++	-	-
Excretory pore cell	+++	-	-
Epithelial system			
Seam cells	-	+++	-
Hypodermis	-	++	-
Other			
Head and tail region cells	-	+++	-

Expression of *tat-2* and *tat-3* in the developing vulva and the uterine-vulval connection

Morphological development of the vulva in concert with the formation of the uterine-vulval connection is a complicated sequence of events in which an increasing number of cells induce each other to assume certain fates and certain spatial positions using signaling molecules (Sundaram, 2005; Newman and Sternberg, 1996). The process begins with the selection from two candidates of the single AC. The AC then degrades the gonadal and ventral epidermal basement membranes and induces 3

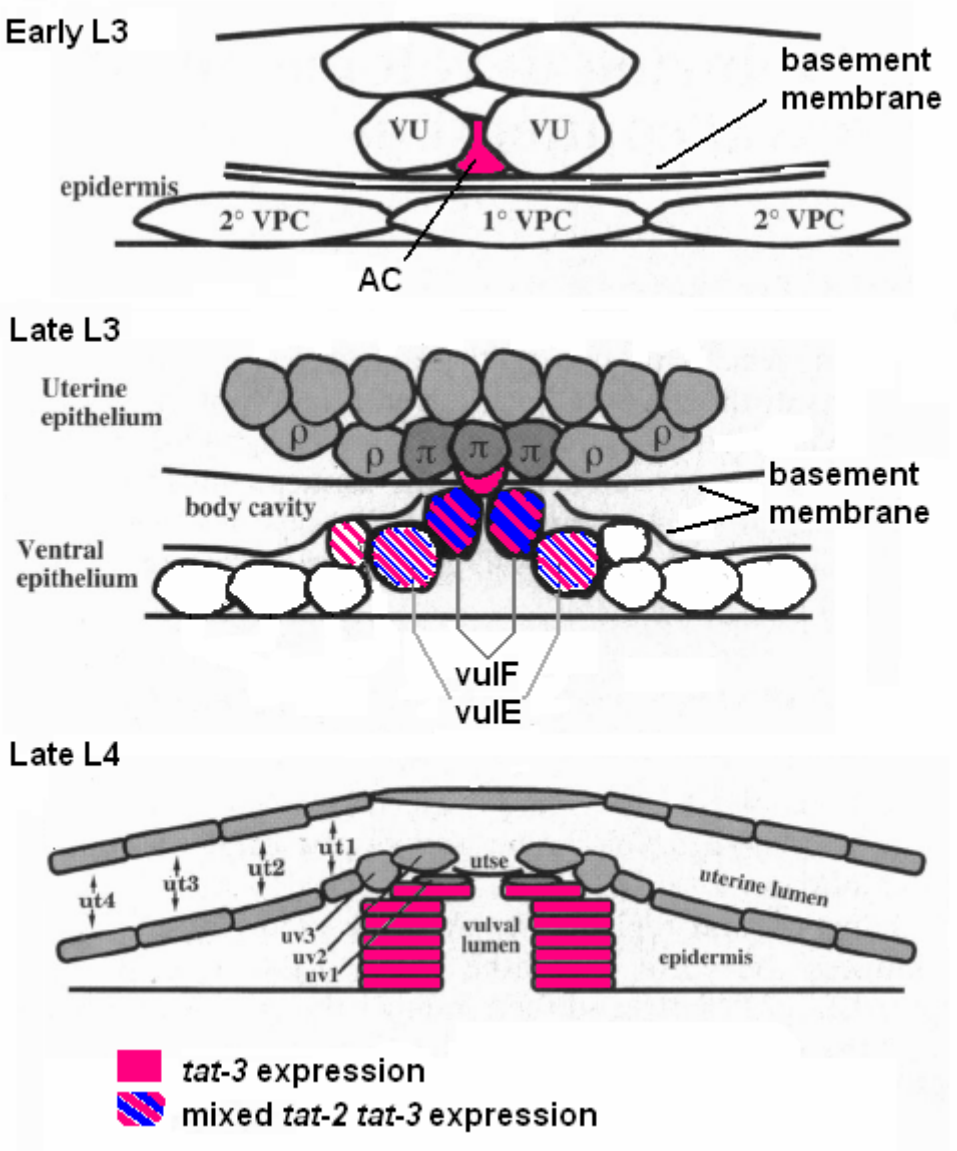

Figure 14. Expression of *tat-2* and *tat-3* in the developing vulva and the uterine-vulval connection. (This figure was adopted and modified from Newman and Sternberg, 1996.)

epidermal VPCs to divide (Sherwood, 2006) (Figure 14). The 1° (P6.p) VPC undergoes 3 rounds of division to produce 8 grand-granddaughters, which become vulF and vulE cells. At the late L3, the AC resides ventrally over the developing vulva and in contact with the vulF cells. *tat-3* reporter is strongly expressed in the AC as soon as it is specified (Figure 11F and 14), but neither this nor the *tat-2* reporter are active in the VPCs. By the L3, both genes are strongly on in the vulF cells, and *tat-3*, but probably not *tat-2*, is also active in the vulE lineage (Figure 9A and B, 11G and 14). Neither gene is notably expressed in the 2° progeny. At the middle L4, the AC fuses with the utse, *tat-2* is still strongly transcribed in the vulF cells, and *tat-3* still forms an expression gradient from the intense signal in the vulF lineage to no fluorescence in the 2° progeny. In the adult vulva, *tat-2* is not expressed and *tat-3* is active in all cells. Preferential localization of the TAT-2 reporter to the plasma membrane regions of the vulF cells that contact the AC and other uterine cells allows for the conclusion that members of the vulF lineage, just as the AC (Sherwood, 2006), are polarized. The developmentally coordinated expression of *tat-2* and *tat-3* in the reproductive system may indicate that these genes are involved in morphogenesis of the vulva and the uterine-vulval connection.

Expression and localization homology between TAT-2 and its mammalian counterparts

The human ATP8B1 (FIC1) and murine Atp8b1 are close homologs of the *C. elegans* TAT-2 in the respective organisms (Figure 1). Mutations in the gene encoding the human homolog cause several kinds of intrahepatic cholestasis, impaired bile flow, which in the most severe cases leads to liver cirrhosis (Bull et al., 1998). A murine model of this disorder exhibits unimpaired bile secretion and no liver damage but

reduced bile salt efflux into bile, reduced resistance of the hepatic canalicular membrane to hydrophobic bile salts and disrupted overall bile salt homeostasis (Paulusma et al., 2006; Pawlikowska et al., 2004). Atp8b1 is expressed in various tissues of the digestive system, such as the liver, small intestine and pancreas, where it localizes to the apical regions of the plasma membrane (Walkowiak et al., 2006; van Mil et al., 2004; Ujhazy et al., 2001). Similarly, TAT-2 is found in various cells of the *C. elegans* digestive system and also resides in the plasma membrane region (Figure 8B-D). Thus, TAT-2, ATP8B1 and Atp8b1 exhibit not only amino acid sequence similarities, but also expression-pattern and subcellular localization homology.

tat-5 is the most broadly expressed of the 4 investigated *tats*

Unlike *tat-2* through *4*, *tat-5* is expressed broadly in all inspected tissues and cell lineages (Figure 13). The *tat-5* ORF is the second cistron in a three-citron operon that also includes *F36H2.2*, an ORF encoding a peptide with similarity to transmembrane nucleoside transporters, and *aph-1*, an essential gene encoding a transmembrane subunit of γ-secretase (Francis et al., 2002 and see Chapter 3). The *tat-5b* expression cassette was constructed by fusing a sequence for NLS-GFP with a *C. elegans* chromosomal DNA segment that includes the first and partly the second *tat-5* exons, the first citron of the *tat-5* operon, the upstream of the operon standalone ORF and the noncoding sequence upstream of the standalone ORF (Figure 6). Since *tat-5b* is unlikely to (no space between the last exon of *F36H2.2* and the first exon of *tat-5b*) and *sph-1* does not (Francis et al., 2002) possess a separate promoter, the whole *tat-5* operon must be expressed off a single promoter located upstream of the first cistron.

The length of the third *tat-5* intron suggested that it might contain a second *cis*-regulatory region independent of the operon promoter. A *tat-5a* expression cassette was constructed by fusing a sequence for NLS-GFP to the second exon of *tat-5a* downstream of a fragment that contains the whole intron 3 (Figure 6). Biolistic transformation with this cassette yielded only a single transgenic line that did not express the reporter. Although other causes, such as inactivation of the GFP by an N-terminal membrane-associated domain of TAT-5a present in the reporter (see above), have not been ruled out yet, the lack of *tat-5a* reporter expression might indicate that exon 3 is devoid of independent *cis*-regulatory elements. Indeed, there might not be a need for a second promoter because the common operon promoter is nearly always on.

References

Bernales S, Papa FR and P Walter. (2006) Intracellular signaling by the unfolded protein response. Annual Review of Cell and Developmental Biology 22:487-508.

Bull LN, van Eijk MJ, Pawlikowska L, DeYoung JA, Juijn JA, Liao M, Klomp LW, Lomri N, Berger R, Scharschmidt BF, Knisely AS, Houwen RH and NB Freimer. (1998) A gene encoding a P-type ATPase mutated in two forms of hereditary cholestasis. Nature Genetics 18:219-224.

Chang C, Newman AP and PW Sternberg. (1999) Reciprocal EGF signaling back to the uterus from the induced *C. elegans* vulva coordinates morphogenesis of epithelia. Current Biology 9:237-246.

Choi J, Richards KL, Cinar HN and AP Newman. (2006) *N*-ethylmaleimide sensitive factor is required for fusion of the *C. elegans* uterine anchor cell. Developmental Biology 297:87-102.

Evans TC. (April 6, 2006) Transformation and microinjection. In The *C. elegans* Research Community (Ed.) *WormBook*. WormBook, doi/10.1895/ wormbook.1.108.1, http://www.wormbook.org.

Francis R, McGrath G, Zhang J, Ruddy DA, Sym M, Apfeld J, Nicoll M, Maxwell M, Hai B, Ellis MC, Parks AL, Xu W, Li J, Gumey M, Myers RL, Himes CS, Hiebsch R, Ruble C, Nye JS and D Curtis. (2002) *aph-1* and *pen-2* are required for Notch pathway

signaling, γ-secretase cleavage of βAPP, and presenilin protein accumulation. Developmental Cell 3:85-97.

Halleck MS, Lawler JF, Blackshaw S, Gao L, Nagarajan P, Hacker C, Pyle S, Newman JT, Nakanishi Y, Ando H, Weinstock D, Williamson P and RA Schlegel. (1999) Differential expression of putative transbilayer amphipath transporters. Physiological Genomics 1:139-150.

Hanna-Rose W and M Han. (1998) Cog-2, a Sox domain protein necessary for establishing a functional vulval-uterine connection in *Caenorhabditis elegans*. Development 126:169-179.

Harris MJ and IM Arias. (2003) FIC1, a P-type ATPase linked to cholestatic liver disease, has homologues (ATP8B2 and ATP8B3) expressed throughout the body. Biochimica et Biophysica Acta 1633:127-131.

Hirokawa T, Boon-Chieng S and S Mitaku. (1998) SOSUI: classification and secondary structure prediction system for membrane proteins. Bioinformatics 14:378-379.

Kinchen JM, Cabello J, Klingele D, Wong K, Feichtinger R, Schnabel H, Schnabel R and MO Hengartner. (2005) Two pathways converge at CED-10 to mediate actin rearrangement and corpse removal in *C. elegans*. Nature 434:93-99.

Maduro M and D Pilgrim. (1995) Identification and cloning of *unc-119*, a gene expressed in the *Caenorhabditis elegans* nervous system. Genetics 141:977-988.

van Mil SW, van Oort MM, van den Berg IE, Berger R, Houwen RH and LW Klomp. (2004) Fic1 is expressed at apical membranes of different epithelial cells in the digestive tract and is induced in the small intestine during postnatal development of mice. Pediatric Research 56:981-987.

Newman AP and PW Sternberg. (1996) Coordinated morphogenesis of epithelia during development of the *Caenorhabditis elegans* uterine-vulval connection. Proceedings of the National Academy of Sciences USA 93:9329-9333.

Okkema PG and M Krause. (December 23, 2005) Transcriptional regulation. In The *C. elegans* Research Community (Ed.), *WormBook*. WormBook, doi/10.1895/wormbook.1.45.1, http://www.wormbook.org.

Olson SA. (2002) EMBOSS opens up sequence analysis. European Molecular Biology Open Software Suite. Briefings in Bioinformatics 3:87-91.

Paulusma CC, Groen A, Kunne C, Ho-Mok KS, Spijkerboer AL, Rudi de Waart D, Hoek FJ, Vreeling H, Hoeben KA, van Marle J, Pawlikowska L, Bull LN, Hofmann AF, Knisely AS and RP Oude Elferink. (2006) Atp8b1 deficiency in mice reduces resistance of the

canalicular membrane to hydrophobic bile salts and impairs bile salt transport. Hepatology 44:195-204.

Pawlikowska L, Groen A, Eppens EF, Kunne C, Ottenhoff R, Looije N, Knisely AS, Killeen NP, Bull LN, Elferink RP and NB Freimer. (2004) A mouse genetic model for familial cholestasis caused by ATP8B1 mutations reveals perturbed bile salt homeostasis but no impairment in bile secretion. Human Molecular Genetics 13:881-892.

Praitis V, Casey E, Collar D and J Austin. (2001) Creation of low-copy integrated transgenic lines in *Caenorhabditis elegans*. Genetics 157:1217-1226.

Sherwood DR. (2006) Cell invasion through basement membranes: an anchor of understanding. Trends in Cell Biology 16:250-256.

Somers DA and I Makarevitch. (2004) Transgene integration in plants: poking or patching holes in promiscuous genomes? Current Opinion in Biotechnology 15:126-131.

Sulston JE and J Hodgkin. (1988) Methods. In WB Wood (Ed.), *The Nematode Caenorhabditis elegans* (pp. 587–606). Cold Spring Harbor, NY: Cold Spring Harbor Laboratory Press.

Sundaram MV. (2005) The love-hate relationship between Ras and Notch. Genes and Development 19:1825-1839.

Tucker ML, Whitelaw CA, Lyssenko NN and P Nath. (2002) Functional analysis of regulatory elements in the gene promoter for an abscission-specific cellulase from bean and isolation, expression, and binding affinity of three TGA-type basic leucine zipper transcription factors. Plant Physiology 130:1487-1496.

Ujhazy P, Ortiz D, Misra S, Li S, Moseley J, Jones H and IM Arias. (2001) Familial intrahepatic cholestasis 1: studies of localization and function. Hepatology 34:768-775.

Walkowiak J, Jankowska I, Pawlowska J, Bull L, Herzig KH and J Socha. (2006) Normal pancreatic secretion in children with progressive familial intrahepatic cholestasis type 1. Scandinavian Journal of Gastroenterology 41:1480-1483.

Wicky S, Schwarz H and B Singer-Kruger. (2004) Molecular interactions of yeast Neo1p, an essential member of the Drs2p family of aminophospholipid translocases, and its role in membrane trafficking within the endomembrane system. Molecular and Cellular Biology 24:7402-7418.

Chapter 6. Phenotypic analysis of *Caenorhabditis elegans* animals with altered expression of *tat-1*, *2*, *3*, *4* or *5*

Introduction

A systematic phenotypic analysis of null mutants with lesions in the genes that encode P-type ATPases in subfamily IV, the group of putative transbilayer amphipath transporters (TATs), has been conducted thus far only in the budding yeast *Saccharomyces cerevisiae* (Pomorski and Menon, 2006; Graham, 2004; Wicky et al., 2004; see Chapter 1). The detected defects for the most part concern energy-dependent cytofacial internalization of fluorescent lipid analogs of phosphatidylserine (PS), phosphatidylethanolamine (PE) and phosphatidylcholine (PC) across polarized cell membranes and bidirectional transport of vesicles between the Golgi apparatus, the endosome and the plasma membrane. At first look it seems straightforward to assume that the deficiencies in vesicular transport arise as a consequence of the disturbances in the structure of the normally polarized lipid membrane (Pomorski amd Menon, 2006; Graham, 2004). However, there is really no solid basis for such inference. As Devaux et al. (2006) suggest, membrane lipid polarization could be established primarily in the Golgi apparatus, whose membranes are comparatively cholesterol-poor and thin and where lipid translocation against the concentration gradient requires little energy. Maintenance of the lipid asymmetry in the cholesterol-rich plasma membrane would then depend on the continuous cycling of its membranes through the Golgi. Since presently there is no evidence to support Devaux' et al. (2006) suggestion either, a fair assessment of the yeast mutant phenotypes would simply conclude that yeast P-type ATPases in subfamily IV promote in some fashion both vesicular transport and membrane lipid polarization.

Relatively little is known about functions of the mammalian members of the subfamily IV. Naturally occurring mutations in the human *ATP8B1* (*FIC1*, see Chapter 5, Figure 1) cause intrahepatic cholestasis in the liver and impaired uptake of bile salts in the intestine and secondarily, aberrations of bile salt and cholesterol metabolism (Nagasaka et al., 2005; van Mil et al., 2001; Bull et al., 1998). The primary defects presumably appear as a result of phosholipid scrambling between the two monolayers of the hepatic and enteric apical plasma membranes in which ATP8B1 normally resides and maintains lipid asymmetry (Paulusma et al., 2006). Apical vesicular transport in cells with compromised *ATP8B1* remains to be investigated (this could be conducted in mice with a deletion in *Atp8b1*, the murine homolog of the human gene; Pawlikowska et al., 2004). A close relative of *ATP8B1* (same subclass, 1b), murine *Atp8b3* (also called *SAPLT*) is expressed exclusively in spermatozoa (Wang et al., 2004). Males with null deletions in the gene produce litters of slightly lower size. This mild defect seems to stem from a decrease in the ability of the mutant sperm to bind and penetrate the zona pellucida (ZP), extracellular matrix, of the egg. Mammalian sperm cells upon binding to the ZP undergo the acrosome reaction during which the acrosome membrane fuses with the plasma membrane to release matrix-degrading acrosomal enzymes (Flesch and Gadella, 2000). The reduced ability of *Atp8b3* null spermatozoa to bind and penetrate (two processes not clearly distinguished as sperm cells in the process of penetration are counted as bound) the ZP might be indicative of a deficiency in the acrosomal enzymes, a possibility not yet investigated. The prevalent, but not generally accepted (see Kurz et al., 2005), view is that during a developmental event called capacitation certain areas of the plasma membrane of spermatozoa expose PS on the

surface and become disordered (Flesch and Gadella, 2000). The latter change manifests itself through increased accumulation in the affected areas of merocyanine 540 (MC540), a fluorescent intercalating between lipid acyl chains dye. In contrast to wild type, *Atp8b3* null sperm cells expose PS before capacitation but fail to bind MC540 before or after it (Wang et al., 2004). These observations are presently difficult to interpret except to conclude that Atp8b3 in some way contributes to the regulation of the plasma membrane properties. In addition to ATP8B1 and Atp8b3, four other mammalian TATs, one in subclass 1a (Atp8a1) and class 6 (ATP11A) and two in class 5 (Atp10c and Atp10d) are also currently under investigation. Atp10c and Atp10d are nonessential and may play a role in the genesis of obesity (Dhar et al., 2006; Flamant et al., 2003). Mutants of the other two TATs are not available yet (Soupene and Kuypers, 2006; Zhang et al., 2005). Thus, as in yeast, mutants with compromised expression of mammalian genes that encode TATs exhibit defects in the organization of polarized cell membranes.

Two other noteworthy generalities emerge from the investigations of TAT mutants. First, P-type ATPases in subfamily IV seem to be involved in metabolism of various xenobiotics. Over-expression of *neo1* in yeast confers resistance to neomycin (Prezant et al., 1996); of *ATP11a* in human malignant lymphoblastic leukemia cells, to some inhibitors of the farnesyltransferase and Bcr/Abl kinase (Zhang et al., 2005); and of some members of class 6 in human breast cancers, to cisplatin (MS Halleck, personal communication). Null mutations in *LdMT*, a *Leishmania donovani* P-type ATPase in subfamily IV, turn *L. donovani* protozoa insensitive to miltefosine, a phosphocholine analogue (Perez-Victoria et al., 2003). In the cases where over-abundance of a TAT is

necessary, drug resistance is likely to be a byproduct of the activity of that particular TAT. However, LdMT may indeed be a transporter or a part of a multisubunit transporting complex for miltefosine (Perez-Victoria et al., 2003). Second, most subfamily IV ATPases are non-essential and null mutants of the genes that encode these proteins usually exhibit very mild phenotypes. Among the yeast TATs, only *neo1* is essential under regular growth conditions (Graham, 2004). The human *ATP8B1* is expressed strongly in many tissues, yet it is essential only in the liver (Bull et al., 1998). Curiously, the closest murine relative of *ATP8B1*, *Atp8b1*, is dispensable even in hepatocytes (Pawlikowska et al., 2004). This lack of distinct phenotypes in TAT mutants could be attributed to functional redundancy among the members of the group. However, such an explanation is unsatisfactory hence a number of P-type ATPases in subfamily IV seem to become essential or at least important under certain conditions. Yeast *drs2* and *Arabidopsis thaliana ALA1* are essential in low temperatures (Saito et al., 2004; Gomes et al., 2000). Yeast *dnf3* is critical for growth on a minimal medium (Balhadere and Talbot, 2001). *Atp8b3* would certainly become essential during sperm competition (Dean et al., 2006). And *Atp10c* and *Atp10d* are required to prevent the onset of obesity in mice fed high fat diet (Dhar et al., 2006; Flamant et al., 2003). Thus, the putative TATs may function to facilitate certain processes during periods of strain imposed by suboptimal growth conditions; consequently, TAT mutants must experience appropriate adverse environments in order to exhibit a phenotype.

Here are reported findings of a systematic study to reveal functions of the *C. elegans* P-type ATPases in subfamily IV. Expression of the six nematode putative TATs was disrupted temporarily via RNA interference or permanently through gene sequence

deletion. Some of the mutants were then investigated for changes in PS exposure during apoptosis and for alterations in cholesterol metabolism. The collected data suggest a substantial amount of conservation across various eukaryotic species with respect to function of the novel P-type ATPases.

Materials and methods

C. elegans mutants and transgenes and animal maintenance

Wild-type and mutant *C. elegans* animals var. Bristol strain N2 were employed in this study. The following mutants, transgenes and mutant-transgene combinations were used: *opIs117 [P_{hsp}::sel-1sp::GFP::AnxV]* (Zullig et al., 2007), *ced-5(n1812)* IV; *opIs117* (Zullig et al., 2007; Reddien and Horvitz, 2004), *lin-15(n765); oxEx166 [lin-15(+) unc-122::gfp hsp::Transposase]* (Bessereau et al., 2001), *tat-2(tm1634) IV*, *tat-2(tm1773) IV*, *tat-3(tm1275) III*, *tat-4(tm1801) II* (described here). Deletions in *tat-2*, *tat-3* and *tat-4* (Figure 1) were induced with the TMP (trimethylpsoralen)/UV treatment and then animals carrying mutant alleles were isolated using gene-specific primer sets by the National Bioresource Project for the Experimental Animal Nematode *C. elegans* in Japan (Gengyo-Ando and Mitani, 2000). Deletion mutants were outcrossed to *lin-15(n765); oxEx166* (expresses GFP in coelomocytes) and then N2. After the final cross, animals that lost the *oxEx166* array and whose progeny did not exhibit the *lin-15* phenotype were selected for future work. Except where noted otherwise, nematodes were maintained on standard nematode growth medium (NGM) plates spotted with *Escherichia coli* OP50 at 20ºC (Brenner, 1974).

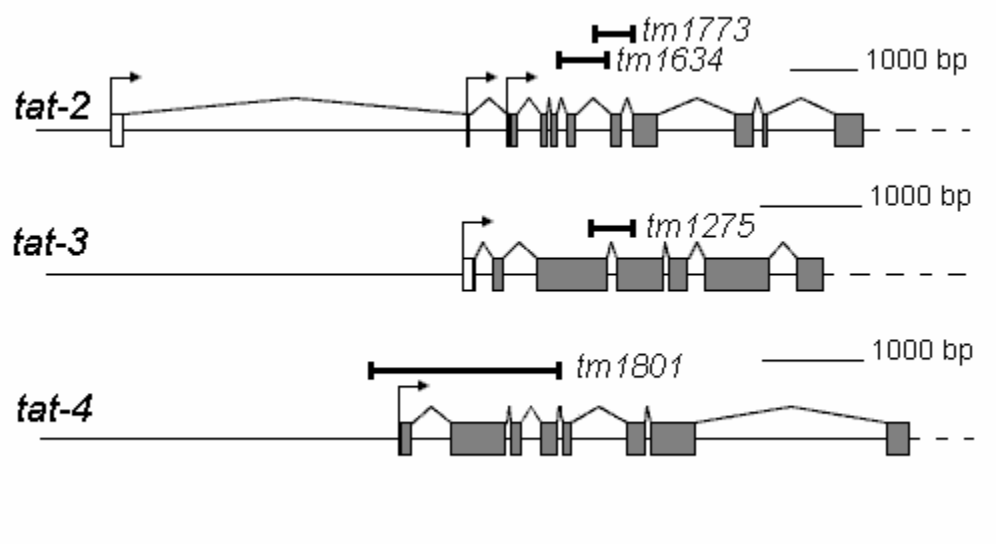

Figure 1. Location of the deleted segments in the *tat-2*, *tat-3* and *tat-4* mutants relative the gene intron-exon structure.

tat RNAi vectors

Partial cDNA clones (expressed sequence tags, ESTs) yk23e10, yk34c11, yk126b10, yk209d5 and yk395e5 were kindly provided by Dr. Kohara (see Chapter 3).Plasmid pPD129.36 (a kind gift of Dr. W Hanna-Rose) contains a multiple cloning site in between two inverted T7 promoters (Timmons and Fire, 1998). 800bp Spe I/Hind III fragment of yk34c11 was fused into Spe I/Hind III cut pPD129.36 to derive pNL16.1. 1.8kb Xho I/Not I fragment of yk209d5 was fused into Xho I/Not I cut pPD129.36 to derive pNL20.10; the latter plasmid was then cut with EcoR I and ligated on itself to derive pNL21.1, which harbors only 500bp of the yk209d5 sequence. 1.1kb Bgl II/Pst I fragment of yk395e5 was fused into Bgl II/Pst I cut pPD129.36 to make pNL19.4. 900bp Xba I fragment yk126b10 was fused into Xba I cut pPD129.36 to make pNL18.8. And finally, 700bp Spe I/Hpa I fragment of yk23e10 was ligated into Spe I/Sma I cut pPD129.36 to obtain pNL10.1. Plasmids pNL16.1 (*tat-1*), pNL21.1 (*tat-2*), pNL19.4 (*tat-3*), pNL18.8 (*tat-4*) and pNL10.1(*tat-5*) were used for production of dsRNA for RNA interference (RNAi) with the targeted genes.

dsRNA feeding of nematodes to induces RNAi

Feeding of N2, *opIs117* and *ced-5(n1812); opIs117* nematodes with dsRNA to induce RNAi against *tat-1*, *tat-2*, *tat-3*, *tat-4* and *tat-5* was conducted as described by Kamath et al. (2000; see protocol 2) with some modifications. pNL16.1, pNL21.1, pNL19.4, pNL18.8, pNL10.1 and pPD129.36 (mock control) plasmids were transformed into bacteria of HT115(DE3) *E. coli* strain. Bacterial cultures carrying one of the plasmids each were grown to OD_{595}=0.4 with shaking at 37ºC in regular Luria Broth (LB) medium enriched with ampicillin to 75µg/ml; IPTG (isopropyl *β*-D-1-

thiogalactopyranoside) was then added to 0.4mM to induce transcription of the gene fragments, and the cultures were incubated at the same conditions for 2 more hours. Subsequently, the cultures were centrifuged to remove the supernatant and then re-suspended in a half of the original volume of fresh LB plus 75μg/ml ampicillin and 0.4mM IPTG. Aliquots of the suspensions were spotted onto regular NGM plates and the plates incubated overnight at room temperature. Synchronized newly hatched in the absence of food larval 1 (L1) stage nematodes were placed 20-30 per *tat* or mock dsRNA plate. The nematodes were first observed for any induced phenotypes 3 days later.

The assay for PS exposure on the surface of apoptotic germ cells

The *opIs117* array carries open reading frames that encode a chimeric peptide composed of the secretion signal domain of SEL-1 (SEL-1sp), complete GFP and complete human Annexin V, in that order, under the control of a heat shock-inducible promoter (Zullig et al., 2007). The peptide is secreted and specifically binds to PS on the cell surface. *ced-5* encodes a protein with similarity to the mammalian DOCK180 and functions in apoptotic cell clearance in the gonad and developing somatic tissues; *ced-5* mutants accumulate un-engulfed cell corpses in the germline and embryo (Wu and Horvitz, 1998). Young adult *opIs117* and *ced-5(n1812)* IV; *opIs117* nematodes that had grown on *tat-1*, *tat-2*, *tat-3*, *tat-4* or mock dsRNA plates were incubated at 30ºC for 30 min. Six hours after the heat-shock, the number of germ cell corpses, which were seen as highly refractile disks in the germ line, and of GFP stained germ cells per gonad arm of the heat treated animals were determined for about 10-15 gonad arms.

Sterol deprivation assay

For the sterol deprivation assay, nematode growth plates were prepared with agarose (8g per liter) and ether extracted peptone (sterol modified NGM, smNGM), instead of agar and raw peptone (Brenner, 1974). Cholesterol was added to the final concentration of 1000ng/mL, 100ng/mL, 10ng/mL or 1ng/mL. OP50 strain *E. coli* culture used to spot the plates was grown in a minimal medium (20mM NH_4Cl, 0.2% w/v D-glucose, 2mg/ml uracil in M9 buffer) overnight at 37ºC. The culture was then divided into 4 aliquots, which were centrifuged down to remove the supernatant, re-suspended in the same volume of the peptone solution (0.5 % w/v peptone in M9 buffer) and enriched with cholesterol to the 4 final concentrations as the plates. The suspensions were then pipetted very carefully to produce roughly similar in area spots onto the corresponding cholesterol concentration plates. The spotted plates were kept overnight at room temperature. N2 and *tat* mutant nematodes were synchronized at L1 by hatching eggs on smNGM plates without bacterial food. The eggs were obtained from hermaphrodites grown on regular cholesterol-containing NGM plates using the hypochlorite treatment, followed by exhaustive washing. L1 stage larva were transferred from no-food plates to spotted plates, exactly 30 animals per plate, by suspending an animal in a drop of M9 buffer, then sucking the liquid with the animal into a Pasteur pipette and finally, expelling the buffer with the animal onto a new plate. This nematode transfer method was employed to minimize animal injury. 3 replica plates were seeded per cholesterol concentration per genotype. The nematodes were allowed to grow at 20ºC for as long as several weeks with periodic observations. Photographs of the growing nematode

populations were obtained with a dissecting microscope (kindly provided by Dr. GH Thomas).

Results

tat-5 is an essential gene

tat-5 dsRNA feeding induced in N2 nematodes gonadal abnormalities and embryonic lethality (Figure 2). The proximal, after the turn, portion of the gonad arm frequently (22% of 41 arms) developed a constriction, a region of gonad narrowing from which oocytes were squeezed out (Figure 2C). In some *tat-5(RNAi)* hermaphrodites a constriction seemed to be in the process of formation (Figure 2B). Such abnormalities of gonad morphology were not observed even in very old (no longer producing eggs) similarly treated but not fed *tat-5* dsRNA N2 animals and nematodes fed with dsRNA for the other 4 *tat* genes (Figure 2A and data not shown). The uterus of *tat-5(RNAi)* hermaphrodites also often (quantitative data not collected) contained disintegrating unfertilized oocytes and eggs (Figure 2E). Unfertilized oocytes normally appear in the uterus of hermaphrodites that used up all spermatozoa. However, in the case of *tat-5(RNAi)* animals with oocytes in the uterus, sperm cells seemed to still be present in spermathecas (data not shown). Finally, development of *tat-5(RNAi)* embryos was severely compromised. *tat-5(RNAi)* plates contained many structurally intact (as opposed to those that disintegrated) *tat-5(RNAi)* embryos exhibiting signs of extensive necrosis (Figure 2F). Thus, it seems that *tat-5* is an essential gene whose suppression in the most severe cases leads to embryonic lethality, lack of oocyte fertilization and defects in gonad morphology.

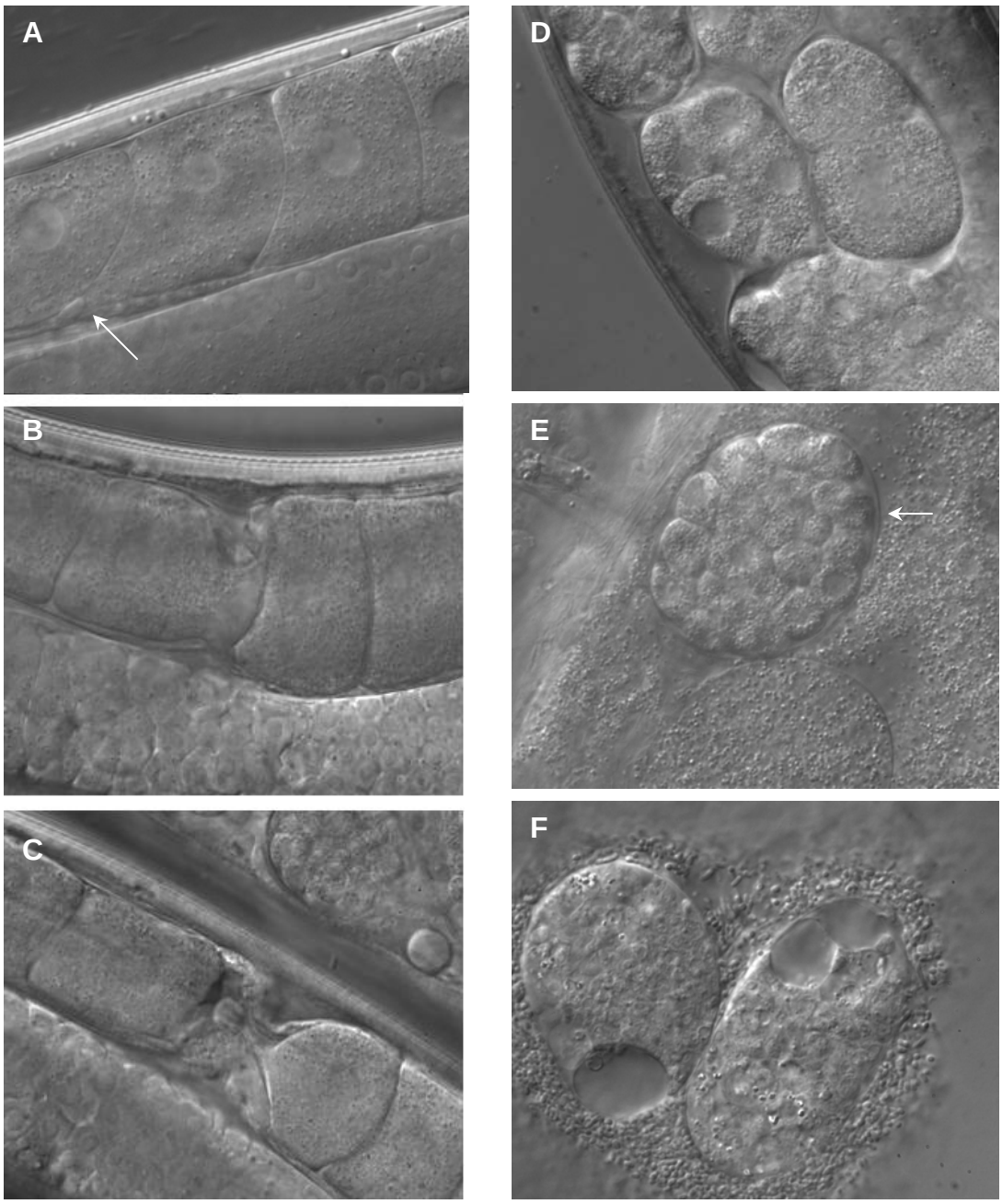

Figure 2. *tat-5(RNAi)* phenotype. After the turn of the gonad arm, wild-type oocytes are arranged in a closely packed row (A). *tat-5(RNAi)* oocytes formed a partial or a complete discontinuity (B and C). This discontinuity could have been introduced by invaginating gonadal sheath cells (arrow in A). The uterus of wt hermaphrodites is filled with embryos in various stages of development (D). The uterus of some *tat-5(RNAi)* hermaphrodites was filled with intact (arrow) embryos and unfertilized oocytes (E). Those embryos that escaped the uterus failed to develop properly (F).

tat-1, *tat-2*, *tat-3* and *tat-4* are nonessential and not required for apoptotic cell clearance

tat-1, *tat-2*, *tat-3* and *tat-4* dsRNA feeding failed to induce notable defects in N2 nematodes. RNAi interference against *tat-1* was successful as evidenced by the GFP-Annexin V apoptotic corpse staining phenotype (see below). *tat-2(tm1634)*, *tat-2(tm1773)*, *tat-3(tm1275)* and *tat-4(tm1801)* mutants are also homozygous viable and no less vigorous and fertile than wild-type nematodes (data not shown). Deletions in *tat-2(tm1773)* and *tat-3(tm1275)* change the reading frame of the downstream sequence and together with *tat-4(tm1801)*, in which a fragment that includes a proximal promoter portion and a sequence encoding the first 323 amino acids (forming the first two transmembrane helices) is missing, are most likely to be null (Figure 1). *tat-2(tm1634)* may not be null because deletion of the sixth exon, encoding 45 amino acids, in this mutant preserves the correct translational frame in the downstream coding region. *tat-1(RNAi)* animals did not notably accumulate un-engulfed germ cell corpses (see bellow). Germline cell corpse clearance is fully functional in *tat-2(tm1634)*, *tat-2(tm1773)*, *tat-3(tm1275)* and *tat-4(tm1801)* mutants (Figure 3). Thus, the four *tats* are nonessential and not required for engulfment of apoptotic cells.

Apoptotic germline cell corpse staining with GFP-Annexin V is compromised in *tat 1(RNAi)* animals

To determine whether *tat-1*, *tat-2*, *tat-3* or *tat-4* were involved in the internalization of PS that spontaneously diffused to the outer monolayer of the plasma membrane, wild-type and *ced-5(n1812)* nematodes carrying the *opIs117* array were grown on *tat(RNAi)* or mock dsRNA plates to adulthood and then heat shocked to induce expression of the chimeric SEL-1sp-GFP-Annexin V peptide. Six hours later the

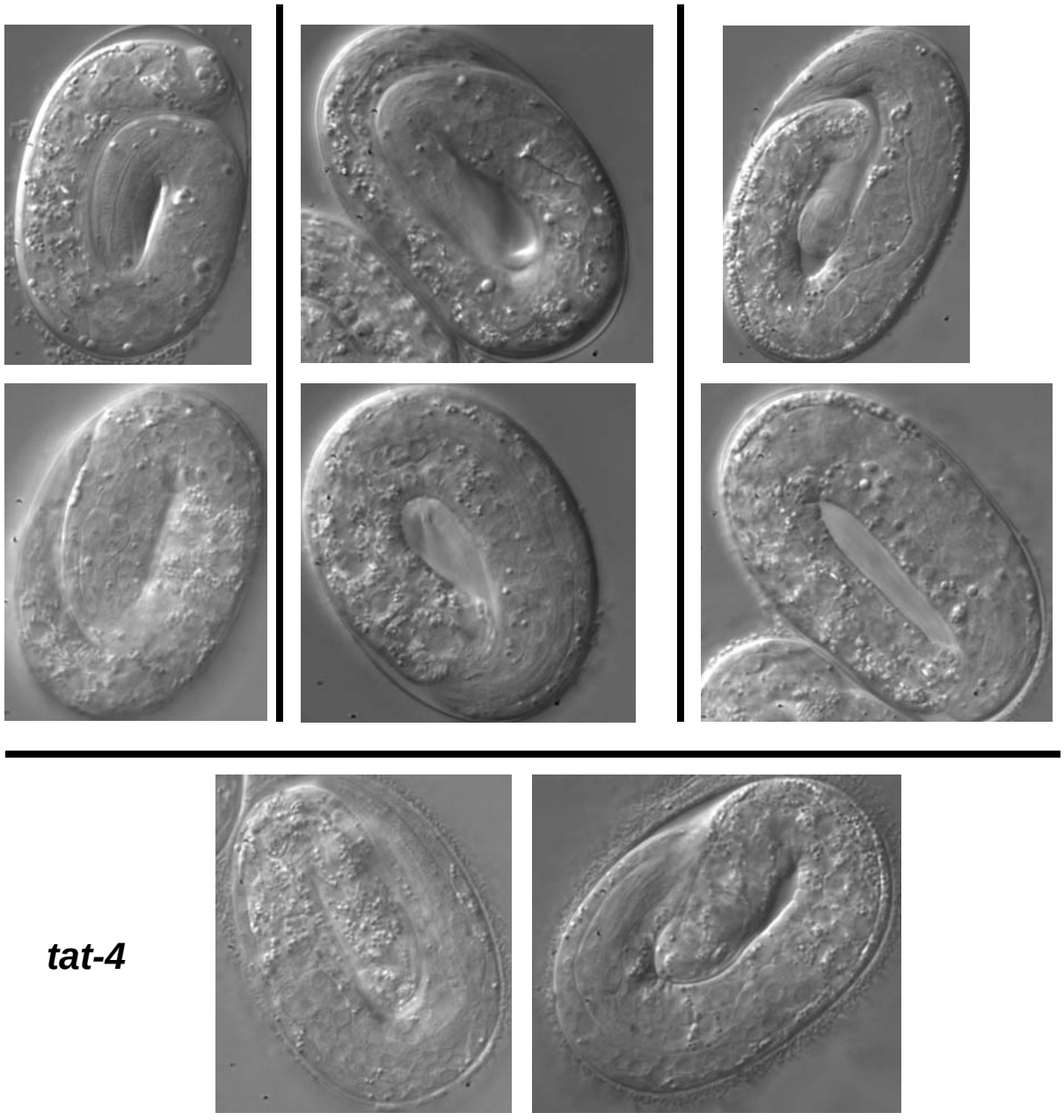

Figure 3. The absence of persistent cell corpses in deletion mutants of *tat-2*, *tat-3* and *tat-4*.

animal gonads were scored for the presence of cell corpses visually with Nomarski microscopy and of GFP stained cells with fluorescent microscopy. For mock dsRNA fed (Figure 4) and regularly grown (data not shown) *opIs117* and *ced-5(n1812); opIs117* nematodes only a subpopulation of presumably apoptotic cells was both recognized visually as apoptotic and stained with the GFP-Annexin V. PS exposure is a very early event in the progression of apoptosis (Schlegel and Williamson, 2001); thus, those cells that stained with the GFP-Annexin V but were not visually identified as corpses probably committed to undergoing cell death but did not exhibit significant morphological changes yet. On the other hand, those corpses that were still observed visually but did not stain with the GFP-Annexin V were already engulfed by the gonadal sheath cells and resided in an acidic environment detrimental to the GFP reporter (Zullig et al., 2007). RNAi against the four *tats* failed to affect cell corpse clearance as measured by the visual count of cell corpses in dsRNA-fed *opIs117* and *ced-5(n1812); opIs117* nematodes (Figure 4 and data not shown). Surprisingly, however, GFP-Annexin V staining of gonadal apoptotic cells was significantly compromised in *tat-1(RNAi)* animals (Figure 4). The reduction in the number of stained corpses in both the *ced-5(n1812)* and wild-type backgrounds was dramatic, suggesting that this phenotype was independent of *ced-5*. Expression and secretion of the chimeric reporter seemed to occur in *tat-1(RNAi)* mutants properly, because GFP fluorescence emanated from the nematode coelom and an occasional apoptotic cell exhibited bright staining with the reporter (data not shown and Zullig et al., 2007). Thus, *tat-1* is necessary for PS exposure on the surface of apoptotic germ cells, as determined by corpse staining with the GFP-Annexin V reporter.

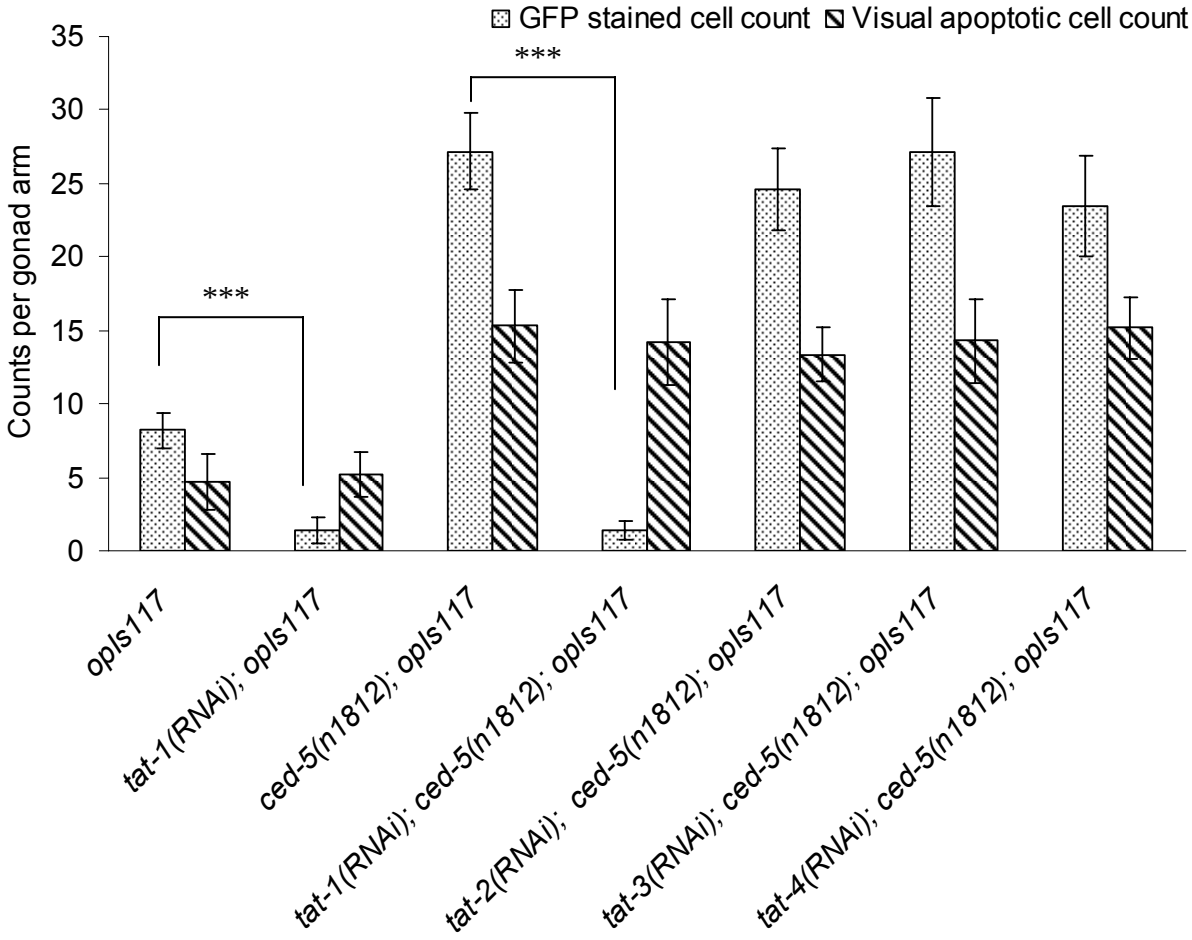

Figure 4. Compromised GFP-Annexin V staining of germline cell corpses in *tat-1(RNAi)* nematodes. Error bars are standard deviations; *** - P<0.005.

tat-2 and *tat-4* mediation of sterol metabolism

The living lipid membrane has a certain capacity to maintain its properties at relatively constant levels vis-à-vis changing external environmental conditions (Hayward et al., 2007) and fluctuating exogenous precursor lipids availabilities (Jesch et al., 2006). It is possible that in an optimum environment, *C. elegans* cell membranes can compensate in some fashion for the absence of the seemingly nonessential TATs as well. This compensatory capacity may be significantly impaired and TAT phenotypes revealed when a second critical membrane structural component is lacking. Since *C. elegans* is a sterol heterotroph (Entchev and Kurzchalia, 2005), depriving nematodes of exogenous sources of this nutrient, a major component of the lipid membrane, is a relatively simple method of affecting membrane structure.

To observe synthetic phenotypes of sterol limitation in the *tat-2*, *tat-3* or *tat-4* mutants, sterol modified NGM (smNGM) and a sterol deprivation assay were developed. In smNGM, agar was substituted with high purity agarose and raw peptone with ether extracted peptone. *C. elegans* nematodes are highly adapted to survival on tiny amounts of a wide variety of steroid alcohols. Furthermore, hermaphrodites load oocytes with enough sterol to completely satisfy sterol needs of the next generation. The first generation grown on smNGM without cholesterol supplementation developed to adulthood and produced progeny, the second generation, however, halted growth at L1 or L2 stages (data not shown). This indicated that smNGM medium without cholesterol is substantially sterol free.

For sterol deprivation survival tests, smNGM plates were enriched with cholesterol to final concentrations of 1000ng/ml, 100ng/ml, 10ng/ml or 1ng/ml, 30 L1

nematodes were seeded per plate and then the resultant populations observed for 2-3 weeks. On regular NGM supplemented with cholesterol to 5 µg/ml (standard conditions; Brenner, 1974), *tat-2(tm1634)*, *tat-3* and *tat-4* mutants are indistinguishable in growth and reproduction from wild-type animals (data not shown and Zullig et al., 2007). On cholesterol-supplemented smNGM plates, the timing of wild-type hermaphrodite development was a function of cholesterol concentration: the lower the cholesterol content, the slower the growth (Figure 5). By the fifth day, N2 populations persisting on 1000ng/ml and 100ng/ml cholesterol plates cleared all food and began to starve (Figure 5A). By day 7, 10ng/ml cholesterol plates became starved; food on 1ng/ml cholesterol plates was exhausted 3 days later. *tat-3* mutant populations exhibited slightly slower but comparable to the wild-type growth rates (Figure 5). However, growth of *tat-2(tm1634)* and *tat-4* mutant populations on msNGM cholesterol supplemented plates lagged dramatically behind that of wild-type and *tat-3* populatons (Figure 5). *tat-2(tm1634)* and *tat-4* populations fed 1000ng/ml cholesterol cleared all food by day 7 (Figure 5B). 100ng/ml cholesterol plates became food free by day 10. After that time mark, most remaining plates began showing clear sings of bacterial and fungal infection (infected during the opening of plates for photographing). Some populations exhibited explosive growth, which was likely fueled by newly synthesized fungal sterol. Only two plates escaped infection, one 10ng/ml and one 1ng/ml both *tat-4*; on both plates all animals eventually died out without consuming all food. *tat-2(tm1773)* mutants exhibited hypersensitivity to sterol scarcity as well (data not shown). Since it is unlikely that 3 independently derived deletion alleles in two related genes would all contain secondary mutations that cause an identical phenotype, mutations in specifically *tat-2*

A

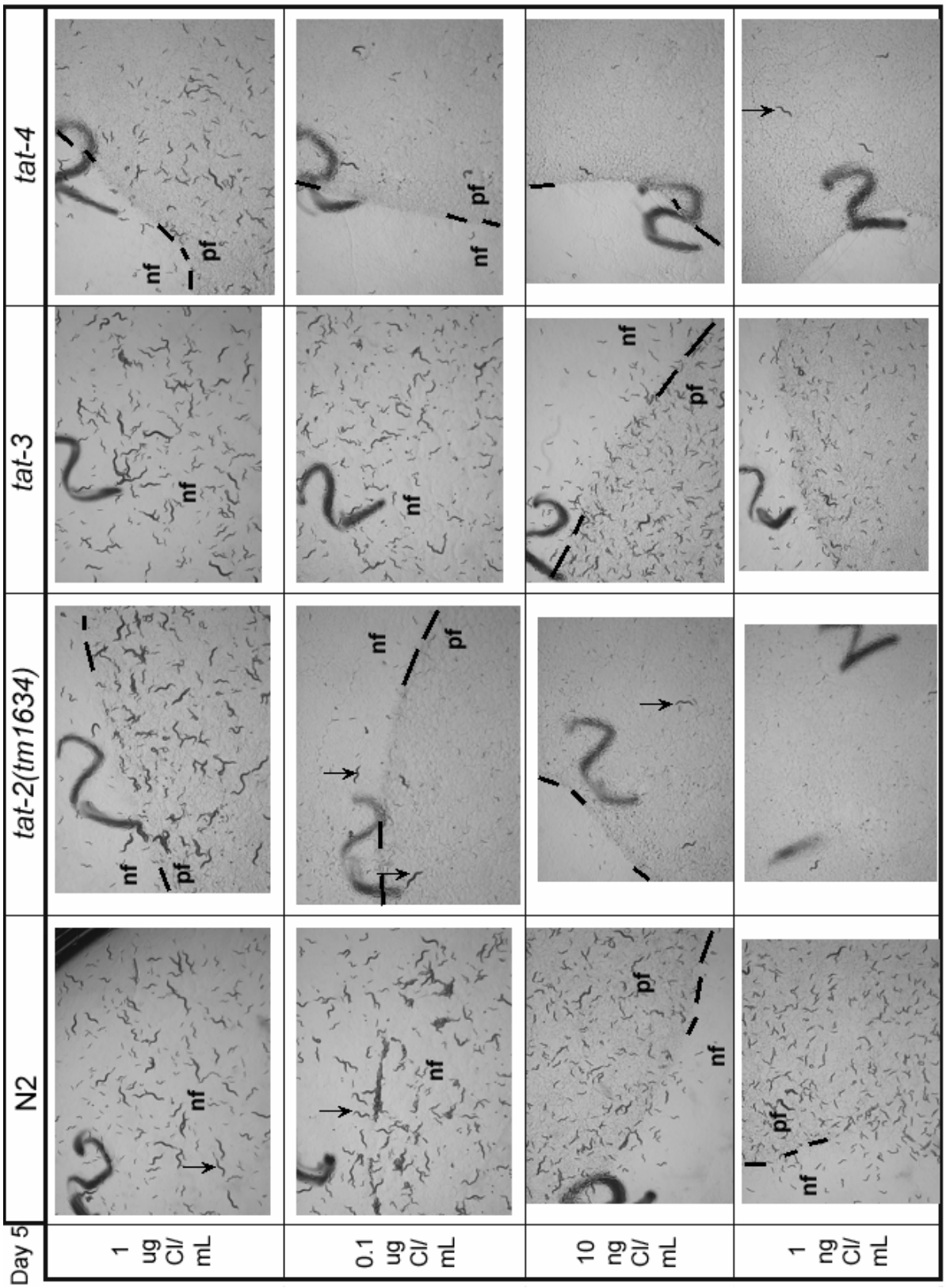

Figure 5 (continues on the next page).

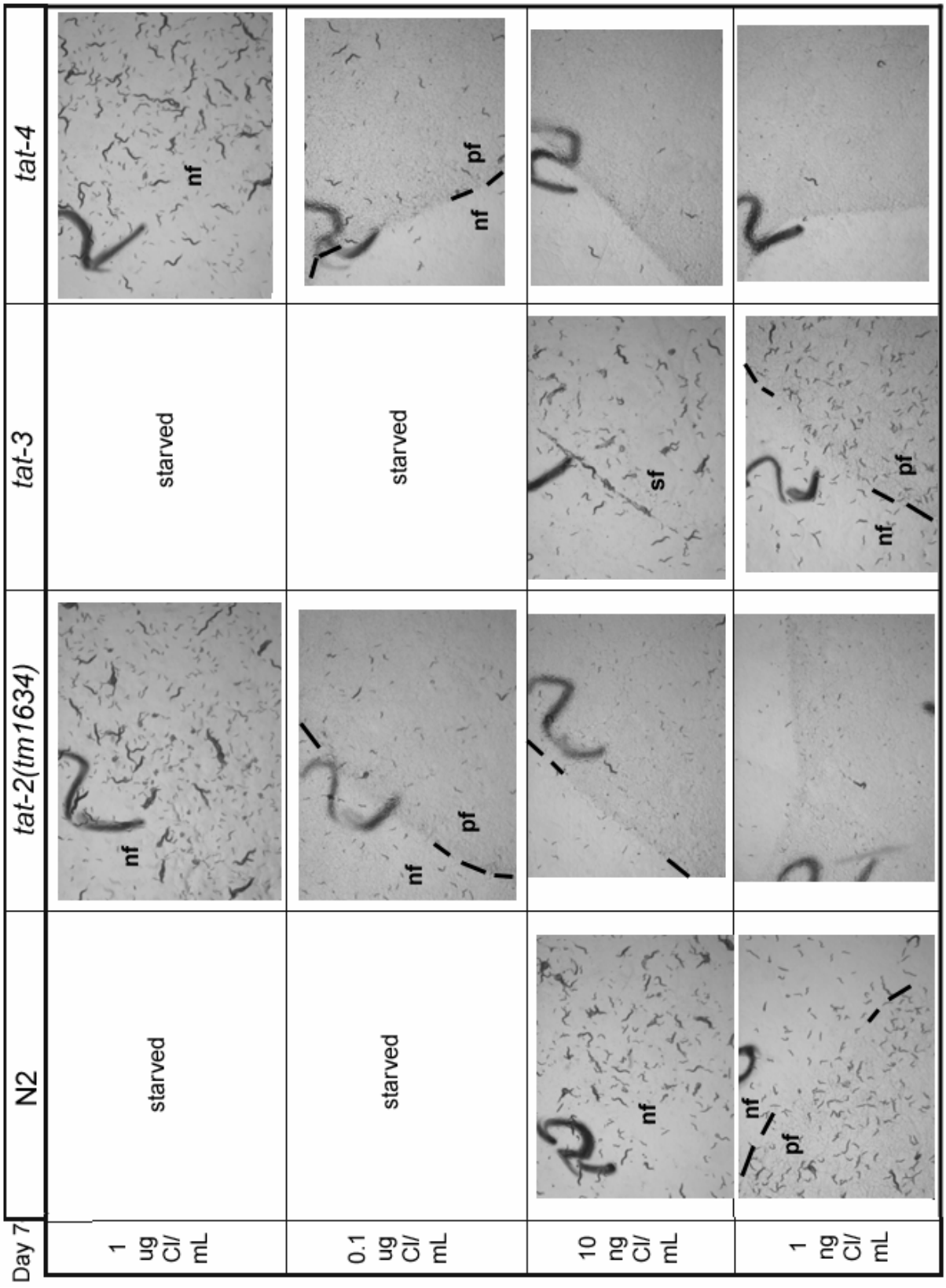

Figure 5 (continues on the next page).

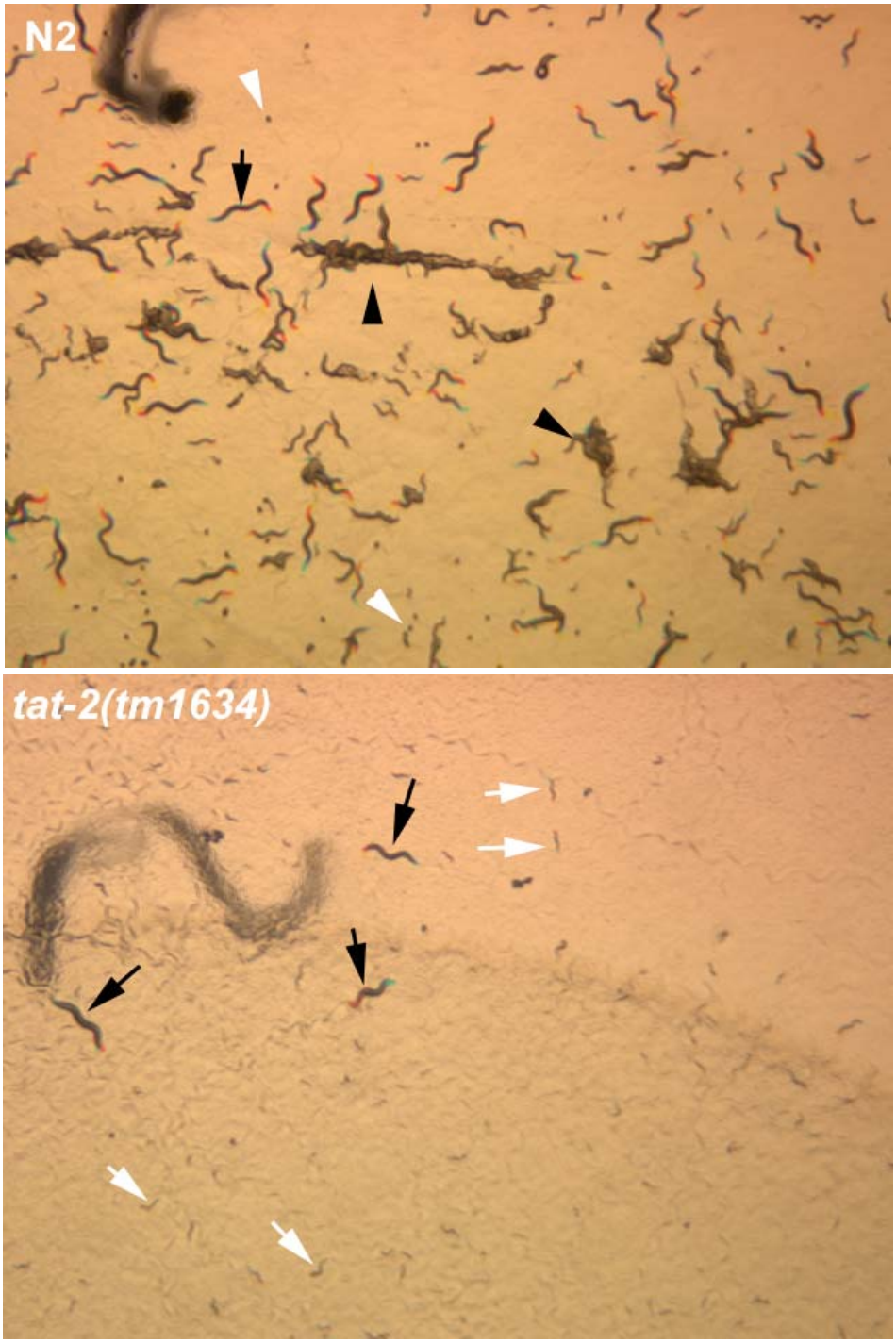

C1

Figure 5 (continues on the next page).

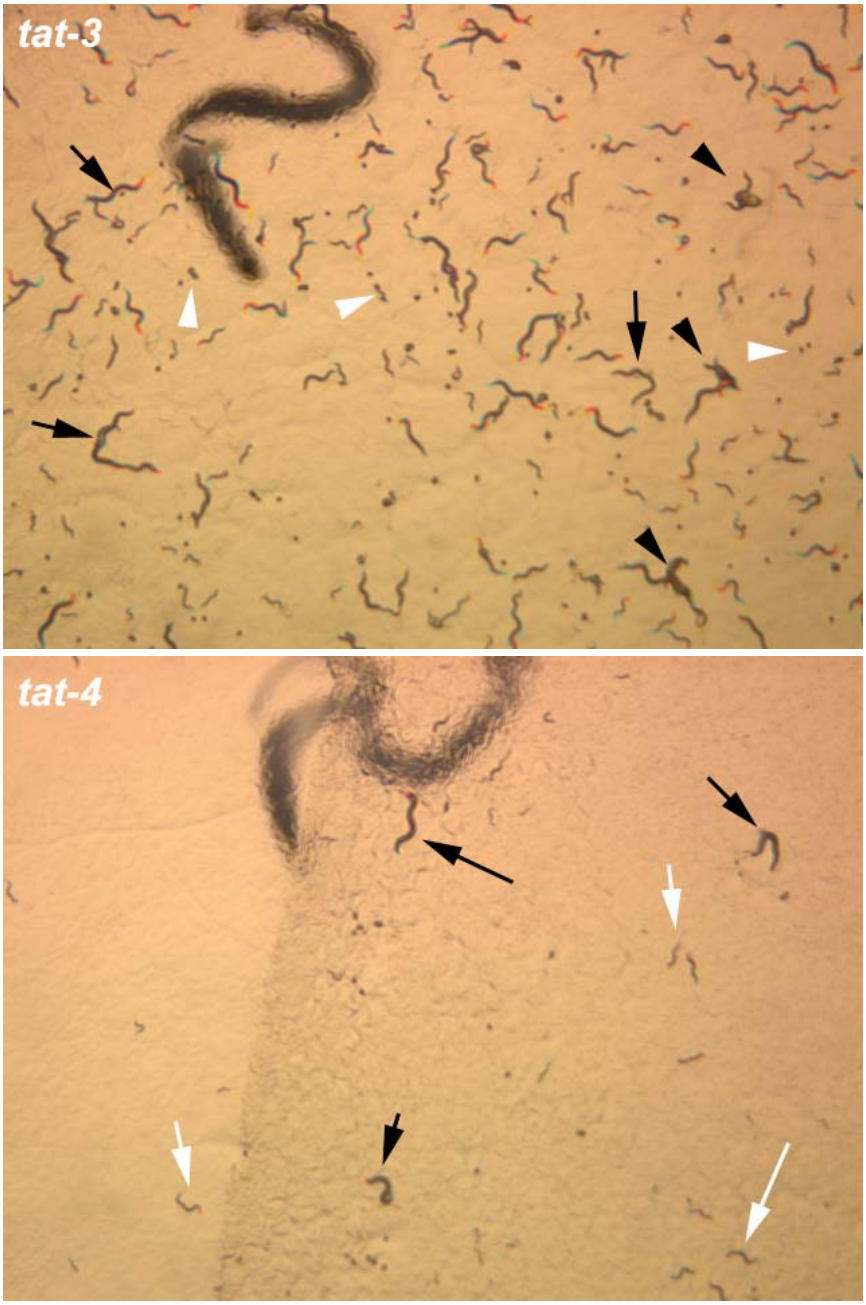

C2

Figure 5 (starts on page 175). Hypersensitivity of *tat-2(tm1643)* and *tat-4* mutants to sterol deprivation. (A) N2 and *tat* plates after 5 days of growth. (B) N2 and *tat* plates after 7 days of growth. (C) Up-close views of representative 100ng/mL cholesterol plates after 5 days of incubation; adult nematodes on *tat-2* and *tat-4* plates are first generation animals. Notations: nf – no food; pf – plenty of food; black arrows – individual adult nematodes; black arrowheads – nematode clumps; white arrows – second generation larva; white arrowheads – eggs; dashes – partial outlines of food edges.

and *tat-4* seem to induce hypersensitivity to sterol deprivation.

Neither *tat-2* nor *tat-4* mutants exhibited on low cholesterol any particular abnormal phenotypes that were not seen in sterol starved N2 and *tat-3* nematodes. On low sterol, second and subsequent generations of N2 animals progressed through the larval developmental stages slower than normally on regular NGM. A subset of eggs failed to hatch and some larva failed to molt properly at the L3 and L4 molts. *tat-2* and *tat-4* nematodes did not seem to encounter higher rates of embryonic death and abnormal molting. These mutants simply grew slower in comparison with N2 and *tat-3* animals. By the fifth day, for example, many N2 and *tat-3* second generation hermaphrodites surviving on 100ng/mL cholesterol plates reached adulthood and produced eggs; in contrast, none of the *tat-2(tm1643)* and *tat-4* animals on the same cholesterol level became adults (Figure 5C). Thus, *tat-2* and *tat-4* mutants seem to need more sterol to satisfy developmental needs.

tat-3; tat-4 double mutant is viable

Since *tat-3* and *tat-4* belong to the same class of subfamily IV P-type ATPases, *tat-3; tat-4* double mutants were derived to determine the extent of functional redundancy between the two genes (Chapter 4, Figure 1). *tat-3; tat-4* mutants are viable, lack any notable developmental or morphological defects. *tat-3; tat-4* mutant populations seem to be slightly more sensitive to sterol deprivation than *tat-4* single mutant populations (Figure 6). Thus, class 5 *tats* are nonessential as a group.

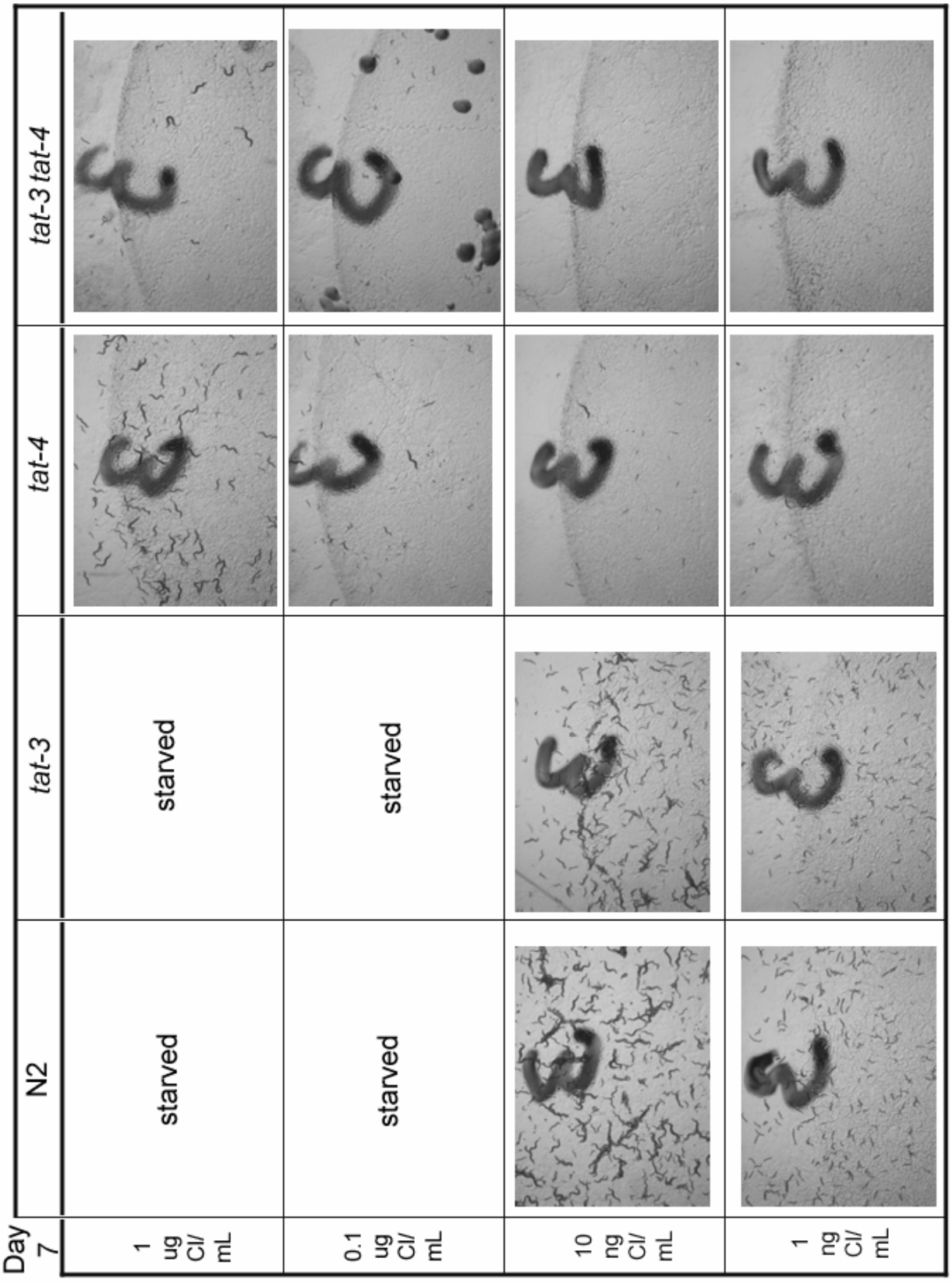

Figure 6 (continues on the next page).

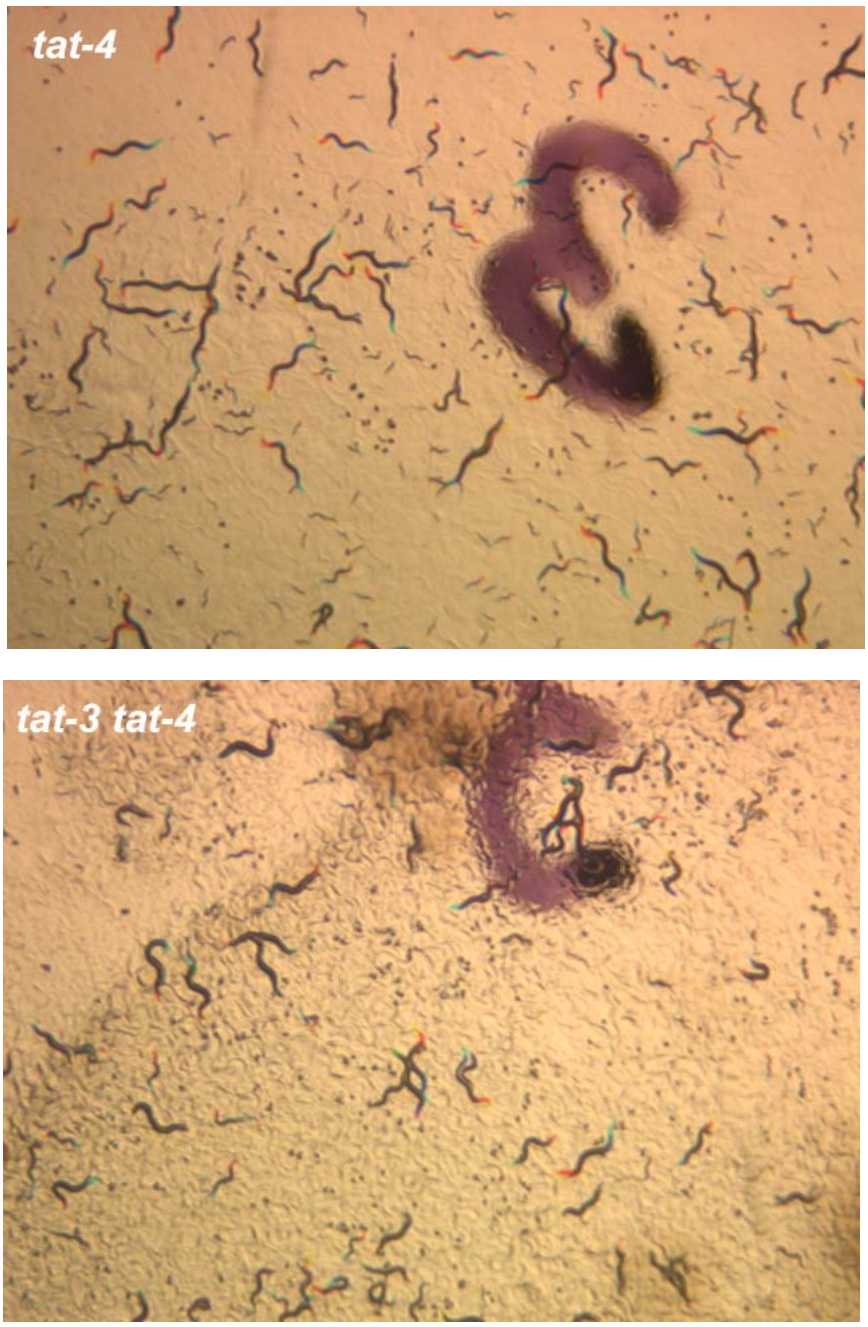

B

Figure 6 (starts on page 180). Slight increase in sensitivity to sterol deprivation in *tat-3; tat-4* double mutants. (A) N2, *tat-3*, *tat-4* and *tat-3; tat-4* populations after 7 days of growth on smNGM plates. (B) Up-close views of representative *tat-4* and *tat-3; tat-4* populations after 8-days of growth on 100ng/mL cholesterol plates.

Discussion

tat-5 might be a housekeeping gene

The broad, if not ubiquitous, expression and the embryonic lethality of *tat-5(RNAi)* together suggest that *tat-5* is likely to be a housekeeping gene. The *tat-5(RNAi)* defects observed in this study are identical with those detected in systematic RNAi screens for genes whose suppression induces clear morphological and developmental abnormalities. Fraser et al. (2000), Maeda et al. (2001), Simmer et al. (2003) and Sonnichsen et al. (2005) all found that RNAi against *tat-5* induces either embryonic lethality or hermaphrodite sterility. Three deletion mutants of *tat-5* (*tm1823*, *tm1772* and *tm1741*) are presently in existence. A preliminary analysis failed to isolate viable nematodes homozygous for the deletion alleles or to identify homozygous mutant dead embryos (unpublished observations). The presence of unfertilized oocytes in the uterus of *tat-5(RNAi)* hermaphrodites suggests that either *tat-5(-)* oocytes or sperm are incapable of participating in fertilization and perhaps, undergo apoptosis. This would explain the inability to find dead *tat-5(-/-)* tissues. The closest yeast homolog of *tat-5*, *neo1*, is also an essential gene (Graham, 2004). The two mammalian genes in class 2, the group to which *tat-5* and *neo1* also belong, seem to be cumulatively expressed in all tissues (MS Halleck, personal communication; Halleck et al., 1999). Thus, class 2 TATs seem to be housekeeping genes individually or as a group in animals and fungi.

Involvement of the putative TATs in sterol metabolism

Eukaryotic organisms generally employ cholesterol and similar steroid alcohols for three major functions: cell membrane structural organization, steroid hormone

biosynthesis and protein activity and structure modulation (Mouritsen and Zuckermann, 2004). The bulk of mammalian un-esterified cell cholesterol resides in the plasma membrane, where it is essential for establishing proper structural organization of this organelle (Hao et al., 2001). Mammals generally require large amounts of cholesterol. In contrast, *C. elegans* nematodes, sterol heterotrophs, can survive on miniscule levels of many steroid alcohols and at least under sterol-limiting conditions, are unlikely to contain substantial amounts of 7-dehydrocholsterol, the major endogenous sterol of this organism, in the plasma membrane (Merris et al., 2004; Kurzchalia and Ward, 2003; Chitwood, 1999). The mechanisms that allow the nematode plasma membrane to adapt to sterol scarcity are presently unknown.

C. elegans animals deprived of sterol exhibit growth defects primarily related to inadequate steroid hormone biosynthesis. *C. elegans* larval development involves two major steroid hormones. 3-keto bile acid-like steroids, called dafachronic acids, promote reproductive development and suppress the dauer pathway, a branch of the nematode lifecycle leading to a special dispersal stage (Motola et al., 2006; Gerish et al., 2001). Another steroid hormone, of presently unknown nature, mediates molting (Gissendanner et al., 2004). On the medium with plenty of bacterial food but without sterol, wild-type L1 animals become dauer-like and halt growth (Matyash et al., 2004). In the presence of some, but not fully sufficient, sterol, the rate of nematode growth is proportional to sterol concentration (Figure 5). At the lower concentrations, a subset of animals fails to properly molt at the L3-L4 and L4-adult transitions, perhaps because at these stages animals are large and require higher amounts of the molting hormone (data not shown; Merris et al., 2004). Thus, the *C. elegans* growth rate is a sensitive

indicator of sterol availability to the enzymes synthesizing growth-promoting and molting hormones.

Under the conditions of sterol deprivation, *tat-2* and *tat-4* seem to be essential genes exhibiting a phenotype that could be explained by defects in sterol delivery to the sites of hormone biosynthesis. NGM plates supplemented with 5µg/ml cholesterol (Brenner, 1974) likely provide an excessive amount of this compound. The growth rate of N2 nematodes on smNGM-1000ng/ml cholesterol was essentially the same as under regular conditions (46 hour post hatching development, plus 58 hour second generation development from fertilization add up to 104 hours; see adult second generation nematodes after 118 hours – roughly 5 days – in Figure 5A) (see also Merris et al., 2003). The abundance of cholesterol in NGM plates masks sterol metabolism defects in *tat-2* and *tat-4* mutants. However, with decreasing cholesterol concentrations in the medium, *tat-2* and *tat-4* hermaphrodites experience more severe sterol shortages, due to inefficient sterol turnover, than wild-type and *tat-3* animals. As a result, *tat-2* and *tat-4* mutants do not exhibit any specific phenotype not seen in N2 nematodes with the same treatment, but simply lack growth-promoting hormones and grow much slower (Figure 5 and 6).

In the absence of TAT-2 and TAT-4, cell membranes where these proteins normally reside may require higher than normal levels of sterol in order to ensure proper membrane functioning. In other words, sterol acts as a “band-aid” to ameliorate the injury caused by deletion of *tat-2* and *tat-4*. With higher amounts of sterol tied up in cell membranes, less of it is available for hormone biosynthesis. Alternatively, TAT-2 and TAT-4 may directly participate in sterol metabolism; a defect in any one step of the

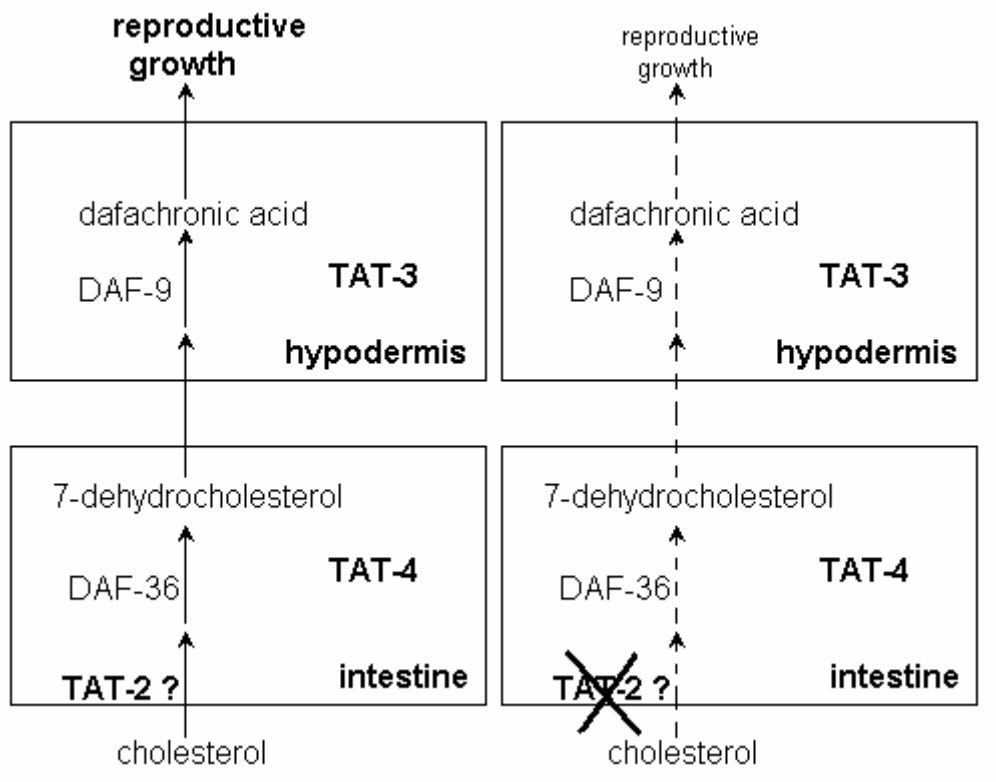

Figure 7. A speculative model of TAT-2 and TAT-4 involvement in sterol metabolism in *C. elegans* (see Rottiers et al., 2006; Gerish and Antebi, 2004; Matyash et al., 2001; Gerish et al., 2001; Yochem et al., 1999).

sterol uptake and delivery pathway that supplies the hormone-synthesizing enzymes could cause the phenotype observed in *tat-2* and *tat-4* mutants (Figure 7). The presently available data are insufficient to confidently choose one of these two explanations over the other.

tat-2 and *tat-4* are strongly expressed in the tissues of the digestive system (see Chapter 4). Both are active in the intestine, the pharyngeal-intestinal valve and the rectal gland cells. *tat-2* is also on in the gland cells of the pharynx. Neither of the two genes is expressed in the epidermis or the XXX cells. In contrast, *tat-3*, whose mutants exhibit little sterol deprivation hypersensitivity, is not transcribed in the digestive tissues with *tat-2* and *tat-4* expression. *tat-2* and *tat-4* transcripts are also found in the developing vulva, the uterus and the spermatheca; these tissues, however, begin developing in the late L3, while mutants of the two genes exhibit uniformly delayed development throughout the larval portion of the nematode lifecycle. Thus, sterol metabolism defects in *tat-2* and *tat-4* mutants likely reside in the intestine.

Involvement of subclass 1b subfamily IV P-type ATPases, the group which includes *tat-2*, in sterol metabolism seems to be evolutionarily conserved between *C. elegans* and mammals. The closest mammalian homologs of *tat-2*, the human *ATP8B1* and murine *Atp8b1*, are expressed in the liver and the intestine and participate in bile salt and cholesterol turnover (Nagasaka et al., 2005; van Mil et al., 2004; Jansen and Sturm, 2003; Eppens et al., 2001; van Mil et al., 2001; Ujhazy et al., 2001). Homozygous individuals for certain types of mutations in *ATP8B1* suffer from chronic progressive familial intrahepatic cholestasis (PFIC), a disorder that requires liver transplantation in the first or second decade of life (Jansen and Sturm, 2003). A liver

transplant fails, however, to eliminate all symptoms of the disorder. In particular, PFIC patients with a transplanted liver continue to suffer from diarrhea and exhibit higher than normal levels of bile salts in the stool (van Mil et al., 2001). Furthermore, mutations in *ATP8B1* seem to be proatherogenic (Black, 2005). Homozygous for the mutant *ATP8B1* alleles individuals contain normal levels of low-density lipoprotein (LDL)-cholesterol but half the regular amount of high density lipoprotein (HDL)-cholesterol and 10 times more than usual of oxidized cholesterol (Nagasaka et al., 2005). Mice with the orthologous mutations in *Atp8b1* do not develop cholestasis but instead secrete twice as much cholesterol in bile, in comparison with wild-type animals (Paulusma et al., 2006). The bile and cholesterol secretion defects in humans and mice are thought to arise due to abnormalities in the structure of the hepatic apical plasma membrane, which stem from a loss of lipid asymmetry and appearance of PS in its exofacial monolayer (Paulusma et al., 2006; Ujhazy et al., 2001). The mechanism of sterol absorption in *C. elegans* is presently unknown. Based on the homologous expression patterns and involvement in cholesterol metabolism, *tat-2* and its two mammalian homologs may perform the same or closely analogous functions.

tat-3 and *tat-4* are more similar to each other than to any mammalian P-type ATPase in subfamily IV (Chapter 4, Figure 1). However, expression patterns of the two genes hardly overlap (Chapter 4, Table I). The closest mammalian homolog of *tat-3* and *tat-4* with some functional data is *Atp10c* (also identified as *Atp10a*; Chapter 4, Figure 1*)*. *Atp10c* is expressed in adipose and muscle tissues and seems to mediate insulin signaling; *Atp10c* mutant mice fed high calorie diet tend to develop the metabolic syndrome characterized by insulin resistance, obesity and specifically in males,

elevated levels of serum cholesterol (Dhar et al., 2006; 2004). In *C. elegans*, the role of adipose tissues is performed by the intestinal cells (McKay et al., 2003). Since *tat-4* is expressed in the intestine, the functions of this gene could be similar to those carried out by the mammalian *Atp10c*.

In yeast, deletion mutants of *drs2*, a class 1a TAT, are synthetically lethal with mutations affecting the late steps of ergosterol biosynthesis (Kishimoto et al., 2005). Mutants of *tat-1*, the *C. elegans* homolog of *drs2*, only very recently became available and remain to be investigated for sterol deprivation hypersensitivity. However, if TAT-1 involvement in sterol metabolism is confirmed, it would indicate that all nonessential nematode TATs mediate sterol turnover strongly (TAT-2 and TAT-4) or weakly (TAT-3) .

Lipid asymmetry and TATs

The now classic hypothesis postulates that an energy-consuming transporter translocates spontaneously diffused PS and with lower affinity, PE from the exofacial to the cytofacial monolayer of the plasma membrane and instills asymmetric lipid distribution across this organelle; preferential sequestration of PS and PE in one leaflet then restricts choline phospholipids, PC and sphingomyelin, to the opposite monolayer (Devaux, 1991; Chapter 1). P-type ATPases in subfamily IV were identified as the transporters which in accordance with the hypothesis pump PS and PE (Tang et al., 1996). In recent years several observations modified these views; most notably, investigations in yeast unexpectedly found active internalization of the plasma membrane PC, in addition to PS and PE, (Pomorski and Menon, 2006). The lipid translocation hypothesis predicts that, first, the housekeeping TAT would be encoded by

a ubiquitously expressed gene or a group of related genes, with at least one member of the group active in each cell type. And second, inactivation of the APLT would lead to the appearance of PS in the outer monolayer of the plasma membrane, scrambling of the lipid asymmetry across polarized membranes and certainly in the most severe cases, lethality. The findings presented here identify which one of the TATs may provide the housekeeping activity that internalizes PS in all healthy cells. The 4 subfamily IV P-type ATPases in classes 1 and 5 do not seem to fit the two criteria individually or as a group. *tat-1*, *tat-2*, *tat-3* and *tat-4* are individually nonessential; *tat-3; tat-4* double mutants are also perfectly viable. *tat-1*, *tat-2, tat-3* and *tat-4* exhibit tissue specific expression patterns, which suggests that these genes perform tissue specific functions (this study and Nilsson and Tuck, 2006). Furthermore, some *C. elegans* cell types, coelomocytes for example, neither express *tat-2*, *tat-3* or *tat-4* nor contain PS on the surface (this study and Zullig et al., 2007). This would imply then that *tat-1* must function in such tissues, but this gene *promotes* PS externalization (Figure 4). Hence, the presently available evidence strongly suggests that *C. elegans* subfamily IV P-type ATPases in classes 1 and 5 are not the housekeeping TATs individually or as a group.

The *C. elegans* genome contains two genes encoding subfamily IV P-type ATPases in class 2. *tat-6* is a nonessential poorly expressed recent duplication of *tat-5* (see Chapter 3 and *ok1984* allele). *tat-5* alone fulfils the requirements of the candidate TAT. It is broadly, likely ubiquitously, expressed and seems to be essential for survival from very early embryonic stages of development, if not even from before fertilization. The sole *S. cerevisiae* member of class 2 is *neo1*. It is also an essential gene but its product may preferentially reside in the endosome and the Golgi apparatus (Wicky et

al., 2004). This suggests that the plasma membrane lipid asymmetry may be established, as Devaux et al. (2006) pointed out, in the endosomal and Golgi compartments, by subfamily IV P-type ATPases in class 2.

Future research directions

In the short term, involvement of TAT-2 and TAT-4 in sterol turnover needs to be further elucidated. The model of *tat-2* and *tat-4* sterol deprivation hypersensitivity advanced here (Figure 7) predicts that mutants of the two genes would exhibit phenotypes similar to those of *daf-36*. *daf-36* mutant animals live longer and are more prone to enter the dauer developmental pathway than wild-type nematodes (Rottiers et al., 2006). Thus, experiments should be conducted to determine the lifespan and readiness to become dauers of *tat-2* and *tat-4* mutants. Second, *tat-2; tat-4* double mutants should be made to determine whether these genes act sequentially or in parallel: sterol deprivation sensitivity of the double mutant would be equivalent and exceed those of the single mutants in the former and the latter cases, respectively. Third, investigations with dehydroergosterol, a fluorescent naturally-occurring physiologically-active analog of cholesterol (Matyash et al., 2001), would visualize sterol turnover in the nematode body and reveal whether sterol uptake in the intestine or sterol efflux from the intestine or some other step in sterol transport is defective when TAT-2 and TAT-4 are nonfunctional. These three lines of experimentation should provide a better understanding of the roles that the two P-type ATPases perform in sterol turnover.

In the long term, the most challenging task is to directly show that the putative TATs do indeed translocate lipids. With the presently available methods, this is impossible. However, as the close association of TATs with proteins in the Cdc50p family in yeast suggests (Graham, 2004), lipid translocation and maintenance of lipid membrane properties may require multi-protein complexes. In *L. donovani* inactivation of a P-type ATPase in subfamily IV confers resistance to miltefosine, a lipid analog (Perez-Victoria et al., 2003). If this finding could be extended to *C. elegans* by showing that at least some *tat* mutants (most like those expressed in the intestine) are insensitive to miltefosine, then a mutagenic screen for nematodes resistant to the drug could be conducted. The screen should net mutant alleles of the resistance-conferring *tats*, as well mutant alleles of those genes whose products function in a complex or in the same process as these TATs. Perhaps, after a list of protein parts mediating lipid translocation is complete, an approach becomes apparent leading to direct demonstration of lipid translocation by TATs.

References

Balhedere PV and NJ Talbot. (2001) PDE1 encodes a P-type ATPase involved in appressorium-mediated plant infection by the rice blast fungus *Magnaporthe grisea*. Plant Cell 13:1987-2004.

Bessereau J-L, Wright A, Williams DC, Schuske K, Davis MW and EM Jorgensen. (2001) Mobilization of a *Drosophila* transposon in the *Caenorhabditis elegans* germ line. Nature 413:70-74.

Black DD. (2005) Chronic cholestasis and dyslipidemia: what is the cardiovascular risk? Journal of Pediatrics 146:306-307.

Brenner S. (1974) The genetics of *Caenorhabditis elegans.* Genetics 77:71-94.

Bull LN, van Eijk MJ, Pawlikowska L, DeYoung JA, Juijn JA, Liao M, Klomp LW, Lomri N, Berger R, Scharschmidt BF, Knisely AS, Houwen RH and NB Freimer. (1998) A

gene encoding a P-type ATPase mutated in two forms of hereditary cholestasis. Nature Genetics 18:219-224.

Chitwood DJ. (1999) Biochemistry and function of nematode steroids. Critical Reviews in Biochemistry and Molecular Biology 34:273-284.

Dean MD, Ardlie KG and MW Nachman. (2006) The frequency of multiple paternity suggests that sperm competition is common in house mice (*Mus domesticus*). Molecular Ecology 15:4141-4151.

Dhar MS, Yuan JS, Elliott SB and C Sommardahl. (2006) A type IV P-type ATPase affects insulin-mediated glucose uptake in adipose tissue and skeletal muscle in mice. Journal of Nutritional Biochemistry 17:811-820.

Dhar MS, Sommardahl CS, Kirkland T, Nelson S, Donnell R, Johnson DK and LW Castellani. (2004) Mice heterozygous for *Atp10c*, a putative amphipath, represent a novel model of obesity and type 2 diabetes. Journal of Nutrition 134:799-805.

Devaux PF, Lopez-Montero I and S Bryde. (2006) Proteins involved in lipid translocation in eukaryotic cells. Chemistry and Physics of Lipids 141:119-132.

Devaux PF. (1991) Static and dynamic asymmetry in cell membranes. Biochemistry 30:1163-1173.

Entchev EV and TV Kurzchalia. (2005) Requirement of sterols in the life cycle of the nematode *Caenorhabditis elegans*. Seminars in Cell and Developmental Biology 16:175-182.

Eppens EF, van Mil SW, de Vree JM, Mok KS, Juijn JA, Oude Elferink RP, Berger R, Houwen RH and LW Klomp. (2001) FIC1, the protein affected in two forms of hereditary cholestasis, is localized in the cholangiocyte and the canalicular membrane of the hepatocyte. Journal of Hepatology 35:436-443.

Flamant S, Pescher P, Lemercier B, Clément-Ziza M, Képès F, Fellous M, Milon G, Marchal G and C Besmond. (2003) Characterization of a putative type IV aminophospholipid transporter P-type ATPase. Mammalian Genome 14:21-30.

Flesch FM and BM Gadella. (2000) Dynamics of the mammalian sperm plasma membrane in the process of fertilization. Biochimica et Biophysica Acta 1469:197-235.

Fraser AG, Kamath RS, Zipperlen P, Martinez-Campos M, Sohrmann M and JA Ahringer. (2000) Functional genomic analysis of *C. elegans* chromosome I by systemic RNA interference. Nature 408:325-330.

Gengyo-Ando K and S Mitani. (2000) Characterization of mutations induced by ethyl methanesulfonate, UV, and trimethylpsoralen in the nematode *Caenorhabditis elegans*. Biochemical and Biophysical Research Communications 269:64-69.

Gerisch B and A Antebi. (2004) Hormonal signals produced by DAF-9/cytochrome P450 regulate *C. elegans* dauer diapause in response to environmental cues. Development 131:1765-1776.

Gerish B, Weitzel C, Kober-Eisermann C, Rottiers V and A Antebi. (2001) A hormonal signaling pathway influencing *C. elegans* metabolism, reproductive development, and life span. Developmental Cell 1:841-851.

Gissendanner CR, Crossgrove K, Kraus KA, Maina CV and AE Sluder. (2004) Expression and function of conserved nuclear receptor genes in *Caenorhabditis elegans*. Developmental Biology 266:399-416.

Gomes E, Jakobsen MK, Axelsen KB, Geisler M and MG Palmgren. (2000) Chilling tolerance in *Arabidopsis* involves ALA1, a member of a new family of putative aminophospholipid translocases. Plant Cell 12:2441-2454.

Graham TR. (2004) Flippases and vesicular-mediated protein transport. Trends in Cell Biology 14:670-677.

Halleck MS, Lawler JF, Blackshaw S, Gao L, Nagarajan P, Hacker C, Pyle S, Newman JT, Nakanishi Y, Ando H, Weinstock D, Williamson P and RA Schlegel. (1999) Differential expression of putative transbilayer amphipath transporters. Physiological Genomics 1:139-150.

Hao M, Mukherjee S and FR Maxfield. (2001) Cholesterol depletion induces large scale domain segregation in living cell membranes. Proceedings of the National Academy of Sciences USA 98:13072-13077.

Hayward SA, Murray PA, Gracey AY and AR Cossins. (2007) Beyond the lipid hypothesis: mechanisms underlying phenotypic plasticity in inducible cold tolerance. Advances in Experimental Medicine and Biology 594:132-142.

Jansen PLM and E Sturm. (2003) Genetic cholestasis, causes and consequences for hepatobiliary transport. Liver International 23:315-322.

Jesch SA, Liu P, Zhao X, Wells MT and SA Henry. (2006) Multiple endoplasmic reticulum-to-nucleus signaling pathways coordinate phospholipid metabolism with gene expression by distinct mechanism. Journal of Biological Chemistry 281:24070-24083.

Kamath RS, Martinez-Campos M, Zipperlin P, Fraser AG and J Ahringer. (2000) Effectiveness of specific RNA-mediated interference through ingested double-stranded RNA in *Caenorhabditis elegans*. Genome Biology 2:research0002.1-0002.10.

Kishimoto T, Yamamoto T and K Tanaka. (2005) Defects in structural integrity of ergosterol and the Cdc50p-Drs2p putative phospholipid translocase cause accumulation of endocytic membranes, onto which actin patches are assembled in yeast. Molecular Biology of the Cell 16:5592-5609.

Kurz A, Viertel D, Herrmann A and K Muller. (2005) Localization of phosphatidylserine in boar sperm cell membranes during capacitations and acrosome reaction. Reproduction 130:615-626.

Kurzchalia TV and S Ward. (2003) Why do worms need cholesterol? Nature Cell Biology 5:684-688.

Maeda I. Kohara Y, Tamamoto M and A Sugimoto. (2001) Large-scale analysis of gene function in *Caenorhabditis elegans* by high-throughput RNAi. Current Biology 11:171-176.

Matyash V, Entchev EV, Mende F, Wilsch-Brauninger M, Thiele C, Schmidt AW, Knolker H-J, Ward S and TV Kurzchalia. (2004) Sterol-derived hormone(s) controls entry into diapause in *Caenorhabditis elegans* by consecutive activation of DAF-12 and DAF-16. PLoS Biology 2(10):e280.

Matyash V, Geier C, Henske A, Mukherjee S, Hirsh D, Thiele C, Grant B, Maxfield FR and TV Kurzchalia. (2001) Distribution and transport of cholesterol in *Caenorhabditis elegans*. Molecular Biology of the Cell 12:1725-1736.

McKay RM, McKay JP, Avery L and JM Graff. (2003) *C. elegans*: a model for exploring the genetics of fat storage. Developmental Cell 4:131-142.

Merris M, Kraeft J, Tint GS and J Lenard. (2004) Long-term effects of sterol depletion in *C. elegans*: sterol content of synchronized wild-type and mutant populations. Journal of Lipid Research 45:2044-2051.

Merris M, Wadsworth WG, Khamrai U, Bittman R, Chitwood DJ and J Lenard. (2003) Sterol effects and sites of sterol accumulation in *Caenorhabditis elegans*: developmental requirement for 4α-methyl sterols. Journal of Lipid Research 44:172-181.

van Mil SW, van Oort MM, van den Berg IE, Berger R, Houwen RH and LW Klomp. (2004) Fic1 is expressed at apical membranes of different epithelial cells in the digestive tract and is induced in the small intestine during postnatal development of mice. Pediatric Research 56:981-987.

van Mil SW, Klomp LW, Bull LN and RH Houwen. (2001) FIC1 disease: a spectrum of intrahepatic cholestatic disorders. Seminars in Liver Disease 21:535-544.

Motola DL, Cummins CL, Rottiers V, Sharma KK, Li T, Li Y, Suino-Powell K, Xu HE, Auchus RJ, Antebi A and DJ Mangelsdorf. (2006) Identification of ligands for DAF-12 that govern dauer formation and reproduction in *C. elegans*. Cell 124:1209-1223.

Mouritsen OG and MJ Zuckermann. (2004) What's so special about cholesterol? Lipids 39:1101-1113.

Nagasaka H, Yorifuji T, Egawa H, Yanai H, Fujisawa T, Kosugiyama K, Matsui A, Hasegawa M, Okada T, Takayanagi M, Chiba H and K Kobayashi. (2005) Evaluation of risk for atherosclerosis in Alagille syndrome and progressive familial intrahepatic cholestasis: two congenital cholestatic diseases with different lipoprotein metabolisms. Journal of Pediatrics 146:329-335.

Nilsson L and S Tuck. (2006) *C. elegans* NUM-1 modulates endocytosis by targeting the TAT-1 phospholipid flippase. Abstract. European Worm Meeting.

Paulusma CC, Groen A, Kunne C, Ho-Mok KS, Spijkerboer AL, Rudi de Waart D, Hoek FJ, Vreeling H, Hoeben KA, van Marle J, Pawlikowska L, Bull LN, Hofmann AF, Knisely AS and RP Oude Elferink. (2006) Atp8b1 deficiency in mice reduces resistance of the canalicular membrane to hydrophobic bile salts and impairs bile salt transport. Hepatology 44:195-204.

Pawlikowska L, Groen A, Eppens EF, Kunne C, Ottenhoff R, Looije N, Knisely AS, Killeen NP, Bull LN, Elferink RP and NB Freimer. (2004) A mouse genetic model for familial cholestasis caused by ATP8B1 mutations reveals perturbed bile salt homeostasis but no impairment in bile secretion. Human Molecular Genetics 13:881-892.

Perez-Victoria FJ, Gamarro F, Ouellette M and S Castanys. (2003) Functional cloning of the miltefosine transporter. A novel P-type phospholipid translocase from *Leishmania* involved in drug resistance. Journal of Biological Chemistry 278:49965-49971.

Pomorski T and AK Menon. (2006) Lipid flippases and their biological functions. Cellular and Molecular Life Sciences 63:2908-2921.

Prezant TR, Chaltraw WE and N Fischel-Ghodsian. (1996) Identification of an expressed yeast gene which prevents aminoglycoside toxicity. Microbiology 142:3407-3414.

Reddien PW and HR Horvitz. (2004) The engulfment process of programmed cell death in *Caenorhabditis elegans*. Annual Review of Cell and Developmental Biology 20:193-221.

Rottiers V, Motola DL, Gerisch B, Cummins CL, Nishiwaki K, Mangelsdorf DJ and A Antebi. (2006) Hormonal control of *C. elegans* dauer formation and life span by a Rieske-like oxygenase. Developmental Cell 10:473-482.

Saito K, Fujimura-Kamara K, Furuta N, Kato U, Umeda M and K Tanaka. (2004) Cdc50p, a protein required for polarized growth, associates with the Drs2p P-type ATPase implicated in phospholipid translocation in *Saccharomyces cerevisiae*. Molecular Biology of the Cell 15:3418-3432.

Schlegel RA and P Williamson. (2001) Phosphatidylserine, a death knell. Cell Death and Differentiation 8:545-548.

Simmer F, Moorman C, van der Linden AM, Kuijk E, van den Berghe PVE, Kamath FS, Fraser AG, Ahringer J and RHA Plasterk. (2003) Genome-wide RNAi of C. elegans using the hypersensitive rrf-3 strain reveals novel gene functions. PLoS Biology 1:77-84.

Sonnichsen B, Koski LB, Walsh A, Marschall P, Neumann B, Brehm M, Alleaume AM, Artelt J, Bettencourt P, Cassin E, Hewitson M, Holz C, Khan M, Lazik S, Martin C, Nitzsche B, Ruer M, Stamford J, Winzi M, Heinkel R, Roder M, Finell J, Hantsch H, Jones SJ, Jones M, Piano F, Gunsalus KC, Oegema K, Gonczy P, Coulson A, Hyman AA and CJ Echeverri. (2005) Full-genome RNAi profiling of early embryogenesis in *Caenorhabditis elegans.* Nature 434:462-469.

Soupene E and FA Kuypers. (2006) Identification of an erythroid ATP-dependent aminopospholipid transporter. British Journal of Haematology 133:436-438.

Tang X, Halleck MS, Schlegel RA and P Williamson. (1996) A subfamily of P-type ATPases with aminophospholipid transporting activity. Science 272:1495-1497.

Timmons L and A Fire. (1998) Specific interference by ingested dsRNA. Nature 395:854.

Ujhazy P, Ortiz D, Misra S, Li S, Moseley J, Jones H and IM Arias. (2001) Familial intrahepatic cholestasis 1: studies of localization and function. Hepatology 34:768-775.

Wang L, Beserra C and DL Garbers. (2004) A novel aminophospholipid transporter exclusively expressed in spermatozoa is required for membrane lipid asymmetry and normal fertilization. Developmental Biology 267:203-215.

Wicky S, Schwarz H and B Singer-Kruger. (2004) Molecular interactions of yeast Neo1p, an essential member of the Drs2p family of aminophospholipid translocases, and its role in membrane trafficking within the endomembrane system. Molecular and Cellular Biology 24:7402-7418.

Wu YC and HR Horvitz. (1998) *C. elegans* phagocytosis and cell-migration protein CED-5 is similar to human DOCK180. Nature 392:501-504.

Yochem J, Tuck S, Greenwald I and M Han. (1999) A gp330/megalin-related protein is required in the major epidermis of *Caenorhabditis elegans* for completion of molting. Development 126:597-606.

Zhang B, Groffen J and N Heisterkamp. (2005) Resistance to farnesyltransferase inhibitors in Bcr/Abl-positive lymphoblastic leukemia by increased expression of a novel ABC transporter homolog ATP11a. Blood 106:1355-1361.

Zullig S, Jovanovic M, Neukomm L, Charette SJ, Lyssenko N, Halleck MS, Reutelingspeger C, Schlegel RA and MO Hengartner. (2007) Phosphatidylserine exposure is an early marker of apoptosis in *C. elegans* and depends on the P-type ATPases TAT-1. Current Biology 17:994-999.

Nicholas N. Lyssenko
The Huck Institutes of the Life Sciences and
Department of Biochemistry and Molecular Biology
The Pennsylvania State University
University Park, PA16802

Education

Doctor of Philosophy in Integrative Biosciences 08/2007
The Huck Institutes of the Life Sciences and
Department of Biochemistry and Molecular Biology
Pennsylvania State University - University Park

Bachelor of Science in Cell and Molecular Biology and Genetics (CMBG) 08/1999
University of Maryland College Park

Fellowships

1. American Heart Association Predoctoral Fellowship 07/2005 – 06/2006
2. American Heart Association Predoctoral Fellowship 07/2003 – 06/2005
3. The Huck Institutes of the Life Sciences Fellowship 09/2001 – 06/2003
Pennsylvania State University, University Park

Selected conference presentations

1**.** Speaker, an abstract selected short talk, Gordon Research Conference 07/2005
Molecular and Cellular Biology of Lipids
2. Poster presenter, Gordon Research Conference Apoptotic Cell 06/2005
Recognition and Clearance

Recent Publications

Lyssenko NN, Miteva Y and RA Schlegel. (2007) The *C. elegans* P-type ATPase subfamily of putative transbilayer amphipath transporters includes a single housekeeping gene and two candidate mediators of intestinal sterol metabolism. Manuscript in preparation.

Lyssenko NN, Hanna-Rose W and RA Schlegel. (2007) A cognate nuclear localization signal effects strong nuclear localization of a GFP reporter and facilitates gene expression studies in *C. elegans*. Biotechniques. Accepted with revisions.

Zullig S, Jovanovic M, Neukomm L, Charette SJ, Lyssenko NN, Halleck MS, Reutelingspeger C, Schlegel RA and MO Hengartner. (2007) Phosphatidylserine exposure is an early marker of apoptosis in *C. elegans* and depends on the P-type ATPase TAT-1. Current Biology 17:994-999.